



City Research Online

City, University of London Institutional Repository

Citation: Henderson, F.A. (1992). The application of polybipyridine ruthenium complexes to immunoassay techniques. (Unpublished Doctoral thesis, City, University of London)

This is the accepted version of the paper.

This version of the publication may differ from the final published version.

Permanent repository link: <https://openaccess.city.ac.uk/id/eprint/28513/>

Link to published version:

Copyright: City Research Online aims to make research outputs of City, University of London available to a wider audience. Copyright and Moral Rights remain with the author(s) and/or copyright holders. URLs from City Research Online may be freely distributed and linked to.

Reuse: Copies of full items can be used for personal research or study, educational, or not-for-profit purposes without prior permission or charge. Provided that the authors, title and full bibliographic details are credited, a hyperlink and/or URL is given for the original metadata page and the content is not changed in any way.

THE APPLICATION OF POLYBIPYRIDINE RUTHENIUM COMPLEXES
TO IMMUNOASSAY TECHNIQUES

FIONA ANN HENDERSON

A THESIS SUBMITTED FOR THE DEGREE OF
DOCTOR OF PHILOSOPHY

CITY UNIVERSITY, LONDON

THE DEPARTMENT OF CHEMISTRY

DECEMBER 1992

TABLE OF CONTENTS

	<u>PAGE</u>
ACKNOWLEDGEMENTS	11
DECLARATION	12
ABSTRACT	13
CHAPTER 1: The Synthesis of di-4,4'-substituted-2,2'-bipyridines, mono-4-substituted-2,2'-bipyridines and their corresponding Ruthenium (II) complexes	14
1:0:1 Introduction	15
1:0:2 The Synthesis of Substituted 2,2'-bipyridines	17
1:1:1 Preparation of 4- and 4,4'-amino substituted 2,2'-bipyridine	24
1:1:2 Preparation of 4- and 4,4'-hydroxy substituted 2,2'-bipyridines	33
1:1:3 Preparation of a Ruthenium Complex Containing a Vinyl Bipyridine	50
1:2:1 Synthesis of Ruthenium Polybipyridine Complexes for Investigation of their Photophysical Properties	52
1:2:2 Synthesis of Bis(2,2'-bipyridine) (4,4'-dibromo-2,2'-bipyridine) Ruthenium (II) Hexafluorophosphate	54
1:2:3 The Synthesis of Ruthenium Complexes Bearing Ester Derivatised Bipyridine Ligands	57
1:3:0 Experimental	59
1:4:0 References	91
CHAPTER 2: Luminescence and the Luminescent Properties of Substituted Tris-(2,2'-bipyridine) Ruthenium (II) Complexes	93
2:0:0 Introduction	94
2:0:1 The Nature of Light	94
2:0:2 Principles of Photochemistry	95
2:1:1 Mechanisms of Photoluminescence	96

	<u>PAGE</u>
2:1:3 The Franck-Condon Principle	100
2:1:4 Energy Difference in the O-O Transitions	101
2:1:5 Quantitative Aspects of Light Absorption and Emission	103
2:1:6 Transition, Probability and Lifetime . .	104
2:1:7 Phosphorescence	104
2:2:1 Inorganic Photochemistry	106
2:2:2 Bonding	106
2:2:3 Inorganic Luminescence	111
2:2:4 Excited States of Electronic Spectra . .	111
2:2:5 The Effect of Solvent on Electronic Tran- sitions	118
2:3:1 Ruthenium Polybipyridines	118
2:3:2 Low-Lying Energy Levels in Ru(bipy) ₃ ²⁺ .	119
2:3:3 The Temperature Dependence of the Photo- physical Properties of the Ru(bipy) ₃ ²⁺ Ion in Aqueous Solution	124
2:3:4 Substituent Effects on the Photophysics of Ruthenium (II) Bipyridine Complexes .	128
2:4:1 Luminescent Properties of Mixed Polybipy- ridine Ruthenium (II) Complexes	129
2:5:1 Room Temperature Luminescence (RTL) . .	132
2:5:2 Mechanisms of Room Temperature Phospho- rescence	132
2:5:3 Matrix Effects in RTP	136
2:5:4 Mechanism of RTP with Sodium Acetate Support	138
2:5:5 Heavy-atom Effect on RTP	140
2:5:6 Analytical Use of RTP	141
2:5:7 RTL in Ruthenium Polybipyridine Com- plexes	142
2:5:8 Initial Evaluation of RTL in Ruthenium Polybipyridine Complexes	142
2:5:9 Standardisation of RTL Procedure	148

	<u>PAGE</u>
2:5:10 Evaluation of RTL as an Analytical Technique	152
2:6:0 Experimental	153
2:7:0 References	163
CHAPTER 3: Immunoassays and the Application of Ruthenium Tris Bipyridine Complexes as Luminescent Labels in Immunoassay	166
3:0:0 Introduction	167
3:0:1 The Immune Response	167
3:1:1 Immunoglobulins	169
3:1:2 The Basic Structure of the Immunoglobulins	170
3:1:3 Variations in Structure of the Immunoglobulins	172
3:1:4 Structural Variation in Relation to Antibody Specificity	172
3:1:5 Variations in Structure not Related to Antibody Specificity	173
3:2:1 Immunoassays in General	179
3:2:2 Immunoassay	180
3:2:3 Immunometric Assay	182
3:2:4 Discrimination between Bound and Free Fractions	184
3:2:5 Time-resolved Fluorescence Immunoassay .	185
3:2:6 DELFIA	188
3:3:0 Ruthenium Complexes in Time-resolved Immunoassay	191
3:3:1 Assessment of Ruthenium Tris Bipyridine Complexes as Antibody Labels	191
3:3:2 Examination of the Luminescent Properties of Ruthenium Tris Bipyridine Complexes Labelled to Human IgG	194
3:3:3 Examination of Conjugated Ruthenium Probes by RTL	197

	<u>PAGE</u>
3:3:4 Evaluation of Ruthenium Tris Bipyridine Complexes as Antibody Probes in Immunoassay	198
3:4:0 Experimental	200
3:5:0 References	203

LIST OF TABLES

2-1 Photophysical Data Relating to a Series of Complexes [Ru(bipy) ₂ (X)] ²⁺	130
2-2 Relative Intensities of Sodium 4-Biphenyl-carboxylate	133
2-3 Comparison of Phosphorescence Signals at Room Temperature and at 77K	135
2-4 Influence of Number of Ionic Sites upon Phosphorescence Signals at 77K and at Room Temperature .	136
2-5 Effect of Added Substances (0.5M) on the First Observable Half-Life of Phosphorescence of 2-naphthalene sulphonate on Filter Paper	137
2-6 Luminescence Lifetime of Ru(bipy) ₃ ²⁺ Adsorbed on a Paper Substrate	143
2-7 Effect of Concentration on the Luminescent Lifetime of Ru(bipy) ₃ ²⁺	144
2-8 Variation of RTL Signal with Solid Phase (I)	146
2-9 Limit of Detection of RTL Signal of Ru(bipy) ₃ ²⁺	147
2-10 Effect of Drying Time and Sample Size on RTL Results	149
2-11 Variation of RTL Signal with Solid Phase (II)	150
2-12 The Limit of Detection of Ru(bipy) ₃ ²⁺ by RTL	151
2-13 Effect of Variation of Sampling Technique	152
3-1 Physical Properties of Major Human Immunoglobulin Classes	177
3-2 Biological Properties of Major Immunoglobulin Classes in the Human	178
3-3 Table Showing the Application of Detection Methods to Immunoassay Systems	184
3-4 Fluorescence Decay Time of some Fluorophores and Proteins	187

3-5 Luminescent Lifetimes of Ruthenium Tris Bipyridine Antibody Probes	197
3-6 Evaluation of the RTL Behaviour of a Ruthenium Complex Human IgG Conjugate	198

LIST OF ILLUSTRATIONS

Fig. 1-1 Figure Showing the Dibrominated Product formed on Reaction of 4,4'-dimethyl-2,2'-bipyridine with NBS	28
Fig. 1-2 Figure Showing Tautomerisation of 4,4'-di-hydroxy-2,2'-bipyridine	34
Fig. 1-3 Diagram Illustrating Possible Carbon Signals seen by ^{13}C nmr	39
Fig. 2-1 Diagram Showing vibrational Levels of the Excited State	97
Fig. 2-2 Example of a Molecular Absorption Spectrum. .	98
Fig. 2-3 Diagram Illustrating the Franck-Condon Principle for a Diatomic Molecule	101
Fig. 2-4 Diagram Illustrating Change of Solvation after Excitation or Emission	102
Fig. 2-5 Diagram Illustrating Phosphorescence	105
Fig. 2-6 Diagram Illustrating the Energy Differences Established in d-orbitals in an O_h Complex .	107
Fig. 2-7 Diagram Showing Possible Bonding of t_{2g} Orbitals to Ligand π Orbitals	108
Fig. 2-8 Bonding Diagram for a Ligand having Orbitals of π Symmetry Filled with Electrons and Low in Energy	109
Fig. 2-9 Bonding Diagram for a Ligand having Vacant High-Energy π Orbitals	110
Fig. 2-10 Diagram Illustrating Bonding of Pyridine in $\text{W}(\text{CO})_5\text{Pyr}$	112
Fig. 2-11 Diagram Showing Ground State Relative to Excited State	115
Fig. 2-12 Diagram Illustrating the Orbital Ordering of $[\text{W}(\text{CO})_5\text{piperidine}]$ and $[\text{W}(\text{CO})_5(4\text{-formylpyridine})]$	116
Fig. 2-13 Diagram Showing the Ordering of Low-Lying Charge-transfer States in $\text{Ru}(\text{bipy})_3^{2+}$ According to the EIP Model	121

Fig. 2-14 Relative Energies of the $(d\pi)^5(\pi^*_{B_2})^1$ Excited States and the $(d\pi)^6$ Ground State of $\text{Ru}(\text{bipy})_3^{2+}$ ES Model	123
Fig. 2-15 Effect of Temperature Variation on the Luminescence Spectra of $\text{Ru}(\text{bipy})_3^{2+}$	125
Fig. 2-16 Diagram Illustrating the Presence of Ligand Field Orbitals lying above the ${}^3\text{MLCT}$ State of $\text{Ru}(\text{bipy})_3^{2+}$	127
Fig. 2-17 Relative Intensities of NaBPCA Samples in Ar (Curve A = $I_{Ar}, -$) and O ₂ (Curve B = $I_{O_2}, ---$) as a Function of Humidity	134
Fig. 2-18 Degree of O ₂ Quenching Represented by Q_{O_2}/I_{Ar} Plotted as a Function of Relative Humidity for NaBPCA Samples	134
Fig. 2-19 Room Temperature Phosphorescence Intensity Plotted as a Function of Quenching Time for 4-phenylcarboxylic acid Adsorbed on Paper and Sodium Citrate Impregnated Paper	137
Fig. 2-20 Adsorption of PABA on a Sodium Acetate Surface	140
Fig. 2-21 Fluorescence and Phosphorescence Spectra of Cinoxacin. Excitation (A) and Emission (A') Spectra of Cinoxacin on Paper Strip Treated with Lead Tetra-acetate. Excitation (B) and Emission (B') Spectra of Cinoxacin on Plain Paper	141
Fig. 2-22 Diagram Showing Fluorescence Microscope Modular Bench	154
Fig. 3-1 Experiments Conducted to Establish Immunoglobulin Structure	170
Fig. 3-2 Model for the Structure of Immunoglobulins .	171
Fig. 3-3 Diagram Showing the Hypervariability in the Immunoglobulin Structure	173
Fig. 3-4 Diagram Showing Immunoglobulin Domains . . .	175
Fig. 3-5 Diagram Representing the Principle of Immunoassay	180
Fig. 3-6 Diagram Showing the Relationship of Bound Antigen to Antigen Concentration in Immunoassay	181
Fig. 3-7 Diagram Demonstrating the Principle of Immuno-metric Assay	182

	<u>PAGE</u>
Fig. 3-8 Diagram Showing the Relationship of Bound Antibody to Antigen Concentration in Immuno-metric Assay	183
Fig. 3-9 Principle of Time Delayed Measurement of Fluorescence	187
Fig. 3-10 Diagram Illustrating the DELFIA System	189
Fig. 3-11 Diagram Showing the Form of the Stabilised Fluorescent Europium Chelate	190
Fig. 3-12 UV Spectra Showing Incorporation of Ruthenium Complex (19) into IgG	193
<u>LIST OF SCHEMES</u>	
SCHEME 1-1 An Example of the Synthesis of a Substituted 2,2'-bipyridine	17
SCHEME 1-2 An Example of an Ullman Type Reaction . .	18
SCHEME 1-3 An Example of the type A Synthetic Scheme for the Preparation of Pyridines	19
SCHEME 1-4 An Example of the Type B Synthetic Scheme for the Preparation of Pyridines	20
SCHEME 1-5 An Example of the Guareschi-Thorpe Synthesis of 2-pyridones	21
SCHEME 1-6 An Example of the Kröhnke Synthesis of Substituted Pyridines	22
SCHEME 1-7 Examples of Other Methods of Synthesis of Pyridines	23
SCHEME 1-8 Proposed Synthetic Route to the Preparation of 4-aminomethyl -2,2'-bipyridine (5)	25
SCHEME 1-9 Synthetic Scheme for the Synthesis of 4,4'- diaminomethyl -2,2'-bipyridine (11)	27
SCHEME 1-10 Synthetic Scheme for the Synthesis of 4,4'-diamino-2,2'-bipyridine (18)	30
SCHEME 1-11 Alternative Scheme for the Synthesis of 4,4'-diamino-2,2'-bipyridine	32
SCHEME 1-12 Synthetic Scheme for the Synthesis of a 4,4'-dihydroxy-2,2'-bipyridine Ruthenium (II) Complex	35
SCHEME 1-13 Reaction Mechanism for the N-Oxidation of Bipyridine	36

SCHEME 1-14	Reaction Mechanism for the Nitration of Bipyridine N-Oxides	37
SCHEME 1-15	Synthetic Scheme for the Synthesis of a 4-hydroxy-2,2'-bipyridine Ruthenium (II) Complex	41
SCHEME 1-16	Projected Mechanism for the Deoxygenation of 4-nitro-2,2'-bipyridine by Phosphorus Trichloride [19]	43
SCHEME 1-17	Scheme Showing Possible Synthetic Routes to Alkyl Hydroxy Bipyridine Ruthenium (II) Complexes	46
SCHEME 1-18	Synthetic Scheme for the Synthesis of bis(4,4'-diphenyl-2,2'-bipyridine)(4-[3-hydroxypropyl]-4'-methyl-2,2'-bipyridine) Ruthenium (II) Hexafluorophosphate . . .	49
SCHEME 1-19	Synthetic Scheme for the Synthesis of bis(2,2'-bipyridine)(4-vinyl-4'-methyl-2,2'-bipyridine) Ruthenium (II) Hexafluorophosphate (40)	51
SCHEME 1-20	Scheme Showing Synthetic Routes to bis-(2,2'-bipyridine)(4,4'-dimethyl-2,2'-bipyridine) Ruthenium (II) Chloride (41) and bis(2,2'-bipyridine)(4,4'-diphenyl-2,2'-bipyridine) Ruthenium (II) Hexafluorophosphate (43)	53
SCHEME 1-21	Synthetic Scheme for the Synthesis of bis(2,2'-bipyridine)(4,4'-dibromo-2,2'-bipyridine) Ruthenium (II) Hexafluorophosphate (46)	56
SCHEME 1-22	Scheme Showing Synthetic Routes to the Synthesis of Ruthenium Complexes Bearing Ester Derivatised Bipyridine Ligands .	58
SCHEME 3-1	Scheme Showing the Conjugation of IgG to bis(2,2'-bipyridine)(4,4'-diamino-2,2'-bipyridine) Ruthenium (II) Hexafluorophosphate (19)	192
SCHEME 3-2	Scheme Showing the Conjugation of Ruthenium Complexes to IgG Utilising Phosgene	195
SCHEME 3-3	Scheme Showing the Conjugation of IgG to Ruthenium Complexes Utilising EDC and Vinyl Derivatives	196

LIST OF GRAPHS

GRAPH 2-1 Effect of Concentration on the Luminescent Lifetime of Ruthenium Tris Bipyridine	144
GRAPH 2-2 Graph Showing the Limit of Detection of the RTL Signal of Ruthenium Tris Bipyridine . . .	148

ACKNOWLEDGEMENTS

I would like to take this opportunity to thank Professor R. S. Davidson for his help during my PhD. I would also like to thank Boots Celltech Limited for funding this work, and Dr. J. Wright for his advice during the project.

My thanks go to Mr. A. Murphy for conducting the microanalysis of the compounds, and to Mr. A. Taylor for keeping Anthony company.

I would like to dedicate this work to my parents. Special thanks to Paul; finally the light at the end of the tunnel has been reached.

DECLARATION

I hereby declare that I grant powers of discretion to the University Librarian to allow the thesis to be copied in whole or in part without further reference to the author. This permission covers only single copies made for study purposes, subject to normal conditions of acknowledgement.

ABSTRACT

A series of ruthenium (II) complexes bearing three 2,2'-bipyridine ligands, one of which was mono-substituted or disubstituted with functional groups, which could be easily activated towards conjugation with an antibody, were synthesized. Examination of the luminescent properties of these complexes, indicated that they exhibited similar characteristics to the parent complex, ruthenium (II) tris 2,2'-bipyridine and were, therefore, suited to application to time-resolved immunoassay. The absorption maxima of the substituted complexes were red shifted relative to that of the parent complex, but the nature of the substituent appeared to have little effect on the degree of shift observed. Also, the emission maxima exhibited red shift relative to ruthenium (II) tris 2,2'-bipyridine, with the degree of shift being greater in the disubstituted complexes. It was noted that the position of the observed emission maximum appeared to be influenced by the mesomeric and inductive effects the substituents exerted on the ligand and, thus, on the complex. The luminescent lifetime of the complexes appeared to be similarly affected; the measured lifetime decreasing with increasing Stokes shift. Examination of the room temperature luminescence (RTL) effect, exhibited by ruthenium (II) tris 2,2'-bipyridine, showed an increase in the luminescence lifetime of the complex when immobilised onto a suitable solid phase, together with a possible detection limit of the complex in the picomolar range. These properties, therefore, highlighted the possible application of this type of complex to solid phase immunoassay. It was found to be possible to conjugate the functionalised ruthenium complexes to immunoglobulin G (IgG), with retention of the required luminescent properties of the parent complex, ruthenium (II) tris 2,2'-bipyridine. It is, therefore, possible that these complexes could be utilised as the detection label in time-resolved immunoassay.

CHAPTER 1

THE SYNTHESIS OF DI-4,4'-SUBSTITUTED-2,2'-BIPYRIDINES, MONO-4-SUBSTITUTED-2,2'-BIPYRIDINES AND THEIR CORRESPONDING RUTHENIUM
(III) COMPLEXES

The purpose of this project was to devise an immunoassay, utilising a luminescent transition metal complex as the system label. It was believed, that the type of immunoassay best suited to this application was one involving the use of time-resolved luminescence as its detection system (ref. Chapter 3). Time-resolved luminescence immunoassay has certain requirements, which are necessary in order for its label to perform adequately in the assay. The chosen transition metal label must therefore demonstrate the following properties:-

- 1) High quantum yield of luminescence
- 2) Large Stokes shift
- 3) Long luminescence lifetime

One transition metal complex which has been reported to exhibit the above mentioned luminescent properties, is the tris (2,2'-bipyridine) ruthenium (II) cation [1]. It was, therefore, proposed to synthesize a series of ruthenium (II) complexes bearing three bipyridine ligands, one of which should be mono-substituted or disubstituted with functional groups, which could be easily activated towards conjugation with an antibody. It was believed, that in synthesizing such a series of complexes, the luminescent properties of ruthenium tris-bipyridine would be maintained, and at the same time produce a compound, that could be used as an antibody label.

As it was proposed to synthesize a series of substituted bipyridines, it appeared that the 6 position on the bipyridine ring was the most apt for this purpose, being highly activated towards substitution reactions. However, it was not ideally suited to our purposes for two main reasons.

- 1) 6-substitution of bipyridines produces a sterically hindered ruthenium complex. Such distortion of the complex from the original tris (2,2'-bipyridine) ruthenium (II) complex causes perturbation of the luminescent properties, resulting in decreases in both the luminescent quantum

yield and lifetime [2], compared with that of the parent complex.

- 2) On ligation 6-substituents cause the bipyridine ligands to twist [2], and probably this distortion could cause the ring substituents to be less accessible to reactants, thus hindering conjugation of antibody to the complex.

By way of contrast, substitution of the 4 position of bipyridine does not lead to distortion of the resulting ruthenium complex. Therefore, substitution of this position has, generally, little effect on the luminescent properties of the complex, when compared with $\text{Ru}(\text{bipy})_3^{2+}$ [3]. It is also probable, that the approach of reactants to the ring substituents in this type of complex would not be hindered, therefore allowing conjugation of antibody to the 4-substituted complex.

5-substituted ligands can be utilised towards complexation to ruthenium. Although the 5-position of bipyridine is the most activated towards electrophilic attack, harsh conditions are required before substitution can occur. Alternatively, N-oxidation of bipyridine activates the 4-position towards easy electrophilic attack. Therefore, a range of derivatives are more readily accessible via the 4-position [4], and it was decided to concentrate on 4-substituted bipyridines for the purpose of this project.

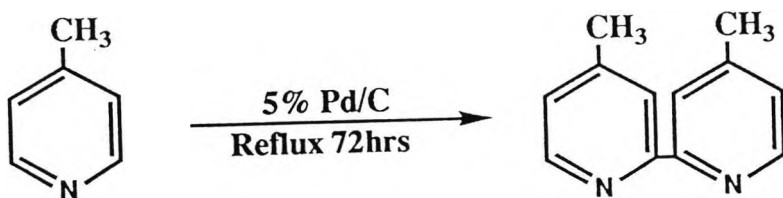
For the development of a ruthenium complex for its intended use as an immunoassay label, the substituents it bears must be readily activatable towards conjugation with antibodies. Two such functional groups are amine and hydroxyl (ref. Chapter 3). The following reports the synthesis of bipyridines substituted at the 4-positions with amino and hydroxy functionalities.

1:0:2 THE SYNTHESIS OF SUBSTITUTED 2,2'-BIPYRIDINES

Preparative routes to substituted bipyridines appear to follow two main synthetic procedures. One route demonstrated by Sasse et al [5,6], involves the reaction of alkyl substituted pyridines in the presence of 5% Pd/C, (Scheme 1-1).

SCHEME 1-1

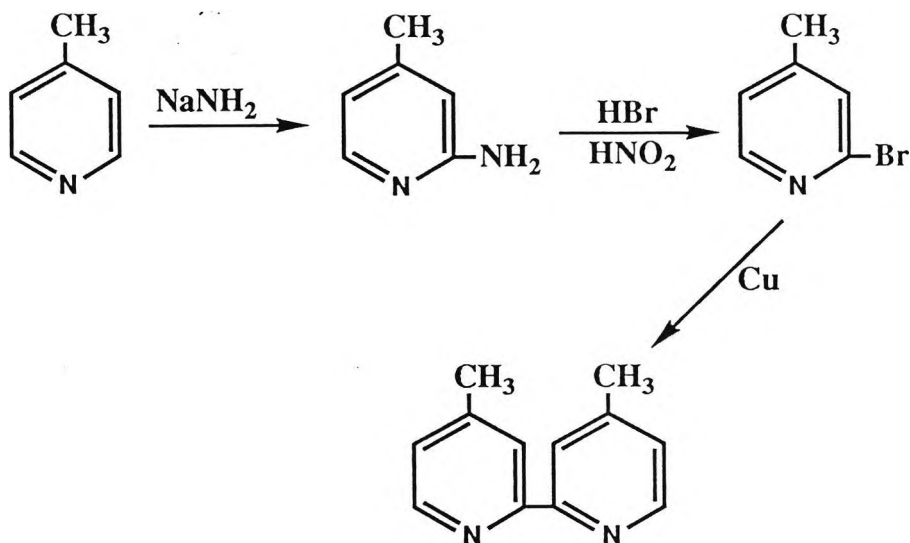
AN EXAMPLE OF THE SYNTHESIS OF A SUBSTITUTED 2,2'-BIPYRIDINE



The second synthetic route is exhibited by the Ullman reaction [7], which comprises the coupling of 2-halopyridines in the presence of copper. An example of the Ullman reaction is given in Scheme 1-2.

Both synthetic procedures referred to above required previously substituted pyridines. There are many general procedures for the synthesis of substituted pyridines, the majority of which are based on cyclisation reactions. The most common of these reactions is the Hantzsch Synthesis, (Scheme 1-3), which is an example of a type A cyclisation reaction.

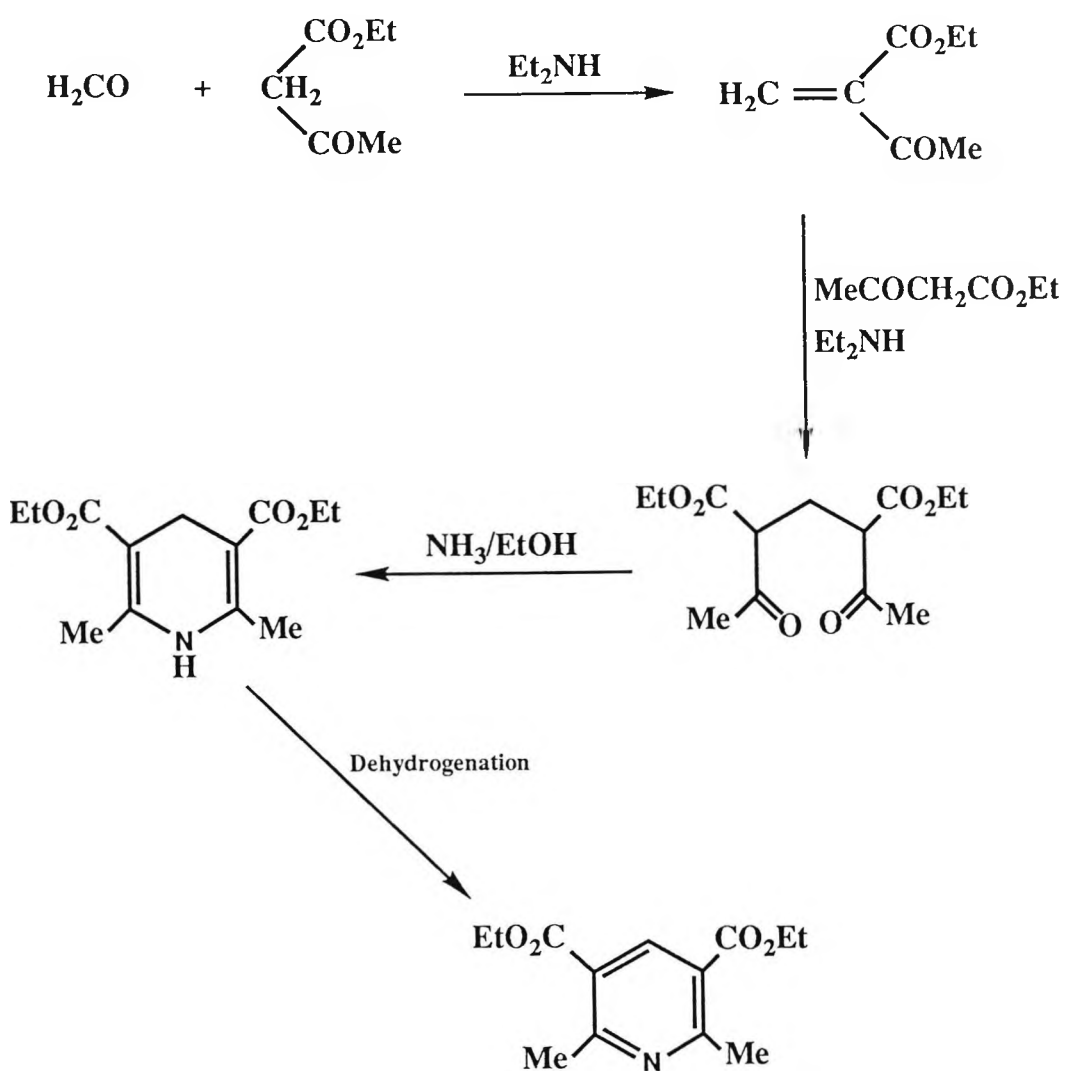
SCHEME 1-2
AN EXAMPLE OF AN ULLMAN TYPE REACTION



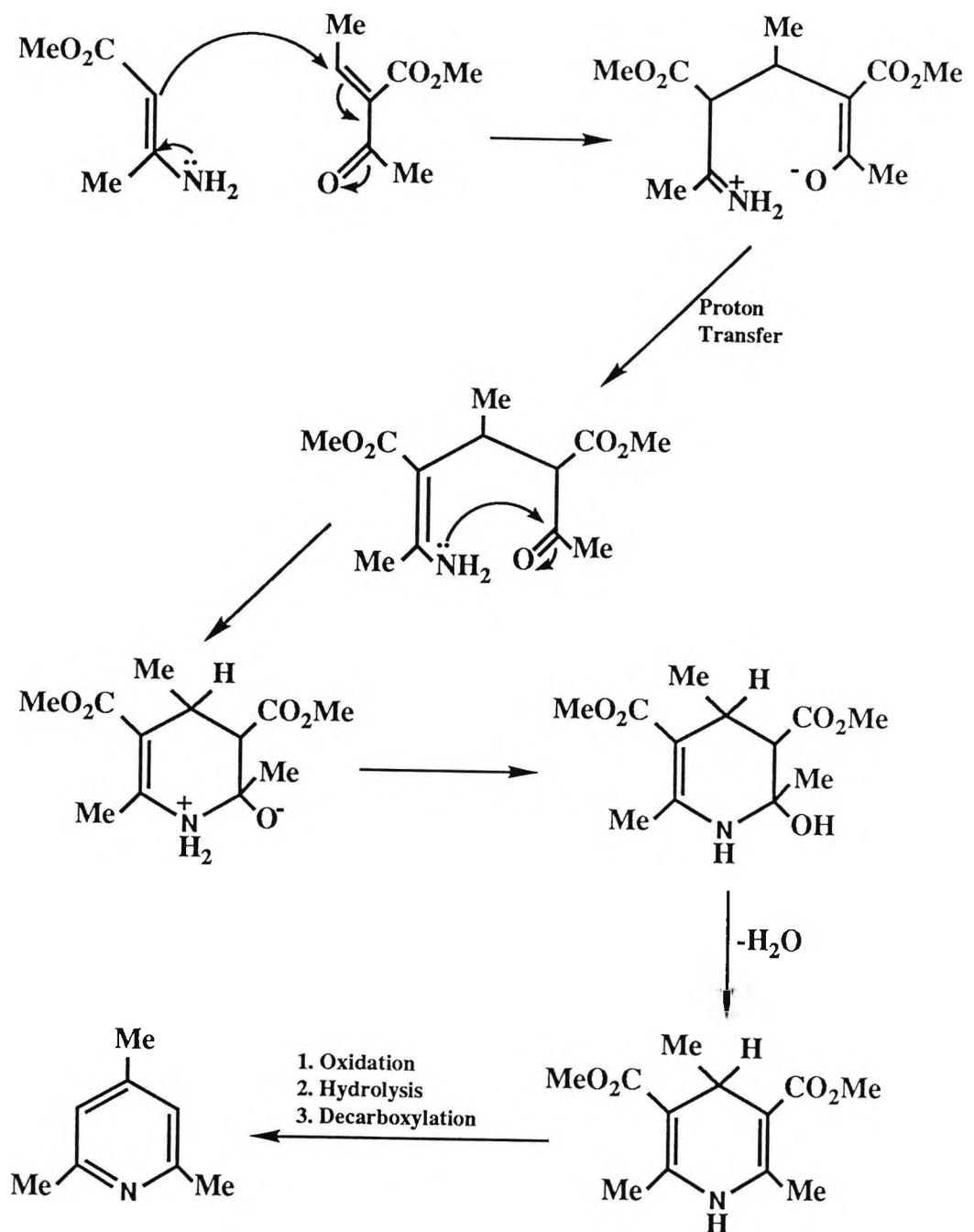
This involves the reaction of a β -ketoester or other activated methylene compound with an aldehyde in the presence of ammonia. The reaction can be represented, as involving the construction of a saturated 1,5-dicarbonyl compound by successive aldol and conjugate addition reactions followed by cyclisation with ammonia.

Another route to the synthesis of substituted pyridines is demonstrated by the type B reaction, illustrated in Scheme 1-4.

SCHEME 1-3
AN EXAMPLE OF THE TYPE A SYNTHETIC SCHEME FOR THE PREPARATION
OF PYRIDINES

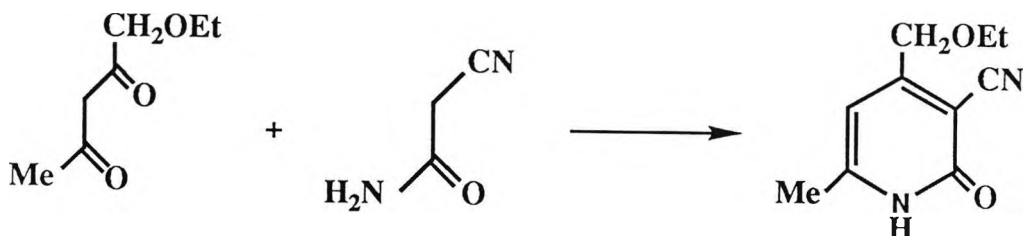


SCHEME 1-4
**AN EXAMPLE OF THE TYPE B SYNTHETIC SCHEME FOR THE PREPARATION
 OF PYRIDINES**



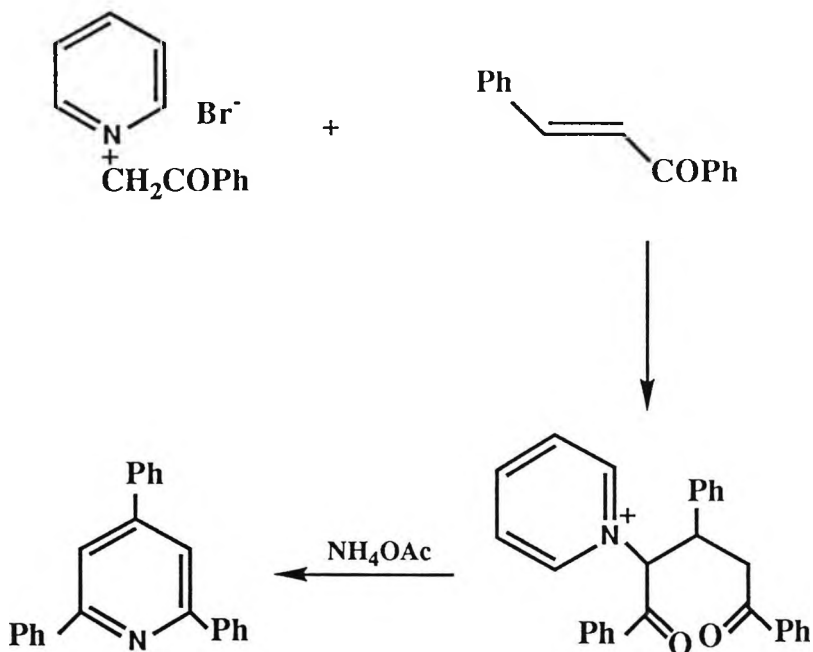
Other less common examples of related processes, in which substituted pyridines are formed in moderate to good yields, include the Guareschi-Thorpe synthesis, (Scheme 1-5), which results in the preparation of 2-pyridones. This synthesis utilises the reaction of cyanoacetamide as the nitrogen containing component in a cyclisation reaction with a 1,3-diketone or β -ketoester.

SCHEME 1-5
AN EXAMPLE OF THE GUARESCHI-THORPE SYNTHESIS OF 2-PYRIDONES.



A good general route, especially for those pyridines with substituents at the 2-, 4-, and 6-positions, is demonstrated by the Kröhnke Synthesis (Scheme 1-6). This involves the conjugate addition of a pyridinium ylide to an α,β -unsaturated carbonyl compound, leading to the construction of a 1,5-diketone, which is at the correct oxidation state for cyclisation directly to an aromatic pyridine in the presence of ammonia.

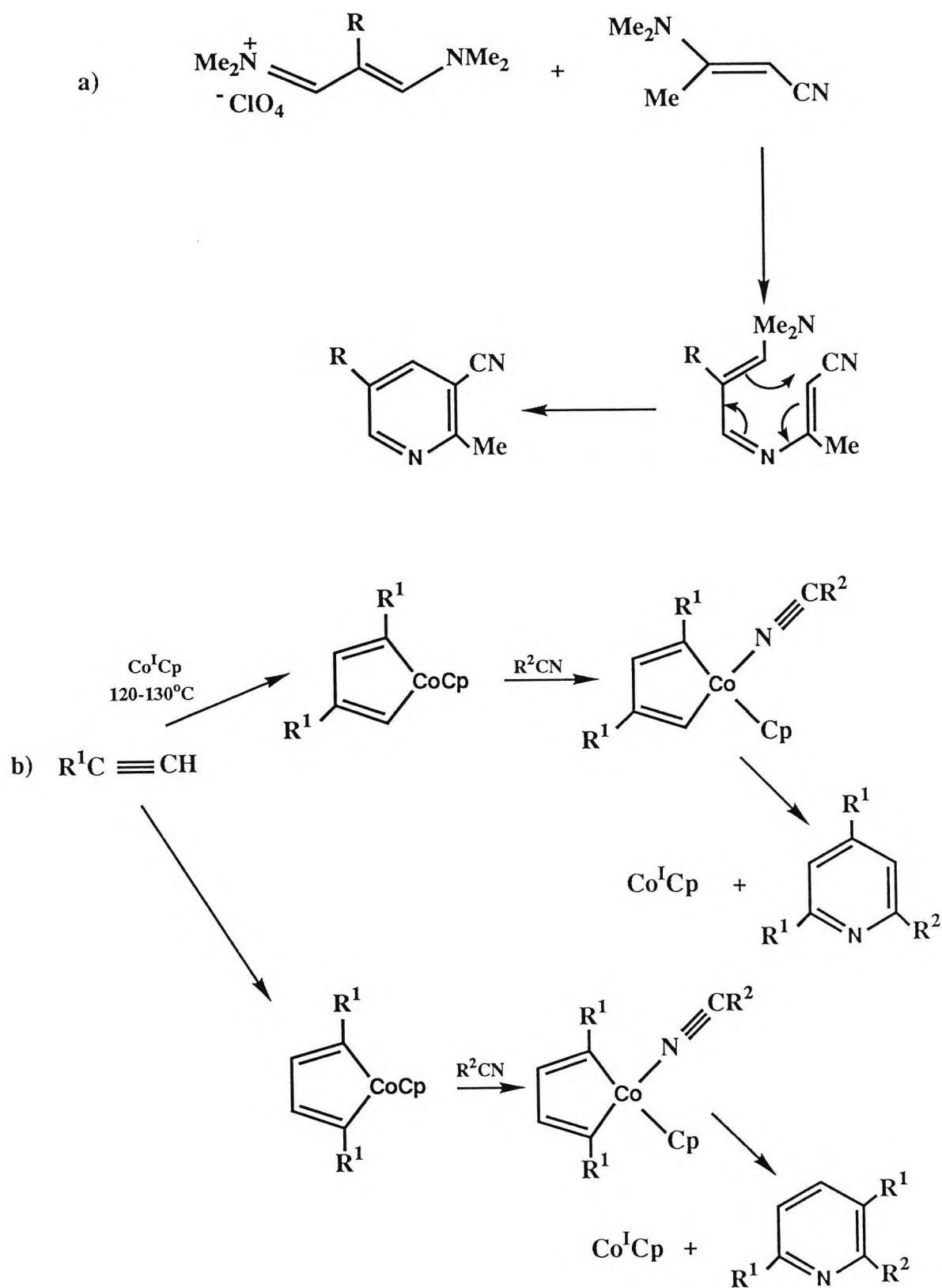
SCHEME 1-6
AN EXAMPLE OF THE KRÖHNKE SYNTHESIS OF SUBSTITUTED PYRIDINES



Other methods of preparation of substituted pyridine include [4+2] cycloadditions (e.g. Scheme 1-7(a)), and the combination of alkynes and nitriles using organocobalt catalysts (e.g. Scheme 1-7(b)).

In reviewing the attempted syntheses of bipyridines identified for this project, it was found there were accessible routes to these compounds, utilising nucleophilic and electrophilic substitution of readily available bipyridine starting materials. It was, therefore, not necessary to conduct Ullman type reactions for the preparation of the substituted bipyridines. This was perhaps an advantage, as the yields from the pyridine coupling reactions are reportedly low, and the separation of the required compound from the reaction by-products is often complex and lengthy.

SCHEME 1-7
EXAMPLES OF OTHER METHODS OF SYNTHESIS OF PYRIDINES



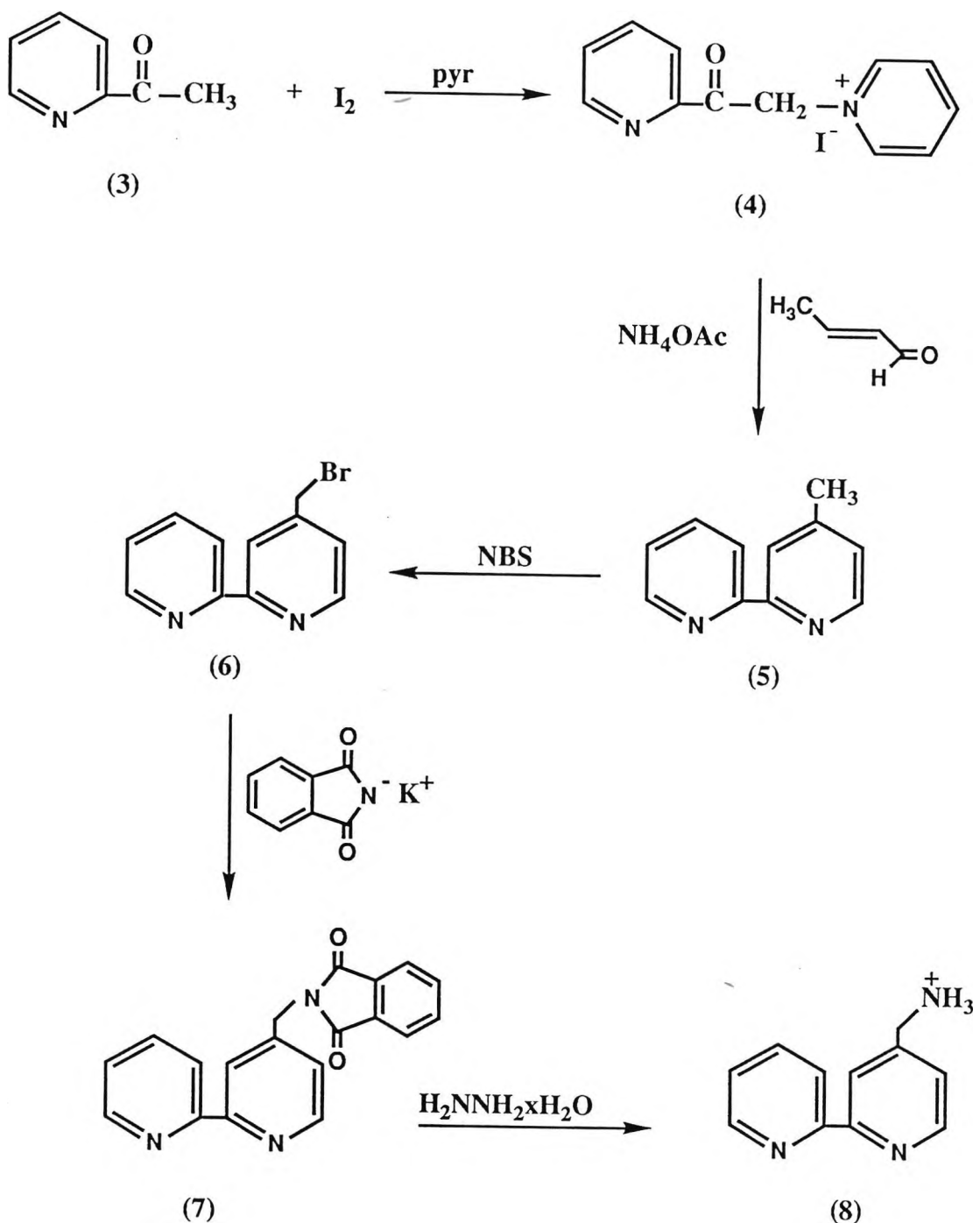
1:1:1 PREPARATION OF 4- AND 4,4'-AMINO SUBSTITUTED 2,2'-BIPYRIDINE

The preparation of 4-aminomethyl-2,2'-bipyridine (8) by the synthetic route shown below was attempted (Scheme 1-8). One of the key intermediates in this synthetic protocol was 4-methyl-2,2'-bipyridine (5). The suggested method of preparation of (5) was that of Kröhnke [8], which involved the conjugate addition of a pyridinium ylide to an unsaturated carbonyl compound yielding a 1,5-diketone. The 1,5-diketone thus formed, was then cyclised in the presence of ammonia, to form, in this case, a 4-methyl pyridine, attached via its 2-position to the pyridine present in the starting material (3). As can be seen from Scheme 1-8, the first step in the proposed reaction sequence involved the preparation of 1-(2-acetylpyridine) pyridinium iodide (4). This preparation was attempted according to the method of Kröhnke and Gross [9]. However, two main problems were encountered following this protocol. Firstly, that quantities of pyridine hydrogen iodide were formed, due to complexation of iodine to pyridine present in the reaction media. Secondly, it proved difficult to remove iodine from the isolated product. The iodine was finally removed by the use of decolourising charcoal, while the pyridine hydrogen iodide was removed by washing the product with water.

It was found that both of the above procedures resulted in the loss of quantities of (4), thus rendering the yield of this required product low. It was also observed, that the pyridine hydrogen iodide contaminant could not be completely removed from the reaction product.

It was, therefore, decided to abandon the method of Kröhnke and Gross [9] and pursue an alternative method of preparation of (4), that of King [10]. This method was found to improve the yield of the pyridinium iodide (4) from the original figure of 5% to approximately 18%. The proposed synthetic scheme, (Scheme 1-8), was then continued as far as the preparation of 4-methyl-2,2'-bipyridine (5) via the protocol of Huang and Brewer [11].

SCHEME 1-8
PROPOSED SYNTHETIC ROUTE TO THE PREPARATION OF 4-AMINOMETHYL
2,2'-BIPYRIDINE (5)



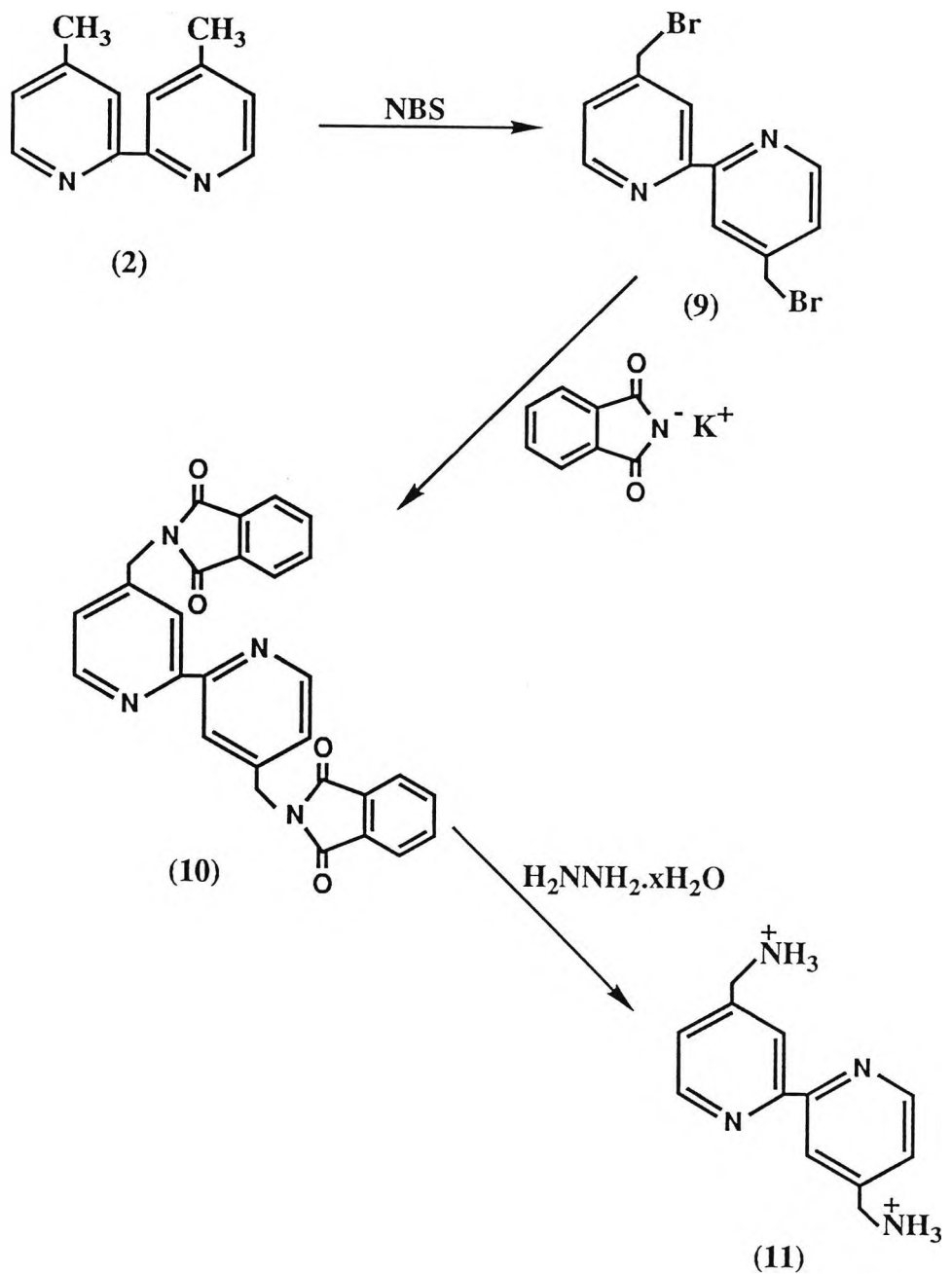
It was, however, this step in the synthetic scheme that proved to be a major problem in the synthesis of 4-aminomethyl -2,2'-bipyridine (8). The reaction of (4) with 2-butenal resulted in the recovery of crude (5) in low yield. Subsequent attempts to purify the crude product by column chromatography, using a column of basic alumina, eluted with a hexane\acetone mixture (9:1), resulted in the decomposition of the reaction products.

Parker [12] had reported a similar protocol to that of Huang and Brewer [11] for the preparation of 5-methyl-2,2'-bipyridine. This method was, therefore, applied to the synthesis of (5) in an attempt to increase the reaction yield. Parker's synthesis differed from that of [11] in two respects. Firstly, it used a larger excess of ammonium acetate (13 fold), and secondly, substituted formamide for methanol. The resulting yield of crude (5) was increased. However, purification of the crude product by column chromatography (alumina column (activity II-III) eluted with dichloromethane/hexane (90:10)), resulted in (5) being obtained in low yield and in an impure form, (impurities were found to be present when tested by ^1H nmr spectroscopy). It was at this point, that, due to the problems encountered in the synthetic Scheme 1-8, regarding the low yields and the contaminant problems in the preparation of both (4) and (5), this synthesis was abandoned.

With the failure of the reaction Scheme 1-8, at the point of synthesis of 4-methyl-2,2'-bipyridine (5), it was decided to continue the synthesis of an aminomethyl bipyridine derivative via the sequence outlined in Scheme 1-9, utilising a readily available starting material, namely 4,4'-dimethyl-2,2'-bipyridine (2). The proposed synthetic route results in the synthesis of 4,4'-diaminomethyl -2,2'-bipyridine (11) via a procedure analogous to that proposed by Parker [12], for the synthesis of 5-aminomethyl -2,2'-bipyridine. The first stage in this protocol involved the monobromination of (2) with N-bromo succinimide (NBS). Initial reaction conditions utilised a 1:2 molar ratio of (2) to NBS: the reaction being monitored by ^1H nmr spectroscopy. After 17 hours, a distinct singlet was observed in the nmr spectrum at 4.28.

SCHEME 1-9

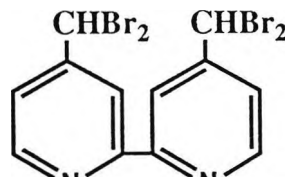
SYNTHETIC SCHEME FOR THE SYNTHESIS OF 4,4'-DIAMINOMETHYL -2,2'-BIPYRIDINE (11)



This singlet was assigned to the pyr-CH₂Br protons of the monobrominated bipyridine derivative (9). Also indicated to be present in the reaction mixture was starting material (2). The reaction was allowed to continue for 27 hours; however, examination of the reaction mixture at this time by ¹H nmr spectroscopy, revealed that (9) was not the major product and that there was still a heavy presence of starting material.

In an attempt to drive the reaction to completion and so increase the yield of (9), a further molar equivalent of NBS was added to the reaction mixture after 5 hours of reaction. Again, the reaction was monitored by ¹H nmr spectroscopy. This increase in the molar ratio of NBS resulted in a decrease in the amount of starting material present in the reaction mixture. However, ¹H nmr spectroscopy revealed a further singlet at 6.28. This singlet was assigned to the pyr-CHBr₂ protons. Therefore, the increase in the molar ratio of NBS had resulted in the formation of the dibrominated derivative (12).

Fig. 1-1 Figure Showing the Dibrominated Product formed on Reaction of 4,4'-dimethyl-2,2'-bipyridine with NBS



(12)

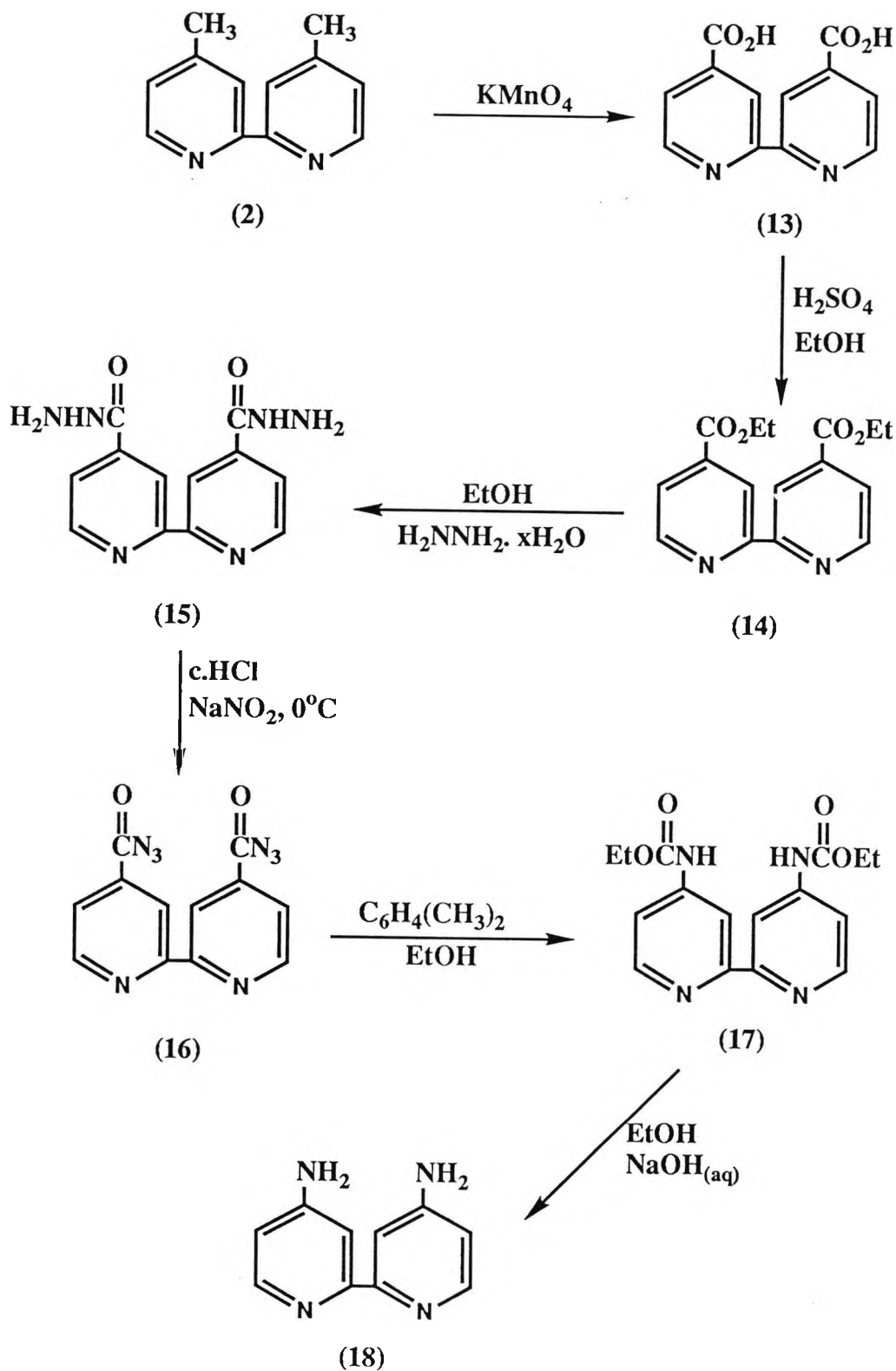
The bromination of (2) was again attempted, using an initial molar ratio of 1:3 4,4'-dimethyl-2,2'-bipyridine to NBS. This exhibited an improvement on previous methods but the product was still contaminated with starting material (2) and the dibrominated derivative (12). At this point, it was decided to continue with the synthesis of 4,4'-diaminomethyl-2,2'-bipyridine (11) using the crude product from the bromination reaction, in the belief that the resulting mixture of products could then be separated to yield the product (11). This strategy, however, resulted in the recovery of material in low yield, which analysis showed did not contain the required product (11).

Another attempt to drive the monobromination to completion involved the utilisation of chloroform as the reaction solvent. This, however, resulted solely in the formation of bromine. It was noted, that, if the concentration of NBS in the reaction mixture was too high, polymerisation resulted in the reaction mixture.

At this point, the overall synthetic strategy of this aspect of the project was assessed. It was decided to concentrate synthetic efforts on the direct substitution of the aromatic rings with amino functionalities. 4,4'-diamino-2,2'-bipyridine (18) was, therefore, defined as the new target molecule. It was proposed to prepare (18) by adaptation of a synthetic route proposed by Whittle [4] for the synthesis of 5,5'-substituted bipyridines (Scheme 1-10).

The first stage in the scheme involved the preparation of a dicarboxylic acid derivative (13), via oxidation of 4,4'-dimethyl-2,2'-bipyridine (2) with potassium permanganate. The resulting yield of this reaction was low. This was believed to be due, at least in part, to the poor solubility of the starting material (2) in the reaction solvent; a fact borne out by the recovery of unreacted (2) at the filtration step of the reaction workup. Attempts to raise the reaction yield failed.

SCHEME 1-10
SYNTHETIC SCHEME FOR THE SYNTHESIS OF 4,4'-DIAMINO-2,2'-BIPYRIDINE (18)



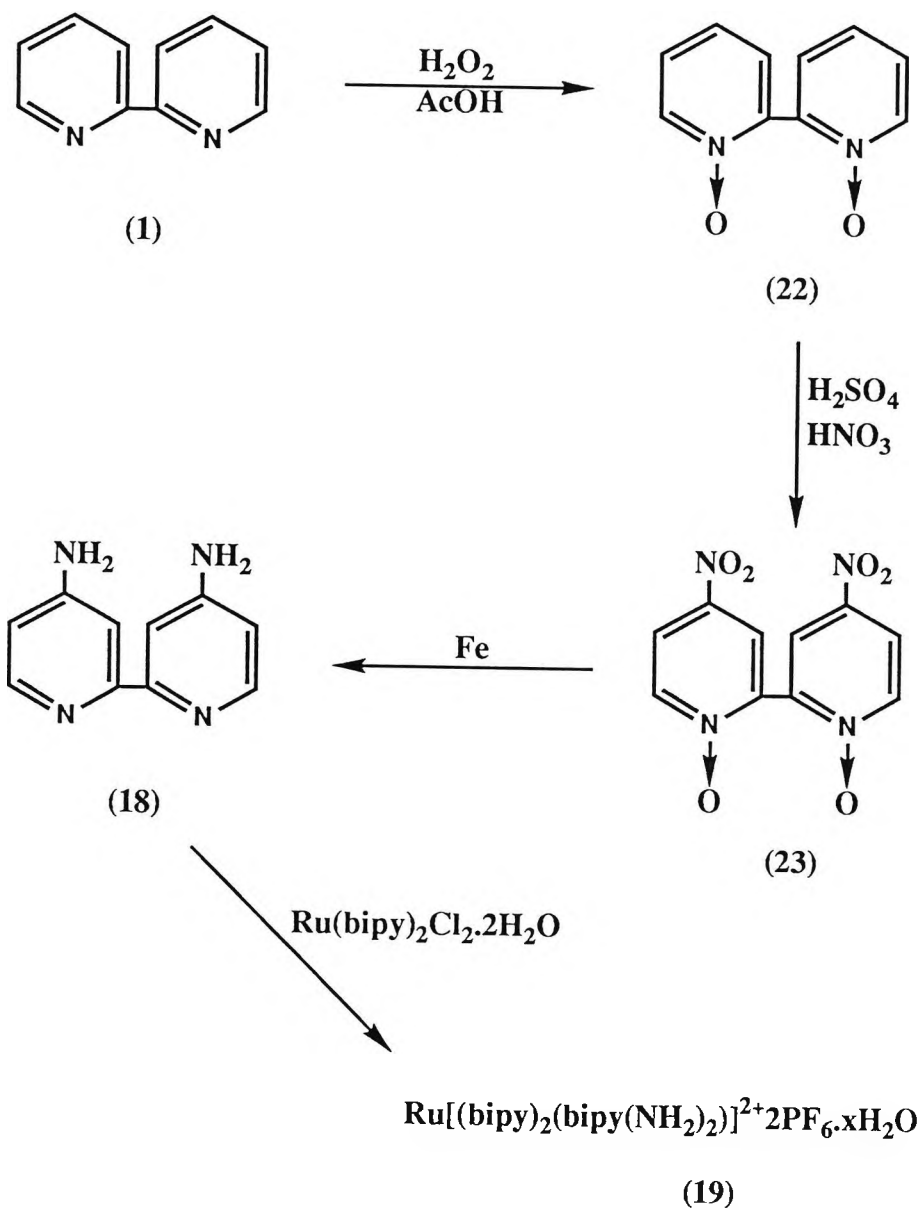
The next two stages in Scheme 1-10 which would result in the preparation of both the ethyl ester derivative (14) and the dicarbazide (16) appeared to proceed well and in good yield. Problems were, however, encountered in the next stage of the reaction sequence involving the preparation of 4,4'-di(ethoxy-carbonylamino)-2,2'-bipyridine (17). The reaction originally appeared to proceed well resulting in a solid, (thought to be the required product), being isolated. The assumption that the recovered material was the required product appeared to be supported by infra-red spectroscopy, (KBr disc), which seemed to indicate the presence of functional groups consistent with the structure of (17). However, the structure of the product could not be confirmed by ^1H nmr spectroscopy due to the high insolubility of the solid in organic solvents. CHN analysis, however, appeared to indicate that the solid was not the required product.

It can be seen from Scheme 1-10 that the synthetic step involving the formation of (17) was a Curtius-type rearrangement. From the literature [4], it would appear that this rearrangement proceeds well for the 5,5'-bipyridine derivatives. The failure of this method must, therefore, be related to the difference in the substitution positions between the literature product [4] and the required product (17). It may be that steric hindrance present in the preparation of the 4-substituted derivative, is in some way elevated in the 5-substituted derivative.

On the basis of the infra-red spectroscopy information received on the product from the Curtius rearrangement, it was decided to continue with the synthesis of 4,4'-diamino-2,2'-bipyridine (18). However, material was only recovered from this reaction in very low yield and, although infra-red spectroscopy of the product appeared encouraging, CHN analysis was not consistent with the required product (18).

At this point, the above synthetic strategy was abandoned in favour of the synthetic scheme outlined in Scheme 1-11. This synthetic route involved the reduction of 4,4'-dinitro-2,2'-

SCHEME 1-11
ALTERNATIVE SCHEME FOR THE SYNTHESIS OF 4,4'-DIAMINO-2,2'-BIPYRIDINE (18)

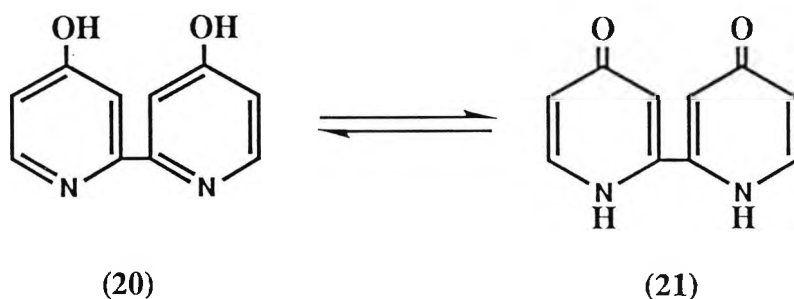


bipyridine N,N'-dioxide (23) with iron resulting in the preparation of 4,4-diamino-2,2'-bipyridine (18), via the protocol of Maerker and Case [13]. The N-oxide starting materials (22) and (23) required for this strategy were prepared according to the method reported by Seddon et al [14], which will be discussed later in some detail in the section on the synthesis of hydroxy substituted bipyridines (Section 1:1:2). Material was recovered in low yield from the reduction of 4,4'-dinitro-2,2'-bipyridine N,N'-dioxide (23) with iron. Infra-red spectroscopy, (KBr disc), appeared to give information consistent with the functionalities present in (18), but CHN analysis indicated that the product was not pure. Although the isolated material was impure, it was decided to proceed with the crude (18) towards the preparation of bis(2,2'-bipyridine) (4,4'-diamino-2,2'-bipyridine) ruthenium (II) hexafluorophosphate (19) via a method submitted by Constable [15] for the synthesis of ruthenium complexes of this type. ^{13}C nmr spectroscopy of the material obtained from the above reaction appeared to indicate that it contained the required product (19), but the nmr spectrum also indicated the presence of a carbon impurity, a fact confirmed by CHN analysis. An attempt was then made to purify the crude material by gel permeation chromatography (Sephadex LH-20 eluted with ethanol). The resulting material was confirmed to be (19) by CHN analysis, thus indicating that the impurity in the crude product was probably unreacted organic starting material.

1:1:2 PREPARATION OF 4 AND 4,4'-HYDROXY SUBSTITUTED 2,2'-BIPYRIDINES

The initial intention was to prepare 4,4'-dihydroxy-2,2'-bipyridine (20) directly by nucleophilic attack on the 4 positions of bipyridine. However, a synthesis of this type would be problematical, as, not only does nucleophilic attack favour the 6 position on this heterocyclic species, but 4,4'-dihydroxy-2,2'-bipyridine is also believed to tautomerise easily (Fig. 1-2), and is, therefore, thought to be highly unstable.

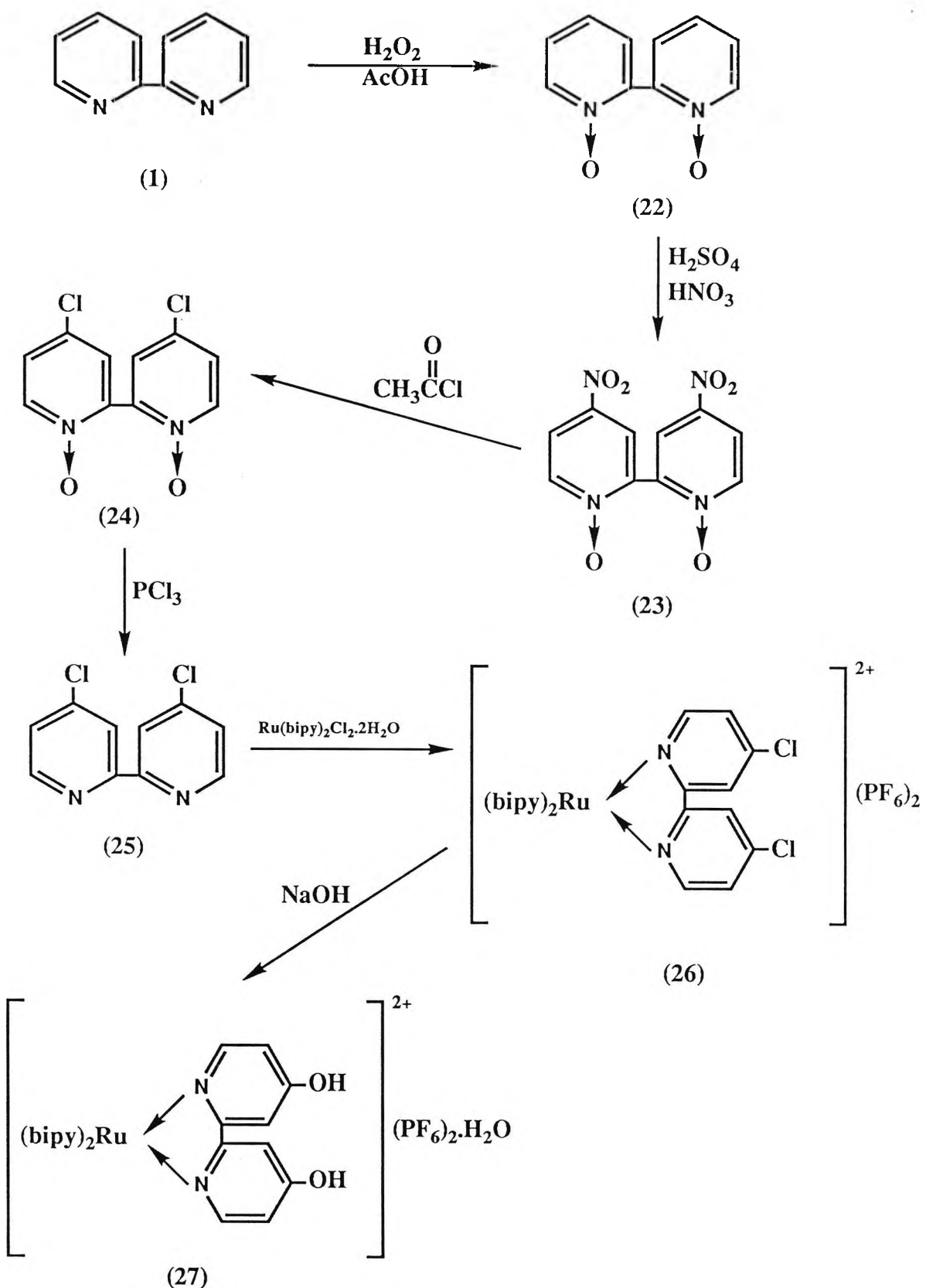
Fig. 1-2 Figure showing Tautomerisation of 4,4'-dihydroxy-2,2'-bipyridine



A preparation of 4,4'-dihydroxy-2,2'-bipyridine has however, been reported by Constable [15], in which the hydroxy compound is prepared via nucleophilic attack of 4,4'-dichloro-2,2'-bipyridine once it is co-ordinated to ruthenium (II), (Scheme 1-12). The basis of this paper, is that co-ordination of 2,2'-bipyridine to ruthenium, results in a lowering of the energy of the LUMO at the 2 and 4 positions, thus activating these positions towards nucleophilic attack.

SCHEME 1-12

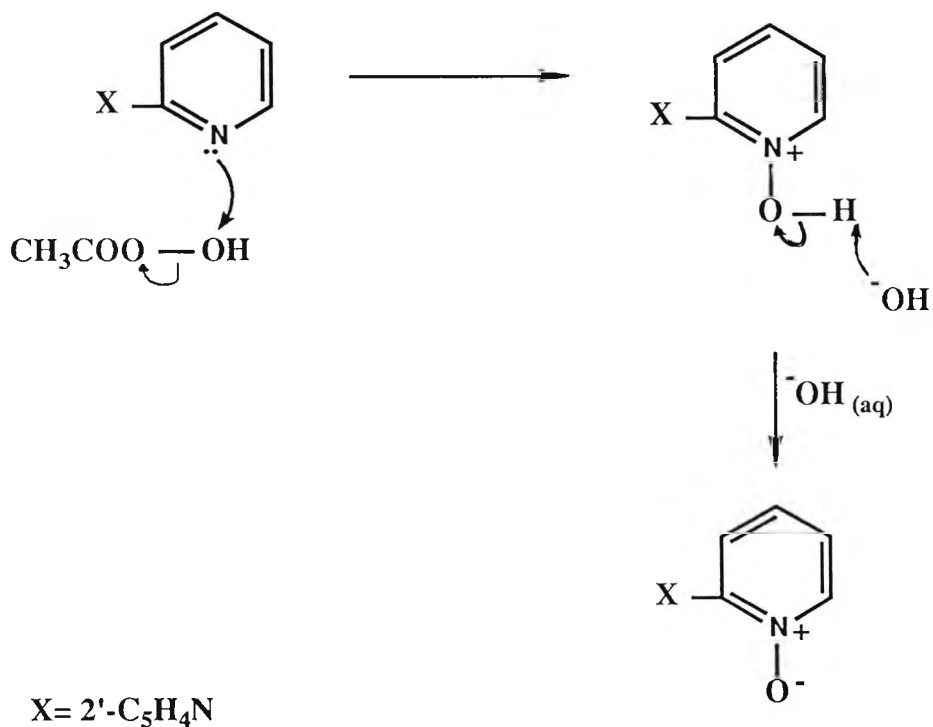
SYNTHETIC SCHEME FOR THE SYNTHESIS OF A 4,4'-DIHYDROXY-2,2'-BIPYRIDINE RUTHENIUM (II) COMPLEX



The proposed synthetic route (Scheme 1-12), therefore, involved synthesis of 4,4'-dichloro-2,2'-bipyridine (25) and its later co-ordination to ruthenium.

As has been previously mentioned, in section 1:0:1, the 4-position on 2,2'-bipyridine is not the most highly activated towards substitution reactions. Therefore, synthesis of (25) must first involve activation of this position. This activation is achieved by reaction of 2,2'-bipyridine with peracetic acid, resulting in the oxidation of the nitrogen of bipyridine (Scheme 1-13).

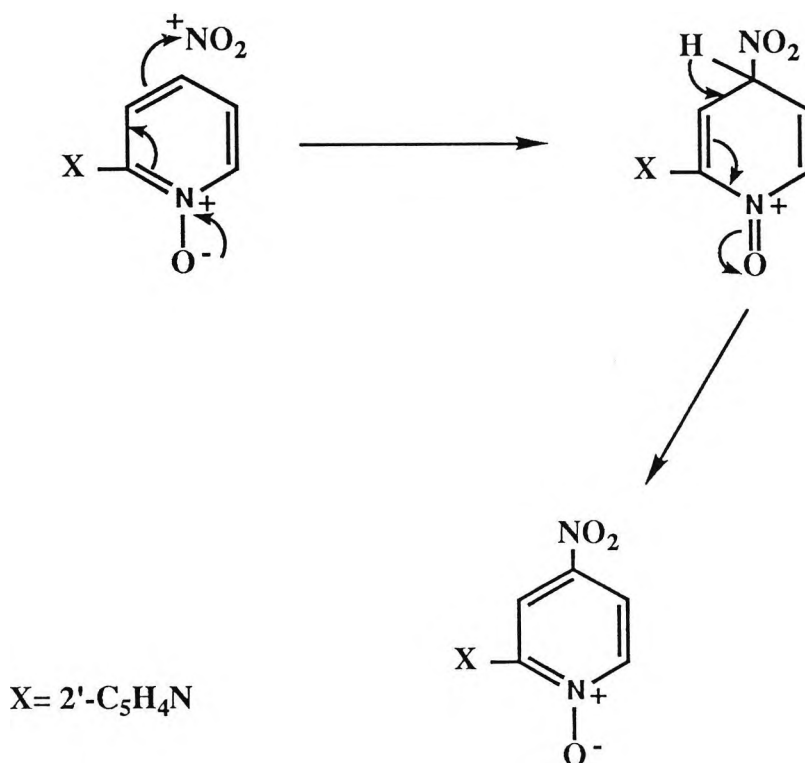
SCHEME 1-13
REACTION MECHANISM FOR THE N-OXIDATION OF BIPYRIDINE



As a consequence of the formation of 2,2'-bipyridine N,N'-dioxide (22), the 4 position of the heterocyclic ring is activated towards electrophilic attack (Scheme 1-14). Therefore, in the presence of the electrophile NO_2^+ the dinitro product (23) is formed. The nitro groups then readily exchange with nucleophiles; in this case a chloride ion, resulting in the formation of 4,4'-dichloro-2,2'-bipyridine N,N'-dioxide (24). This leaves (24) to be deoxygenated in the presence of phosphorus trichloride thus yielding 4,4'-dichloro-2,2'-bipyridine (25), [13,14].

SCHEME 1-14

REACTION MECHANISM FOR THE NITRATION OF BIPYRIDINE N-OXIDES



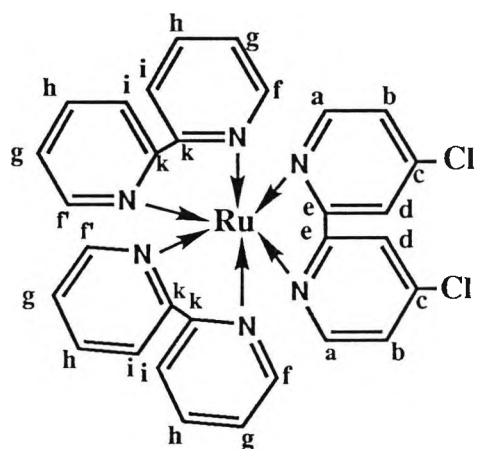
Two literature procedures are quoted for the preparation of 2,2'-bipyridine N,N'-dioxide (22), namely that of Maerker and Case [13], and the proposal of Seddon et al [14]. These literature procedures differ only in their methods of generation of peracetic acid. Maerker and Case [13] quote a prior publication of Haginiwa [16], which proposes the addition of hydrogen peroxide at the commencement of the reaction only. However, the protocol of Seddon et al [14] advocates the addition of hydrogen peroxide in two portions, firstly at the commencement, and secondly, 3 hours into the reaction time.

Repetition of both these methods resulted in a slightly higher yield being obtained, when the method of Seddon et al [14] was followed. Presumably, the increased yield was due to the generation of a greater quantity of peracetic acid under these reaction conditions. It should be noted, that during the course of preparation of 2,2'-bipyridine N,N'-dioxide, the reaction yield was strongly affected by both thermal decomposition and decomposition due to exposure of the reaction product to light. A similar problem was noted during the synthesis of 4,4'-dinitro-2,2'-bipyridine N,N'-dioxide (23). Reaction yields of (23) were found to be variable due to the extreme sensitivity of this compound to decomposition under reaction conditions.

4,4'-dichloro-2,2'-bipyridine N,N'-dioxide (24) was obtained easily as proposed in Scheme 1-12 [14]. However, repeated recrystallisations of the crude reaction product from dimethyl-formaldehyde (DMF), resulted in decomposition of (24). Consequently, the synthetic route was continued to the synthesis of 4,4'-dichloro-2,2'-bipyridine (25) using crude (24), via an analogous procedure to that conducted by Maerker and Case, [13], for the preparation of 4,4'-dibromo-2,2'-bipyridine. This method resulted in the preparation of (25) in low yield. A factor contributing to the low yield of (25) may have been, that the presence of moisture in the reaction starting materials was found to severely depress the resulting yield of 4,4'-dichloro-2,2'-bipyridine (25).

The preparation of bis(2,2'-bipyridine) (4,4'-dichloro-2,2'-bipyridine) ruthenium (II) hexafluorophosphate (26) was attempted via the protocol of Constable [15]. This involved the reaction of cis-dichloro bis(2,2'-bipyridine) ruthenium (II) with 4,4'-dichloro-2,2'-bipyridine (25). Material isolated from this reaction was examined by ^{13}C nmr spectroscopy and found to exhibit 11 aromatic carbon signals. Initial examination of the structure of (26), however, gave rise to the expectation of 10 aromatic signals. On re-examination of the structure of (26), it can be seen from Fig. 1-3, that there are possibly 3 chemical environments for the carbon atoms at the 6 and 6' positions in the heterocyclic rings, corresponding to a, f and f' (Fig. 1-3).

Fig. 1-3 Diagram Illustrating possible Carbon Signals seen by ^{13}C nmr



Considering the first environment a; from Figure 1-3, it can be seen that this corresponds to the 6 and 6' carbon atoms of the dichloro substituted bipyridine ligand, giving rise to one signal in the ^{13}C nmr spectra.

Taking the two similar unsubstituted bipyridines into account, again from Figure 1-3, it appears that 6 and 6' carbon atoms of these ligands are in two different chemical environments.

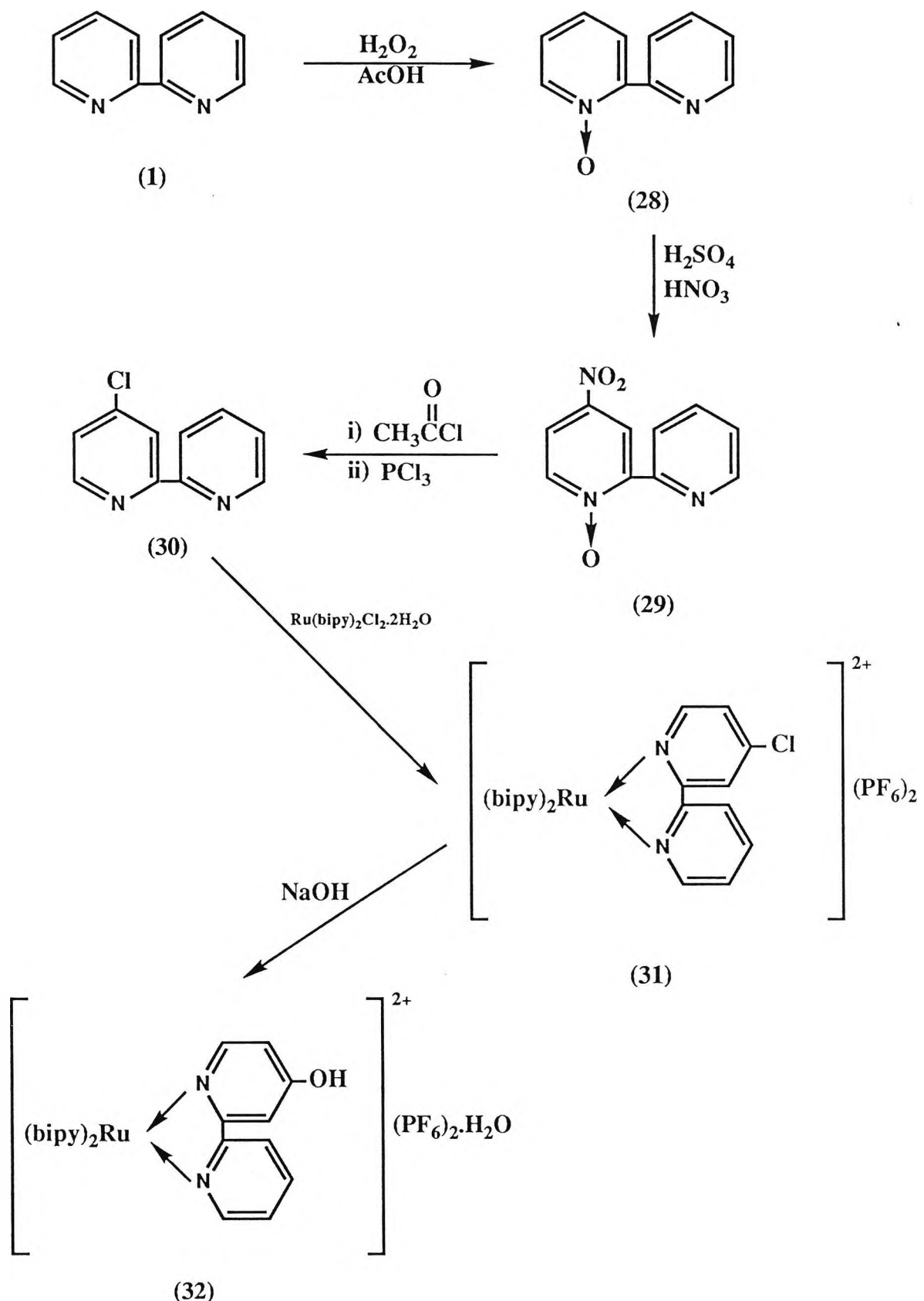
Firstly, these carbon atoms can either be adjacent to the substituted bipyridine ligand, resulting in environment f, corresponding to an aromatic carbon signal, or secondly in close proximity to the unsubstituted bipyridine, giving rise to another environment f' and thus a further aromatic carbon signal. Thus three carbon signals arise due to the different chemical environments of the 6 and 6' carbon atoms of the heterocycles, instead of the initially expected two. This, therefore, explains the presence of the unexpected signal in the aromatic region of the ^{13}C nmr spectra of (26).

At this point it was considered to be beneficial to prepare bis(2,2'-bipyridine) (4-hydroxy-2,2'-bipyridine) ruthenium (II) hexafluorophosphate (32) as well as the dihydroxy substituted complex (27). (32) would thus give a comparison with complex (27), indicating the effect exhibited by one point of attachment to an antibody, as opposed to two that would be obtained utilising complex (27).

The proposed synthesis of bis (2,2'-bipyridine) (4-hydroxy-2,2'-bipyridine) ruthenium (II) hexafluorophosphate (32) was via a route similar to that conducted for the preparation of (27) (Scheme 1-15). The initial stage of the synthesis involved the preparation of 2,2'-bipyridine N-oxide (28) via a method proposed by Jones et al [17]. However, this procedure resulted only in the isolation of 2,2'-bipyridine N,N'-dioxide (22), despite reducing both the suggested reaction temperature and the proportion of hydrogen peroxide in the reaction mixture.

A broadly similar protocol for the synthesis of (28), that of Mlochowski [18, 19] was attempted. This resulted in an alteration of the reaction solvent to toluene and an increase in the reaction temperature from 50°C to 75°C. Monitoring of the reaction by TLC (SiO_2 : ethyl acetate, methanol and ammonia (4:2:1)), showed that the reaction time could be reduced from

SCHEME 1-15
SYNTHETIC SCHEME FOR THE SYNTHESIS OF A 4-HYDROXY-2,2'-BIPYRIDINE RUTHENIUM (II) COMPLEX



12 to 5.5 hours. These alterations to the reaction conditions of Jones et al [17] did in fact result in the isolation of (28).

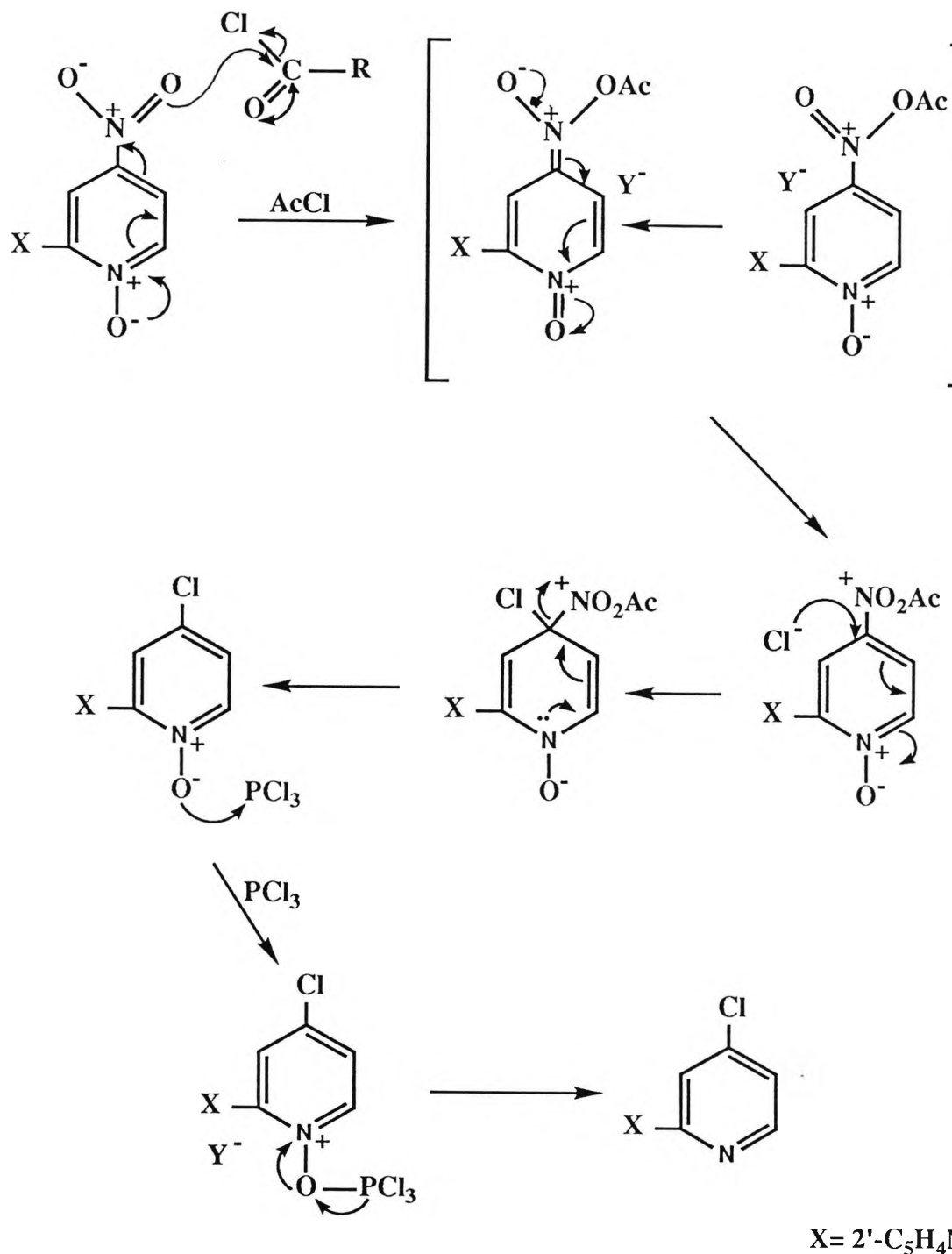
4-chloro-2,2'-bipyridine (30) was prepared by reaction of 4-nitro-2,2'-bipyridine N-oxide (29) with acetyl chloride and phosphorus trichloride via a modification of the Jones procedure [17] reported by Cook et al [20]. In the Jones protocol [17], both acetyl chloride and phosphorus trichloride are added at the commencement of the reaction. However, Cook et al [20] report that this probably results in the deoxygenation of (29) by phosphorus trichloride, before it reacts with acetyl chloride, thus deactivating the aromatic ring towards nucleophilic attack and preventing the formation of the desired product. Cook et al [20] therefore proposed the refluxing of 4-nitro-2,2'-bipyridine N-oxide (29) with excess acetyl chloride, prior to the addition of phosphorus trichloride, to overcome this problem. In fact, in our hands, the reaction was found to proceed well and in good yield following this modification [20].

The mechanism of the formation of 4-chloro-2,2'-bipyridine (30) appears to be uncertain. The experimental evidence would appear to point to a mechanism of the type shown in Scheme 1-16, [19]. This proposes that the exposure of (29) to acetyl chloride results in nucleophilic attack by the nitro group of (29) on the carbonyl of acetyl chloride, giving rise to the formation of an intermediate and the production of a chloride ion. The intermediate thus formed is prone to nucleophilic attack, which occurs from the liberated chloride ion, thus producing 4-chloro-2,2'-bipyridine N-oxide. The chlorinated bipyridine N-oxide can then be deoxygenated by phosphorus trichloride thus yielding the desired product 4-chloro-2,2'-bipyridine (30).

The synthesis of bis (2,2'-bipyridine) (4-chloro-2,2'-bipyridine) ruthenium (II) hexafluorophosphate (31) was carried out via the protocol of Constable [15]. The material obtained from this reaction was confirmed to be (31) by ^{13}C nmr spectroscopy and CHN analysis.

SCHEME 1-16

PROJECTED MECHANISM FOR THE DEOXYGENATION OF 4-NITRO-2,2'-BIPYRIDINE BY PHOSPHORUS TRICHLORIDE [19]



The ^{13}C nmr spectra of bis(2,2'-bipyridine) (4-chloro-2,2'-bipyridine) ruthenium (II) hexafluorophosphate (31) was found to give an extra carbon aromatic signal from that expected; a similar situation to that observed in the ^{13}C nmr spectra of the ruthenium complex (26). As for (26), this extra signal could probably be assigned to signals resulting from the different chemical environments of the 6 and 6' carbon atoms of the unsubstituted bipyridine ligands.

As both the chloro complexes (26) and (31) had now been isolated, the synthesis could be carried through to the hydroxy complexes (27) and (32), using the proposed method of Constable [15]. This method involves nucleophilic attack at the chlorinated positions on the heterocycles, by treating them with sodium hydroxide, resulting in the formation of the hydroxy complex. Initial attempts to form the dihydroxy complex (27) yielded material, that, upon examination by CHN analysis was found to be neither the required product nor the starting material; a fact confirmed by infra-red spectroscopy. ^{13}C nmr spectroscopy of the reaction product indicated the presence of bipyridine type structures, but did not clearly indicate the presence of (27). The reaction time was then increased to 48 hours and the progress of the reaction monitored by ^{13}C nmr spectroscopy. The spectroscopy showed that two materials were present; starting material (26) and the required product (27). Further attempts to drive the reaction to completion by lengthening the reaction time failed.

The mono-chloro complex (31) was found to exhibit similar behaviour to (26). Therefore, as it was clear that the hydroxy complexes (27) and (32) could only be obtained in low yield, it was decided to abandon this synthesis.

All the target molecules discussed so far have involved the direct attachment of antibody to the bipyridine ring. However, separation of the luminescent centre from the antibody may prove to be of greater advantage than direct attachment. It is probable, that this separation may lead to better linkage of the label to the protein. Also, possibly, conjugation of the label

to the antibody via a linker may result in improved preservation of antibody affinity, which can be severely affected by direct conjugation. Such a separation can be achieved via an alkyl chain, the length of which must, however, be controlled, because alkyl chains are flexible. Therefore, a chain which is too long may cause the complex to fold back on itself and so reassociate with the antibody.

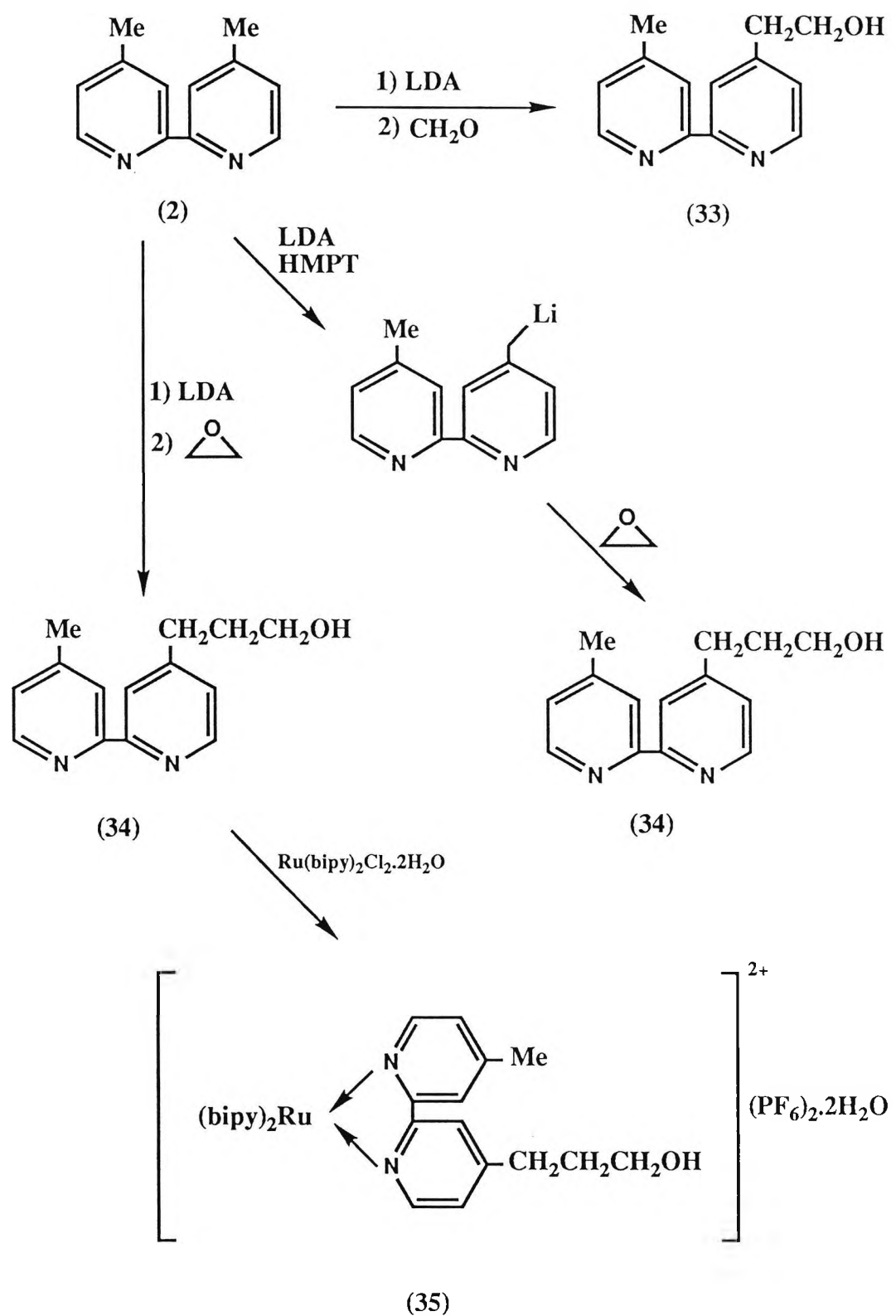
It was proposed that the first complex of this type to be synthesised, would contain the substituted ligand 4-hydroxyethyl-4'-methyl-2,2'-bipyridine (33), the proposed synthesis of which, utilised the method of Ghosh and Spiro [21], shown in Scheme 1-17.

This protocol uses the starting material 4,4'-dimethyl-2,2'-bipyridine (2), which is lithiated by lithium diisopropylamine (LDA), resulting in the removal of the most acidic proton, namely one of the protons from the methyl substituent. Subsequent reaction of the lithiated species with formaldehyde should then yield the product (33), [21]. In our hands, the reaction of (2) with LDA appeared to give the lithiated product, which was indicated by the orange-brown colouration of the reaction mixture. Next, attempts were made to introduce formaldehyde gas, generated by heating paraformaldehyde in a separate vessel. These attempts failed, due to repolymerisation of the gas, before introduction into the reaction mixture.

Due to the problems encountered by the introduction of formaldehyde into the reaction vessel, the gas was substituted with ethylene oxide, which does not have the above handling problems of formaldehyde. Such a substitution would result in the formation of the bipyridine ligand 4-(3-hydroxypropyl)-4'-methyl-2,2'-bipyridine (34). This reaction appeared to proceed well, yielding a brown semi-solid oil, that, on examination by ¹H nmr spectroscopy, appeared to contain some of the required product (34). However, spectroscopy also revealed heavy contamination of the crude product by starting material (2). Subsequent attempts to find a suitable recrystallisation solvent failed.

SCHEME 1-17

SCHEME SHOWING POSSIBLE SYNTHETIC ROUTES TO ALKYL HYDROXY BIPYRIDINE RUTHENIUM (II) COMPLEXES



Trituration of the crude product with ethanol was therefore attempted, this resulted in the precipitation of a white solid, which, upon analysis was identified as (2). Ethanol was removed from the triturate under vacuo yielding a brown oil. The identification of a TLC system (silica: ethyl acetate: pet. ether 60°/80°, 1:9), which was capable of separating this oil, resulted in the attempted separation of the oil by column chromatography. However, the crude material appeared to decompose during chromatography. The experiment was, therefore, repeated exchanging the trituration solvent ethanol for ether. This again resulted in the precipitation of a white solid. However, ¹H nmr spectroscopy of this material appeared to indicate that it was the disubstituted product 4,4'-di-(3-hydroxypropyl)-2,2'-bipyridine. Removal of the solvent from the triturate under vacuum gave a brown oil, which analysis by ¹H nmr spectroscopy showed was the desired product (34), contaminated with starting material (2). Column chromatography of the isolated oil was attempted, using a pressure column to reduce the risk of decomposition of the product during chromatography. The system used was, as before, silica eluted with ethyl acetate: pet. ether 60°/80° (1:9). The proportion of ethyl acetate in the elutant was gradually increased, until the elution solvent was totally ethyl acetate. At this point two substances were eluted. The first of these materials was identified as starting material (2), and the second as the required product (34) contaminated with aliphatic material. The experiment was again repeated and an acid-base extraction was performed on the oil isolated from the ether trituration of the crude reaction product. This procedure however, resulted only in the isolation of starting material (2).

An attempt was then made to prepare (34), by a modification of the procedure reported by Kaiser and Petty [22] (Scheme 1-17), which utilises a 1:1 complex of LDA to hexamethylphosphoric-triamide. This method yielded aliphatic material as its major product, with starting material (2) and the desired product (34) as minor products. An attempted Kugel distillation of this crude material, however, resulted in decomposition.

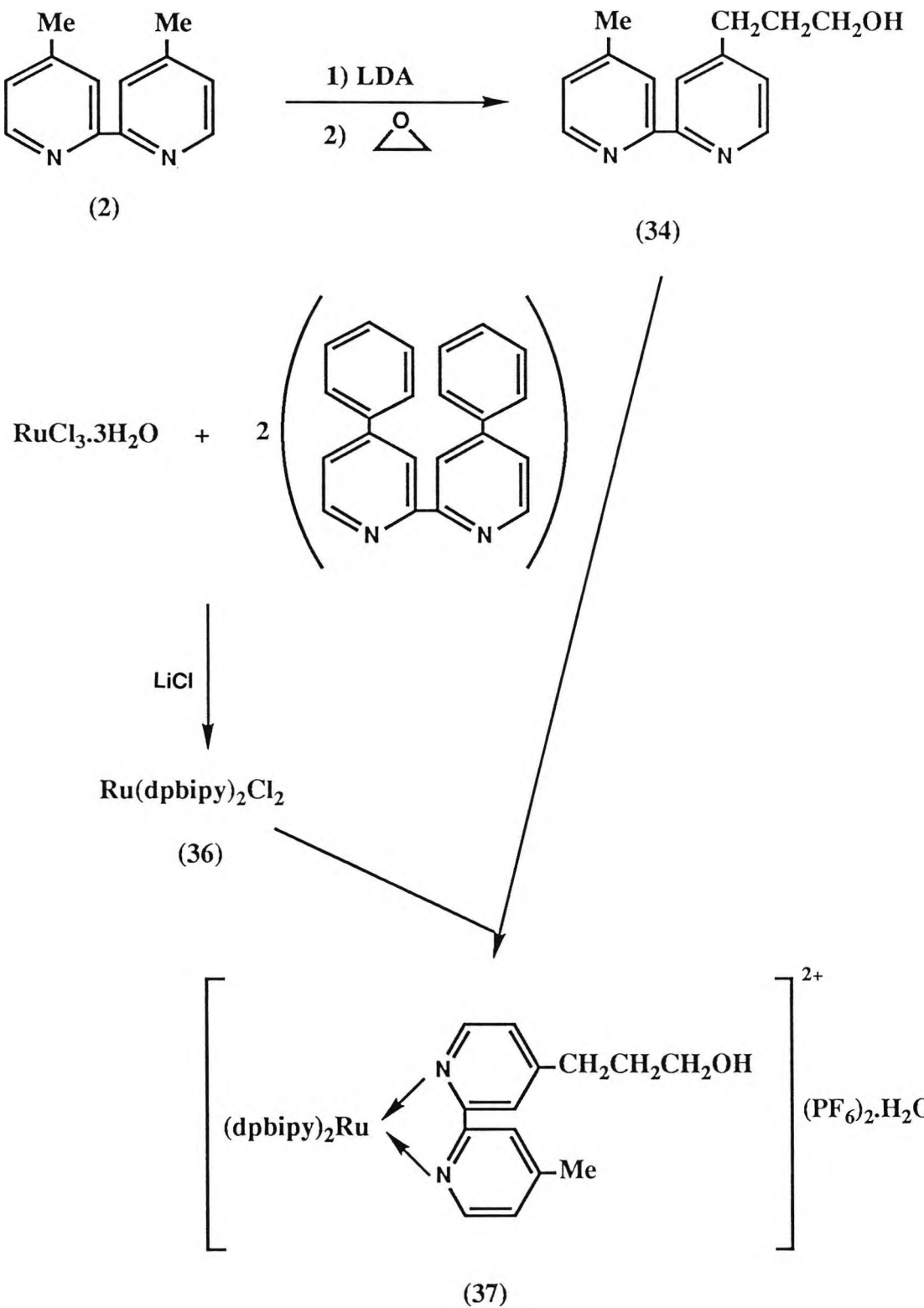
It was now clear, that, due to the instability of (34), it would be difficult to isolate quantities of it in a pure form. It was decided that it would be possible to continue the synthesis to the preparation of the ruthenium complex (35) (Scheme 1-17), using the crude product (34) isolated by column chromatography (see above). It was possible to use this material as although it was impure, its contaminants are only aliphatic in nature, and, as such would not affect chelation of the required bipyridine ligand (34) to ruthenium. The synthesis was, therefore, continued, via a procedure analogous to that proposed by Constable [15] for the preparation of bis(2,2'-bipyridine) (4,4'-dichloro-2,2'-bipyridine) ruthenium (II) hexafluorophosphate (26). The material thus isolated, was confirmed to be the required complex (35) using CHN analysis, ¹H nmr, and ¹³C nmr spectroscopy. ¹³C nmr spectroscopy again exhibited 3 signals corresponding to the 6 and 6' carbon atoms of the bipyridine ligands. Therefore, it appears, that this unexpected carbon signal in the aromatic region of the ¹³C nmr spectra of ruthenium complexes, containing one dissimilar bipyridine ligand, is becoming a characteristic of this type of ruthenium complex.

A further ruthenium complex using ligand (34) was prepared, substituting 4,4'-diphenyl-2,2'-bipyridine for the unsubstituted bipyridines. This would then provide a direct comparison with complex (35), thus showing the effect a higher degree of rigidity and greater conjugation would have on the luminescent lifetime of ruthenium tris bipyridine complexes.

Bis (4,4'-diphenyl-2,2'-bipyridine) (4-[3-hydroxypropyl]-4'-methyl-2,2'-bipyridine) ruthenium (II) hexafluorophosphate (37) was prepared by a method similar to that of (35); again analogous to the protocol reported by Constable [15] (Scheme 1-18). CHN analysis of the material isolated from this reaction showed the complex to be slightly impure. ¹³C nmr spectroscopy showed, that, whilst the spectrum was consistent with the proposed structure, one carbon signal was present in the aromatic region of the spectrum which could not be accounted for in the structure of (37).

SCHEME 1-18

SYNTHETIC SCHEME FOR THE SYNTHESIS OF BIS(4,4'-DIPHENYL-2,2'-BIPYRIDINE) (4[3-HYDROXYPROPYL]-4'-METHYL-2,2'-BIPYRIDINE) RUTHENIUM (II) HEXAFLUOROPHOSPHATE (37)

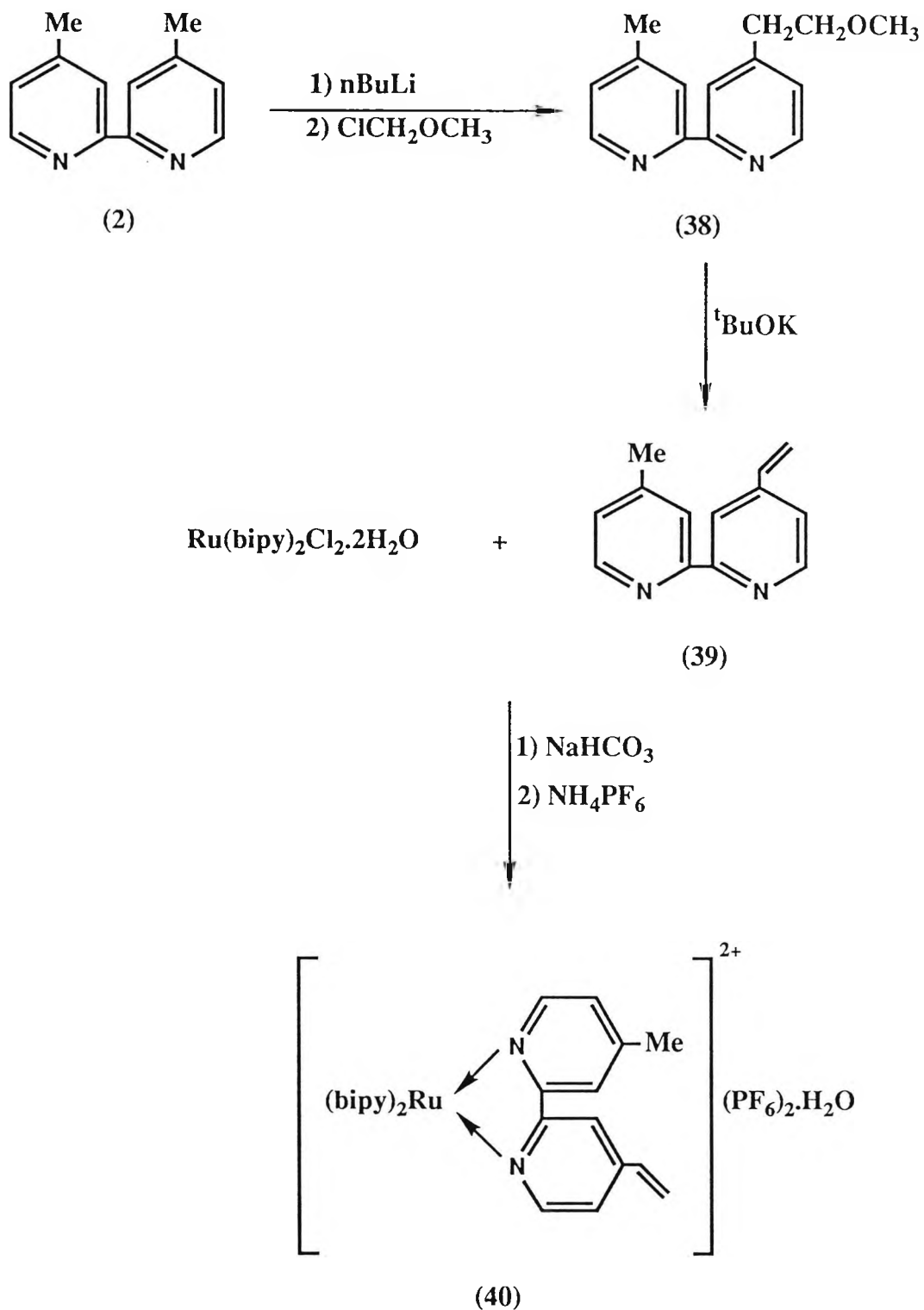


The work conducted so far has concentrated on the production of amino and hydroxy functionalised ruthenium complexes, with the primary purpose of conjugation of these compounds to antibodies, (ref. Chapter 3). With this objective in view, one further functional group should be considered, i.e. the vinyl group. This functionality is open to attack from thiol groups on the protein at high pH. A potential problem in the use of this functionality lies in the fact, that not all proteins bear readily accessible thiol functionalities. However, these can be easily introduced into the protein without incurring loss of biological activity, by modification with Traut's reagent, [23], or NHS-SATA, [24]. In light of this fact, it was decided to synthesize bis(2,2'-bipyridine) (4-vinyl-4'-methyl-2,2'-bipyridine) ruthenium (II) hexafluorophosphate (40) via the synthetic scheme 1-19.

The first step in the synthesis of (40) involved the preparation of 4-vinyl-4'-methyl-2,2'-bipyridine (39). The synthesis of this ligand was achieved via a modification of the procedure of Ghosh and Spiro [21] reported by Abruna et al [25]. This protocol comprises the lithiation of one of the methyl groups of 4,4'-dimethyl-2,2'-bipyridine (2), thus removing the most acidic proton. A nucleophile is formed, which then readily attacks (chloromethyl)methyl ether resulting in the elimination of a chloride ion, hence forming the methoxy methyl derivative (38). ¹H nmr spectroscopy of the material obtained from the lithiation of (2), appeared to confirm the presence of a structure consistent with that expected for (38). However, the spectrum also revealed impurities in the aliphatic region. The next step in the synthesis of 4-vinyl-4'-methyl-2,2'-bipyridine (39) involves treatment of the methoxymethyl derivative (38) with potassium tertiary butoxide resulting in the abstraction of the most acidic proton from (38) and the subsequent elimination of the methoxy group giving the required vinyl derivative (39).

SCHEME 1-19

SYNTHETIC SCHEME FOR THE SYNTHESIS OF BIS(2,2'-BIPYRIDINE) (4-VINYL-4'-METHYL-2,2'-BIPYRIDINE) RUTHENIUM (II) HEXAFLUOROPHOSPHATE (40)



Treatment of the crude (38) obtained above with potassium tertiary butoxide resulted in the isolation of some material, which when examined by ^1H nmr spectroscopy appeared to have a structure consistent with (39), but CHN analysis, revealed that the material was impure. However, the ^1H nmr spectrum of this product suggested that any impurity present was probably inorganic. As it was felt that an impurity of this nature would not interfere with the ligation of (39) to ruthenium the synthesis of bis(2,2'-bipyridine) (4-vinyl-4'-methyl-2,2'-bipyridine) ruthenium (II) hexafluorophosphate (40), was attempted using crude (39), [21]. Infra-red spectroscopy of the material isolated from this reaction, appeared to confirm the presence of the vinyl functionality, and CHN analysis was consistent with the required product (40).

1:2:1 SYNTHESIS OF RUTHENIUM POLYBIPYRIDINE COMPLEXES FOR INVESTIGATION OF THEIR PHOTOPHYSICAL PROPERTIES

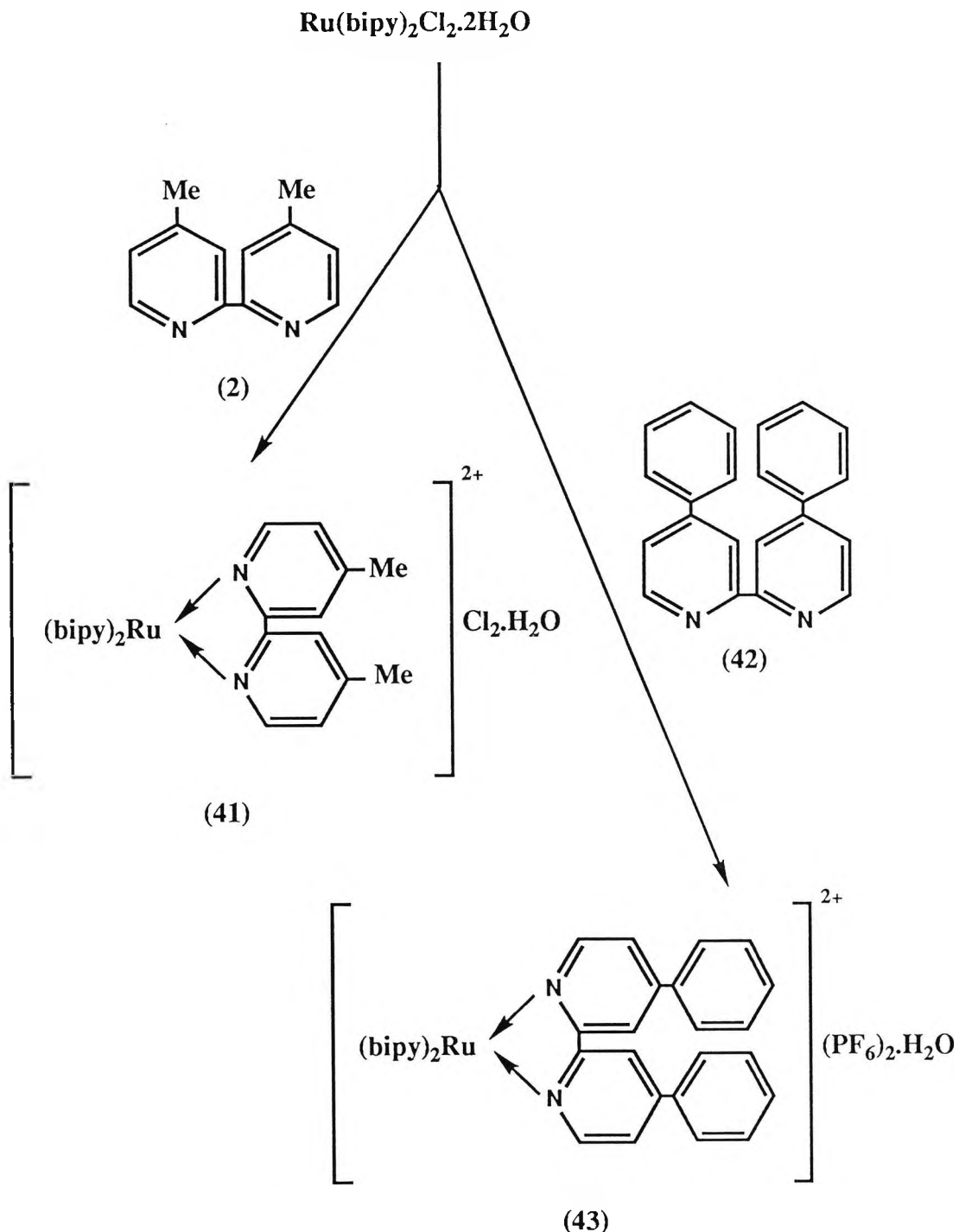
The ruthenium tris bipyridine complexes considered so far could all be conjugated to an antibody and for this reason, were targeted for this specific purpose. It was also believed that it would be of interest to monitor the effect, which various functionalities on the third bipyridine ligand of the complex had on the photophysical processes undergone by such ruthenium compounds.

With this purpose in mind, two complexes were identified for synthesis utilising commercially available ligands. These complexes were bis(2,2'-bipyridine) (4,4'-dimethyl-2,2'-bipyridine) ruthenium (II) chloride (41) and bis(2,2'-bipyridine) (4,4'-diphenyl-2,2'-bipyridine) ruthenium (II) hexafluorophosphate (43), (Scheme 1-20).

The first of these complexes was prepared by refluxing 4,4'-dimethyl-2,2'-bipyridine (2) with cis-dichloro bis(2,2'-bipyridine) ruthenium (II) for 48 hours, then precipitating the complex from the reaction mixture with acetone. Examination of the product obtained from this reaction by ^{13}C nmr spectroscopy, showed its structure to be consistent with that expected for complex (41).

SCHEME 1-20

SCHEME SHOWING SYNTHETIC ROUTES TO BIS(2,2'-BIPYRIDINE) (4,4'-DIMETHYL-2,2'-BIPYRIDINE) RUTHENIUM (II) CHLORIDE (41) AND BIS(2,2'-BIPYRIDINE) (4,4'-DIPHENYL-2,2'-BIPYRIDINE) RUTHENIUM (II) HEXAFLUOROPHOSPHATE (43)



The spectrum obtained revealed two signals corresponding to the 6 and 6' carbons of the bipyridine ligands, which in fact, was the number of signals, that would be expected on initial examination of the structure of (41). However, all ruthenium complexes of this type, in which the third bipyridine ligand differs from the other two, have exhibited three signals corresponding to the 6 and 6' carbons of the bipyridine ligands. The fact that this extra signal was not observed in this case may have been due to the very weak nature of the ^{13}C nmr spectrum obtained.

The second complex (43) was prepared by a procedure analogous to that proposed by Constable [15] for the synthesis of bis(2,2'-bipyridine) (4,4'-dichloro-2,2'-bipyridine) ruthenium (II) hexafluorophosphate (26). Analysis of the isolated product by microanalysis, showed that it was probably the required product. ^1H nmr spectroscopy showed only the presence of aromatic protons.

1:2:2 SYNTHESIS OF BIS(2,2'-BIPYRIDINE) (4,4'-DIBROMO-2,2'-BIPYRIDINE) RUTHENIUM (II) HEXAFLUOROPHOSPHATE (46)

The reason for targeting (46) as a complex for synthesis was two-fold. Firstly, the complex (46) would provide a comparison of its photophysical properties with the previously prepared bis(2,2'-bipyridine) (4,4'-dichloro-2,2'-bipyridine) ruthenium (II) hexafluorophosphate (26); thus providing information on the effects, which halogen substituents have on the luminescent properties of this type of ruthenium complex. Secondly, synthesis of (46) would involve the preparation of the 4,4'-dibromo-2,2'-bipyridine ligand (45). This ligand could provide an ideal starting point for further work, as the bromo substituent can easily be replaced in organometallation reactions, thus allowing the easy introduction into the bipyridine ligand of spacer groups, which bear functionalities active towards antibodies.

The proposed synthetic scheme for the preparation of 4,4'-dibromo-2,2'-bipyridine (45) was by a route analogous to that

conducted for the synthesis of 4,4'-dichloro-2,2'-bipyridine (25) (Scheme 1-21). This route involves nucleophilic attack by a bromide ion upon 4,4'-dinitro-2,2'-bipyridine N,N'-dioxide (23), via a mechanism similar to that proposed in Scheme 1-16, resulting in the formation of 4,4'-dibromo-2,2'-bipyridine N,N'-dioxide (44). The (44) so isolated, would then be deoxygenated with phosphorus tribromide, to yield 4,4'-dibromo-2,2'-bipyridine (45).

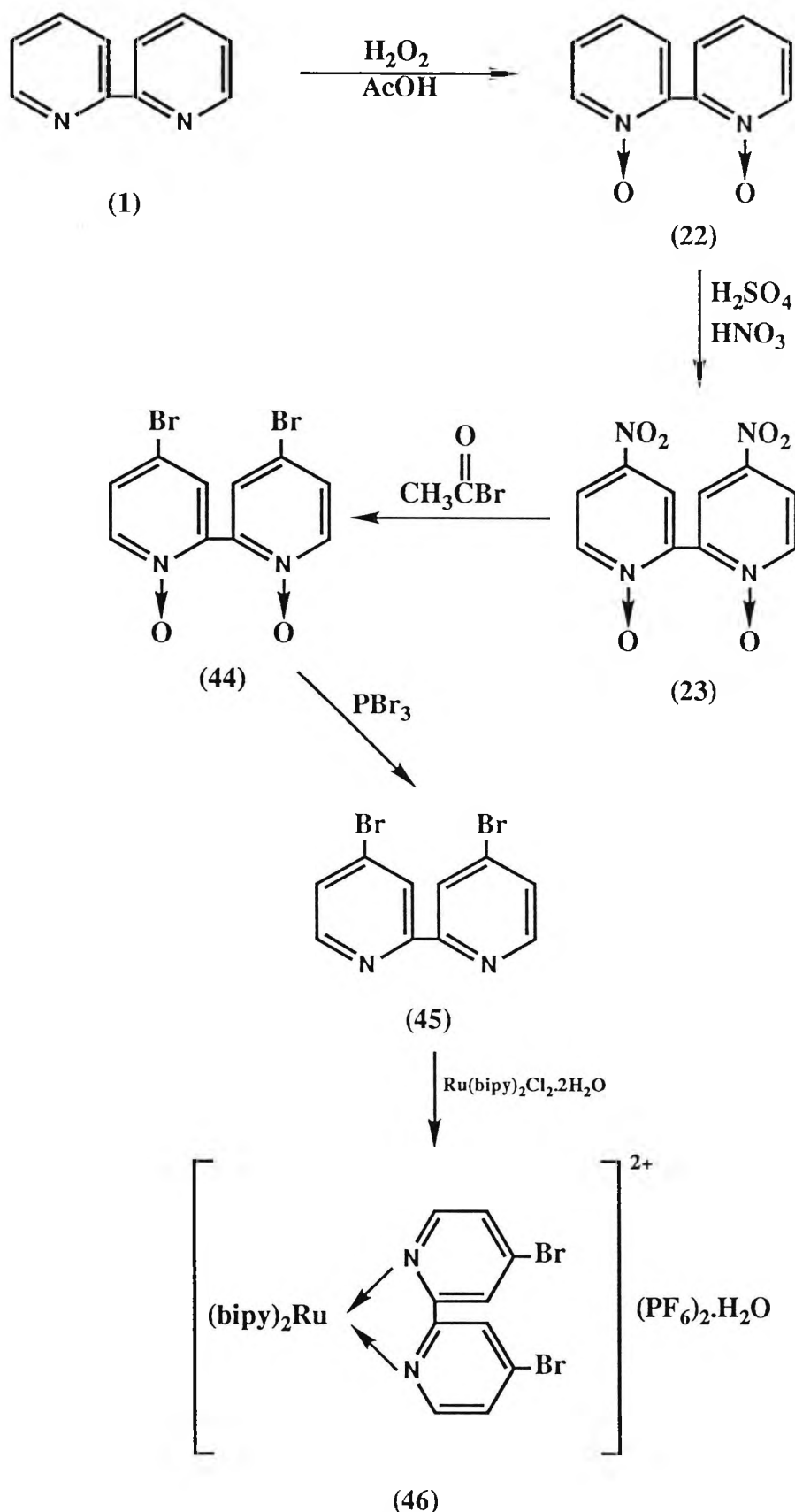
The preparation of 4,4'-dibromo-2,2'-bipyridine (45) via the protocol of Maerker and Case [13] was attempted. However, no product was isolated from the deoxygenation of (44) following this method. Repetition of this reaction, using a greater excess of acetyl bromide, resulted in the isolation of some material, which however, decomposed on exposure to the atmosphere.

The preparation of (45) was again repeated, via a modification of the method of Maerker and Case [26]. This modification involves the addition of an excess of acetyl bromide to a suspension of 4,4'-dinitro-2,2'-bipyridine N,N'-dioxide (23) in glacial acetic acid at 60°C, followed by deoxygenation of the product isolated in the above reaction using phosphorus tribromide. Material isolated from these reactions was confirmed to be probably (45) by CHN analysis.

Bis(2,2'-bipyridine) (4,4'-dibromo-2,2'-bipyridine) ruthenium (II) hexafluorophosphate (46) was prepared via the method of Constable [15]. Material isolated from this reaction was confirmed to be (46) by CHN analysis. ^{13}C nmr spectroscopy of the isolated product, showed that it had a structure consistent with that of the required complex (46). Again, three signals were observed in the aromatic region of the ^{13}C nmr spectrum of (46), which could be assigned to the different chemical environments of the 6 and 6' carbon atoms of the bipyridine ligands; a phenomenon, which is becoming characteristic of this type of complex.

SCHEME 1-21

SYNTHETIC SCHEME FOR THE SYNTHESIS OF BIS(2,2'-BIPYRIDINE)
(4,4'-DIBROMO-2,2'-BIPYRIDINE) RUTHENIUM (II) HEXAFLUOROPHOSPHATE (46)



1:2:3 THE SYNTHESIS OF RUTHENIUM COMPLEXES BEARING ESTER DERIVATISED BIPYRIDINE LIGANDS

Initially, it was attempted to prepare bipyridine ligands bearing ester functionalities via the acid chloride derivative (47), (Scheme 1-22). This synthesis involved, firstly, the oxidation of 4,4'-dimethyl-2,2'-bipyridine (2) with potassium permanganate, forming the dicarboxylic acid derivative (13), (the preparation of which has been previously described in Section 1:1:1), with the second step in the synthesis involving the reaction of (13) with thionyl chloride to form the acid chloride derivative (47).

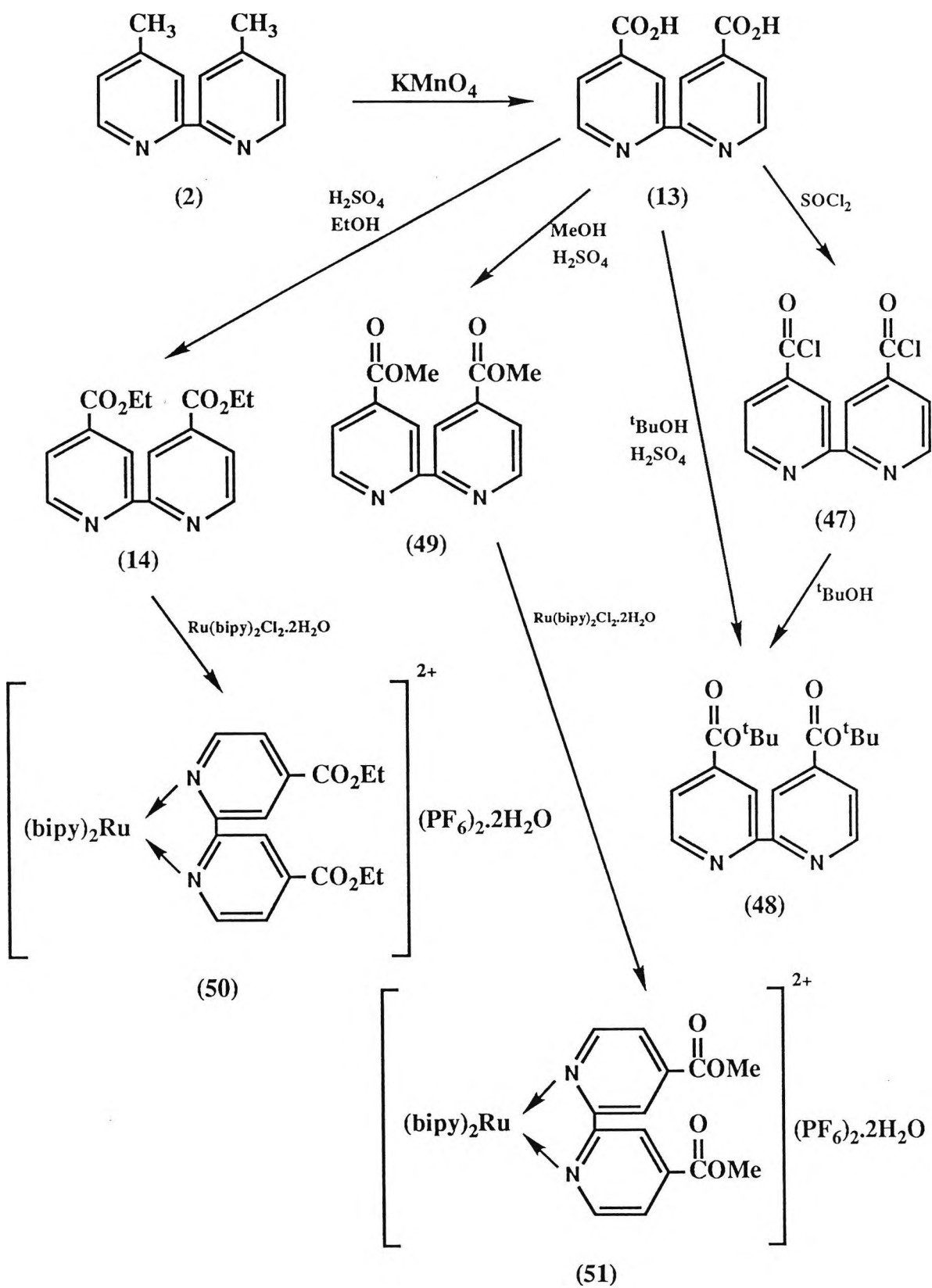
The reaction of (13) with thionyl chloride, initially appeared to proceed well, but the removal of excess thionyl chloride in order to isolate (47) proved extremely difficult. Reaction of the thionyl chloride contaminated acid chloride derivative (47), with t-butanol, resulted in the isolation of the diacid starting material (13).

Attempts to prepare the ester derivatives of 2,2'-bipyridine, were then concentrated on the acid catalysed esterification of the dicarboxylic acid derivative of 2,2'-bipyridine (13). As has been previously mentioned in Section 1:1:1, this reaction was successfully utilised in the preparation of the ethyl ester derivative of 2,2'-bipyridine (14), via modification of the protocol reported by Whittle [4], for the isolation of the 5,5'-substituted ester. Dimethyl (2,2'-bipyridine)-4,4'-dicarboxylate (49) was also prepared, via a procedure analogous to that of the ethyl ester (14). However, an attempt to prepare the t-butyl ester derivative (48) via this method failed, as the reaction yielded only starting material (13).

Ruthenium complexes of the ester derivatives were prepared via the method of Constable [15], (Scheme 1-22). ^{13}C nmr spectroscopy revealed that the material isolated from the attempted preparation of (50), was consistent with that expected for the structure of the ethyl ester complex. However, ^{13}C nmr spectroscopy of the material isolated from the attempted preparation

SCHEME 1-22

SCHEME SHOWING SYNTHETIC ROUTES TO THE SYNTHESIS OF RUTHENIUM COMPLEXES BEARING ESTER DERIVATISED BIPYRIDINE LIGANDS



of the methyl ester complex (51), was consistent with the structure expected for (50). Therefore, it would appear that exchange of the methoxy groups with ethoxy groups had occurred under the reaction conditions for the preparation of the ruthenium complex (51).

1.3.0 EXPERIMENTAL

Preparation of 1-(2-acetylpyridine) pyridinium iodide (4)

Preparation according to the procedure of Kröhnke and Gross [9].

2-acetylpyridine (1.00g, 8.25×10^{-3} moles) in pyridine (10 cm^3) was added to iodine (1.05g, 8.27×10^{-3} moles) which had been stirring in pyridine (20 cm^3) for 30 minutes. The reaction mixture was then left at reflux for 24 hours. After this time, TLC (ethyl acetate/petroleum ether $60^\circ:80^\circ$ (4:1) : silica gel) showed only baseline material thought to be the required product.

After cooling, the reaction mixture was filtered and washed with water. The remaining black solid was recrystallised from ethanol and decolourising charcoal to give white crystals (0.05g, approx. 2% yield based on 2-acetylpyridine).

^1H nmr : 6.56 δ (2H; singlet; pyr-CO-CH₂-pyr); 7.8-9.0 δ (11H; multiplet; aromatic protons). Impurity in the aromatic region due to pyridinium iodide.

Preparation of (4) according to the procedure of King [10].

Iodine (4.19g, 0.033 moles) was added to 2-acetylpyridine (4.00g, 0.033 moles) dissolved in pyridine (14 cm^3) at room temperature. The reaction mixture was heated to reflux for 3 hours, then allowed to cool overnight.

A precipitate formed overnight, which was removed by filtration and washed with a small amount of pyridine, dried, then

recrystallised from ethanol to yield a black crystalline solid (1.93g, 18% yield based on 2-acetylpyridine).

Anal. calcd. for $C_{12}H_{11}N_2IO$: Theory C, 44.19; H, 3.39; N, 8.59%. Found C, 44.03; H, 3.34; N, 8.62%.

1H nmr : 6.56 δ (2H; singlet; pyr-CO-CH₂-pyr); 7.8-9.0 δ (9H; multiplet; aromatic).

Infra-red (KBr disc) : 1711 cm⁻¹ (ketone conjugated aryl str.)

Preparation of 4-methyl-2,2'-bipyridine (5)

Attempted preparation by the procedure of Huang and Brewer [11].

1-(2-acetylpyridine) pyridinium iodide (0.28g, 8.59×10^{-4} moles) 2-butenal (0.071 cm³, 8.59×10^{-4} moles) and a four fold excess of ammonium acetate (0.26g, 3.44×10^{-3} moles) in methanol (20 cm³) were stirred together at 60-65°C for 5 hours, then allowed to cool to room temperature, and the methanol was removed under reduced pressure.

The residue was then extracted with ether, the ether was removed under vacuum and the residue extracted with hexane. Removal of the hexane under reduced pressure yielded a brown oil.

1H nmr : 2.44 δ (3H; singlet; bipy-CH₃); 7.2-8.68 δ (7H; multiplet; aromatic). 1H nmr also shows impurities in both the aromatic and aliphatic regions.

The brown oil was applied to a column of basic alumina, followed by elution with a hexane/acetone (9:1) mixture, which resulted in the loss of all material.

Preparation of (5) by an analogous procedure to that of Parker [12]

To a mixture of 1-(2-acetylpyridine)pyridinium iodide (3.00g, 9.20×10^{-3} moles) and ammonium acetate (9.23g, 0.12 moles) in

formamide (14 cm^3) was added 2-butenal (0.65g , 9.27×10^{-3} moles) and the mixture stirred at 65°C for 8 hours. After cooling, the reaction mixture was extracted with ether ($3 \times 30 \text{ cm}^3$) and hexane ($2 \times 10 \text{ cm}^3$). The solvents were removed from the extracts under reduced pressure to yield a brown oil (0.95g). This oil was then applied to a column of alumina (activity II-III), followed by elution with hexane-dichloromethane (90:10). The first fraction from this column was collected and the solvent removed under vacuum, yielding a colourless oil (0.16g , 10% yield based on 1-(2-acetylpyridine) pyridinium iodide).

^1H nmr : 2.44δ (3H; singlet; bipy-CH₃); $7.2-8.68 \delta$ (7H; multiplet; aromatic). There are however, still impurities present in the aliphatic region, notably at 1.28δ (broad singlet).

Preparation of 4,4'-di(bromomethyl)-2,2'-bipyridine (9)

GENERAL PROCEDURE

To a solution of 4,4'-dimethyl-2,2'-bipyridine (1.0g , 5.43×10^{-3} moles) in dry carbon tetrachloride (60 cm^3) was added N-bromo-succinimide (1.94g , 10.9×10^{-3} moles) and 2,2'-azobisis(2-methylpropanonitrile) (50mg). The reaction mixture was then brought to reflux, and the course of the reaction monitored by ^1H nmr spectroscopy. Once the optimum reaction time had been reached, the reaction mixture was allowed to cool to room temperature, filtered, and the solvent was removed under reduced pressure to yield a green oil.

Variations to the above general procedure included:-

- i) The addition of a further 1 molar equivalent of NBS, after heating the reaction mixture under reflux for 5 hours.
- ii) A change in the molar ratio of NBS to 4,4'-dimethyl-2,2'-bipyridine from 2:1 to 3:1 at the commencement of the reaction.

iii) Exchange of the solvent to chloroform from carbon tetrachloride.

Preparation of (2,2'-bipyridine)-4,4'-diaminomethyl hydrochloride (11) [12]

Crude 4,4'-dibromomethyl-2,2'-bipyridine was prepared according to the general bromination method variation ii) outlined on Page 61. This bromination reaction was terminated after 23 hours, to yield a green oil. To a solution of this oil, (2.32g, 6.78×10^{-3} moles), assuming 100% 4,4'-dibromomethyl-2,2'-bipyridine) in DMF (100 cm³), was added potassium phthalimide (2.59g, 0.014 moles) and the resulting mixture heated at 80°C for 3 hours. The reaction mixture was poured on to crushed ice, and a yellow solid was removed by filtration. This solid was then recrystallised from a large volume of ethanol to give a cream-coloured solid (0.44g).

The above solid was suspended in ethanol (5 cm³) and an excess of hydrazine hydrate (0.14g, 3.71×10^{-3} moles) was added, the resulting mixture was then brought to reflux for 8 hours. After cooling, concentrated hydrochloric acid (5 cm³) was added, and the mixture brought to reflux for a further 30 minutes. After being allowed to cool to room temperature, the reaction mixture was filtered, the solvent was removed under reduced pressure, and the residue was recrystallised from ethanol to give a brown solid (0.05g).

Anal. calcd. for C₁₂H₁₆N₄Cl₂ : Theory C, 50.18; H, 5.61; N, 19.50%. Found C, 53.70; H, 4.07; N, 14.94%.

Preparation of (2,2'-bipyridine)-4,4'-dicarboxylic acid (13)

A mixture of 4,4'-dimethyl-2,2'-bipyridine (7.00g, 0.04 moles) and potassium permanganate (40.00g, 0.25 moles) in water (300 cm³), was heated under reflux for 22 hours. The reaction mixture was then allowed to cool to room temperature and filtered to remove the black precipitate formed during the reaction.

The filtrate was washed with ether (3 x 150 cm³), then acidified with concentrated hydrochloric acid until a permanent precipitate had formed. The precipitate was collected by filtration,

washed with water, then ether, and finally dried to give a white solid (1.86g, 20% yield based on 4,4'-dimethyl-2,2'-bipyridine).

Preparation of diethyl(2,2'-bipyridine)-4,4'-dicarboxylate (14) [4]

A mixture of (2,2'-bipyridine)-4,4'-dicarboxylic acid (2.00g, 8.26×10^{-3} moles), ethanol (30 cm^3) and concentrated sulphuric acid (7.60g) was heated at reflux for 18 hours. The reaction mixture was poured into water (80 cm^3) and the precipitate removed by filtration. The product was then recrystallised from ethanol to give colourless needle-like crystals (1.27g, 51% yield based on (2,2'-bipyridine)-4,4'-dicarboxylic acid).

^1H nmr : 1.36-1.52 δ (6H; triplet; $-\text{OCH}_2\text{CH}_3$); 4.4-4.68 δ (4H; quartet; $-\text{OCH}_2\text{CH}_3$); 7.96-9.12 δ (6H; multiplet; aromatic).

Infra-red (KBr disc) : 3000 cm^{-1} (C-H str., aromatic, weak), 1728 cm^{-1} (C=O str., ester C=O, v. strong), 1597 cm^{-1} and 1554 cm^{-1} (C=C str., (skeletal)aromatic), 1290 cm^{-1} and 1256 cm^{-1} (C-O str., ester C-O, strong).

Preparation of (2,2'-bipyridine)-4,4'-dicarbohydrazide (15) [4]

A mixture of diethyl(2,2'-bipyridine)-4,4'-dicarboxylate (1.58g, 5.26×10^{-3} moles), hydrazine hydrate (8 cm^3), and ethanol (8 cm^3), was heated under reflux at 115°C for 3 hours. The creamy insoluble product was removed by filtration and washed with boiling ethanol to obtain (2,2'-bipyridine)-4,4'-dicarbohydrazide (1.31g, 92% yield based on diethyl(2,2'-bipyridine)-4,4'-dicarboxylate). This material was found to be insoluble in acid, base, and organic solvents.

Preparation of (2,2'-bipyridine)-4,4'-dicarbazide (16) [4]

The finely powdered dihydrazide (15) (1.31g , 4.81×10^{-3} moles) was suspended in concentrated hydrochloric acid (26 cm^3) and the mixture cooled to 0°C . A cold solution of sodium nitrite

(0.78g, 0.01 moles) in water (6 cm³) was added dropwise with stirring, the reaction temperature being maintained below 10°C.

The suspended hydrazide slowly dissolved and the cloudy solution obtained was diluted with water to precipitate the dicarbazide. The precipitate was washed with water and hot ethanol, to give a white powder (0.89g, 63% yield based on (2,2'-bipyridine)-4,4'-dicarbohydrazide).

Anal. Calcd. for C₁₂H₆N₈O₂ : Theory C, 48.98; H, 2.05; N, 38.08%. Found C, 49.17; H, 2.17; N, 37.25%.

Infra-red (KBr disc) : 2160-2190 cm⁻¹ (-N₃, strong), 1689 cm⁻¹ (C=O str., v. strong).

Preparation of 4,4'-di(ethoxycarbonylamino)-2,2'-bipyridine (17) [4]

(2,2'-bipyridine)-4,4'-dicarbazide (0.89g, 3.02 x 10⁻³ moles) was suspended in a mixture of ethanol (26 cm³) and xylene (26 cm³) and heated under reflux for 8 hours. The reaction mixture was allowed to cool and colourless needles, which crystallised out slowly on cooling, were collected and recrystallised from ethanol to give a colourless solid (0.044g, 44% based on (2,2'-bipyridine)-4,4'-dicarbazide).

Anal. Calcd. for C₁₆H₁₈N₄O₄ : Theory C, 58.17; H, 5.47; N, 16.96%. Found C, 52.70; H, 6.08; N, 14.95%.

Insoluble in DMSO.

Infra-red (KBr disc) : 3331-2985 cm⁻¹ (N-H str., v. broad) 1742 cm⁻¹ and 1714 cm⁻¹ (C=O str., strong).

Preparation of 4,4'-diamino-2,2'-bipyridine (18) [4]

A mixture of 4,4'-di(ethoxycarbonylamino)-2,2'-bipyridine (0.29g, 6.36 x 10⁻⁴ moles) (impure), ethanol (3.15 cm³) and 2.5N

sodium hydroxide solution (3.15 cm^3), was stirred at $70\text{--}80^\circ\text{C}$ for 24 hours. The mixture was then cooled to room temperature and filtered. The white powder obtained was recrystallised from a large volume of water containing a few drops of ammonia, yielding a small quantity of colourless needle-like crystals.

Anal. Calcd. for $\text{C}_{10}\text{H}_{10}\text{N}_4\text{O}_2$: Theory C, 55.04; H, 4.61; N, 25.67%. Found C, 62.05; H, 5.35; N, 28.25%.

Infra-red (KBr disc) : 3149 cm^{-1} (N-H str., v. broad).

Preparation of 2,2'-bipyridine N,N'-dioxide (22)

Procedure according to Maerker and Case [13].

30% hydrogen peroxide (10 cm^3) was added to 2,2'-bipyridine (5.00g, 0.03 moles) in glacial acetic acid (25 cm^3) and the reaction mixture was heated at approximately 80°C for 8 hours. After this time, the solution was allowed to cool to room temperature and added slowly to acetone (500 cm^3), precipitating a white solid, which was collected by filtration (4.85g, 81% yield based on 2,2'-bipyridine).

Anal. Calcd. for $\text{C}_{10}\text{H}_8\text{N}_2\text{O}_2$: Theory C, 63.82; H, 4.28; N, 14.88%. Found C, 63.80; H, 4.47; N, 14.79%.

Infra-red (KBr disc) : 3000 cm^{-1} (C-H str., aromatic) 1427 cm^{-1} (C-H ring str.), 1299 cm^{-1} (N^+-O), 1147 cm^{-1} (in-plane and out-of-plane C-H deformation, aromatic), 1098 cm^{-1} and 1022 cm^{-1} (C-H deformation, aromatic), 983 cm^{-1} (C-H in plane ring deformation).

Procedure according to Seddon et al. [14].

2,2'-bipyridine (10.0g, 0.064 moles), hydrogen peroxide (13 cm^3 , 100 vol.) and glacial acetic acid (75 cm^3) were heated at 80°C for 3 hours. Hydrogen peroxide (9 cm^3 , 100 vol.) was then added and the heating continued for a further 4 hours. The reaction

mixture was allowed to cool to room temperature, then poured cautiously into acetone. A precipitate, which formed slowly, was filtered off to give white crystals (11.04g, 92% yield based on 2,2'-bipyridine).

Preparation of 4,4'-dinitro-2,2'-bipyridine N,N'-dioxide (23)[14]

Fuming nitric acid (16.4 cm³) was added slowly to a mixture of 2,2'-bipyridine N,N'-dioxide (8.20g, 0.04 moles), oleum (8.2 cm³) and concentrated sulphuric acid (16.4 cm³) cooled in an ice bath. The mixture was heated to 100°C for 4 hours, with the reflux condenser fitted with a calcium chloride drying tube. After this time, the reaction mixture was allowed to cool to room temperature and cautiously poured on to crushed ice (68g) and water (77 cm³), precipitating out a yellow solid, which was then collected by filtration, washed with water and air dried (7.25g, 65% yield based on 2,2'-bipyridine N,N'-dioxide).

Anal. Calcd. for C₁₀H₆N₄O₆ : Theory C, 43.17; H, 2.17; N, 20.14%. Found C, 42.17; H, 2.29; N, 20.19%.

¹H nmr : (DMSO-d₆) approx. 7 δ (6H; multiplet; aromatic).

Infra-red (KBr disc) : 1600 cm⁻¹ and 1570 cm⁻¹ (str. ring, aromatic, sharp), 1510 cm⁻¹ (-NO₂ str. antisymm., aromatic, broad), 1480 cm⁻¹ (str. ring, aromatic, sharp), 1350 cm⁻¹ (-NO₂ str. symm., aromatic, strong, broad), 1118 cm⁻¹ (β-CH mode, aromatic, sharp), 840 cm⁻¹ (C-N str., aromatic, strong), 750 cm⁻¹ (C-N in-plane deformation, aromatic).

Alternative Preparation of 4,4'-diamino-2,2'-bipyridine (18) [13]

To a solution of 4,4'-dinitro-2,2'-bipyridine N,N'-dioxide (4.0g, 0.014 moles) in glacial acetic acid (160 cm³) at 100°C was added iron powder (8.8g, electrolytic grade). The mixture

was heated at 114°C with stirring for 70 minutes, then cooled to room temperature and added to water (100 cm³). The resulting mixture was made alkaline with 25% sodium hydroxide and finally brought up to a volume of 600 cm³ with water. Filtration afforded a black tarry precipitate, which was allowed to dry in air. The dried precipitate was extracted with industrial methylated spirit until further extraction no longer gave a purple alcoholic solution. The combined extracts were filtered, then acidified, with cooling, with concentrated hydrochloric acid. The resulting suspension was filtered, the white precipitate was washed with industrial methylated spirit and discarded, and the alcoholic wash solution was combined with the filtrate. The alcoholic solution was concentrated to a volume of approx. 250 cm³. On standing, long needles deposited in the concentrate and were collected by filtration. The solid was recrystallised from aqueous ethanol (6.4% water) to give white needle-like crystals of the hydrochloride product. The latter material was dissolved in water and the free-base precipitated by addition of dilute sodium hydroxide solution. The white solid obtained from this was then recrystallised from water to give a colourless crystalline solid (0.25g, 9.6% yield based on 4,4'-dinitro-2,2'-bipyridine N,N'-dioxide).

Anal. Calcd. for C₁₀H₁₀N₄ : Theory C, 64.50; H, 5.41; N, 30.08%. Found C, 63.98; H, 5.42; N, 30.05%.

Infra-red (KBr disc) : 3411 cm⁻¹ and 3303 cm⁻¹ (N-H str., sharp), 3149 cm⁻¹ (C-H, aromatic, broad), 1598 cm⁻¹ (ring str., subs. pyr, sharp), 1556 cm⁻¹ (ring str., subs. pyr, weak).

Preparation of cis-dichlorobis(2,2'-bipyridine) ruthenium (III)

Ruthenium trichloride trihydrate (2.47g, 9.45 x 10⁻³ moles), 2,2'-bipyridine (2.96g, 0.019 moles) & lithium chloride (anhyd.) (4.94g) in DMF (49 cm³) were heated together under reflux for 5½ hours under nitrogen. The solution was cooled to below room temperature, then acetone (247 cm³) was added, with stirring being maintained throughout the cooling process. After this

time, a black solid had formed which was then filtered and washed with water and ether.

The crude product was suspended in a water:ethanol (1:1) mixture (400 cm³) and heated under reflux for 1 hour. Any insoluble material was filtered off and lithium chloride (47.50g) was then added carefully to the filtrate (exotherm). The ethanol was distilled off and the solution quickly cooled and left at 2-4°C overnight. The purple-black crystals formed were then collected by filtration washed with water, then ether, and dried (2.13g, 43% yield based on ruthenium trichloride trihydrate).

Anal. Calcd. for RuC₂₀H₂₀N₄O₂Cl₂ : Theory C, 46.16; H, 3.87; N, 10.76%. Found C, 44.10; H, 3.93; N, 10.27%.

Preparation of bis(2,2'-bipyridine)(4,4'-diamino-2,2'-bipyridine) ruthenium (II) hexafluorophosphate (19) [15]

cis-dichloro bis(2,2'-bipyridine) ruthenium (II) (0.3041g, 5.84 x 10⁻⁴ moles) and 4,4'-diamino-2,2'-bipyridine (0.1087g, 5.84 x 10⁻⁴ moles) were heated under reflux in ethanol (250 cm³) for 20 hours under nitrogen. After this time TLC (SiO₂:MeOH) showed one red spot near the baseline with no starting material being indicated. The reaction mixture was filtered hot, treated with a solution of ammonium hexafluorophosphate (0.58g, 3.58 x 10⁻³ moles) in methanol (12 cm³) and allowed to cool. On cooling, red crystals precipitated out of solution, which were collected by filtration (0.37g, 70% yield based on cis-dichloro bis(2,2'-bipyridine) ruthenium (II)).

Anal. Calcd. for C₃₀H₂₈N₈P₂OF₁₂Ru : Theory C, 39.70; H, 3.11; N, 12.35%. Found C, 40.19; H, 2.85; N, 12.45%.

¹³C nmr (acetone-d₆): 157.11 ppm (C₂, substituted, quaternary), 156.85 ppm (C₂, unsubstituted, quaternary), 155.90 ppm (Carbon impurity), 155.41 ppm (C₄, substituted, quaternary), 151.12, 150.80, 149.24 ppm (C₆, carbon signals, substituted and unsubstituted), 136.80 ppm (C₄, unsubstituted, quaternary), 127.47

ppm (C_5 , unsubstituted), 124.08 ppm (C_3 , unsubstituted), 111.81 ppm (C_5 , substituted), 107.20 ppm (C_3 , substituted).

Infra-red (KBr disc) : 3400 cm^{-1} (N-H str., broad), 1553 cm^{-1} (ring str., subs. pyr., sharp), 1463-1421 cm^{-1} (ring str., aromatic, weak).

A sample of the above red solid was dissolved in ethanol, to give a concentrated solution. This solution was then applied to a Sephadex LH-20 column, followed by elution with ethanol. The main fast running red band was collected and the solvent evaporated off. The resulting red solid was then analysed.

Anal. Calcd. for $C_{30}H_{28}N_8P_2OF_{12}Ru$: Theory C, 39.70; H, 3.11; N, 12.35%. Found C, 39.62; H, 3.01; N, 12.14%.

Preparation of 4,4'-dichloro-2,2'-bipyridine N,N'-dioxide (24)[14]

Glacial acetic acid (27 cm^3), ethanoyl chloride (18 cm^3) and 4,4'-dinitro-2,2'-bipyridine N,N'-dioxide (1.71g, 6.15×10^{-3} moles) were heated together at 100°C for 2 hours. The cooled mixture was poured on to ice (141g). On neutralisation of the solution with sodium hydroxide solution (30% w/v), a yellowish-coloured solid was precipitated, which was collected by filtration, washed with water and air-dried (1.29g, 82% yield based on 4,4'-dinitro-2,2'-bipyridine N,N'-dioxide).

Anal. Calcd. for $C_{10}H_6N_2O_2Cl_2$: Theory C, 46.72; H, 2.35; N, 10.89%. Found C, 46.61; H, 2.56; N, 10.80%.

Infra-red (KBr disc) : 740 cm^{-1} (C-Cl str., aromatic, sharp).

Preparation of 4,4-dichloro-2,2'-bipyridine (25)

Procedure analogous to that used by Maerker and Case [13] for the preparation of 4,4'-dibromo-2,2'-bipyridine.

A suspension of crude 4,4'-dichloro-2,2'-bipyridine N,N'-dioxide (1.66g, 6.46×10^{-3} moles) in anhydrous chloroform (42 cm³) was cooled to -3°C and phosphorous trichloride (8.2 cm³, 0.094 moles) was added. The reaction mixture was brought to reflux for 75 minutes, then allowed to cool to room temperature and poured into an ice-water mixture. After phase separation, the chloroform layer was extracted repeatedly with distilled water and the aqueous extracts were combined with the water layer from the reaction mixture. Neutralisation of this aqueous solution with 25% sodium hydroxide gave a white precipitate, which was collected by filtration and washed thoroughly with water. The solid collected was then recrystallised from petroleum ether to give white needles (225mg, 15% yield based on 4,4'-dichloro-2,2'-bipyridine N,N'-dioxide).

Anal. Calcd. for C₁₀H₆N₂Cl₂ : Theory C, 53.36; H, 2.66; N, 12.44%. Found C, 53.46; H, 2.62; N, 12.42%.

Infra-red (KBr disc): 731 cm⁻¹ (C-Cl str., aromatic, strong).

¹H nmr(CDCl₃) : 7.36-7.48 δ (2H; multiplet; 5 and 5' aromatic protons), 8.56 δ (2H; doublet; 3 and 3' aromatic protons), 8.64-8.72 δ (2H; doublet; 6 and 6' aromatic protons).

¹³C nmr (CDCl₃) : 122.07 ppm (C₃), 124.67 ppm (C₅), 145.67 ppm (C₄, quaternary), 150.34 ppm (C₆), 156.74 ppm (C₂, quaternary).

Preparation of bis(2,2'-bipyridine)(4,4'-dichloro-2,2'-bipyridine) ruthenium (II) hexafluorophosphate (26) [15]

cis-dichlorobis(2,2'-bipyridine) ruthenium (II) (484mg, 1mmol) and 4,4'-dichloro-2,2'-bipyridine (225mg, 1mmol) were heated together in ethanol (250 cm³) under reflux for 22 hours under nitrogen. The reaction was monitored by TLC (SiO₂:MeOH) and after 22 hours TLC showed a predominant orange spot at the baseline (product), and a very slight fast running purple spot (starting material).

The reaction mixture was filtered hot, treated with a solution of ammonium hexafluorophosphate (1.00g) in methanol (20 cm³) and allowed to cool. On cooling, red crystals precipitated out

slowly, which were collected by filtration (0.076g, 80% yield based on Ru(bipy)₂Cl₂.2H₂O).

Anal. Calcd. for C₃₀H₂₄N₆Cl₂ORuP₂F₁₂ : Theory C, 38.07; H, 2.55; N, 8.87%. Found C, 37.77; H, 2.50; N, 8.61%.

Infra-red (KBr disc) : approx. 3000 cm⁻¹ (C-H str., aromatic, broad), 750 cm⁻¹ (C-Cl str., aromatic, sharp).

¹H nmr (acetone-d₆) : 7.64-7.88 δ (6H; multiplet; 5 and 5' aromatic protons), 8.16-8.48 δ (10H; multiplet; 3,3' and 4,4' aromatic protons), 8.96-9.04 δ (4H; doublet; 6,6' protons of unsubstituted bipyridine), 9.20-9.24 δ (2H; doublet; 6,6' protons of substituted bipyridine).

¹³C nmr (acetone-d₆) : 125.65 ppm (C₃ of unsubstituted bipyridine), 126.69 ppm (C₃ of substituted bipyridine), 129.10 ppm (C₅ of unsubstituted bipyridine), 129.43 ppm (C₅ of substituted bipyridine), 139.45 ppm (C₄ of unsubstituted bipyridine), 146.68 ppm (C₄ substituted bipyridine, quaternary), 152.99 and 153.32 ppm (C₆ of unsubstituted bipyridine), 154.04 ppm (C₆ of substituted bipyridine), 158.40 (C₂ of unsubstituted bipyridine, quaternary), 159.05 ppm (C₂ of substituted bipyridine, quaternary).

Mass spec. : 786 m/e (M⁺).

Preparation of 2,2'-bipyridine N-oxide (28)

Procedure according to Jones et al. [17].

Hydrogen peroxide (25 cm³; 100 vol) was added to a vigorously stirred solution of 2,2'-bipyridine (5.00g, 0.032 moles) in glacial acetic acid (20 cm³) and the reaction mixture was heated at 50°C for 12 hours. The volatile compounds were then removed giving a pale yellow solid instead of the expected yellow oil. This indicated that 2,2'-bipyridine N,N'-dioxide had been obtained and none of the required product. The above procedure

was repeated using 11 cm³ of hydrogen peroxide instead of 25 cm³, and the reaction was heated at 80°C for 7 hours. This method, however, yielded 2,2'-bipyridine N,N'-dioxide.

Procedure according to McAuliffe [19]

Hydrogen peroxide (5 cm³, 100 vol) was added to a solution of 2,2'-bipyridine (2.65g, 0.017 moles) in glacial acetic acid (17 cm³) and toluene (17 cm³). The mixture was heated to 75°C and, at hourly intervals, a TLC was run (silica; ethyl acetate, methanol and ammonia solution, (4:2:1)). This exhibited three spots, the fastest running being starting material and the lower two being the mono- and di-substituted N-oxides. After 5½ hours, the reaction mixture was concentrated to approximately 9 cm³, water was added (17 cm³) and the reaction mixture again concentrated to approximately 9 cm³. This was repeated twice more and after the second addition, the reaction mixture was evaporated to dryness. The solid obtained was neutralised with ammonium carbonate (10%) and washed with benzene (2 cm³). The required product was then extracted with dichloromethane (3 x 10 cm³) and the extracts were dried with sodium sulphate. The solvents in the extracts were removed under vacuum, to yield a pale yellow oil, which slowly solidified to give a white semi-solid (1.5g, 51% based on 2,2'-bipyridine). This isolated solid was then used immediately in the preparation of 4-nitro-2,2'-bipyridine N-oxide (29).

Preparation of 4-nitro-2,2'-bipyridine N-oxide (29) [19]

After cooling to 0-5°C, concentrated sulphuric acid (27 cm³) was added with care to 2,2'-bipyridine N-oxide (5.05g, 0.03 moles). A mixture of fuming nitric acid (40 cm³) and concentrated sulphuric acid (27 cm³) was then added over 15 minutes, and the reaction mixture heated at 100°C for 2 hours. The mixture was allowed to cool to room temperature and then poured on to ice (133.00g). The pH was adjusted to 5.5 with aqueous sodium hydroxide (15%) and the crude precipitate filtered off. The solid was then purified by soxhlet extraction using absolute ethanol (200 cm³), to give yellow needles of 4-nitro-2,2'-

bipyridine N-Oxide (1.95g, 31% based on 2,2'-bipyridine N-oxide).

mpt. 183-184°C (literature 184°C).

Anal. Calcd. for $C_{10}H_7N_2O_3$: Theory C, 55.30; H, 3.24; N, 19.34%.
Found C, 55.31; H, 3.13; N, 19.02%.

Infra-red (KBr discs) ; 1520 cm^{-1} (N-O asymm. str.(sharp),
1340 cm^{-1} (N-O sym. str., sharp).

Preparation of 4-chloro-2,2'-bipyridine (30) [19]

4-nitro-2,2'-bipyridine N-oxide (3.00g, 0.013 moles) was heated under reflux with ethanoyl chloride (90 cm^3) for 1 hour. The reaction mixture was cooled to 0°C and phosphorus trichloride (15 cm^3) added dropwise. The resulting solution was then brought to reflux for a further 2 hours. The reaction mixture was then allowed to cool to room temperature, poured on to ice (450.00g), and neutralised with sodium hydroxide (20%) to give a white precipitate. The precipitate was extracted with dichloromethane (3 x 75 cm^3), and the extracts were dried with sodium sulphate and evaporated to dryness. The residue was recrystallised with pet. ether (60°-80°) to give 4-chloro-2,2'-bipyridine as colourless needles (1.25g, 51% based on 4-nitro-2,2'-bipyridine N-oxide).

Anal. Calcd. for $C_{10}H_7N_2Cl$: Theory C, 63.00; H, 3.70; N, 14.69%.
Found C, 63.08; H, 3.73; N, 14.46%.

Preparation of bis(2,2'-bipyridine)(4-chloro-2,2'-bipyridine)ruthenium (II) hexafluorophosphate (31) [15]

cis-dichlorobis(2,2'-bipyridine) ruthenium (II) (484mg, 1mmol) and 4-chloro-2,2'-bipyridine (191mg, 1 mmol) were heated together in ethanol (250 cm^3) under reflux for 20 hours under nitrogen.

TLC (silica:MeOH) at this time exhibited one slow running red spot above the baseline. The reaction mixture was filtered hot, treated with a solution of ammonium hexafluorophosphate (1g) in

methanol (20 cm³) and allowed to cool. Red crystals that precipitated out on cooling were then collected by filtration (0.76g, 85% yield based on Ru(bipy)₂Cl₂.2H₂O).

Anal. Calcd. for C₃₀H₂₃N₆ClRuP₂F₁₂ : Theory C, 40.31; H, 2.59; N, 9.40%. Found C, 40.03; H, 2.72; N, 9.41%.

Infra-red (KBr disc) : 1463-1406 cm⁻¹ (ring str., aromatic), 730 cm⁻¹ (C-Cl str., aromatic, sharp).

¹³C nmr (acetone-d₆): 125.58 ppm (C₃, substituted and unsubstituted bipyridine), 129.04 ppm (C₅, substituted and unsubstituted bipyridine), 139.32 ppm (C₄, unsubstituted bipyridine), 146.55 ppm (C₄, substituted bipyridine, quaternary), 153.12 and 153.84 ppm (C₆, unsubstituted bipyridine), 157.55 ppm (C₆, substituted bipyridine), 158.40 ppm (C₂, unsubstituted bipyridine, quaternary), 159.90 ppm (C₂, substituted bipyridine, quaternary).

Preparation of bis(2,2'-bipyridine)(4,4'-bishydroxy-2,2'-bipyridine) ruthenium (II) hexafluorophosphate (27) [15]

Bis(2,2'-bipyridine)(4,4'-dichloro-2,2'-bipyridine) ruthenium (II) hexafluorophosphate (70mg, 0.074 mmol) and sodium hydroxide (80mg, 2 mmol) were dissolved in water (18 cm³) and the solution heated under reflux for 1 hour under nitrogen. The solution was filtered hot and treated with aqueous hexafluorophosphoric acid (0.25 cm³, 75%), which resulted in the precipitation of an orange solid. This solid was collected by filtration and recrystallised from aqueous ethanol to give orange-red crystals (0.04g).

Anal. Calcd. for C₃₀H₂₇N₆F₁₂O_{3.5}P₂Ru : Theory C, 39.22; H, 2.96; N, 9.15%. Found C, 38.64; H, 2.40; N, 8.76%.

Infra-red (KBr disc) : 1600 cm⁻¹ (ring str., aromatic, sharp), 1460 cm⁻¹ (ring str., aromatic, sharp), 1410 cm⁻¹ (ring str., aromatic, weak), 1230 cm⁻¹ (β-CH mode, aromatic, weak).

The reaction time was increased to 48 hours, when examination of the product by ¹³C nmr showed a mixture of products, perhaps of starting material and required product.

Preparation of bis(2,2'-bipyridine)(4-hydroxy-2,2'-bipyridine)ruthenium (II) hexafluorophosphate (32) [15]

Bis(2,2'-bipyridine)(4-chloro-2,2'-bipyridine) ruthenium (II) hexafluorophosphate (67.5mg, 0.075 mmol) and sodium hydroxide (80 mg, 2 mmol) were dissolved in water (20 cm³) and the solution was heated under reflux for 30 minutes under nitrogen. The resulting solution was filtered hot and treated with aqueous hexafluorophosphoric acid (0.2 cm³, 75%), yielding an orange precipitate, which was then collected by filtration (0.06g).

Anal. Calcd. for C₃₀H₂₆N₆O₃P₂F₁₂Ru : Theory C, 39.62; H, 2.88; N, 9.24%. Found C, 39.40; H, 2.50; N, 8.91%.

¹³C nmr (acetone-d₆) : nmr gave many signals in the region where it is expected that bipyridine signals would be seen, indicating a mixture of products.

Preparation of 4-hydroxyethyl-4'-methyl-2,2'-bipyridine (33) [21]

n-Butyl lithium (25 cm³ of a 1.12M solution) was added to a solution of diisopropylamine (4 cm³) in dry THF (15 cm³) and the resulting mixture was stirred under nitrogen for 15 minutes. 4,4'-dimethyl-2,2'-bipyridine (5.00g, 0.027 moles) in dry THF (125 cm³) was then slowly added, changing the colour of the reaction mixture to orange-brown. After 2 hours stirring, it was attempted to bubble formaldehyde gas through the solution. However, all attempts, including cooling the gas, did not prevent polymerisation to paraformaldehyde.

Preparation of 4-(3-hydroxypropyl)-4'-methyl-2,2'-bipyridine (34)

n-Butyl lithium (18 cm³ of a 1.57M solution) was added to a solution of diisopropylamine (4 cm³) in dry THF (15 cm³) and the resulting mixture was stirred under nitrogen for 15 minutes. 4,4'-dimethyl-2,2'-bipyridine (5.00g, 0.03 moles) in dry THF (125 cm³) was then added slowly. After 2 hours, a saturated solution of ethylene oxide (1.26g, 0.03 moles in 10 cm³ THF) was added at < 0°C. Stirring was continued for a further 30 minutes at 0°C and then 15 minutes under gentle reflux. After this time, the reaction mixture had turned red. Water was added to the solution, which was then extracted with ether. The ether extract was dried with anhydrous Na₂SO₄, filtered and removed under vacuo, to give a brown oil containing a white solid (starting material). This oil was triturated with a small quantity of ethanol, precipitating out the white solid. The triturate was filtered and the ethanol removed under reduced pressure, to give a brown semi-solid oil.

¹H nmr(CDCl₃): 1.68-1.92 δ (2H; multiplet; pyr-CH₂CH₂CH₂OH), 2.24 δ (3H; singlet; pyr-CH₃), 2.52-2.68 δ (2H; triplet; pyr-CH₂CH₂CH₂OH), 3.36-3.48 δ (2H; triplet; pyr-CH₂CH₂CH₂OH), 4.28 δ (1H; broad singlet; -OH), 6.68-8.08 δ (6H; aromatic including 6.68-6.76 δ doublet, 7.76 δ singlet, and 7.96-8.08 δ multiplet). nmr impurity 4,4'-dimethyl-2,2'-bipyridine.

TLC analysis of this semi-solid oil (silica; ethyl acetate : pet.ether 60/80 (1:9)), exhibited three spots; the middle running spot was identified as starting material, with the remaining spots running near the baseline and at the solvent front.

Due to the result of the TLC analysis, a chromatographic analysis of the oil was conducted (silica gel; ethyl acetate; pet.ether 60/80 (1:9)); the analysis yielded 7 fractions. ¹H nmr spectroscopy of the fractions appeared to indicate that decomposition had occurred, but the seventh fraction appeared to contain a small quantity of the desired product.

Attempted alternative purification methods:-

- i) Trituration with ethanol was replaced by ether. This yielded a waxy white precipitate. ^1H nmr spectroscopy of this precipitate showed that it was probably 4,4'-di(3-hydroxypropyl)-2,2'-bipyridine.

^1H nmr (CDCl_3) : 1.64-1.84 δ (4H; multiplet; pyr- $\text{CH}_2\text{CH}_2\text{CH}_2\text{OH}$), 2.44-2.60 δ (5H; triplet; pyr- $\text{CH}_2\text{CH}_2\text{CH}_2\text{OH}$), D_2O shake removes broadness in triplet indicating OH), 3.32-3.44 δ (4H; triplet; pyr- $\text{CH}_2\text{CH}_2\text{CH}_2\text{OH}$), 6.72-8.16 δ (6H; aromatic including 6.72-6.80 δ multiplet, 7.8 δ singlet, 8.08-8.16 δ doublet). All integration is approximate due to a slight impurity of starting material.

The solvent from the filtered ether triturate was removed under vacuum without heating to give a yellow oil. The trituration was repeated and the ether again removed under vacuum. The oil isolated by this procedure was examined by ^1H nmr spectroscopy. This indicated that the oil was probably the required product, contaminated with starting material.

The isolated oil was applied to a pressure column (silica 60 Art. 9385; ethyl acetate : pet.ether 60/80° (1:9)). Once the material was loaded onto the column, the amount of ethyl acetate in the eluent was increased gradually to 100%. At this point, two bands were eluted from the column. The solvent was then removed from both collected bands under vacuum and the residues were examined by ^1H nmr spectroscopy (CDCl_3). The first band appeared to be starting material and the second band appeared to be the required product contaminated with aliphatic material. The aliphatic contaminants were found at 0.80-1.04 δ and 1.18-1.42 δ ; all other assignments were as previously stated for the required product. Removal of the solvent from the second band under reduced pressure yielded a brown oil, which slowly solidified to give a brown solid.

A small scale attempt was made to further purify the residue from the second band by forming the HCl salt. HCl gas was bubbled through an ether solution of the residue, precipitating a white sticky solid, which was recrystallised from acetonitrile to give a white powder. The powder was dissolved in 20% sodium hydroxide, boiled for approximately 10 minutes, and then extracted with ether. The ether was removed under vacuum, to yield a light yellow oil. A repetition of the HCl salt preparation on a larger scale resulted in the decomposition of the salt whilst recrystallising in acetonitrile.

- ii) The above preparative procedure was repeated up to the point that the ether extracts of the reaction mixture were removed under reduced pressure to give a yellow oil. The oil was dissolved in hydrochloric acid (50%) and extracted with pet.ether 60/80° (20 cm³) and dichloromethane (2 x 20 cm³). The aqueous layer was boiled for 10 minutes in decolourising charcoal and then made basic using potassium hydroxide pellets, to give a milky white solution. This basic solution was extracted with ether (3 x 30 cm³), the ether extracts were combined, washed with water, and dried over Na₂SO₄, and the ether finally removed under reduced pressure to give a white semi-solid. ¹H nmr spectroscopy of this solid showed some product, but recrystallisation with methanol gave a white solid which was shown to be starting material.

Attempted preparation of (34) by modification of the procedure of Kaiser and Petty [22]:-

To a solution of diisopropylamine (3.5 cm³, 2.53g, 0.025 moles) in dry THF (10 cm³) at 0°C under nitrogen, was added n-butyl lithium (27 cm³, 0.025 moles of a 0.91M solution). The resulting pale yellow solution was maintained at 0°C for 30 minutes, then treated with hexamethylphosphoric triamide (5.0 cm³, 4.5g, 0.025 moles). The resulting solution was stirred at 0°C for a further 15 minutes;

after this time, a solution of 4,4'-dimethyl-2,2'-bipyridine (4.61g, 0.025 moles) in dry THF (100 cm³) was added to the reaction mixture over a period of 5 minutes. After 30 minutes at 0°C, the reaction mixture was treated with ethylene oxide (1.09g, 0.025 moles) in dry THF (15 cm³). The resulting mixture was stirred for 1 hour at 25°C and then poured into 10% hydrochloric acid (100 cm³) giving a two layered system. The layers were separated and the aqueous layer was made basic with solid sodium hydroxide pellets. The basic solution was extracted with diethyl ether. The combined organic extracts were washed with water, dried over magnesium sulphate and concentrated to give a yellow oil. This oil appeared to decompose with time, giving a brown oil.

¹H nmr spectroscopy (CDCl₃) appeared to have the signals required for the product; however, further examination of the spectra and the integration showed that the oil may be a small quantity of starting material, with the major product being an alkyl hydroxy chain not attached to the bipyridine ring.

Due to the lack of clarity of the ¹H nmr it was decided to further purify the product by Kugel distillation; however, this resulted in decomposition of the product.

Preparation of bis(2,2'-bipyridine)(4-[3-hydroxypropyl]-4'-methyl-2,2'-bipyridine) ruthenium (II) hexafluorophosphate (35) [15]

cis-dichloro bis (2,2'-bipyridine) ruthenium (II) (484 mg, 1 mmol) and 4-(3-hydroxypropyl)-4'-methyl-2,2'-bipyridine (273.9 mg, 1.2 x 10⁻³ moles, a slight excess is used to allow for the impurities present), were heated together in ethanol (250 cm³) under reflux for 19 hours. After this time a clear red solution was obtained, which on TLC (silica; MeOH) showed no presence of starting material, only indicating a slow running red spot, characteristic of a tris bipyridine ruthenium complex. The reaction mixture was filtered hot, treated with a solution of ammonium hexafluorophosphate (1g) in methanol (20 cm³) and

allowed to cool. As no crystals were obtained on cooling, a few drops of concentrated hydrochloric acid were added and the solution left at 2-4°C overnight. After this time red crystals had precipitated out, which were collected by filtration (0.04g, 40% yield based on cis-dichloro bis(2,2'-bipyridine) ruthenium (II)).

Anal. Calcd. for $\text{RuC}_{34}\text{H}_{36}\text{N}_6\text{O}_3\text{P}_2\text{F}_{12}$: Theory C, 42.20; H, 3.74; N, 8.68%. Found C, 42.51; H, 3.37; N, 8.85%.

^{13}C nmr (acetone-d₆) : 158.53 ppm (C₂, unsubstituted bipyridine, quaternary), 158.07 ppm (C₂, substituted bipyridine, quaternary), 155.99 ppm (C₄, 3-hydroxypropyl substituted bipyridine, quaternary), 152.84 ppm, 152.15 ppm, and 151.95 ppm (C₆, carbon signals), 151.69 ppm (C₄, methyl substituted bipyridine, quaternary), 138.99 ppm (C₄, unsubstituted bipyridine), 129.75 ppm (C₅, substituted bipyridine), 128.97 ppm (C₅, unsubstituted bipyridine), 126.30 ppm (C₃, substituted bipyridine), 125.52 ppm (C₃, unsubstituted bipyridine). Aliphatic signals; 21.16 ppm (pyr-CH₃), 61.52 ppm (-CH₂CH₂CH₂OH), -CH₂CH₂CH₂OH signals probably under acetone-d₆ signal.

Preparation of *cis*-dichloro (4,4'-diphenyl-2,2'-bipyridine) ruthenium (II) (36)

A mixture of ruthenium trichloride trihydrate (0.42g, 1.62×10^{-3} moles) 4,4'-diphenyl-2,2'-bipyridine (1.0g, 3.24×10^{-3} moles) and lithium chloride (anhyd.) (0.85g, 0.02 moles) in DMF (9 cm³) was heated under reflux for 5½ hours, under a nitrogen atmosphere.

The reaction mixture was allowed to cool to room temperature overnight, maintaining a nitrogen atmosphere over the reaction. The solution was then cooled to below room temperature and acetone (43 cm³) was added with stirring to the reaction mixture. The resulting solution was left at 2-4°C until a black precipitate had formed. The precipitate was removed by filtration, washed with water, then with ether to yield a dark

brown/black solid (0.85g, 64% yield based on ruthenium trichloride trihydrate).

Anal. Calcd. for $C_{44}H_{34}N_4Cl_2ORu$: Theory C, 65.51; H, 4.25; N, 6.95%. Found C, 66.36; H, 3.99; N, 7.18%.

Preparation of bis(4,4'-diphenyl-2,2'-bipyridine)(4-[3-hydroxypropyl]-4'-methyl-2,2'-bipyridine) ruthenium (II) hexafluorophosphate (37) [15]

cis-dichloro bis(4,4'-diphenyl-2,2'-bipyridine) ruthenium (II) (824.7 mg, 1 mmol) and 4-(3-hydroxypropyl)-4'-methyl-2,2'-bipyridine (273.9 mg, 1.2×10^{-3} moles, excess used due to impurities present in this material) were heated together in ethanol (250 cm³) under reflux for 20 hours, after which time a red solution was obtained. TLC, (silica ; MeOH), of the reaction mixture exhibited a fast running red spot and a faint baseline spot, probably starting material. The reaction mixture was then filtered hot, treated with a solution of ammonium hexafluorophosphate (1g) in methanol (20 cm³) and allowed to cool. A black precipitate formed on cooling, which was probably unreacted starting material; this was removed by filtration, a few drops of concentrated hydrochloric acid were added to the filtrate, and the resulting solution was left at 2-4°C overnight. After this time, a red microcrystalline solid had precipitated out, and this was collected by filtration (0.47g, 37% yield based on cis-dichloro bis (4,4'-diphenyl-2,2'-bipyridine) ruthenium (II)).

Anal. Calcd. for $C_{58}H_{50}N_6O_2P_2F_{12}Ru$: Theory C, 55.55; H, 4.02; N, 6.70%. Found C, 56.02; H, 3.90; N, 6.70%.

¹³C nmr (acetone-d₆) : 159.05 ppm (C₂, phenyl-bipyridine, quaternary), 158.07 ppm (C₂, alkyl-hydroxy bipyridine, quaternary), 155.99 ppm (C₄, attached to alkyl chain of alkyl-hydroxy bipyridine, quaternary), 153.06 ppm, 151.69-150.65 ppm (C₆, three signals from bipyridine ligands), 151.69 ppm (C₄, attached to methyl group of alkyl-hydroxy bipyridine, quaternary), 150.65 ppm and 137.04 ppm (C₄ of pyridine ring of phenyl bipyridine, quaternary and quaternary carbon on phenyl

ring of phenyl-bipyridine), 131.51 ppm, 126.23 ppm, and 123.11 ppm (phenyl carbons of phenyl-bipyridine), 131.51 ppm (C_5 , phenyl bipyridine), 129.82 ppm (C_4 , alkyl-hydroxy bipyridine), 129.17 ppm (C_3 , alkyl-hydroxy bipyridine), 128.58 ppm (C_3 , phenyl bipyridine). Impurity 125.78 ppm. Aliphatic signals, 61.52 ppm (-CH₂CH₂CH₂OH), 21.22 ppm (pyr-CH₃), -CH₂CH₂CH₂OH signals probably under acetone-d₆ signal.

Preparation of 4-vinyl-4'-methyl-2,2'-bipyridine (39) [25]

To a solution of diisopropylamine (3.8 cm³, 0.028 moles) in dry THF (30 cm³) was added n-butyl lithium (13.77 cm³, 0.027 moles of a 1.96M solution) at 0°C under nitrogen. This was followed by the dropwise addition of 4,4'-dimethyl-2,2'-bipyridine (5g, 0.027 moles) in dry THF (117 cm³). After the resulting deep brown reaction mixture had been stirred for 15 minutes at 0°C, (chloromethyl)methyl ether (2.3 cm³, 0.03 moles) in dry THF (20 cm³) was added dropwise. The reaction mixture slowly changed colour to give a pale yellow solution. The reaction mixture was stirred at 0°C for 30 minutes, quenched with water (30cm³) and saturated sodium hydrogen carbonate solution (17 cm³), and ether (50 cm³) added. Following two additional ether extractions (2 x 50 cm³), the combined ether extracts were dried over sodium sulphate and concentrated, to give a pale yellow oil. This oil was then filtered through a flash grade silica gel (ether elution), concentrated in vacuo and left standing at room temperature for 2-3 days, after which time unreacted starting material deposited as white crystals, leaving an orange-red oil (2.15g, 35% yield based on 4,4'-dimethyl-2,2'-bipyridine).

¹H nmr (CDCl₃) : 2.20 δ (3H; singlet; pyr-CH₃), 2.63-2.87 δ (2H; triplet; pyr-CH₂CH₂OCH₃), 3.13 δ (3H; singlet; pyr-CH₂CH₂OCH₃), 3.37-3.60 δ (2H; triplet; pyr-CH₂CH₂OCH₃), 6.80-8.43 δ (6H; aromatic, including 6.80-7.03 δ, multiplet, 2H, 8.06-8.17 δ, multiplet, 2H, 8.30-8.43 δ, multiplet, 2H). Impurities are present in the aliphatic region at approximately 1.0 δ.

To a solution of the oil isolated above (2.15g, 9.42 x 10⁻³ moles) in dry THF (55 cm³) at -78°C under nitrogen, was added

dropwise potassium t-butoxide (2.13g, 0.017 moles) in dry THF (36 cm³). After the reaction mixture had been stirred for 1½ hours at -78°C and at room temperature for an additional 15 minutes, the reaction was quenched with water (26 cm³) and extracted with ether (3 x 51 cm³). The combined ether extracts were dried over sodium sulphate and the ether was removed under vacuum, to give a pale orangey-brown solid. Following filtration through a 5cm column of 230-400 mesh silica gel (ether elution), to remove polymeric impurities, the resulting pale yellow solid was recrystallised from ether/hexane to yield a white crystalline solid (0.82g, 44% yield based on the methoxyethyl derivative of 4,4'-dimethyl-2,2'-bipyridine).

Anal. Calcd. for C₁₃H₁₂N₂ : Theory C, 79.56; H, 6.16; N, 14.27%. Found C, 79.03; H, 6.37; N, 14.15%.

¹H nmr (CDCl₃) : 2.30 δ (3H; singlet; pyr-CH₃), 5.27-6.70 δ (3H; complex consisting of 5.27 δ, doublet; 5.43 δ, doublet; 5.77 δ, doublet; 6.07 δ, doublet; 6.43 δ, singlet; 6.60 δ, singlet; 6.70 δ, singlet; vinyl protons), 8.13-8.53 δ (6H; aromatic, including 6.93-7.20 δ, multiplet, 8.13 δ, singlet, 8.30-8.53 δ, multiplet).

Preparation of bis(2,2'-bipyridine)(4-vinyl-4'-methyl-2,2'-bipyridine) ruthenium (II) hexafluorophosphate (40) [21]

A mixture of cis-dichloro bis(2,2'-bipyridine) ruthenium (II) (468.2 mg, 8.997 × 10⁻⁴ moles)(4-vinyl-4'-methyl-2,2'-bipyridine (176.6 mg, 8.997 × 10⁻⁴ moles) and sodium hydrogen carbonate (0.27g, 3.21 × 10⁻³ moles) in a methanol-water solution, 2:3, (21 cm³, i.e. 3.4 cm³ methanol, 12.6 cm³ water), was heated under reflux for 20 hours under nitrogen. After this time, TLC (silica; MeOH) indicated no presence of the faster running purple starting material. The reaction mixture was filtered hot and a solution of ammonium hexafluorophosphate (1g) in methanol (20 cm³) was added; this resulted in the precipitation of a red solid. An attempt to recrystallise this solid from dichloromethane/acetone, however, gave a red oil, which, when the solvent was removed under vacuum, slowly solidified.

This solid was then recrystallised from ethanol/dichloromethane yielding a red solid (0.46g, 55.71% yield based on cis-dichloro bis (2,2'-bipyridine) ruthenium (II)).

Anal. Calcd. for $C_{33}H_{30}N_6OP_2F_{12}Ru$: Theory C, 43.19; H, 3.30; N, 9.16%. Found C, 43.39; H, 3.27; N, 8.98%.

Infra-red (KBr disc) : 3084 cm^{-1} (C-H str., asymm., vinyl, broad), 1618 cm^{-1} (C=C str., vinyl, sharp), 1482 cm^{-1} (C-H str., aromatic, sharp).

Preparation of bis(2,2'-bipyridine)(4,4'-dimethyl-2,2'-bipyridine) ruthenium (II) chloride (41)

A mixture of cis-dichloro bis(2,2'-bipyridine) ruthenium (II) (999.7 mg, 1.92×10^{-3} moles) and 4,4'-dimethyl-2,2'-bipyridine (353.0 mg, 1.92×10^{-3} moles) in ethanol (250 cm^3) was heated under reflux under nitrogen for 48 hours. After this time, the reaction mixture was cooled to room temperature and the solvent was removed under reduced pressure to give a red solid. This solid was dissolved in DMF (5 cm^3) and acetone (60 cm^3) was added, precipitating out a red-orange solid which was collected by filtration (1.22g, 89% yield based on cis-dichloro bis(2,2'-bipyridine) ruthenium (II)).

Infra-red (KBr disc) : 3409 cm^{-1} (water of crystallisation), 1601 cm^{-1} and 1462 cm^{-1} (C=C str., aromatic, sharp).

^{13}C nmr (DMSO-d₆) : 156.83 ppm (C₂, unsubstituted bipyridine, quaternary), 156.25 ppm (C₂, substituted bipyridine, quaternary), 151.30 and 150.00 ppm (C₆, carbon signals), 150.39 ppm (C₄, substituted bipyridine, quaternary), 137.89 ppm (C₄, unsubstituted bipyridine), 128.71 ppm (C₅, substituted bipyridine), 127.93 ppm (C₅, unsubstituted bipyridine), 125.32 ppm (C₃, substituted bipyridine), 124.61 ppm (C₃, unsubstituted bipyridine), 20.64 ppm (pyr-CH₃).

Preparation of bis(2,2'-bipyridine)(4,4'-diphenyl-2,2'-bipyridine) ruthenium (II) hexafluorophosphate (43) [15]

A mixture of cis-dichloro bis(2,2-bipyridine) ruthenium (II) (458 mg, 8.805×10^{-4} moles) and 4,4'-diphenyl-2,2'-bipyridine (272 mg, 8.805×10^{-4} moles) in ethanol (250 cm^3) was heated under reflux under a nitrogen atmosphere, and the reaction was monitored by TLC (silica:MeOH). After 26 hours, TLC indicated only a trace of starting material, (fast running purple spot at solvent front). The reaction mixture was filtered hot, treated with a solution of ammonium hexafluorophosphate (1g) in methanol (20 cm^3) and allowed to cool. On cooling red crystals precipitated out, which were collected by filtration. This solid was recrystallised from ethanol to give a red crystalline solid (0.66g, 73% yield based on cis-dichloro bis(2,2'-bipyridine) ruthenium (II)).

Anal. Calcd. for $\text{C}_{42}\text{H}_{34}\text{N}_6\text{OP}_2\text{F}_{12}\text{Ru}$: Theory C, 48.99; H, 3.33; N, 8.16%. Found C, 48.94; H, 3.11; N, 7.86%.

Infra-red (KBr disc) : 1613 cm^{-1} and 1446 cm^{-1} (C=C str., aromatic, sharp).

^1H nmr (acetone-d₆) : Only aromatic protons are observed in the region 7.57-9.33 δ , as a complex multiplet.

Preparation of 4,4'-dibromo-2,2'-bipyridine (45)

Procedure according to Maerker and Case [13].

To a suspension of 4,4'-dinitro-2,2'-bipyridine N,N'-dioxide (1.0g, 3.59×10^{-3} moles) in glacial acetic acid at 60°C , was added acetyl bromide (7.8 cm^3 , 12.97g, 0.11 moles) and the mixture was heated under reflux for 2 hours. After approximately 30 minutes of heating, a yellow precipitate formed and a brown gas was evolved. The reaction mixture was cooled to room temperature, poured on to approximately 140g of ice, and the resulting mixture was brought to neutral pH with 15% sodium

carbonate solution. This resulted in the precipitation of a pale yellow solid which was collected by filtration (0.85g, crude 4,4'-dibromo-2,2'-bipyridine N,N'-dioxide).

A suspension of crude 4,4'-dibromo-2,2'-bipyridine N,N'-dioxide (0.85g, 2.46×10^{-3} moles) in anhydrous chloroform (22 cm^3) was cooled to -3°C and phosphorus tribromide (3.4 cm^3 , 9.69g, 0.036 moles) was added. The mixture was then brought to reflux for 1 hour. During this time a yellow solid remained. The mixture was allowed to cool to room temperature and poured into an ice-water mixture. After phase separation, the chloroform layer was extracted repeatedly with water, and the aqueous extracts were combined with the water layer from the reaction mixture. At this point neutralisation of the aqueous solution with 25% sodium hydroxide was supposed to give a white precipitate; however, no such precipitate was obtained and the method was abandoned.

Procedure with excess of acetyl bromide

To a suspension of 4,4'-dinitro-2,2'-bipyridine N,N'-dioxide (4.30g, 0.015 moles) in glacial acetic acid (67 cm^3), was added acetyl bromide (44 cm^3 , 0.60 moles) and the reaction mixture was heated to 100°C for 2 hours. During this time the solution became clear, then precipitated out a dark brown solid, and a brown gas was evolved from the reaction mixture. The mixture was then cooled to room temperature, the liquid decanted off and poured on to ice (287g). The solution thus obtained was neutralised with sodium hydroxide solution (30%) to give a yellow precipitate, which was collected by filtration, washed with water and air-dried. The wet solid appeared to be slightly air sensitive.

Anal. Calcd. for $\text{C}_{10}\text{H}_6\text{N}_2\text{O}_2\text{Br}_2$: Theory C, 34.71; H, 1.74; N, 8.09%. Found C, 31.83; H, 1.67; N, 7.64%.

Procedure as per reference [26]

To a suspension of 4,4'-dinitro-2,2'-bipyridine N,N'-dioxide (4.60g, 0.017 moles) in glacial acetic acid (68 cm³) at 60°C, was added acetyl bromide (36 cm³, 59.87g, 0.49 moles) dropwise. The temperature of the solution was then increased slowly to reflux temperature on a water bath and maintained at reflux for 2 hours. The solution was cooled to room temperature, poured on to ice (678.69g) and then neutralised with 15% sodium carbonate. The resulting precipitate formed was filtered off and dried in an oven at 90°C to give crude 4,4'-dibromo-2,2'-bipyridine N,N'-dioxide.

A suspension of crude 4,4'-dibromo-2,2'-bipyridine N,N'-dioxide (2.0g, 5.83 x 10⁻³ moles) in chloroform (52 cm³) was cooled to -3°C and phosphorus tribromide (8 cm³, 0.044 moles) was added. The mixture was then brought to reflux with stirring on a water bath and maintained at this temperature for 1.25 hours. The reaction mixture was then cooled to room temperature and poured into an ice-water mixture. After phase separation the chloroform layer was extracted repeatedly with water and the aqueous extracts were combined with the water layer from the reaction mixture. Neutralisation of this aqueous solution with 25% sodium hydroxide, caused separation of a white precipitate, which, after cooling of the mixture to 0°C, was isolated by filtration and washed thoroughly with water. The crude solid was then recrystallised from pet.ether 60/80°, to give pale yellow crystals (0.30g, 17% yield based on 4,4'-dinitro-2,2'-bipyridine N,N'-dioxide).

Anal. Calcd. for C₁₀H₆N₂Br₂ : Theory C, 38.25; H, 1.92; N, 8.92%. Found C, 38.43; H, 1.79; N, 8.76%.

Preparation of bis(2,2'-bipyridine)(4,4'-dibromo-2,2'-bipyridine) ruthenium (II) hexafluorophosphate (46) [15]

A mixture of cis-dichloro bis(2,2'-bipyridine) ruthenium (II) (340.6 mg, 6.55 x 10⁻⁴ moles) and 4,4'-dibromo-2,2'-bipyridine (203.8 mg, 6.55 x 10⁻⁴ moles) in ethanol (176 cm³) was heated under reflux for 48 hours.

After this time, TLC (silica:MeOH), indicated a small quantity of starting material. The resulting dark red solution was filtered hot, treated with a solution of ammonium hexafluorophosphate (1g) in methanol (20 cm³) and allowed to cool. On cooling, red crystals precipitated out, which were collected by filtration (0.55g, 81% yield based on *cis*-dichloro bis(2,2'-bipyridine) ruthenium (II)).

Anal. Calcd. for C₃₀H₂₄N₆Br₂OP₂F₁₂Ru : Theory C, 34.80; H, 2.34; N, 8.12%. Found C, 34.81; H, 2.24; N, 7.78%.

Infra-red (KBr disc) : 1592 cm⁻¹ and 1460 cm⁻¹ (C=C str., aromatic, sharp).

¹³C nmr (acetone-d₆) : 158.59 ppm (C₂, substituted bipyridine, quaternary), 158.27 ppm (C₂, unsubstituted bipyridine, quaternary), 153.65 ppm, 153.25 ppm, and 152.86 ppm (C₆ carbon signals), 139.39 ppm (C₄, unsubstituted bipyridine), 134.96 ppm (C₄, substituted bipyridine, quaternary), 132.35 ppm (C₅, substituted bipyridine), 129.49 ppm (C₃, substituted bipyridine), 129.04 ppm (C₅, unsubstituted bipyridine), 125.52 ppm (C₃, unsubstituted bipyridine).

Preparation of di-t-butyl-(2,2'-bipyridine)-4,4'-dicarboxylate (48)

METHOD 1

Distilled thionyl chloride (134 cm³) was added in excess to (2,2'-bipyridine)-4,4'-dicarboxylic acid (2.00g, 8.6 x 10⁻³ moles) and the reaction mixture was heated under reflux for 20 hours. The solution was then allowed to cool to room temperature and thionyl chloride was removed under reduced pressure. However, analysis of the solid obtained, indicated that there was a vast excess of thionyl chloride still present. Several further attempts were made to remove the thionyl chloride completely, but all failed.

Addition of the solid formed above (0.25g, 8.94×10^{-4} moles) to t-butanol (0.10g, 1.38×10^{-3} moles) in a slight excess of 8% sodium hydroxide solution (0.75 cm³), resulted in the evolution of HCl, but only the diacid was recovered from the reaction mixture.

METHOD 2 [4]

(2,2'-bipyridine)-4,4'-dicarboxylic acid (0.33g, 1.36×10^{-3} moles), t-butyl alcohol (11 cm³) and concentrated sulphuric acid (1.25g) were heated together at reflux for 18 hours. Only the diacid starting material was recovered from the reaction mixture.

Preparation of dimethyl(2,2'-bipyridine)-4,4'-dicarboxylate (49)[4]

(2,2'-bipyridine)-4,4'-dicarboxylic acid (1.92g, 7.93×10^{-3} moles), methanol (31 cm³), and concentrated sulphuric acid (7.30g), were heated together at reflux for 18 hours.

The reaction mixture was allowed to cool to room temperature and poured on to water (77 cm³). A precipitate was formed, which was removed by filtration and recrystallised from methanol to give a white crystalline solid (0.85g, 39% yield based on (2,2'-bipyridine)-4,4'-dicarboxylate).

Anal. Calcd. for C₁₄H₁₂N₂O₄ : Theory C, 61.76; H, 4.44; N, 10.28%. Found C, 61.54; H, 4.45; N, 10.12%.

¹H nmr (CDCl₃) : 3.92 δ (6H; singlet; pyr-C-OCH₃), 7.80-8.84 δ (6H; multiplet; aromatic).

Preparation of bis(2,2'-bipyridine)(diethyl[2,2'-bipyridine]-4,4'-dicarboxylate)ruthenium (II) hexafluorophosphate (50) [15]

A mixture of cis-dichloro bis(2,2'-bipyridine) ruthenium (II) (484 mg, 1 mmol) and diethyl(2,2'-bipyridine)-4,4'-dicarboxylate (300.3 mg, 1 mmol) in ethanol (250 cm³) was heated under reflux for 22 hours.

After this time, TLC (silica:MeOH) indicated one slow-running spot just above the baseline. The reaction mixture was filtered hot, treated with a solution of ammonium hexafluorophosphate (1g) in methanol (20 cm³) and allowed to cool. Dark red crystals precipitated out slowly, which were collected by filtration (0.37g, 36% yield based on *cis*-dichloro bis(2,2'-bipyridine) ruthenium (II)).

Anal. Calcd. for C₃₆H₃₆N₆O₆P₂F₁₂Ru : Theory C, 41.59; H, 3.30; N, 8.08%. Found C, 41.01; H, 3.18; N, 8.30%.

Infra-red (KBr disc) : 1731 cm⁻¹ (C=O str., aromatic ester, sharp), 1299 cm⁻¹ and 1145 cm⁻¹ (C-O str., aromatic ester, sharp).

¹³C nmr (acetone-d₆) : 164.52 ppm (C₂, unsubstituted bipyridine, quaternary), 159.24 ppm (C₂, substituted bipyridine, quaternary), 158.27 ppm (-C-OEt, quaternary), 154.17 ppm, 153.25 ppm, and 152.93 ppm (C₆ carbon signals), 139.97 ppm (C₄, substituted bipyridine, quaternary), 139.776 ppm (C₄, unsubstituted bipyridine), 129.23 ppm (C₅, unsubstituted bipyridine), 127.93 ppm (C₅, substituted bipyridine), 125.78 ppm (C₃, unsubstituted bipyridine), 124.94 ppm (C₃, substituted bipyridine), 63.41 ppm and 27.93 ppm (ethyl ester aliphatic carbon signals).

Preparation of bis(2,2'-bipyridine)(dimethyl[2,2'-bipyridine]-4,4'-dicarboxylate)ruthenium (II) hexafluorophosphate (51) [15]

A mixture of *cis*-dichloro bis(2,2'-bipyridine) ruthenium (II) (484.0 mg, 1 mmol), dimethyl (2,2'-bipyridine)-4,4'-dicarboxylate (272.3 mg, 1 mmol) in ethanol (250 cm³) was heated under reflux for 22 hours. After this time, TLC (silica:MeOH) indicated one slow-running spot just above the baseline. The reaction mixture was filtered hot, treated with a solution of ammonium hexafluorophosphate (1g) in methanol (20 cm³) and allowed to cool, during which time dark red crystals precipitated out, which were collected by filtration.

¹³C nmr analysis of this compound showed that it was not in fact the methyl ester complex, but the ethyl ester derivative.

REFERENCES

1. COOK, M.J., LEWIS, A.P., McAULIFFE, G.S.G., SKARDA, V. and THOMSON, A.J., (1984), J. Chem. Soc. Perkin Trans. II, 1303.
2. FABIAN, R.H., KLASSEN, D.M. and SONNTAG, R.W., (1980), Inorg. Chem., 19, 1977.
3. NAKAMARU, K., (1982), Bull. Chem. Soc. Jpn., 55, 2697.
4. WHITTLE, C.P., (1977), J. Heterocyclic Chem., 14, 191.
5. BADGER, G.M. and SASSE, W.H.F., (1956), J. Chem. Soc., 616.
6. SASSE, W.H.F. and WHITTLE, C.P., (1961), J. Chem. Soc., 1347.
7. CASE, F.H., (1946), J. Am. Chem. Soc., 68, 2574.
8. KRÖHNKE, F., (1976), Synthesis, 1.
9. KRÖHNKE, F. and GROSS, K.F., (1959), Chem. Ber., 92, 24.
10. KING, L.C., (1944), J. Am. Chem. Soc., 66, 894.
11. HUANG, T.L.J. and BREWER, D.G., (1981), Can. J. Chem., 59, 1689.
12. PARKER, D., University of Durham, Private communication.
13. MAERKER, G. and CASE, F.H., (1958), J. Am. Chem. Soc., 80, 2745.
14. ANDERSON, S., CONSTABLE, E.C., SEDDON, K.R., TURP, J.E., BAGGOTT, J.E. and PILLING, M.J., (1985), J. Chem. Soc. Dalton Trans., 2247.
15. CONSTABLE, E.C., (1984), Inorg. Chem. Acta, 82, 53.
16. HAGINIWA, J., (1955), J. Pharm. Soc., Jpn., 71, 263. C.A., 50, 3435, (1956).
17. JONES, R.A., RONEY, B.D., SASSE, W.H.F. and WADE, K.O., (1967), J. Chem. Soc. (B), 106.
18. SKARZEWSKI, J. and MLOCHOWSKI, J., (1979), Heterocycles, 12, 1403.
19. McAULIFFE, G.S.G., (1980), MSc. Thesis, University of East Anglia.
20. COOK, M.J., LEWIS, A.P., McAULIFFE, G.S.G., SKARDA, V., THOMSON, A.J., GLASPER, J.L. and ROBBINS, D.J., (1984), J. Chem. Soc. Perkin Trans. II, 1293.

21. GHOSH, P.K. and SPIRO, T.G., (1980), J. Am. Chem. Soc., 102, 5543.
22. KAISER, E.M. and PETTY, J.D., (1975), Synth. Comm., 705.
23. TRAUT, R.R., BOLLEN, A., SUN, T-T., HERSEY, J.W.B., SUNBERG, J. and PIERCE, L.R., (1973), Biochem., 12, 3266.
24. DUNCAN, R.J.S., WESTON, P.D. and WRIGGLESWORTH, R., (1983), Anal. Biochem., 132, 68.
25. ABRUNA, H.D., BREIKSS, A.I. and COLLUM D.B., (1985), Inorg. Chem., 24, 987
26. COOK, M.J., University of East Anglia, Private Communication.

CHAPTER 2

LUMINESCENCE AND THE LUMINESCENT PROPERTIES OF SUBSTITUTED TRIS-(2,2'-BIPYRIDINE) RUTHENIUM (II) COMPLEXES

2:0:0 INTRODUCTION

In the following sections we consider the properties of light itself, the interaction of light with molecular systems, the nature of the resulting excited molecules, and finally their physical reactions.

2:0:1 THE NATURE OF LIGHT

To account for the interaction of light with matter, it is necessary to regard light as either a collection of particles or waves; ie, to apply the theory of the wave particle duality of light. According to the electromagnetic theory of Maxwell, light forms waves by displacements of varying electric and magnetic fields. These electric and magnetic oscillations take place in directions at right angles to one another and to the direction of travel. The interaction of light with matter is, therefore, due to interactions between the electric oscillations of the waves and the electrons of the atoms. The wave properties of light are related by the equation (1):

$$\lambda\nu = c \quad (\text{Eqn. 1})$$

ν = frequency

λ = wavelength

c = velocity of light in vacuo ($3.00 \times 10^8 \text{ ms}^{-1}$)

The processes of absorption and emission can only be explained by the application of Quantum Theory. The basis of this is that radiant energy can only be absorbed in definite units or quanta and this can be related to Equation (1) as follows:-

$$E = h\nu = hc/\lambda \quad (\text{Eqn. 2})$$

E = energy per photon

h = Planck's constant ($6.62 \times 10^{-34} \text{ Js}$)

It is convenient to have a unit of radiant energy, which is equivalent to 6.023×10^{23} photons. This is defined as an

Einstein. The visible portion of the spectrum extends from 400 to 700 nm, so, due to the Planck relationship (Eqn. 2) an Einstein represents about 300 to 170 kJmol^{-1} , respectively, at these extremes.

2:0:2 PRINCIPLES OF PHOTOCHEMISTRY

A quantitative study of the photochemistry of molecules has led to the derivation of two principal laws.

The first law states, that only optical irradiation that is absorbed by the reacting system can be effective in producing chemical changes. In terms of molecular species, applying quantum theory, only those molecules which absorb the incident light, can undergo primary excited-state events.

The second law states, that one photon or light quantum, can excite one molecule. Molecules endowed with excitation energy, $h\nu$, are often reactive and short-lived. In studying such species, two general types of quantitative measurements have been made:

- i) Absolute rates of reaction and decay.
- ii) Efficiency of the decay or reaction process, based on the number of photons absorbed.

The efficiency of a light-induced process is the quantum yield Φ , defined according to Equation 3.

$$\Phi = \frac{\text{molecules undergoing the process}}{\text{photons absorbed by the molecules}} \quad (\text{Eqn. 3})$$

Light emission generally arises from only two of the processes that take place after the primary act of light absorption, and the quantum efficiency of photo-luminescence never exceeds unity.

2:1:1 MECHANISMS OF PHOTOLUMINESCENCE

As with the duality treatment of light, it is also necessary to treat the electrons and nuclei of atoms as both electrically charged particles and as waves. This duality of electrons is expressed mathematically in the Schrödinger equation, a differential equation, whose particular solutions for any one system represent the energies of the various possible states, or energy levels, in which the system can exist.

The absorption of a photon of light by an atom or molecule can, therefore, only occur if the energy of the photon is exactly equal to the energy difference between two existing energy levels of the system concerned:-

$$h\nu = E_2 - E_1 \quad (\text{Eqn. 4})$$

The vibrational and rotational motions of a molecule are also quantised, ie. vibrational and rotational energy can be taken up or lost only in discrete quantum units. Thus the total energy of a particular state of a molecule may be represented as follows:-

$$\begin{aligned} E &= E_e + E_v + E_r \quad (\text{Eqn. 5}) \\ E &= \text{Total energy} \\ E_e &= \text{Electronic excitation energy} \\ E_v &= \text{Vibrational energy} \\ E_r &= \text{Rotational energy} \end{aligned}$$

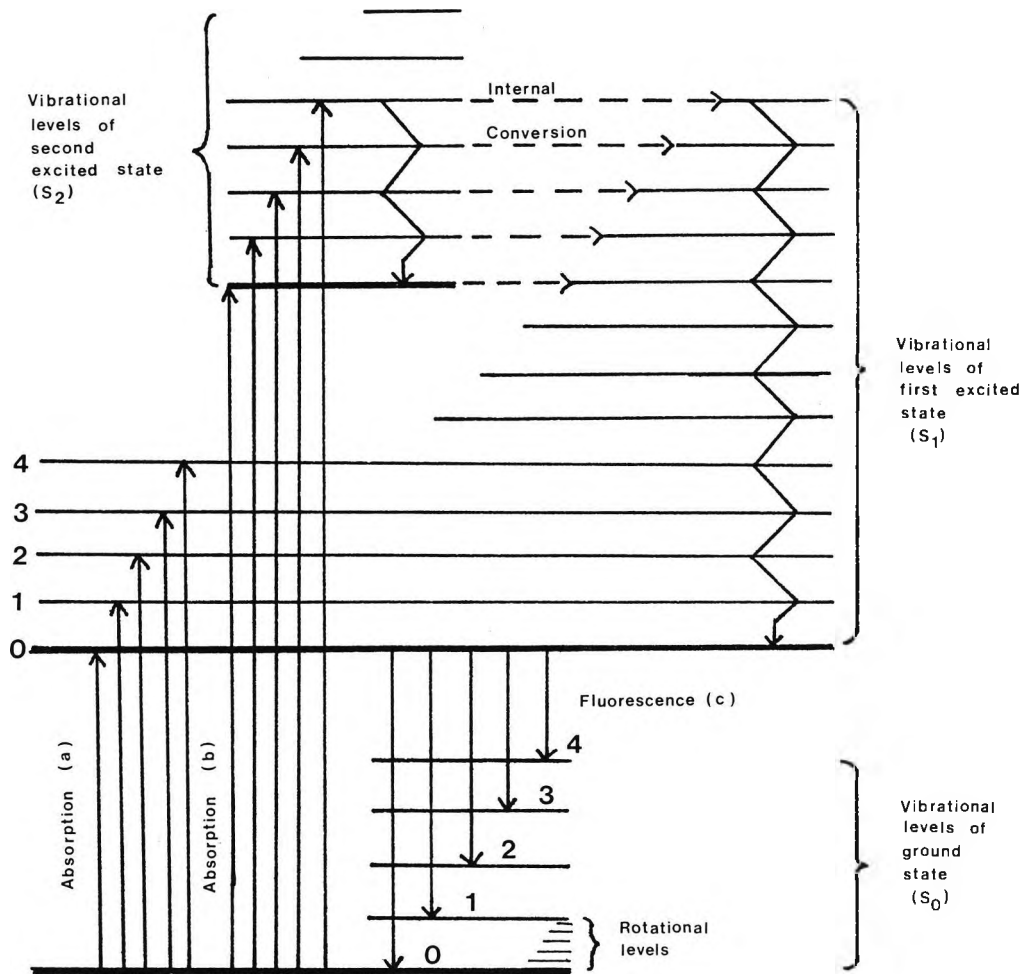
Expansion of Equation 5 gives:-

$$h\nu = \Delta E_e + \Delta E_v + \Delta E_r \quad (\text{Eqn. 6})$$

The energy required to excite each level is as follows:-

$$E_e > E_v > E_r$$

Fig. 2-1 Diagram Showing Vibrational Levels Of The Excited State



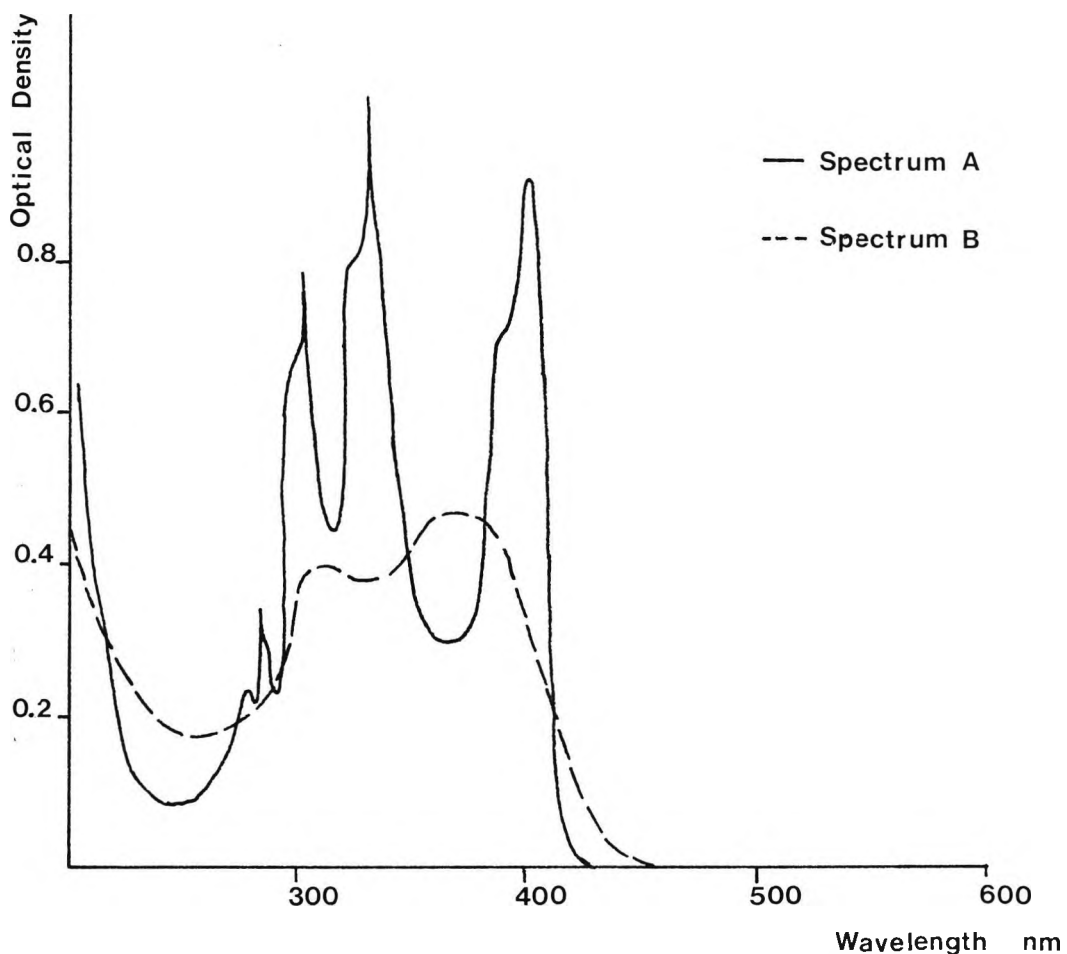
2:1:2 FLUORESCENCE

Fluorescence is the commonest photoluminescence. At room temperature, most molecules are in the lowest vibrational level of the ground state (0 of S_0). It is from this state that transitions take place upwards on the absorption of light (transitions a and b in Fig. 2-1). The rotational levels for all molecules in solution are so closely spaced that they cannot be easily distinguished spectroscopically.

The absorption spectra of molecules vary according to the complexity of their vibrational levels. If these levels are

comparatively simple, the spectrum appears as a series of well separated maxima (Fig. 2-2A).

Fig. 2-2 Example of a Molecular Absorption Spectrum



However, with molecules which possess complex vibrational levels, a broad absorption band is seen, (Fig. 2-2B), due to all the transitions - (a) in Fig. 2-1 - to the various vibrational levels of the first excited state. Another broad absorption band is also seen at shorter wavelengths, corresponding to transitions to vibrational-rotational levels of the second electronic excited state.

When most systems are raised to an upper electronic state higher than the first, they undergo internal conversion, whereby the molecule passes from a low vibrational level of the upper state

to a high vibrational level of the lower state, retaining the same total energy (Fig. 2-1). Once internal conversion has occurred, the molecule loses excess vibrational energy by collision with solvent molecules. Therefore, all energy transitions to levels higher than that of the lowest vibrational level of the first excited state, rapidly fall to this level. Some reactions do occur at higher levels, but they must take place rapidly to compete with internal conversion and loss of vibrational energy by collision. Similarly, for light emission from the upper states to be appreciable, it would have to come from a rapid process, and therefore, such emissions are rarely seen. However, light emission or chemical reaction from the lowest vibrational level of the first excited state does not need to be so rapid, as internal conversion from here to the ground state is a relatively slow process.

From the vibrational level 0 of the first excited state (S_1) (Fig. 2-1), the molecule may return to any one of the vibrational-rotational levels of the ground state with the emission of fluorescence. If all excited molecules return to the ground state in this way, the quantum yield is unity. However, if other mechanisms are used to achieve the ground state, eg. photochemical reaction or singlet to triplet transition, there is a corresponding decrease in the quantum yield.

At room temperature, absorption is mainly from the lowest vibrational level of the ground state and emission is usually from the lowest vibrational level of the first excited singlet state. Therefore, only one transition, the 0-0 transition, is common to both the emission and absorption spectra, all other transitions in absorption (as in Fig. 2-1), requiring more energy than all the transitions observed in the emission spectrum. The fluorescence emission spectrum, therefore, overlaps the longest wavelength absorption band at the wavelength corresponding to the 0-0 transition and the rest of the spectrum lies to the long wavelength side of the first absorption band.

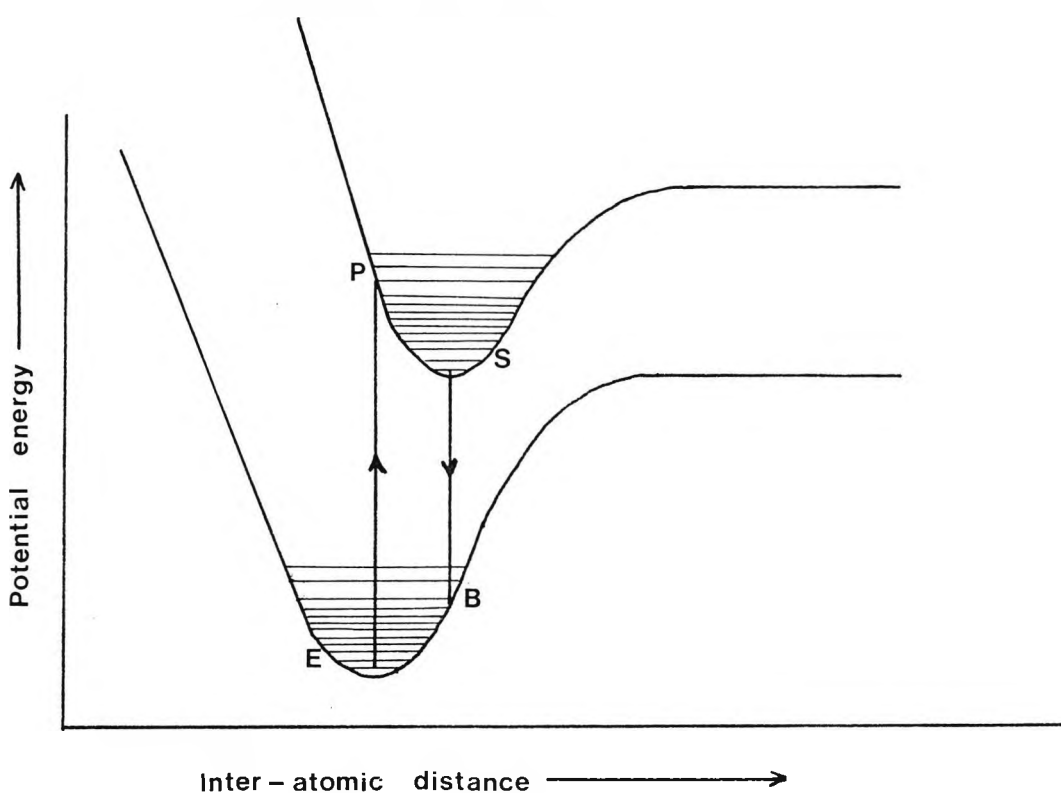
Frequently, the emission is an approximate mirror image of the first absorption band, because the distribution of the vibrational levels of the first excited state, which determine the shape of the first absorption band is often similar to the distribution of vibrational levels in the ground state, that determines the shape of the fluorescence emission spectrum. It is found, that the wavelength of emission is always longer than that of the exciting light (Fig. 2-1); this is referred to as Stokes Shift. Shift to shorter wavelength is anti-Stokes shift and can occur as a very weak absorption band, due to a small proportion of thermally excited molecules in the lower vibrational levels of the ground state, eg. 1 of S₀, which gives a transition from 0 to 1.

2:1:3 THE FRANCK-CONDON PRINCIPLE

The spectra explained so far, would give a series of sharp equally intense bands in either the emission or absorption spectrum. This, however, is not found to be the case, as the spectra obtained consist of broad bands. This can be explained by the fact that molecules possess vibrational and rotational energy in each of their ground states. Since the size and shape of the molecule will, in general, be different in each electronic state, the Franck-Condon effect leads to broad band molecular spectra.

This effect is based on the fact that light absorption takes place within the period of vibration of the light wave. During this time, the heavy nuclei of the atoms in the molecule do not appreciably change their position and momentum, and, therefore, the nuclear conformation and relative motions in the excited state immediately after absorption are identical to those in the ground state immediately before absorption of light, line EP (Fig. 2-3).

Fig. 2-3 Diagram Illustrating the Franck-Condon Principle for a Diatomic Molecule



The orbital occupied by the electron in the excited state, is generally more expanded in space than that occupied in the ground state; therefore, the equilibrium position in the excited state corresponds to a greater inter-atomic distance than that of the ground state. It is, therefore, this equilibrium of the vibrational states, which causes the broadening of the observed bands, and the shape of the emission spectrum will thus depend on the relative positions of the minima of the upper and lower curves, (Fig. 2-3).

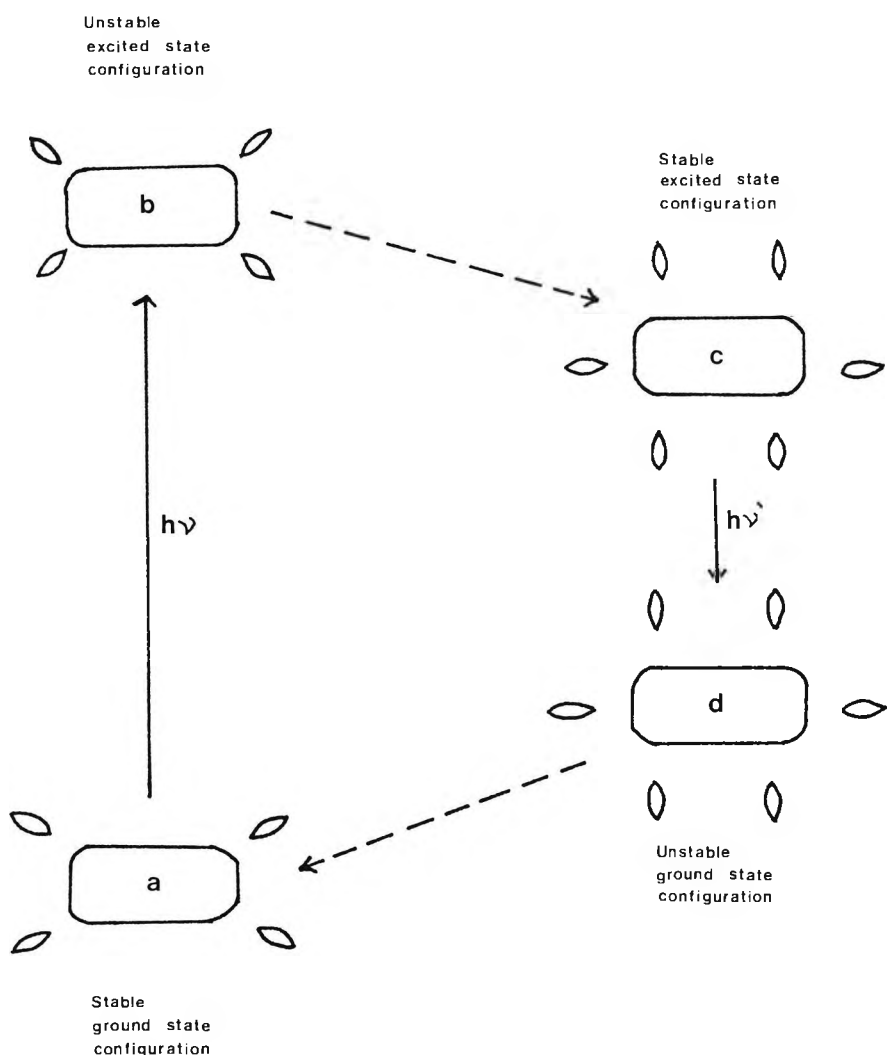
2:1:4 ENERGY DIFFERENCE IN THE O-O TRANSITIONS

In both the absorption and fluorescent states, the molecule is solvated by dipolar interaction due to:-

- i) Permanent dipoles in the solute and solvent
- ii) Induced dipoles in one or the other

The electron distribution is different in the excited state from that of the ground state. Therefore, the dipole moment and/or polarisability will be different and hence the degree of solvation.

Fig. 2-4 Diagram Illustrating Change of Solvation after Excitation or Emission



In fluid solution, at room temperature, solvent molecules will not have time to re-orient themselves during the process of light absorption. Hence the molecule immediately after excitation, finds itself in a state of solvation corresponding to a higher energy than its preferred equilibrium condition. The molecule normally has time to relax to a lower energy

equilibrium configuration before emitting. Immediately after emission, the molecule in the ground state is in a state of solvation corresponding to the equilibrium configuration in the excited state. Therefore, the process of absorption of light requires slightly more energy than that released during the process of light emission, although both processes correspond to the 0-0 transition. Therefore, the 0-0 transition in absorption and fluorescence do not coincide.

The difference between 0-0 transitions depends on the different degrees of solvation in the two states. This difference is, therefore, greatest for molecules showing a large change in dipole, on excitation to the first excited state, and so is greater in more polar solvents.

2:1:5 QUANTITATIVE ASPECTS OF LIGHT ABSORPTION AND EMISSION

The Beer-Lambert Law of absorption of light is of great importance. It relates the absorbance (Abs) of a material with the light path length, l , and concentration of absorbant, c , with the incident, I_0 , and transmitted intensity, I_t , and so with the optical density of the solution, $(\log_{10} I_0/I_t)$:-

$$\text{Abs} = \log_{10}(I_0/I_t) = \epsilon cl \quad (\text{Eqn. 7})$$

The molar extinction coefficient (ϵ), is a function of the wavelength of incident light; ϵ is also related to k , the specific cross-sectional area of the molecule at a particular wavelength, as follows:-

$$k = 2,300\epsilon/N \quad (\text{Eqn. 8})$$

N = Avagadro's number

The Beer-Lambert Law cannot be obeyed, if the incident light is polychromatic over a range in which ϵ is not constant. Further, if there are equilibria in the system so that the concentration of absorbing species is not proportional to the stoichiometric concentration, again the Law will not be valid.

2:1:6 TRANSITION, PROBABILITY AND LIFETIME

The relative probabilities of transitions to various vibrational levels of the upper electronic excited state, can have a marked effect on the relative absorption intensities of these transitions. The absolute probabilities of the electronic transitions themselves depend on the types of the electronic states involved, and so they determine the overall intensity of the corresponding absorption bands. Optical transitions that are probable on absorption are also probable in emission, so therefore there , exists a direct relationship between the probability of fluorescence emission and the molecular extinction coefficient of the corresponding absorption band.

Another major factor governing the fluorescence intensity observed in solution at room temperature, is the radiative lifetime. This is defined as the lifetime which would be observed in the absence of all other processes, by which the molecule can return to the ground state.

$$\tau_r = \frac{1}{k_1} \quad (\text{Eqn. 9})$$

τ_r = radiative lifetime.

k_1 = 1st order rate constant for the process of fluorescence emission.

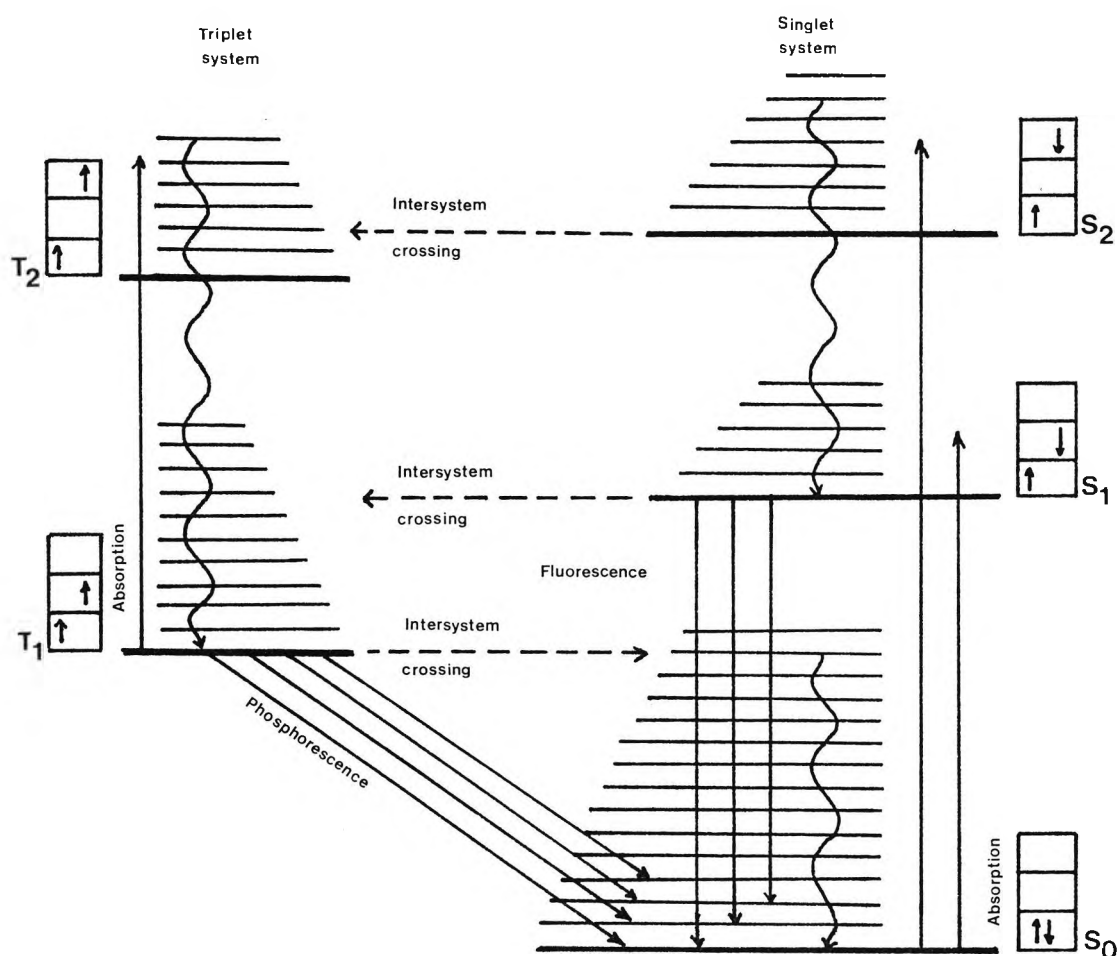
If the lifetime is long, there is a much greater chance of radiationless processes competing successfully with the radiative process that gives rise to fluorescence, and the intensity of the latter will, therefore, be lower.

2:1:7 PHOSPHORESCENCE

In luminescence, there is another possible transition, which can give rise to the emission of light. This involves a spin forbidden transition from the singlet state to the triplet state via intersystem crossing. Intersystem crossing is a process by which the electron promoted to an upper orbital may flip its

spin, and thus, have its spin orientated in the same direction ("parallel") as that electron in the ground state, and so be, triplet in nature. This electron, therefore, enters the triplet system at an energy equivalent to that it possessed in the singlet system (Fig. 2-5) and can decay to the lowest excited triplet vibrational energy. The final emission of light that occurs from the lowest excited triplet vibrational level to the ground state is then termed phosphorescence. Although this radiative transition is formally spin forbidden, in practice, because of spin-orbit coupling, these transitions do take place, although with extremely low probability compared with singlet-singlet or triplet-triplet transitions.

Fig. 2-5 Diagram Illustrating Phosphorescence



2:2:1 INORGANIC PHOTOCHEMISTRY

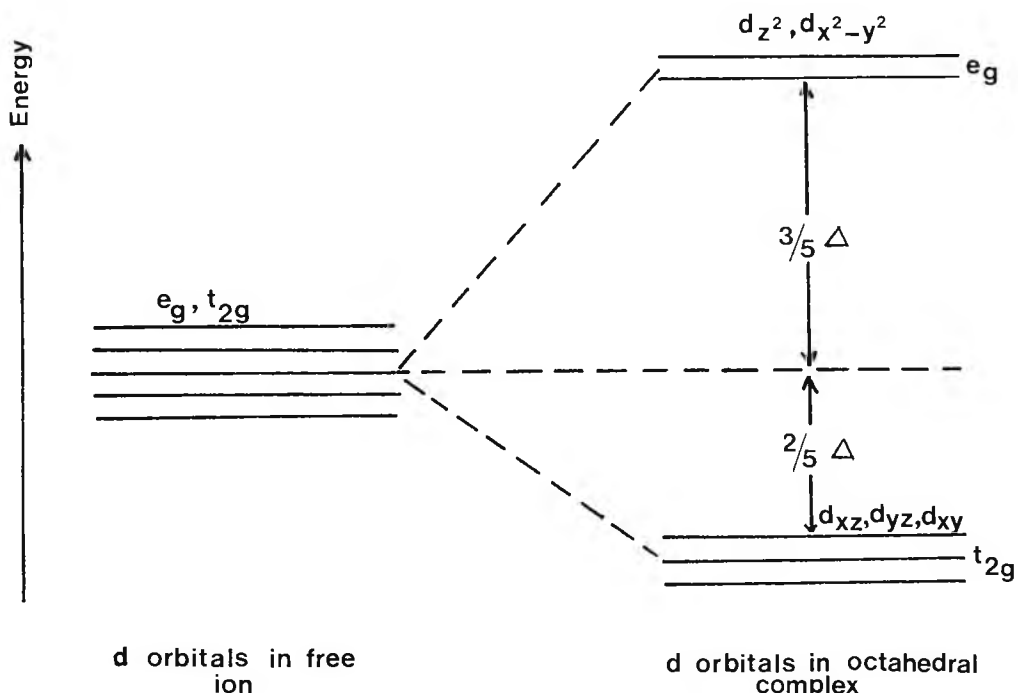
Before investigating the nature of the electronic spectra of transition metal complexes, it is necessary to have an understanding of the nature of bonding in these complexes.

2:2:2 BONDING

A simplified view can be of bonding as an electrostatic attraction between a charged central metal ion and a set of negatively charged ions, or the negative ends of dipoles of co-ordinated neutral ligands, eg. water or the sets of nitrogen non-bonding electrons on bidentate ligands. In this view, the stability of a complex is a consequence of purely electrostatic forces. If the central ion is a transition metal ion with an open d-shell, then these excess d-electrons contribute nothing to the bonding. Indeed, they shield the central nucleus and reduce its effective charge. The approach of the negative ligands repels the electrons in the d-orbitals and raises their energies both with respect to those residing on the ligands, and also those remaining on the central core.

In the following, we are mainly concerned with those complexes of octahedral or pseudo-octahedral symmetry, and, in these cases, not all the d-electrons are destabilised equally by the ligand cage. Those electrons residing in the d-orbitals that point towards the ligands, dx^2-y^2 , and dz^2 (e_g set), are repelled more by the negative ligands than those residing in the d-orbitals that are directed between the ligands dxy dyz dxz (t_{2g} set). The difference in destabilization energy leads to the splitting of the d-orbital energies and is indicated by Δ in Fig. 2-6.

Fig. 2-6 Diagram Illustrating the Energy Differences Established in d-orbitals in an O_h Complex

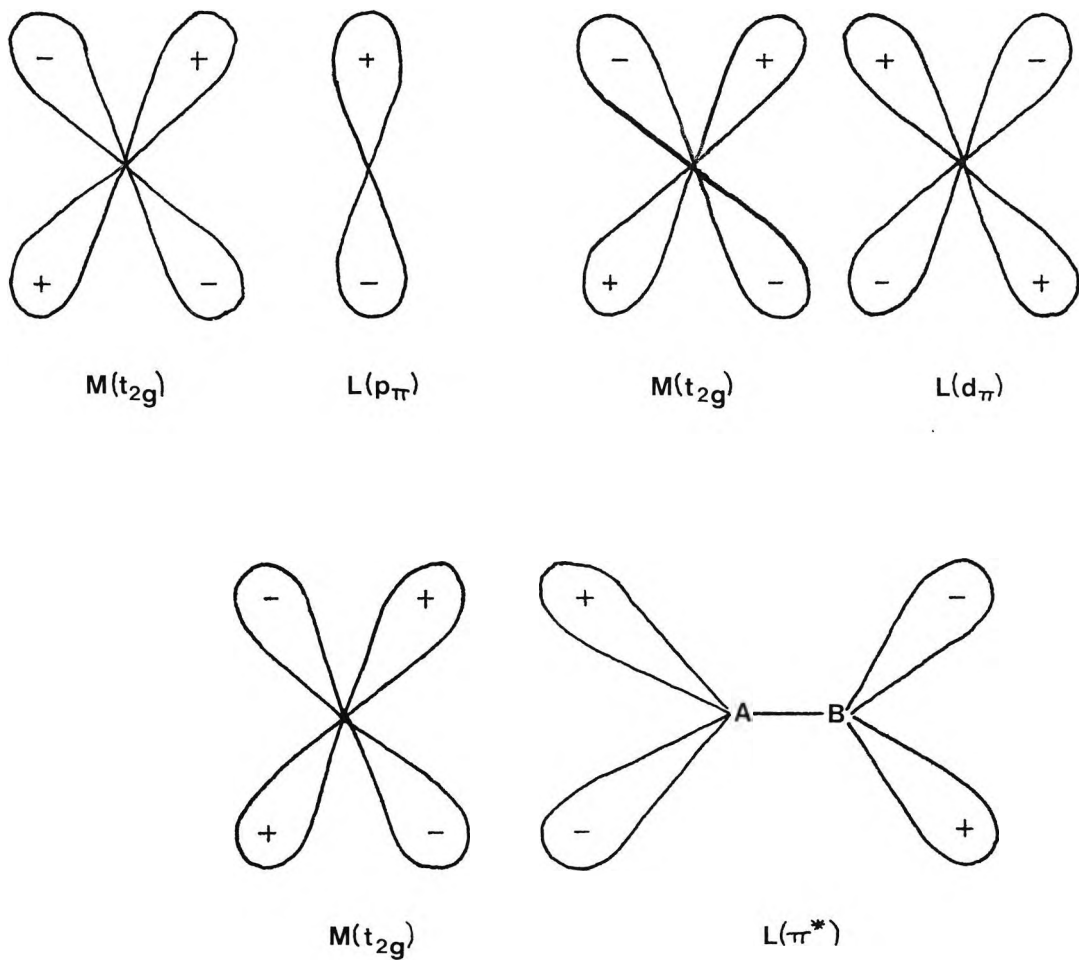


The magnitude of Δ is determined by several factors; the radius of the metal ion, the charge on the central ion, and the chemical nature of the ligands. For a given central metal ion with a specified ionic charge, the magnitude of Δ can vary widely. Common ligands have been arranged in order of their effect on Δ . This is called the spectrochemical series, e.g. $I^- < Br^- < Cl^- < S^{2-} < F^- < OH^- < CH_3COO^- < C_2O_4^{2-} < H_2O < Py \approx NH_3 < en < bipy < phen < PR_3 < CN^-$. The ligands are arranged in order of increasing ligand field strength.

It can be seen from the above that the electrostatic model fails, since bipyridine, a neutral ligand, is associated with a much larger value of Δ than $C_2O_4^{2-}$, a dinegative ion. There must, therefore, be a degree of covalence introduced to account for these findings, as is done in ligand-field theory.

The spectrochemical series can be better understood through the consideration of π -bonding. The t_{2g} orbitals are considered non-bonding with respect to σ -bonding ligands, but become bonding orbitals with ligands having π symmetry. The ligand orbitals may be p or d orbitals, or π^* molecular orbitals, (Fig. 2-7).

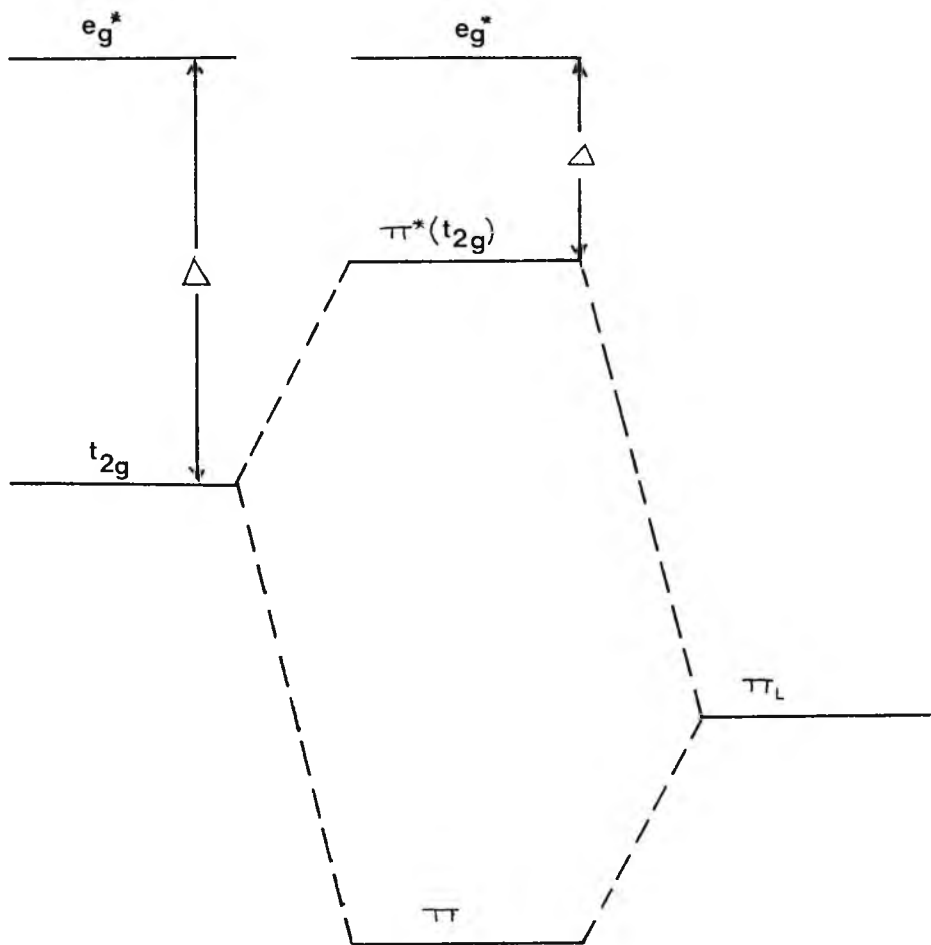
Fig. 2-7 Diagram Showing Possible Bonding of t_{2g} Orbitals to Ligand π Orbitals



The effects that π -bonding can have on the value of Δ can be considered, by examining two extreme cases:-

- i) A ligand having orbitals of π symmetry filled with electrons and low in energy, eg. filled p orbitals on F^- or Cl^- .

Fig. 2-8 Bonding Diagram for a Ligand having Orbitals of π Symmetry Filled with Electrons and Low in Energy

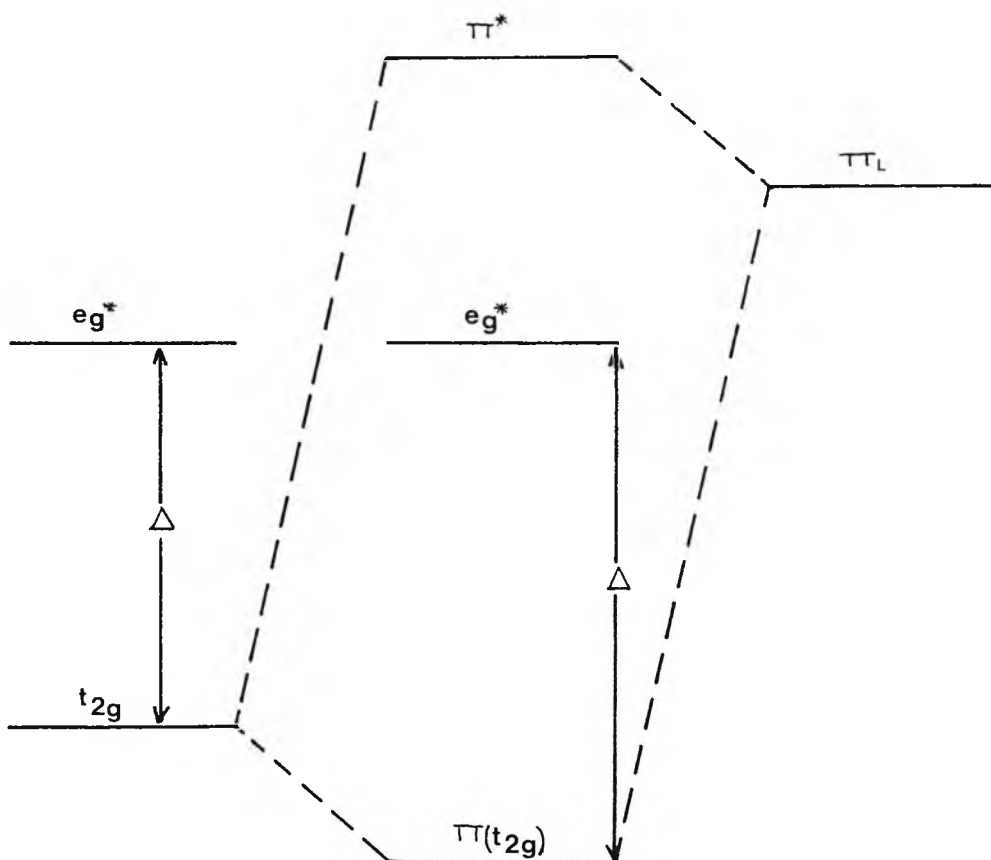


It can be seen from Fig. 2-8, that the π -bonding molecular orbital formed is lower in energy than the p_{π} atomic orbitals, from which it was formed, and contains the electrons from the filled ligand π orbitals. Therefore, this can be considered as a $L \rightarrow M \pi$ interaction, with the ligand regarded as a π -electron donor. The π^* orbital is higher in energy than the original t_{2g} metal orbital, and, since the bonding π orbital is filled, the $\pi^*_{t_{2g}}$ orbital must contain the metal electron. The net effect is a decrease

in Δ , and such ligands would be expected to be found at the weak-field end of the spectrochemical series.

- ii) A ligand having vacant high-energy π orbitals, eg. phosphorus, arsenic, and sulphur donors, which possess vacant d orbitals.

Fig. 2-9 Bonding Diagram for a Ligand having Vacant High-Energy π Orbitals



This is a $M \rightarrow L \Delta$ interaction, with the π -acceptor ligands stabilising the t_{2g} orbital, and therefore increasing Δ .

Ligands which give a small Δ value are referred to as weak field, and, as Δ is less than the pairing energy for electrons, the complexes formed are usually high-spin in nature. However, if Δ is large, the ligands are high field, and Δ is greater

than the pairing energy; therefore, the electrons couple to give a low spin complex.

2:2:3 INORGANIC LUMINESCENCE

The terms phosphorescence and fluorescence have little meaning in inorganic or organometallic systems, because in many such systems the multiplicity of the excited and ground states is not restricted to just singlet and triplet. Therefore, it is generally more appropriate to describe emissions as luminescence.

2:2:4 EXCITED STATES OF ELECTRONIC SPECTRA

The excitation of a molecule from the electronic ground state, to an electronic excited state, corresponds to absorption of light in the near infra-red, visible, or ultraviolet regions of the spectrum. For transition metal complexes, the absorption bands in the first two of these regions are relatively weak, and are associated with transitions largely localised on the metal atom. The ultraviolet bands, however, are intense, and are associated with the transfer of an electron from one atom to another, and are called charge-transfer bands.

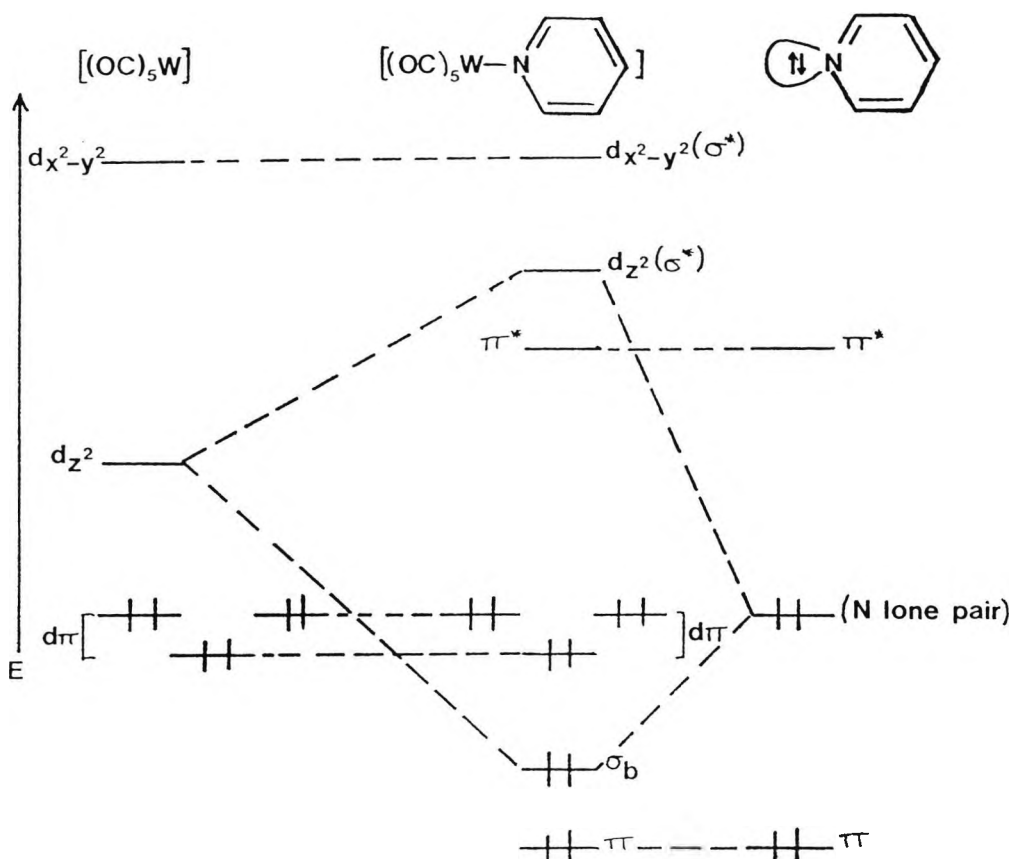
In the following, we will consider these various low lying excited states, which can be populated by optical irradiation:-

A) Intraligand Excited States (IL)

Ligands which co-ordinate to metals have their own set of excited states. Co-ordination to the metal also causes perturbation of the ligand's electronic structure. If the free ligand possesses one electron transitions which either terminate or originate on an orbital centred on the ligating atom, perturbation is so great that it is inappropriate to refer to the transitions as intraligand (IL). If, however, co-ordination gives only a small amount of perturbation, the complex will have excited states not too differ-

ent to that of the free ligand. If bonding of pyridine in $W(CO)_5Pyr$ is considered as an example (Fig. 2-10).

Fig. 2-10 Diagram Illustrating Bonding of Pyridine in $W(CO)_5Pyr$



The complex co-ordination does not alter the $\pi \rightarrow \pi^*$ excitations of the pyridine as they are not involved in the bonding. However, the $n \rightarrow \pi^*$ excitation of pyridine is altered beyond recognition, since the principal mode of bonding to the metal is via the σ interaction of the nitrogen lone-pair. The $n\pi^*$ state, therefore, loses its identity upon co-ordination.

It can, therefore, be said that if a ligand has low-lying transitions involving orbitals which are centred on atoms not directly bonded to the metal, those same

transitions survive in the complex as identifiable intra-ligand transitions.

B) **Ligand-Field Excited States**

(Metal-centred excitations)

These are transitions between d orbitals of the metal, which have been split in a ligand field. These absorptions are usually fairly weak. However, in organometallics they are relatively intense, owing to a large degree of covalence.

The ligand-field (LF) transitions are also affected by the interaction of other electrons with that which is excited. The interactions are couplings between the quantum numbers for the individual electrons. It is assumed that there are 3 types of interaction spin-spin coupling, which is greater than orbit-orbit coupling, which is again greater than spin-orbit coupling. These are considered in the Russel-Saunders scheme and give rise to Russel-Saunders terms [a].

In electronic spectra, certain transitions are disallowed, due to two principal reasons called selection rules:-

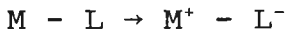
- i) Spin forbidden-transitions. Transitions in which there is a change in the number of unpaired electron spins are forbidden, i.e. for a transition to give optical absorption, $\Delta S = 0$. Transitions for which $\Delta S \neq 0$ are said to be spin-forbidden.
- ii) Orbitally forbidden-transitions (Laporte rule). Transitions involving the redistribution of electrons in a single quantum shell are forbidden. Thus $d \rightarrow d$ and $p \rightarrow p$ transitions are forbidden, but $s \rightarrow p$ and $p \rightarrow d$ transitions are allowed. Transitions should only involve one electron, so that for a

transition to be allowed, $L = \pm 1$. Transitions for the type $g \rightarrow g$ and $u \rightarrow u$ are described as being partially forbidden.

The spin selection rule is relaxed by spin-orbital couplings. As these couplings increase, the intensity of the spin-forbidden bands also increases. The Laporte selection rule may also be relaxed if a complex contains a centre of symmetry, as the complex can then use a vibronic mechanism to show optical absorption.

C) Metal-to-Ligand Charge-Transfer Excited States

Low-valent metal complexes often have low-lying transitions which are termed metal-to-ligand charge-transfer (MLCT). The transition originates in some metal-centred orbital and terminates in some ligand-localised orbital. An extreme approximation of MLCT results in an oxidised metal and a reduced ligand



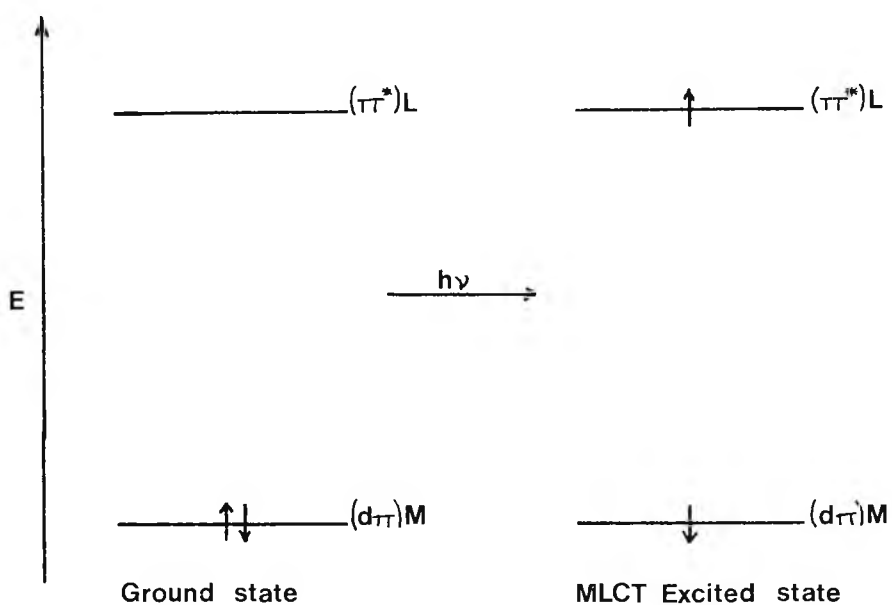
The energy required for this transition is, therefore, dependent on the relative ease of oxidation of the central metal, and the availability of a low-lying acceptor orbital on the ligand.

These transitions would also be expected to affect the nature of the chemistry of the complex. The central metal would be expected to be more susceptible to nucleophilic attack in the MLCT state than in the ground state, and at the same time the ligand would develop radical-anion character and should be more reactive towards electrophiles than the ground-state complex. Except for associative substitution processes, MLCT excited states are typically not substitution-labile enough to undergo reaction within the lifetime of the complex. This conclusion arises from two considerations:-

- i) The transition originates in a filled d orbital, which is usually not that consequential with respect to metal-ligand bonding.
- ii) A ligand-localised orbital is populated, which does not substantially influence metal-ligand bonding.

Indeed, the electrostatic attraction generated in an MLCT state may make the M - L bond more inert.

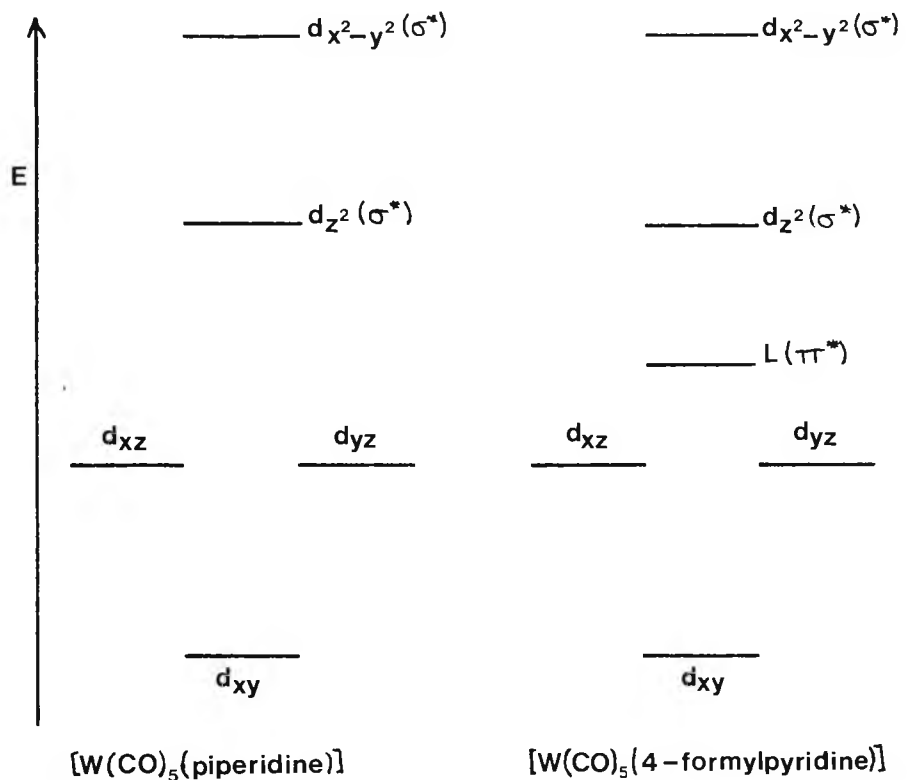
Fig. 2-11 Diagram Showing Ground State Relative to Excited State



From Fig. 2-11, it can be seen that the MLCT state is simultaneously a more powerful oxidant than the ground state. The excited electron in $(\pi^*)L$ is less stable, therefore increasing the reducing power, and the 'hole' in $(d\pi)M$ is more stable, providing the increase in oxidizing power.

MLCT can be illustrated as follows:-

Fig. 2-12 Diagram Illustrating the Orbital Ordering of $[W(CO)_5 \text{ piperidine}]$ and $[W(CO)_5(4\text{-formylpyridine})]$



In comparing the orbital ordering for $[W(CO)_5(\text{piperidine})]$, (I), and $[W(CO)_5(4\text{-formylpyridine})]$, (II), (see Fig. 2-12), the d-orbitals will be the same in each case, as the co-ordination sphere is the same. The LF bonds in (I) are also found in the same position and relative intensity in (II). However, unlike saturated piperidine, 4-formyl pyridine has a low-lying $\pi^*(L)$ acceptor orbital; therefore, (II) exhibits a low-lying extremely solvent-sensitive absorption not present in (I). (I) effectively loses piperidine upon photoexcitation consistent with the population of the d_{z^2} orbital, which has directed σ^* character, and is, therefore, a LF bond, whereas the lowest excited state of (II), is inert with respect to photosubstitution and is, therefore, probably a MLCT band.

D) Ligand-to-Metal Charge-Transfer Excited States

These excited states arise from the excitation of an electron from a ligand-centred orbital to an orbital localised on the metal. Ligand-to-metal charge-transfer (LMCT) depends on the availability of low-lying, empty, or partially filled metal orbitals, and on the relative ease of oxidation of the ligands. LMCT is of little importance in organometallic complexes, as the unfilled d-orbitals are generally not low-lying, arising from the fact that the high ligand field strengths associated with organometallic complexes places the unfilled d-orbitals at high energy.

The shift of electron density from the ligand to the metal in LMCT would be expected to make the ligand more susceptible to nucleophilic attack, and the metal more susceptible to electrophilic attack. However, this is found not to be the case; LMCT is generally associated with homolytic cleavage of M and L instead.

E) Metal-to-Solvent Charge-Transfer Excited States

These are transitions that originate in metal-centred orbitals and terminate in solvent orbitals. Metal-to-solvent charge-transfer (MSCT) tends to oxidise the metal complex and reduce the solvent.

The position of absorption depends on the solvent and its ease of reduction, and on the ease of ionisation of the metal complex.

2:2:5

THE EFFECT OF SOLVENT ON ELECTRONIC TRANSITIONS
(REF. FIG. 2-4)

The wavenumber corresponding to the energy of the absorption band is analogous to the energy difference between the energy of the equilibrium configuration of the ground state (a), and the energy of the state reached immediately after light absorption (b). Therefore, a change in solvent can be interpreted in terms of the net effect of the change in energy of the states (a) and (b). The electron charge distribution of $\pi-\pi^*$ excited state, is more extended than that of the ground state, and is, therefore, more polarisable.

The change to a polar solvent increases the solvent interaction in both states, but the corresponding decrease in energy of the excited state is slightly greater than that of the ground state, and so the absorption band is red shifted.

The charge-transfer state has a much greater permanent dipole moment than the ground state. Therefore, in a polar solvent, there is a larger reduction in energy of the charge-transfer state than in the ground state corresponding to a large red shift.

For $n \rightarrow \pi^*$ transitions, polar solvents in the ground state are hydrogen bonded at the n-electron site, and promotion of a non-bonding electron to the π -electron system reduces hydrogen bonding forces in the excited state. Therefore, a polar solvent reduces the energy of the ground state to a greater degree than that of the excited state, and the absorption band shifts to higher wave numbers resulting in a blue shift.

2:3:1

RUTHENIUM POLYPYRIDINES

For many years, there has been much interest generated in the luminescent properties of ruthenium polypyridines, particularly the tris 2,2'-bipyridine ruthenium (II) dication, $\text{Ru}(\text{bipy})_3^{2+}$. Most of the work on this complex in recent years, has been

centred on its use as a catalyst in energy conversion schemes involving the photochemical decomposition of water. Our interest in complexes of this type has also been due to their luminescent properties, but in this instance, it is because they have ideal properties for use as labels in time-resolved immunoassay, (described in more detail in Chapter 3). In the following, an attempt is made to set out a model explaining the luminescence properties of ruthenium polybipyridine complexes.

2:3:2 LOW-LYING ENERGY LEVELS IN Ru(bipy)₃²⁺

There has been much debate over a number of years, as to the nature of the emission from Ru(bipy)₃²⁺. Initially, it was assigned as a charge-transfer fluorescence by Paris and Brandt [1]. This assignment was disputed by later authors, who assigned the emission as "d-d" phosphorescence [2], "d-d" fluorescence [3], charge transfer [4], charge-transfer fluorescence, and charge-transfer phosphorescence. However, the bulk of the research carried out now seems to indicate that the emission is charge-transfer in nature. At this point, it would be easier to put forward a simplified model for the luminescence properties of Ru(bipy)₃²⁺ at low temperature, and then enter into a discussion as to the exact multiplicity of these transitions.

Examination of the emission shows that excitation of Ru(bipy)₃²⁺ in any of its absorption bands, leads to a single emission band. This indicates that some fraction of the initial excited states produced by light absorption, decays to a common set of excited states responsible for emission. In fact, studies of the variation of luminescence quantum yield, (Φ_1), with wavelength, show that all excited states attained over the range of wavelengths studied (250-550nm), could relax with unit efficiency (Φ), into the luminescence levels [5]. This and other experimental data, clearly dictates the presence of a multi-state model for the origin of emission [6]. If a single state or group of degenerate states were responsible for luminescence, the τ/Φ ratio should be temperature independent and equal the limiting lifetime, a fundamental molecular property. However,

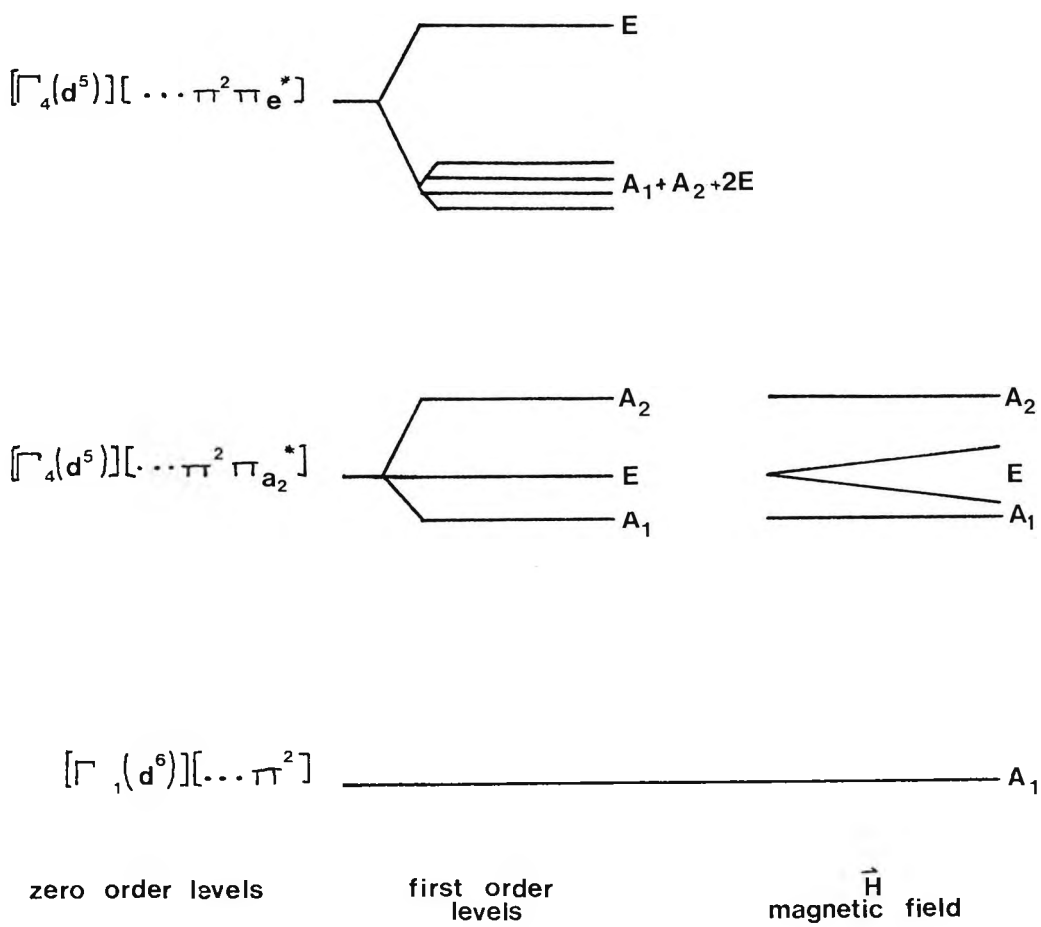
at low temperature, the emission of the system is temperature dependent; therefore, a multi-state must exist.

It is generally accepted that the absorption of light by Ru(bipy)₃²⁺ is dominated by transitions to metal-to-ligand-charge-transfer (MLCT) states, (ie. the promotion of the excited electron from the d-orbitals of the metal to the π^* orbitals of the ligand), which are largely singlet in character. At lower energies, much weaker bands are observed, which are assignable to MLCT states having largely triplet character [7]. Emission is dominated by a closely spaced manifold of at least three of the latter states [8]. Therefore, there must be rapid inter-system crossing from the initially formed singlet MLCT state to the corresponding triplet state before emission. The exact classification of MLCT states to singlet or triplet can, however, be regarded as only formal, since the spin-orbit interaction is large enough to cause a large mixing of the singlet and triplet spin states [9].

The exact nature, type, ordering, and symmetries of the manifold of MLCT states, has also been a matter of close debate. Until recently, the most generally accepted model was that submitted by Crosby et al [8, 10-12]. This model, termed the electron-ion parent coupling (EIP) model or delocalised model, relies on group theory for the assignment of the MLCT states. They visualised the low-lying charge-transfer excited configurations in these systems, to be the result of the promotion of a d electron, initially localised on the metal ion to a π^* anti-bonding orbital delocalised over the ligand system. Assuming D₃ symmetry is maintained, the lowest charge-transfer excited states arise from the Ru (III)(d⁵) core, weakly coupled with the promoted electron residing in a π^* orbital on the ligand system. This π^* orbital must be anti-symmetric with respect to a C₂ axis perpendicular, to the threefold principal axis of the complex, and in D₃ this can only give a₂ or e symmetries. This coupling of the promoted electron with the strongly spin-orbit coupled states of the d⁵ core, results in 16 levels which are comprised of 36 states. The lowest three levels of A₁, E, and A₂ symmetry, which arise from coupling of a $\pi^*(a_2)$ electron with the

ground state of the d^5 core, are believed to be responsible for the luminescence properties at 77K . Of these three levels predicted for $d\pi^* a_2$ excitation, the A_1 and E are seen to be associated with triplet parentages, whereas the A_2 derives formally from a singlet. Since singlets are generally higher than triplets from the same configuration, A_2 is placed as the highest (and shortest-lived) level of the manifold. It is also believed that at 77K, 90% of the emission originates from this level. From group theory, using the selection rules for dipole-induced transitions from the A_1 ground state to the three excited states, A_1 is assigned the lowest (and longest-lived) state in the system being formally forbidden, and the E level is placed as the intermediate level being x,y -allowed.

Fig. 2-13 Diagram Showing the Ordering of Low-Lying Charge-transfer States in $\text{Ru}(\text{bipy})_{3}^{2+}$ According to the EIP Model [10]



However, recent results obtained from techniques such as time-resolved resonance Raman [13], circular dichroism [14], spectroelectrochemistry [15], and luminescence [16], clearly indicate that other models must be sought, to explain all the details of the electronic excited states of $\text{Ru}(\text{bipy})_3^{2+}$.

Taking resonance Raman as an example; from examination of the spectra obtained for the excited state of $\text{Ru}(\text{bipy})_3^{2+}$, it is clear the MLCT state has a symmetry which cannot be D_3 , but is at most C_2 , and could be lower [17]. Comparison of the spectrum of the excited $\text{Ru}(\text{bipy})_3^{2+}$ with that of $\text{Li}^+(\text{bipy}^-)$ shows that the spectrum of $\text{Ru}(\text{bipy})_3^{2+}$ is consistent with a fully reduced bipyridine ring being present in the $d\pi^*$ excited state; this, therefore, suggests that the electron excited into the $d\pi^*$ system resides on a single bipyridine moiety on the vibrational time scale. This model has been referred to as the localised model, and has led to a new scheme being proposed, namely, the electronic structural (ES) model [18].

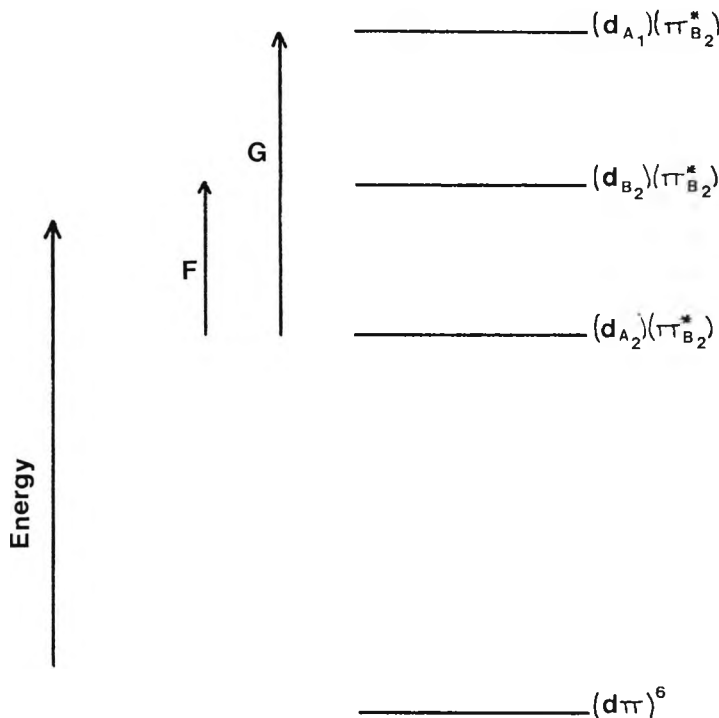
The development of the ES model proceeds in three discrete steps:-

- i) The excited-state configurations resulting from an electron residing in a bipy π^* orbital interacting with the d^5 metal core are presented.
- ii) The resulting configurations are resolved into pure singlet and triplet states by the introduction of spin-spin coupling.
- iii) The effect of spin-orbit coupling due to the presence of the metal ion is calculated.

The result is a model, which differs from the former delocalised model not only in its symmetry allocation of C_2 , but also in its use of spin-orbit coupling considered inappropriate for the EIP model.

It is assumed that the electron is promoted to a π^* orbital of a particular bipyridine ligand. Taking into account the C_{2v} point group now assigned to the excited state of $\text{Ru}(\text{bipy})_3^{2+}$, the lowest energy π^* orbital of bipyridine has B_2 symmetry. The next lowest energy π^* orbital has A_2 symmetry and occurs $\sim 7000\text{cm}^{-1}$ higher in energy. The three $d\pi_{(t_{2g})}$ orbitals transform in this symmetry as A_1 , A_2 , and B_2 . There are five metal valence electrons to be placed in the three $d\pi$ orbitals in the MLCT excited states from which three different $(d\pi)^5 (\pi^*_{B_2})^1$ excited-state configurations can result, depending upon which $d\pi$ orbital is singly occupied.

Fig. 2-14 Relative Energies of the $(d\pi)^5 (\pi^*_{B_2})^1$ Excited States and the $(d\pi)^6$ Ground State of $\text{Ru}(\text{bipy})_3^{2+}$ (ES Model) F and G are positive as shown [18]



The promoted electron is then coupled to the odd electron in the d^5 core, and this transforms as four states: A_1 , which is con-

sidered as of singlet parentage, and three triplet states A_2 , B_1 , and B_2 .

The final step of the development of the model is now included, namely spin-orbit coupling, which results in the mixing of the singlet and triplet character of the excited states.

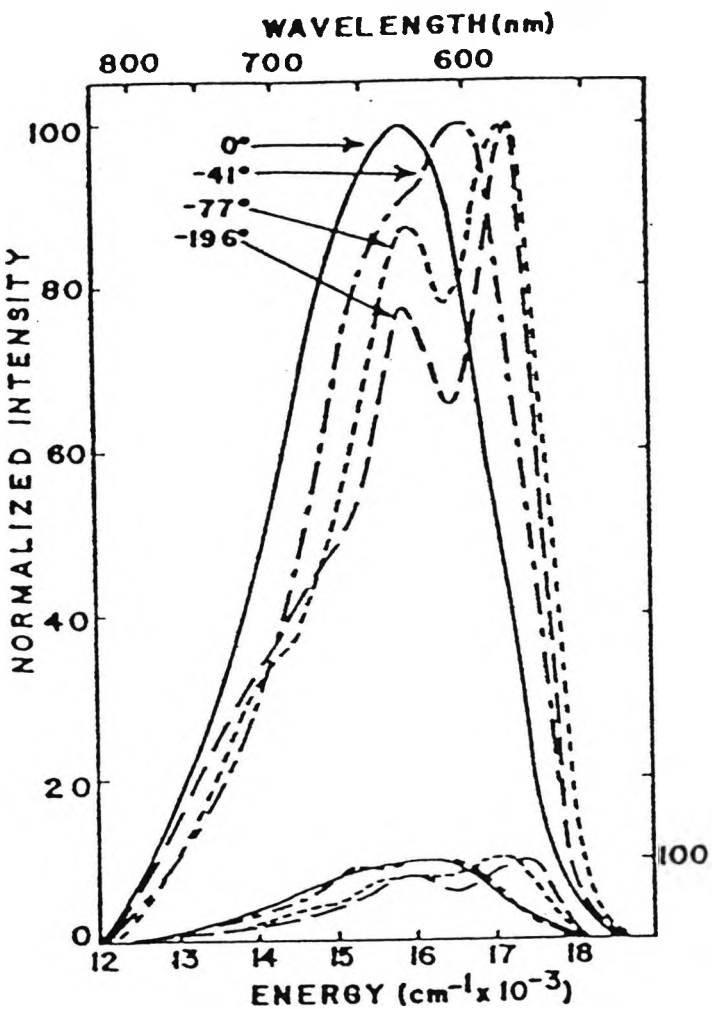
The final result at ambient and lower temperatures is a four-state manifold. The A_2 state is considered to be purely triplet as there are no singlet A_2 states with which it can mix, and it is assigned as the lowest excited state in the manifold. B_1 is attributed to the uppermost state and is essentially all singlet. The ordering of the other two states, B_2 and A_1 , is not yet totally resolved for $\text{Ru}(\text{bipy})_3^{2+}$, but it is understood that they lie close to A_2 with an energy separation within 100cm^{-1} . B_1 , the fourth level, is believed to lie several hundred cm^{-1} above the low-lying manifold.

2:3:3

THE TEMPERATURE DEPENDENCE OF THE PHOTOPHYSICAL PROPERTIES OF THE $\text{Ru}(\text{bipy})_3^{2+}$ ION IN AQUEOUS SOLUTION

Study of the luminescence spectrum of $\text{Ru}(\text{bipy})_3^{2+}$ between -196 and 100°C (Fig. 2-15), shows that the spectrum broadens and red shifts as the temperature is raised, and time-resolved spectra indicate that the luminescence decay is exponential at all temperatures [19].

Fig. 2-15 Effect of Temperature Variation on the Luminescence Spectra of $\text{Ru}(\text{bipy})_3^{2+}$ [19]



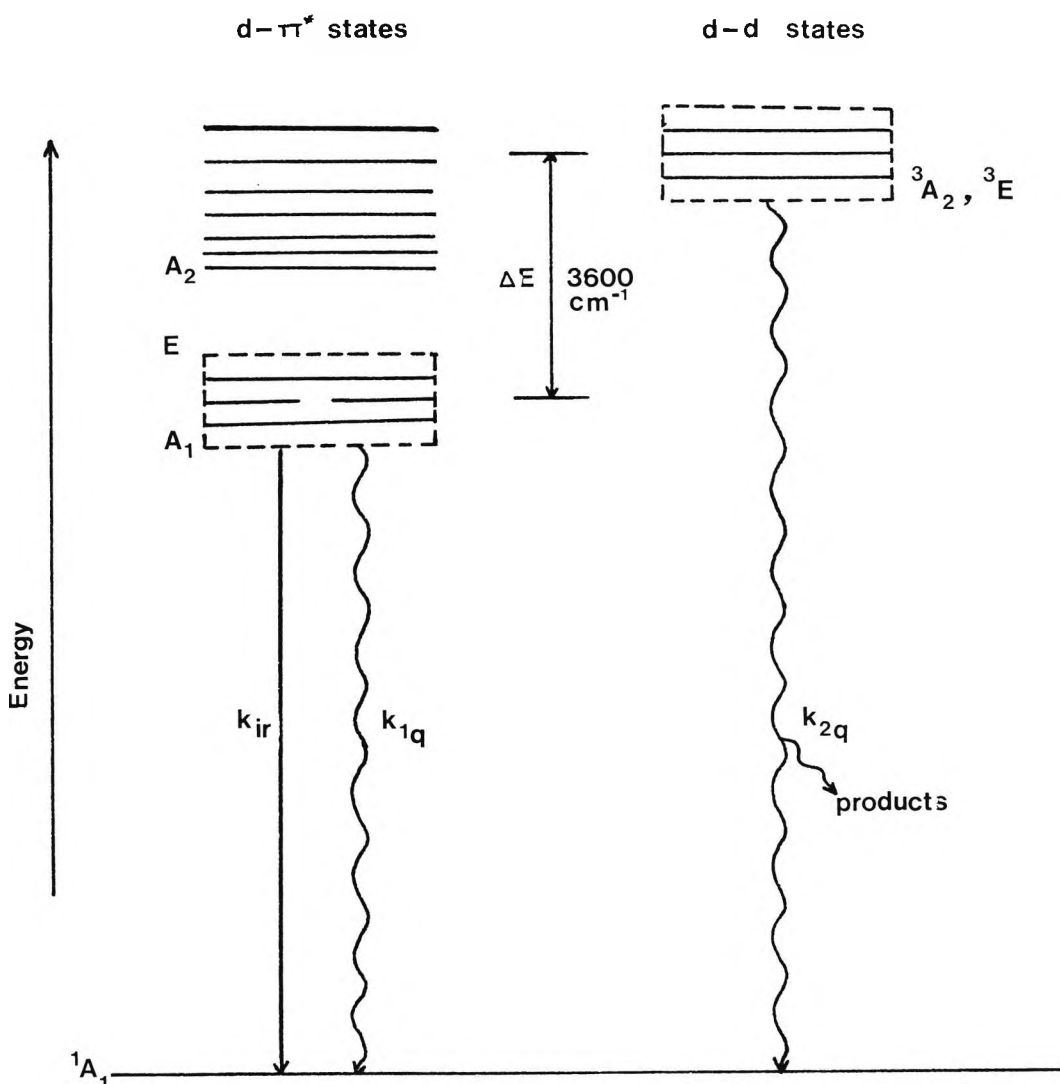
The MLCT states must, therefore, be being affected in some way by the temperature change. One effect of temperature, is that at ambient temperatures, other excited levels, above the low-lying manifold responsible for emission below 77K, become thermally accessible. The existing theoretical models for the excited states of $\text{Ru}(\text{bipy})_3^{2+}$ must, therefore, be extended for higher temperatures; taking the EIP model as an example, as many as 36 spin-orbit coupled states of $d\pi^*$ parentage could lie within about 3000cm^{-1} of the lowest excited levels and could, therefore, contribute to the net decay process. In addition, the low-lying 3T state of an octahedral d^6 complex will split into 3A_2 and 3E components in the D_3 symmetry group of $\text{Ru}(\text{bipy})_3^{2+}$, giving rise to a total of nine states of d-d parentage. There are, therefore, as many as 45 electronic states of $d\pi^*$ and d-d orbital parentage, which may contribute to the

thermally equilibrated excited state manifold at room temperature. Since the complex is photoinert at room temperature, and shows a deuterium effect on its luminescence, the decay of the excited state manifold is probably dominated by weak coupled radiationless transitions to the ground state at room temperature. It is unlikely that these weak-coupled processes would occur any more rapidly from the higher excited states than from the lowest excited state. Thus the Boltzmann factors heavily favour decay via the lowest few levels. Hence, it is anticipated that the number of levels responsible for the properties of the complex at room temperature is nearly the same as at -196°C.

The effects of temperature on luminescence must, therefore, be due to the presence of new decay pathways in fluid solutions, which are absent in rigid media and leads to the conclusion that the radiative lifetime is dependent on the viscosity of the solvent. In other words, the radiative lifetime is altered on going from a rigid to a fluid medium due to structural changes in the solvation sphere, which cause substantial mixing of MLCT states with CTTS configurations [20]. Changes in the quantum yield and quenching rate in the fluid media can also be attributed to efficient radiationless decay pathways, which are associated with the structure of the solvation sphere. It has been indicated that these pathways dissipate energy through the O-H vibrations in water [19]. Energy transfer to solvent is presumably moderated in a rigid medium by alterations of the solvation sphere.

Luminescence from the average triplet state ($^3\text{MLCT}$) displays an additional temperature dependence in the range 273-373K. This behaviour has led to the postulate that a second decay pathway is present at higher temperatures, which is non-radiative and responsible for the noted temperature dependence. This consists of a second set of ligand field levels [19] lying approximately 3600cm^{-1} above the charge transfer levels, that can be thermally populated during the lifetime of the $^3\text{MLCT}$ state, and can decay to the ground state with a radiationless decay constant of 10^{13}s^{-1} , (Fig. 2-16, [21]).

Fig. 2-16 Diagram Illustrating the Presence of Ligand Field Orbitals lying above the $^3\text{MLCT}$ State of $\text{Ru}(\text{bipy})_3^{2+}$ [21]



This strongly-coupled radiationless decay process is believed to be thermally activated by population of the upper levels. Thus, the dissipation of excitation energy in aqueous $\text{Ru}(\text{bipy})_3^{2+}$ can be viewed as a combination of radiative and weakly-coupled radiationless processes through a low-energy set of levels, and a thermally activated strong coupled radiationless process through a higher set of energy levels.

Because the elevated temperature thermally populated state is non-luminescent and decays rapidly to the ground state, the deduction that the complex may be photoactive has been made. This appears to be the case and photochemical data, [19,22,23], indicates, that the photoactivity is due to ligand displacement reactions rather than photoredox processes. This clearly shows, that the lower set of levels are photo-inert, while the upper set are photo-active.

2:3:4 SUBSTITUENT EFFECTS ON THE PHOTOPHYSICS OF RUTHENIUM
 (II) BIPYRIDINE COMPLEXES

In general, the replacement of bipyridine ligands in $\text{Ru}(\text{bipy})_3^{2+}$ with those bearing substituents on their 4 and 4' positions seems to have little observable effect on the absorption and emission spectra of these complexes. The general structure of the spectra at room temperature appears to be consistent with that of the parent. Therefore, it is assumed that there is little or no change in those states responsible for emission and absorption at this temperature. There is, however, a shift to red wavelength of the maxima in both spectra relative to the maxima observed in $\text{Ru}(\text{bipy})_3^{2+}$ [24,25]. This shift is assumed in some extent to be due to extension of the conjugation of the π system, but it seems to be affected in the main by the resonance and field effects of the substituents. For example, examination of the absorption of a series of +M, -I substituents at the 4 and 4' positions on the bipyridine ligands [24], shows that both the mono- and disubstituted bipyridine ligands give a red shift of the absorption maximum. Monosubstituted ligands give a slightly lower shift than disubstituted ligands, but the difference is marginal. The substituents also affect the molar absorptivities ϵ_s , defined at λ_{\max} of the CT band and, it has been shown, that the marked variations in the value of ϵ_s are influenced by the electron donating character of the substituent. Thus, ϵ_s increases over the series of ruthenium complexes with bipyridine ligands bearing NH_2 , OR, H, Cl and Br atoms or groups.

For emission spectra, +M, -I substituents induce shifts similar to that induced in the absorption band maximum, although

substituents having a larger +M effect have a larger effect on the shift of the absorption band. Thus, the apparent Stokes shift [$\lambda_{\max(\text{abs})} - \lambda_{\max(\text{em})}$] for complexes bearing +M, -I substituents in the 4,4'-positions decreases in the series Cl, H, Br, OEt, OPh, NHAc, NH₂, NET₂.

2:4:1 LUMINESCENT PROPERTIES OF MIXED POLYBIPYRIDINE RUTHENIUM (II) COMPLEXES

For the purpose of this thesis, namely, the development of a luminescent label for use in time-resolved immunoassay, it was proposed to synthesize ruthenium (II) complexes with three bipyridine ligands, one of which should be mono-substituted at the 4 position or di-substituted at the 4 and 4' positions. This substituted bipyridine ligand should bear functionalities that could easily be activated towards conjugation with an antibody. The reasons for the choice of complexes of this type are discussed in detail in Chapters 1 and 3. At this point, it will be sufficient to say, that, having found that Ru(bipy)₃²⁺ had the required quantum yield and spectral properties for a luminescent label in immunoassay, we embarked on the synthesis of a series of ruthenium complexes that would retain these properties, but could also be conjugated to an antibody.

All the relevant photophysical data of the synthesized ruthenium complexes are listed in Table 2-1. For all the ruthenium complexes examined, both the emission and absorption spectra maintained the original characteristics of Ru(bipy)₃²⁺. In their absorption spectra, they exhibited an intense d-ligand π* charge-transfer. However, as can be seen from Table 2-1, the absorption maximum was red-shifted relative to the parent complex. It can also be seen, that the presence of different substituents on one of the bipyridine ligands appears to have little or no effect on the degree of red shift observed on the C-T band.

TABLE 2-1

PHOTOPHYSICAL DATA RELATING TO A SERIES OF COMPLEXES $[\text{Ru}(\text{bipy})_2(\text{X})]^{2+}$
 (X = bipy or substituted bipy)

COMPLEX	SPECTRAL LIMITS		maxex	maxem	LIFETIME	* QUANTUM YIELD
	EMISSION	EXCITATION				
$[\text{Ru}(\text{bipy})_3]^{2+}$	550-750nm	320-600nm	450nm	610nm	⁺ 0.855μs	0.035
$[\text{Ru}(\text{bipy})_2(\text{bipy Me vinyl})]^{2+}$ (40)	550-750nm	350-525nm	468nm	615nm	400ns	0.049
$[\text{Ru}(\text{bipy})_2(\text{bipy Me}(\text{CH}_2)_3\text{OH})]^{2+}$ (35)	550-750nm	450-600nm	465nm	615nm	320ns	0.050
$[\text{Ru}(\text{bipy})_2(\text{bipyCl})]^{2+}$ (31)	555-800nm	245-550nm	468nm	625nm	320ns	0.033
$[\text{Ru}(\text{bipy})_2(\text{bipy Me}_2)]^{2+}$ (41)	550-800nm	240-550nm	468nm	620nm	370ns	0.036
$[\text{Ru}(\text{bipy})_2(\text{bipy(dp)}_2)]^{2+}$ (43)	550-800nm	290-550nm	468nm	625nm	#	#
$[\text{Ru}(\text{bipy})_2(\text{bipyBr}_2)]^{2+}$ (46)	550-800nm	280-550nm	468nm	645nm	240ns	0.030
$[\text{Ru}(\text{bipy})_2(\text{bipyCl}_2)]^{2+}$ (26)	580-800nm	220-550nm	468nm	650nm	120ns	0.009
$[\text{Ru}(\text{bipy})_2(\text{bipy(NH}_2)_2)]^{2+}$ (19)	500-850nm	230-600nm	470nm	665nm	80ns	#
$[\text{Ru}(\text{bipy})_2(\text{bipy(CO}_2\text{Et})_2)]^{2+}$ (50)	550-850nm	300-550nm	468nm	670nm	300ns	#
$[\text{Ru}(\text{dpbipy})_2(\text{bipy Me}(\text{CH}_2)_3\text{OH})]^{2+}$ (37)	550-800nm	300-600nm	482nm	630nm	370ns	0.083

* Quantum yields measured in degassed acetonitrile

+ Literature value quoted for the lifetime of $[\text{Ru}(\text{bipy})_3]^{2+}$ [23]

Unmeasured values

The emission spectra obtained for the ruthenium complexes consists of a number of closely spaced emission bands, which, at room temperature lose their fine structure and are recorded as broad bands. Examination of the photophysical data of these complexes, shows that, as with the absorption spectra the λ_{\max} of the emission is red shifted relative to that of the parent complex $\text{Ru}(\text{bipy})_3^{2+}$. However, with emission, the substituents on the bipyridine ligand appear to have a greater effect over the amount of shift observed, than is seen in the absorption spectra. Those complexes containing a di-substituted ligand, eg. (26), appear to give a greater red shift than those containing a mono-substituted ligand, eg. (31). On examination of the substituents present, it can be seen, that the shift in the λ_{\max} of the emission spectra is dependent on the mesomeric and inductive effects, that the substituent exerts on the ligand, and, thus, on the complex. So, a methyl substituent, that has an electron-releasing inductive effect, exhibits little red shift, whereas a substituent with a large mesomeric effect, eg. NH_2 , gives a correspondingly large shift.

From examination of the luminescent lifetimes of the complexes (Table 2-1), it appears they are also affected by the presence of substituents on the ligands. In general, a decrease is seen in the lifetime corresponding with an increase in Stokes shift. The mono-substituted complexes show a smaller decrease in their lifetime, relative to those ruthenium complexes that bear disubstituted ligands.

The structures of the ruthenium complexes (37) and (35) differ only by the fact that complex (37) bears two 4,4'-diphenyl-2,2'-bipyridine ligands instead of the two 2,2'-bipyridine ligands of complex (35). Examination of the absorption and emission spectra of these complexes shows that (37) exhibits a red shift in both emission and absorption maxima relative to (35). This can probably be explained by the fact that the 4,4'-diphenyl-2,2'-bipyridine ligands of (37) give a higher degree of conjugation to the complex.

2:5:1 ROOM TEMPERATURE LUMINESCENCE (RTL)

As well as utilising the ruthenium (II) polybipyridine complexes as labels in time-resolved immunoassay, other properties of the complexes were investigated in an attempt to evaluate their use in other types of immunoassay. One such property was the room temperature luminescence of $\text{Ru}(\text{bipy})_3^{2+}$ which, it was hoped, might result in the use of the complexes in a solid-phase immunoassay.

2:5:2 MECHANISMS OF ROOM TEMPERATURE PHOSPHORESCENCE

Room temperature phosphorescence (RTP) was a phenomenon first noted by Schulman and Walling, [26], whereby ionic organic molecules adsorbed at room temperature on a solid surface, e.g. paper, silica, or alumina, exhibit phosphorescence. This led to the exploitation of room temperature phosphorescence for analytical purposes.

The exact mechanism of RTP appears, at present, to be a matter for debate. However, Schulman and Walling, [26, 27], suggested that the adsorption of ionic organic molecules onto a solid surface, caused them to be held rigidly, so inhibiting collisional deactivation of the triplet state and restricting oxygen quenching when the sample was dried rigorously. This hypothesis was then extended, [28], to the study of the interaction of the phosphor with filter paper and the effects of oxygen and moisture on this interaction. It was found that both oxygen and moisture can independently quench RTP. This was indicated by the relative intensity data obtained from a sample in humidified argon and oxygen (Table 2-2).

Also, from Fig. 2-17 [28], it can be seen, that, in the absence of oxygen, moisture by itself acts as a powerful quenching agent. At low humidities, a moderate quenching effect was noted, while at high humidities quenching was quite dramatic. On the basis of this, it was first suggested, that the mechanism for RTP involved hydrogen bonding of the organic molecules to

hydroxy groups on the solid support, thus providing a rigid sample matrix, and second, that moisture competes with surface hydroxyl functionalities for hydrogen-bonding to the phosphor molecules, thus tying up hydroxyl groups so that the phosphor is not held rigidly; in other words, water "softens" the matrix, allowing collisional deactivation. Quenching by triplet ground state oxygen was also found to occur in the absence of moisture. As the magnitude of oxygen quenching was facilitated by the presence of moisture (Fig. 2-18) [28], it was, therefore, concluded that moisture must be regarded as the most important factor in quenching RTP, because it could both transport oxygen onto the sample matrix and allow collisional deactivation to operate.

TABLE 2-2 RELATIVE INTENSITIES OF SODIUM 4-BIPHENYLCARBOXY-LATE[28]

Samples in Ar and O₂ as a Function of Relative Humidity

%H ^a	I _{Ar^b}	Rsd in Ar ^c	I _{O₂^d}	Rsd in O ₂ ^c	QH ₂ O ^e	Q _{O₂} ^f
0	100	1.2	70.9	1.5	0	29.1
3.2	98.1	1.1	70.3	1.3	1.9	27.8
8.5	91.6	2.4	61.3	1.9	8.4	30.3
18.8	57.6	1.2	25.5	3.8	42.4	32.1
37.1	12.8	2.6	2.5	14	87.2	10.3
58.3	2.6	7.1	0.4	2.9	97.4	2.2
80.5	0.7	4.3	0.1	17	99.3	0.6
100	0.3	11	0.0	-	99.7	0.3

a = % relative humidity of gas at 298K

b = Intensity in argon relative to 0% humidity in argon (I_{Ar°})

c = Calculated from triplicate runs and given in %

d = Intensity in oxygen relative to I_{Ar°}

e = I_{Ar°} - I_{Ar}

f = I_{Ar°} - I_{O₂}

Fig. 2-17 Relative Intensities of NaBPCA Samples in Ar (Curve A = I_{Ar} , -) and O₂ (Curve B = I_{O_2} , ---) as a Function of Humidity [28]

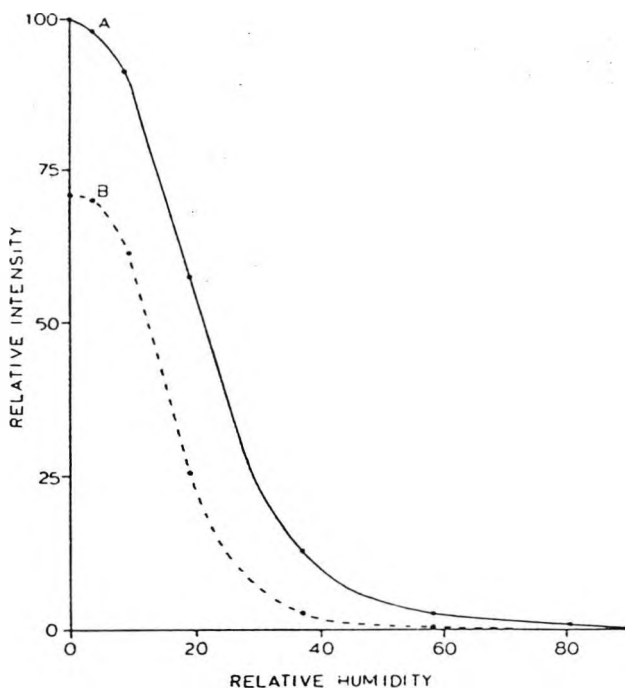
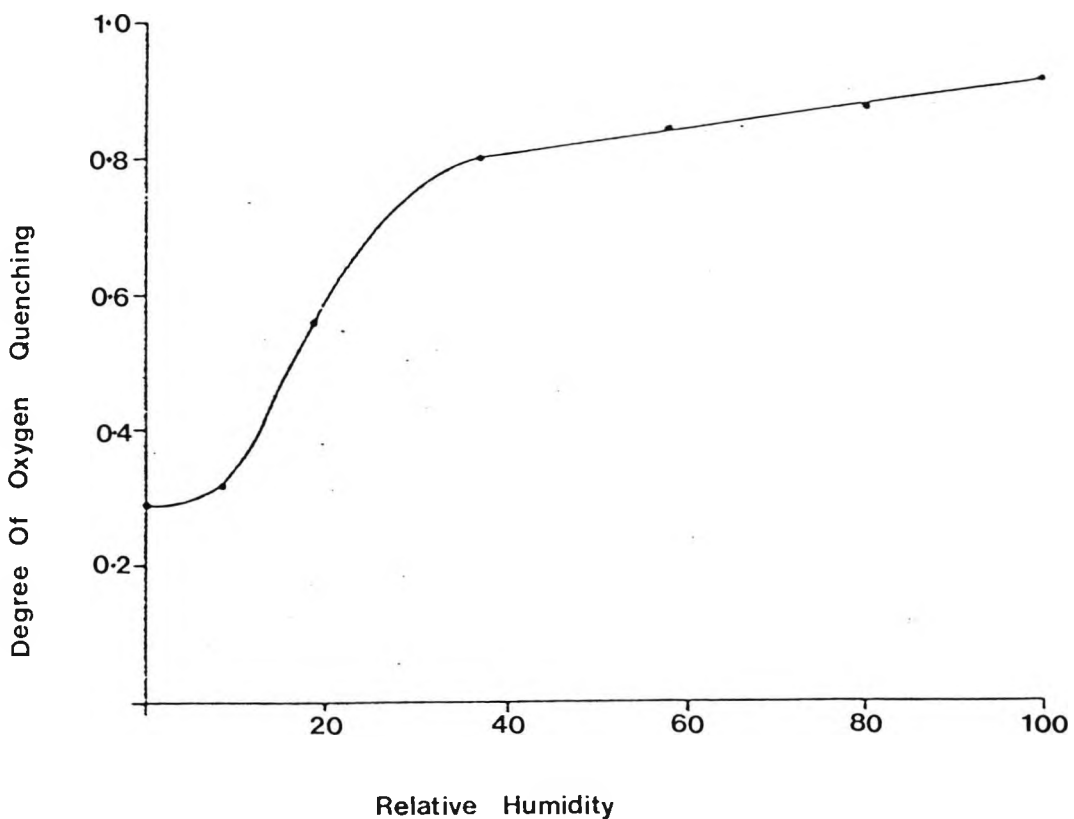


Fig. 2-18 Degree of O₂ Quenching Represented by Q_{O_2}/I_{Ar} Plotted as a Function of Relative Humidity for NaBPCA Samples. [28]



The hypothesis that hydrogen-bonding is responsible, in some part, for the binding of the analyte to the substrate, has been borne out by other work involving phosphorescence investigation of hydrogen bonding [29] and work with silanized paper [28].

Studies comparing the phosphorescence signals of several compounds adsorbed on filter paper at room temperature with those of the same compounds at 77K in a solid matrix (Table 2-3), [30], show that the rigidity, with which molecules are held on filter paper is important. These studies demonstrate, that those molecules which have the most ionic sites, show the greatest rigidity, eg. 2,4 -dithio-pyrimidine, a doubly charged species, shows a better ratio of phosphorescence signals at 77K and at room temperature than 5-acetyl-uracil, an uncharged species, (Table 2-4).

TABLE 2-3 COMPARISON OF PHOSPHORESCENCE SIGNALS AT ROOM TEMPERATURE AND AT 77K [30]

COMPOUND *	Max. Phos. Signal @ 77 K	Max. Phos. Signal @ 330 K
4-amino-benzoic acid	6	
4-methylmercapto-purine	8	
2-amino-6-methyl-mercapto-purine	19	
4-amino-2,6-dihydroxyl pyrimidine	50	
2,4-dithio-pyrimidine	1.8	
sulphaquanidine	110	
tryptophane	10	
5-acetyl-uracil	220	
2-thio-6-amino-uracil	26	
vanillin	1.6	

* All compounds prepared in 1M NaOH.

Concentrations are approximately 5mM.

TABLE 2-4 INFLUENCE OF NUMBER OF IONIC SITES UPON PHOSPHORESCENCE SIGNALS AT 77K AND AT ROOM TEMPERATURE [30]

Phos. Ratio P_{77K}/P_{333K} (1M NaOH)	No. of Ionic Sites	Molecular Species
2	2	4-hydroxy-3-methoxybenzaldehyde
50	1	4-amino-2,6-dihydroxy-1-pyrimidine
220	0	5-acetyl-uracil

2:5:3 MATRIX EFFECTS IN RTP

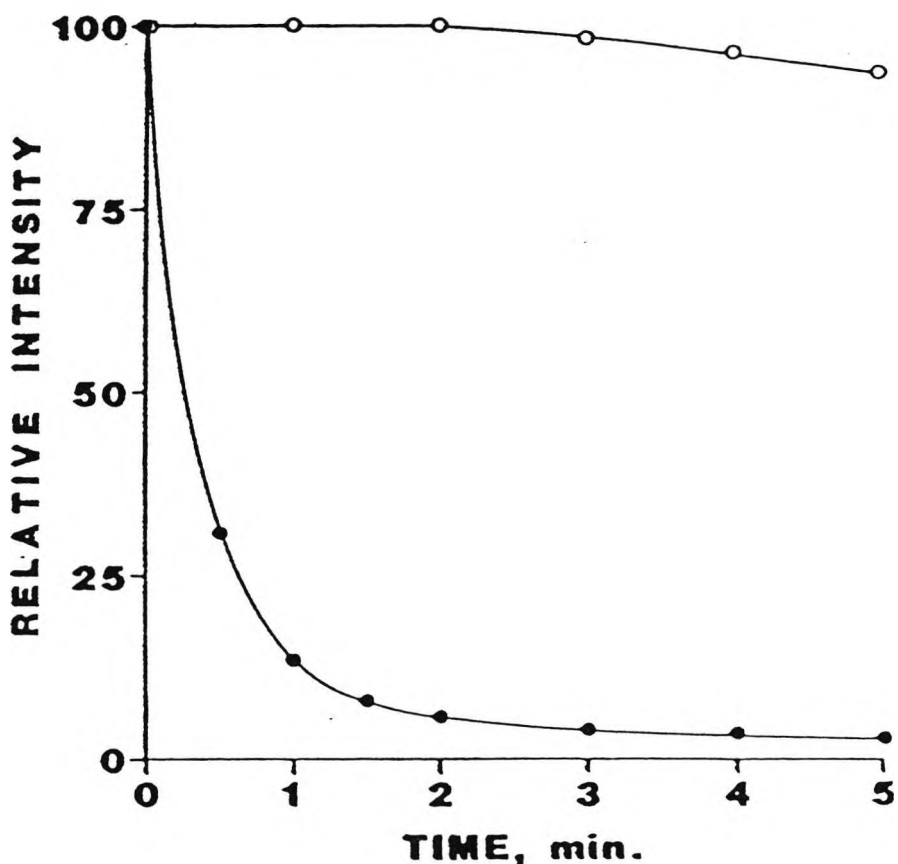
Investigations have also been made into the effect of the matrix on the lifetime of RTP [31]. The phosphorescent half-life of sodium 2-naphthalenesulphonate on filter paper with various compounds also adsorbed onto the paper was measured (Table 2-5).

In every case, the results show that the lifetime increased. These results are consistent with the previously proposed model for RTP (see Section 2:5:2), assuming that packing the matrix with salts and sugars further inhibits the internal molecular motions of the emitting compound. Alternatively, RTP could arise, because compounds become trapped within the matrix, and are thereby protected from quenching by molecular oxygen. Accordingly, it is possible that added compounds act to "plug up" the channels and interstices of the matrix, thus decreasing permeability to oxygen. Further extension of this idea has shown, that impregnation of the filter paper with sodium citrate decreases the oxygen permeability [32] and its inherent quenching effect (Fig. 2-19), allowing analysis of samples at relative humidities of 60% or less.

TABLE 2-5 EFFECT OF ADDED SUBSTANCES (0.5M) ON THE FIRST OBSERVABLE HALF-LIFE OF PHOSPHORESCENCE OF 2-NAPHTHALENE SULPHONATE ON FILTER PAPER [31]

Added Compound	Half-Life ms	Added Compound	Half-Life ms
-	135±6	CH ₃ COONa	256±66
NaF	212±34	KOH	358±38
CaCl ₂	272±42	H ₃ BO ₃	267±38
SrCl ₂	290±10	Glycine	303±40
BaCl ₂	327±46	Alanine	308±28
NH ₄ Cl	207±49	Glucose	506±23
(NH ₄) ₂ CO ₃	175±7	Sucrose	587±27

Fig. 2-19 Room Temperature Phosphorescence Intensity Plotted as a Function of Quenching Time for 4-biphenylcarboxylic acid Adsorbed on Paper (●) and Sodium Citrate Impregnated Paper (○). Quenching was Accomplished by exposure to air at a relative humidity of 58%. [32]



Many materials other than filter paper have been investigated for their possible use as solid supports in RTP; one of these is sodium acetate. In an extensive report, submitted by von Wandruszka and Hurtubise [33], on the RTP behaviour of p-aminobenzoic acid (PABA) on sodium acetate, it was shown that there appeared to be structural requirements for PABA to strongly adsorb onto sodium acetate and to exhibit RTP on this substrate. This led to the following general conclusions about the RTP behaviour of compounds similar to PABA:-

- i) Compounds with a benzene nucleus must have a carboxyl group attached to the 1-position to show RTP, e.g. Aniline gives no RTP signal.
- ii) A hydrogen-bonding substituent attached to the 4-position on the benzene ring is also required; the only suitable groups being amino and hydroxyl groups.
- iii) No RTP is seen for compounds, in which the carbonyl group is displaced one or more carbon atoms from the benzene ring.

Further studies of the pH dependence of the PABA RTP signal when adsorbed onto sodium acetate, indicated that low RTP signals resulted at high acidities. It was thought that this was due to protonation of the hydroxyl and amino groups of PABA, which prevented strong interaction with the sodium acetate. It was also found, that high sodium hydroxide concentrations gave a decrease in the intensity of the RTP signal; this was probably due to precipitation of sodium hydroxide on the surface.

The solvent usually used for the application of materials onto sodium acetate was ethanol. Ethanol is a suitable solvent for RTP, as its volatility meets the required properties. If a solvent is too volatile, it evaporates before the adsorbate applied to the solid substrate has adequately spread across the

solid, leading to the development of concentration gradients on the surface. Water was also used, but this resulted in the formation of sodium acetate trihydrate, which gave a low RTP signal. Other suitable solvents were n-propanol, iso-propanol, and iso-butanol. Aprotic solvents, eg. ether, acetone, DMF, and cyclohexane, gave no RTP signal.

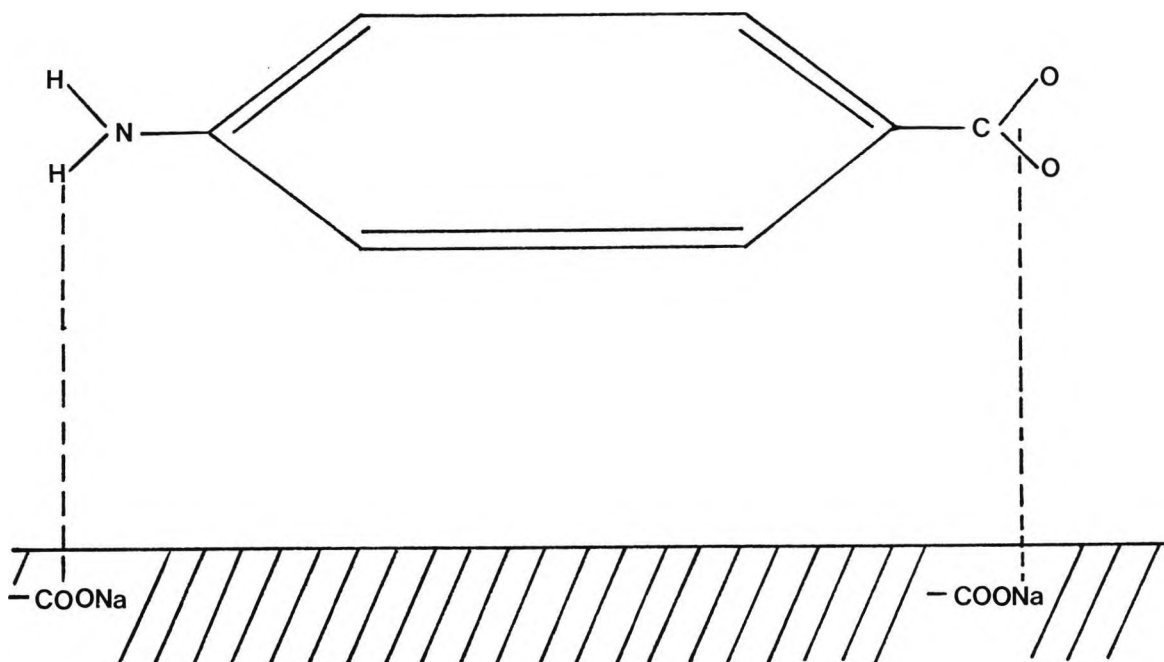
From their results, outlined above, on sodium acetate, von Wandruszka and Hurtubise, [33], put forward a theory for the mechanism of adsorption of PABA onto sodium acetate. They proposed , that the adsorption of PABA was preceded by partial neutralisation with dissolved sodium acetate in alcoholic solution. This proposal was supported by the strong RTP of the sodium salt of PABA (Na-PABA), when it was adsorbed onto sodium acetate in an ethanolic solution. No signal was observed for either PABA or Na-PABA in acetone or DMF, probably due to ion pairing and the formation of a conjugated species in these solvents.

A consequence of an ionised adsorbate strongly adsorbing on sodium acetate is insensitivity of the phosphorescence signal to moisture. Because the chemisorption interactions between adsorbent and adsorbate are so favourable, the adsorbate effectively displaces adsorbed water from the surface, thus the predominant interactions are directly between adsorbent and adsorbate. Water cannot, therefore, effectively compete for occupied sites on the adsorbent.

Infra-red studies [33] showed that the N-H stretching vibrations of PABA shifted to higher wavelengths and broadened; this is thought to indicate hydrogen bonding between both the amino and the carboxyl groups of PABA, and the sodium acetate surface.

As a result of surface area studies, a model for the adsorption of PABA onto sodium acetate was proposed, [33], (Fig. 2-20). It can be seen from Fig. 2-20 that the molecule is adsorbed flatly onto the surface, and that one molecule of PABA requires two of sodium acetate in order to be adsorbed.

Fig. 2-20 Adsorption of PABA on a Sodium Acetate Surface [33]

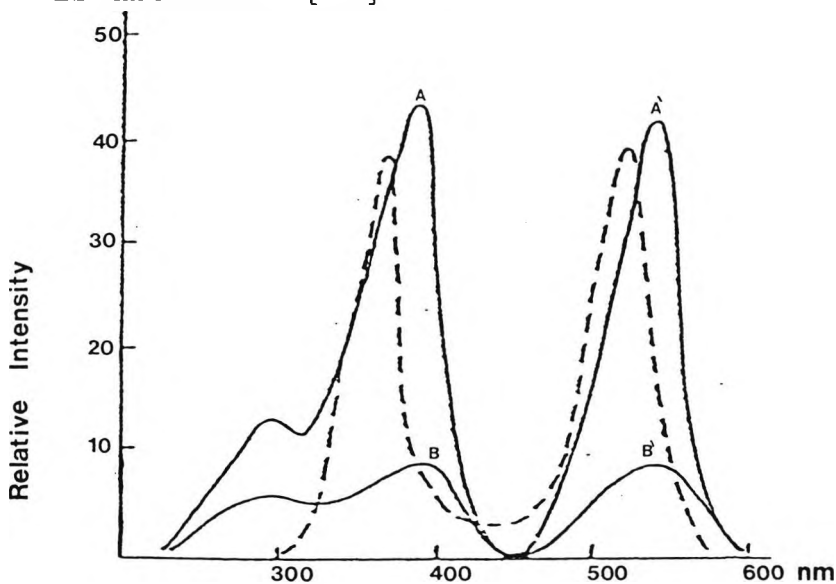


2:5:5 HEAVY-ATOM EFFECT ON RTP

So far, we have only considered RTP of ionic or polar organic molecules. However, RTP has been observed in non-polar as well as polar organic molecules, by the use of a heavy-atom perturber [34-36].

This heavy-atom effect is thought to be due to the presence of a heavy atom which increases the spin-orbit coupling and so enhances spin-forbidden transitions, thus allowing more rapid intersystem crossing. This results in a lowering of the fluorescence yield and an increase in the phosphorescence yield. Fig. 2-21 shows an example of this effect, using lead tetra-acetate as the heavy atom in the RTP of cinoxacin.

Fig. 2-21 Fluorescence (---) and Phosphorescence (-) Spectra of Cinoxacin. Excitation (A) and Emission (A') Spectra of Cinoxacin on Paper Strip treated with Lead Tetra-acetate. Excitation (B) and Emission (B') Spectra of Cinoxacin on Plain Paper. The Real Ratio of A to B is about 80. [37]



2:5:6 ANALYTICAL USE OF RTP

RTP is now on the way to being established firmly as an analytical procedure. Not only does it have a low detection limit (in the nano-gram region for most organic molecules [38]), it is also a relatively simple technique to perform. In the initial stages, it involves the spotting of a certain volume of sample solution onto a pre-dried solid support. After application of the sample, the solid support is again dried. The method and timing of the drying process, in which infra-red lamps and ovens are most commonly employed, varies according to the procedure followed [39]. After drying, the samples are directly mounted into the spectrophotometer to measure the phosphorescence signal.

The exact nature of the sample compartment used for RTP measurement varies. There are, however, two main methods; one designed by Winefordner et al [40], which allows convenient subtraction of blank from sample spectra, and another which is an automated method submitted by Vo-Dinh, Walden and Winefordner [41].

2:5:7 RTL IN RUTHENIUM POLYBIPYRIDINE COMPLEXES

It was decided to attempt to utilise the procedures of RTP for the study of the solid phase behaviour of the ruthenium tris bipyridine cation, $\text{Ru}(\text{bipy})_3^{2+}$, to ascertain whether adsorption of the complex onto a rigid phase would increase the lifetime of the ruthenium complex to a greater extent than that observed at room temperature in solution. The term was changed from RTP to room temperature luminescence (RTL), as luminescence was considered to be a more appropriate term to express the emissive properties of ruthenium complexes.

From the theory put forward for the mechanism of RTP, $\text{Ru}(\text{bipy})_3^{2+}$ should exhibit this phenomenon at room temperature, because not only is it ionic in nature, but it also contains within its structure a heavy atom, namely ruthenium, which should give rise to an internal heavy-atom effect.

2:5:8 INITIAL EVALUATION OF RTL IN RUTHENIUM POLYBIPYRIDINE COMPLEXES

A set of preliminary experiments were conducted to evaluate whether $\text{Ru}(\text{bipy})_3^{2+}$ would exhibit RTL, and also to assess the potential scope of the use of RTL in the detection of low levels of $\text{Ru}(\text{bipy})_3^{2+}$.

One of the first experiments undertaken was the investigation into the effect which the adsorption of $\text{Ru}(\text{bipy})_3^{2+}$ onto Whatman No. 1 filter paper would have on its lifetime; viz. would it be lengthened? This initial experiment involved a soaking method in which a 1.5cm x 0.5cm rectangle of Whatman No. 1 paper was dipped into a concentrated methanol solution of $\text{Ru}(\text{bipy})_3^{2+}$ until it was thoroughly soaked. Subsequently, it was dried in a flow of hot air for approximately 5 minutes. From Table 2-6, it can, in fact, be seen, that the lifetime of $\text{Ru}(\text{bipy})_3^{2+}$ appears to be enhanced by adsorption onto the filter paper.

TABLE 2-6 LUMINESCENT LIFETIME OF $\text{Ru}(\text{bipy})_3^{2+}$ ADSORBED ON A PAPER SUBSTRATE

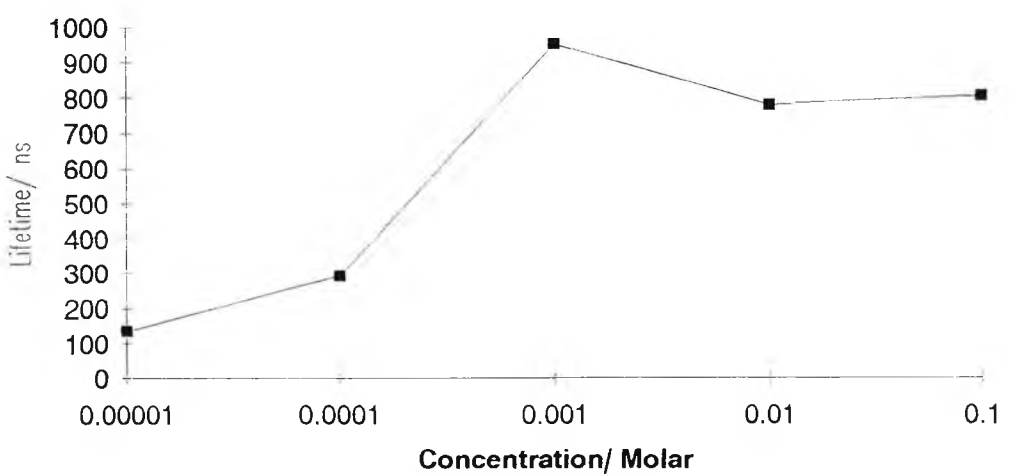
	Lifetime
$\text{Ru}(\text{bipy})_3^{2+}$ in H_2O	460 ns
$\text{Ru}(\text{bipy})_3^{2+}$ in CH_3CN	161 ns
$\text{Ru}(\text{bipy})_3^{2+}$ on paper	635 ns

As the initial experiment demonstrated that adsorption onto filter paper did, in fact, lengthen the lifetime of emission of the ruthenium complex, it was decided to investigate further the RTL effect. One step towards establishing this as an analytical technique for the detection of ruthenium complexes, was to investigate the effect that low concentrations would have on the detection of the complex. This preliminary experiment was again conducted using the soaking method outlined above, but utilising known molar solutions of $\text{Ru}(\text{bipy})_3^{2+}$ in methanol. The results are detailed in Table 2-7. From these results, it can be seen that the ruthenium complex can be detected at low levels. A graph plotted of concentration of $\text{Ru}(\text{bipy})_3^{2+}$ against the luminescent lifetime of the complex (Graph 2-1), shows an increase in the lifetime from $1 \times 10^{-5}\text{M}$ to $1 \times 10^{-3}\text{M}$; however, at concentrations greater than $1 \times 10^{-3}\text{M}$ the measured luminescent lifetime appears to plateau out. This apparent plateau in the RTL signal at high concentrations may be inherent in the method used for the measurement of the signal. As the paper is soaked into the ruthenium solution, the matrix becomes saturated and this can lead to the development of concentration gradients, thus increasing the degree of error in the measured results. At higher concentrations, the concentration gradient effect may become more noticeable.

TABLE 2-7 EFFECT OF CONCENTRATION ON THE LUMINESCENT LIFETIME OF $\text{Ru}(\text{bipy})_3^{2+}$

Concentration of $\text{Ru}(\text{bipy})_3^{2+}$	Lifetime
0.1M	806 ns
0.01M	782 ns
$1 \times 10^{-3}\text{M}$	953 ns
$1 \times 10^{-4}\text{M}$	293 ns
$1 \times 10^{-5}\text{M}$	135 ns
Paper	87 ns

GRAPH 2-1 EFFECT OF CONCENTRATION ON THE LUMINESCENT LIFETIME OF RUTHENIUM TRIS BIPYRIDINE



The preliminary investigations of the RTL effect exhibited by Ru(bipy)₃²⁺ have, therefore, revealed the following:-

- i) Immobilisation of Ru(bipy)₃²⁺ onto a suitable solid support, results in lengthening of the measured lifetime of the complex from that detected in solution.
- ii) Low concentrations, in the region of 1x10⁻⁵M of the ruthenium complex, can be analysed by measurement of the RTL signal.

However, to utilise this technique as a quantitative analysis method for the detection of ruthenium complexes, fuller investigation of the substrate for adsorption and the level of analyte to be added to the substrate, would have to be carried out.

It was, therefore, decided to investigate the effect of different solid phases on the emission spectrum of Ru(bipy)₃²⁺. This set of experiments again utilised the soaking method described above. Although it is clear from the results obtained, that there is a problem with the reproducibility of the results (Table 2-8), various trends can be noted. It can, for example, be seen that those solid phases containing glass fibres exhibited very little signal, compared with that of Ru(bipy)₃²⁺ adsorbed on Whatman No. 1 filter paper. This could lead to the conclusion that the interaction between the ruthenium complex and the silicon dioxide groups of the glass fibre matrix was low. Thus, as the complex was not held rigidly to the matrix, it was, therefore, open to attack by quenching factors such as moisture, so giving rise to a reduction in the intensity of the luminescent signal.

Among those solid phases that showed improved RTL signals relative to the glass fibre-containing substrates, were PVA and polyacrylamide. This increase in the signal was probably due to more than just physical adsorption onto the surface of the matrix. It could be an indication of some ionic interaction, or possibly a hydrogen bonding effect between these matrices and the ruthenium complex.

Although GNT paper (supplied by Wiggins Teape) gave the highest recorded signal, it appeared to behave in a different manner from the other surfaces investigated. When the paper sample was dipped into the ruthenium solution, a floating film was formed on the surface and no adsorption of the solution into the paper appeared to occur. Once dried, the coat of the complex on the paper was uneven, which, in some way, could explain the high standard deviation of the results obtained using this matrix. From the initial appearance of the surface, it was expected that the RTL result would be low. However, as previously stated, this paper gave the highest result. The exact nature of this paper is unknown, but it is possible that it is coated with some type of polymer, which was able to interact with the ruthenium complex. This could result in the Ru(bipy)₃²⁺ being held more rigidly on the surface, so preventing quenching of the luminescent signal.

TABLE 2-8 VARIATION OF RTL SIGNAL WITH SOLID PHASE(1)

Solid Phase	Average Integrated RTL Signal +	Ratio *	Standard Deviation
GNT paper	305.492	1.73	30
100% polyacrylamide 10% PVA binder	199.662	1.27	28
100% PVA	237.341	0.61	77
100% polyacrylamide	153.974	0.33	36
100% 1.8μ glass fibres	62.638	0.17	17
100% polyester fibres	66.111	0.14	31
5μ glass fibres SAN binder	49.19	0.13	11
5μ glass fibres 10% PVA binder + polyacrylonitrile	43.493	0.12	16
5μ glass fibres	27.905	0.08	3

+ Calculated as area under emission curve 500-700nm.

* Ratio of sample RTL signal to that of Whatman No. 1 filter paper under the same conditions.

It has, therefore, been established that $\text{Ru}(\text{bipy})_3^{2+}$ gives an RTL signal, which can be measured to a low level by means of lifetime experiments. It has also been ascertained that:-

- i) The magnitude of the signal is concentration dependent,
and
- ii) changing the adsorption matrix results in variation in the measured RTL signal, depending on the type of interaction of $\text{Ru}(\text{bipy})_3^{2+}$ with the adsorbent surface.

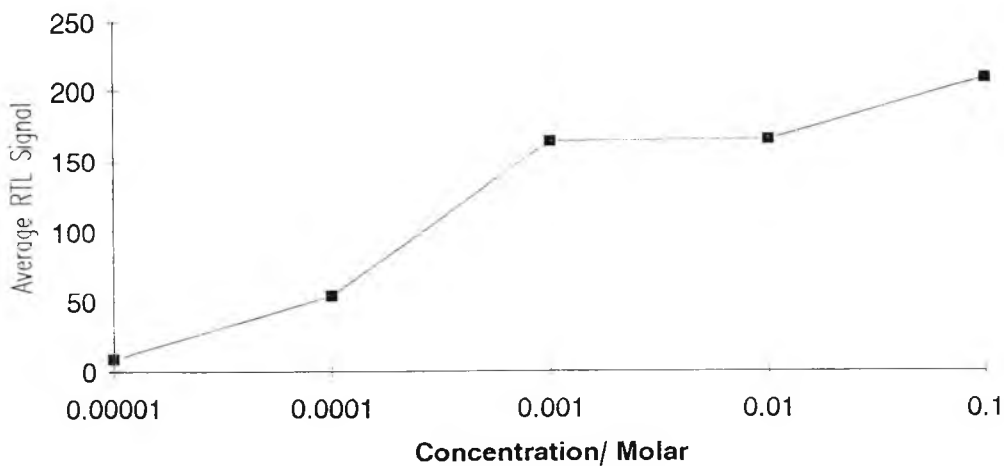
One final set of preliminary experiments was conducted utilising a limited amount of sample ($20\mu\text{l}$), and Whatman No. 1 filter paper as the adsorption matrix. The aim of these experiments was to investigate the limit of detection of the ruthenium complex by RTL. Although, from these experiments, a good limit of detection was established in the region of 1×10^{-9} moles, we were again unable to obtain reproducible results within a reasonable standard deviation (Table 2-9, Graph 2-2). In fact, repeated spectra obtained from the same sample, did not give analogous results. This difficulty in obtaining reproducibility may, in part, be due to concentration gradients set up on adsorption of the complex onto the solid surface, so leading to non-uniform adsorption onto the filter paper. Excitation of the surface in different places on the same sample, would thus give varying emission signals, and so a poor standard deviation of results.

TABLE 2-9 LIMIT OF DETECTION OF RTL SIGNAL OF $\text{Ru}(\text{bipy})_3^{2+}$

Concentration	No. of moles	* Average RTL Signal	SD
0.1M	2×10^{-6} moles	208.05	25
0.01M	2×10^{-7} moles	165.28	34
$1 \times 10^{-8}\text{M}$	2×10^{-8} moles	163.94	33
$1 \times 10^{-9}\text{M}$	2×10^{-9} moles	53.78	12
$1 \times 10^{-10}\text{M}$	2×10^{-10} moles	8.63	-

* Calculated as area under emission curve 510-730nm

GRAPH 2-2 GRAPH SHOWING THE LIMIT OF DETECTION OF THE RTL SIGNAL OF RUTHENIUM TRIS BIPYRIDINE



2:5:9 STANDARDISATION OF RTL PROCEDURE

It is obvious from the results obtained above that RTL of $\text{Ru}(\text{bipy})_3^{2+}$ is a workable procedure which could be utilised to develop an immunoassay system. It is, however, important to remove, or reduce, as far as possible, the problem so far encountered, ie. the reproducibility of the RTL signal. There are two possible approaches to reducing the sampling variation:-

- i) Drying the solid phase more rigorously, both prior to the application of the ruthenium complex and after the application of the complex.
- ii) The addition of less analyte to the solid phase.

The latter procedure, it is believed, would cut down on the development of concentration gradients on adsorption of the complex onto the paper, resulting in uniform spread of the complex across the surface of the solid phase. Drying the adsorption matrix more rigorously should remove the moisture, so reducing quenching of the luminescent signal by oxygen, which could be aided by the presence of moisture in the sample matrix.

In fact, as can be seen from Table 2-10, drying the solid phase overnight at approx. 80°C prior to application of the sample, applying a smaller sized sample, namely 5 μ l of sample, and subsequently drying the specimen for RTL testing at approx. 80°C for a further 40 minutes, did reduce the error in reproducibility of results, showing a significant reduction in the more spurious results.

TABLE 2-10 EFFECT OF DRYING TIME AND SAMPLE SIZE ON RTL RESULTS

Solid Phase	Concentration	* Average RTL Signal	SD
Whatman No. 1 Filter Paper	0.1M	2.317	0.26
Whatman No. 1 Filter Paper	0.01M	2.988	0.28
Whatman Antibiotic Assay Discs	0.1M	+ 1.495	0.25
Whatman Antibiotic Assay Discs	0.01M	+ 2.049	0.15

* Weight of paper within emission spectral limits 500-750nm

+ Signal-blank disc signal

It was decided to investigate further potential matrices for RTL using this new drying and sampling procedure. The solid phases chosen for testing, were commercially available filter papers. As can be seen from Table 2-11, the RTL signal showed variation with the matrix utilised. One matrix, namely the Whatman antibiotic assay discs, gave a higher RTL signal than Whatman No. 1 filter paper, though a higher blank reading was obtained.

TABLE 2-11

VARIATION OF RTL SIGNAL WITH SOLID PHASE (II)

Solid Phase	* Signal due to solid phase (A)	*Signal due to solid phase treated with $[\text{Ru}(\text{bipy})_3]^{2+}$ (B)	* RTL Signal (B)-(A)
Whatman Antibiotic Assay Discs	0.8579	2.9424	2.0845
Whatman No. 1 Filter Paper	0.0972	1.1998	1.1026
Whatman No. 42 Filter Paper	0.0770	1.0167	0.9397
Hardened Whatman No. 50 Filter Paper	0.0701	0.4844	0.4143
Glass Fibre Filter Paper	0.1670	0.2341	0.0671

* All signals weight of paper between spectral limits 500-750nm

Due to the performance of these Whatman antibiotic assay discs, it was decided to assess further their performance against Whatman No. 1 filter paper, with regard to the possible limit of detection of the RTL signal on the two different matrices. From the results obtained, (Table 2-12), it was established that both types of matrix could detect $\text{Ru}(\text{bipy})_3^{2+}$ at 5×10^{-11} moles, although, the results obtained for the Whatman antibiotic discs, indicate that this solid phase is the most likely of the two matrices to have the lowest detection limit. The sole limiting factor to the detection limit of this matrix was the high blank signal of the matrix itself.

TABLE 2-12 THE LIMIT OF DETECTION OF Ru(bipy)₃²⁺ BY RTL

Solid Phase	Concentration	No. of moles	* RTL Signal
Whatman No. 1 Filter Paper (sensitivity 10x4)	0.1M	5 x 10 ⁻⁷ moles	2.6223
	0.01M	5 x 10 ⁻⁸ moles	2.7285
	1 x 10 ⁻³ M	5 x 10 ⁻⁹ moles	1.1803
	1 x 10 ⁻⁴ M	5 x 10 ⁻¹⁰ moles	0.2602
	1 x 10 ⁻⁵ M	5 x 10 ⁻¹¹ moles	0.0589
Whatman Antibiotic Assay Discs (sensitivity 3x5)	0.1M	5 x 10 ⁻⁷ moles	1.2162
	0.01M	5 x 10 ⁻⁸ moles	2.4868
	1 x 10 ⁻³ M	5 x 10 ⁻⁹ moles	1.6741
	1 x 10 ⁻⁴ M	5 x 10 ⁻¹⁰ moles	0.4811
	1 x 10 ⁻⁵ M	5 x 10 ⁻¹¹ moles	0.6535

* Signal calculated from weight of paper between spectral limits 500-700nm - blank weight.

One factor which has yet to be established in this evaluation of RTL, is the effect that variation of the sampling procedure would have on the measured RTL signal. It has already been seen, that the addition of a large volume of sample to the solid phase results in the development of concentration gradients, yielding poor reproducibility of results.

Also, one factor continuously observed is that at concentrations of Ru(bipy)₃²⁺ above 1 x 10⁻³M, the RTL signal appears to plateau out. Therefore, it appears that the application of the sample to the solid phase can have a marked effect on the signal observed. Indeed, this is further demonstrated by the results obtained on variation of the method of application of the sample to the solid phase, (Table 2-13). It appears that allowing the sample to drain by capillary action onto the solid phase, yielded a far better RTL signal than that obtained by concentration of the sample in a defined area. In fact, it is apparent that the more concentrated the sample on the solid phase, the

lower the RTL signal obtained, which could in part be due to a self-quenching effect.

TABLE 2-13 EFFECT OF VARIATION OF SAMPLING TECHNIQUE

Sampling Technique	Observed Signal
Capillary action	2.9753
Medium concentrated spot	1.4361
Small concentrated spot	0.7648

2:5:10 EVALUATION OF RTL AS AN ANALYTICAL TECHNIQUE

From the results obtained above, it would appear that RTL is a useful technique for the analysis of Ru(bipy)₃²⁺ in the picomolar range. However, at present, the scope for the introduction of experimental error is high, particularly with regard to the application of analyte onto the solid phase, and the measurement of the emission spectra.

Before finally developing RTL as an analytical procedure for the detection of ruthenium complexes, it would be advisable to carry out further experiments to investigate more thoroughly the mechanism of adsorption of the complex onto the matrix. With a better understanding of this process, the most suitable matrix could then be selected. From the results obtained above, it is obvious that the method used to apply the analyte to the matrix is of fundamental importance. Therefore, further work should be instigated to develop a more automated, and so less prone to error, method of conducting this procedure.

Errors in the measurement of the emission spectra could, perhaps, be reduced by the design of a procedure, whereby the samples would be introduced into the spectrofluorimeter with the excitation beam having a fixed angle of incidence on the solid matrix. The reproducibility of the method may also be improved by the removal of moisture from the spectrofluorimeter by

purging the sample compartment with dry inert gas, such as nitrogen or argon.

However, it is probable that on definition of the analytical procedure for RTL, that this phenomenon would prove to be a technique which could be utilised in solid phase immunoassay.

2:6:0 EXPERIMENTAL

Measurement of Excitation and Emission Spectra of Substituted Ruthenium (II) Polybipyridine Complexes

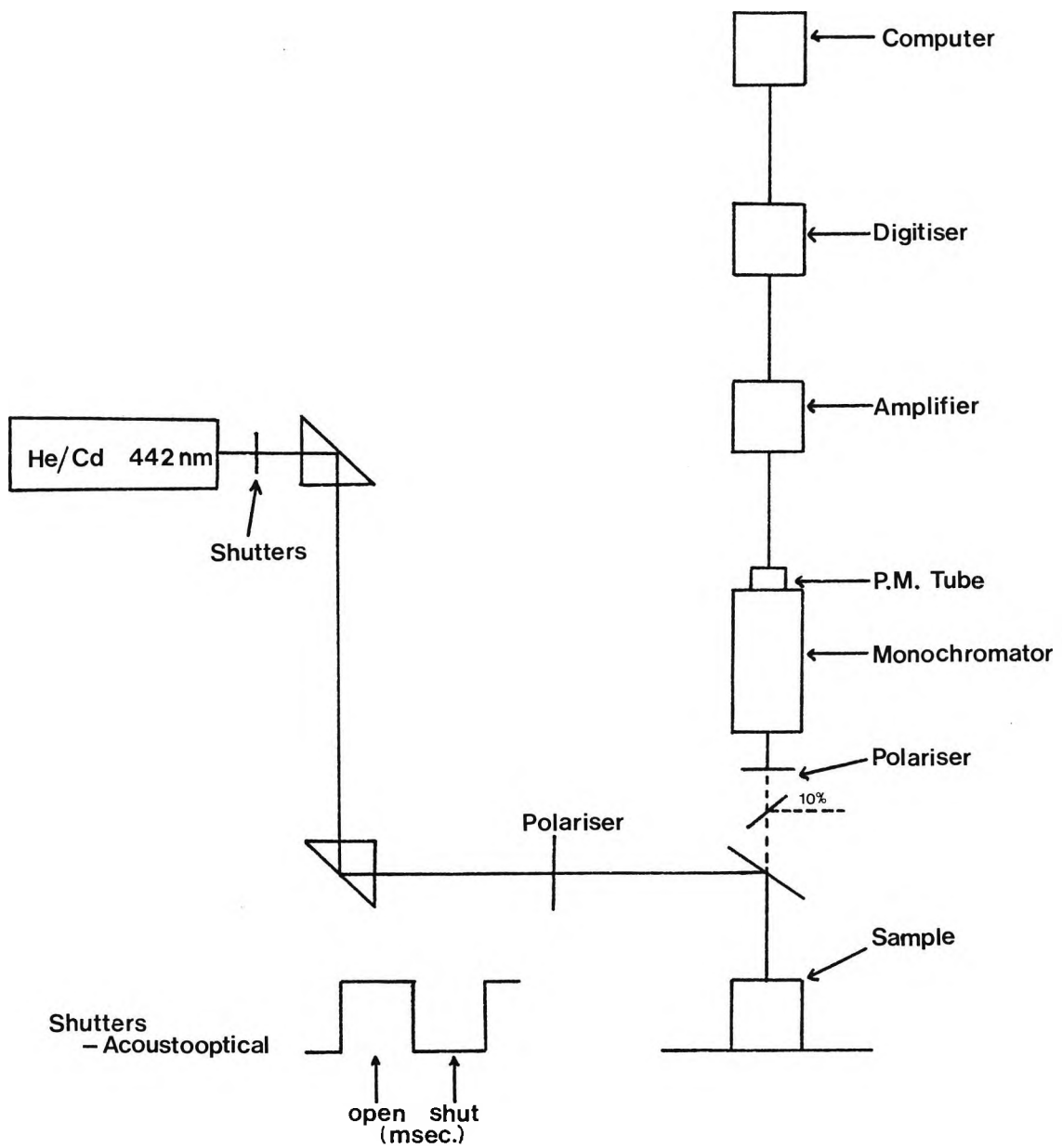
Apparatus: Emission and excitation spectra were measured with a Perkin-Elmer MPF-4 Fluorescence Spectrophotometer.

Reagents: All ruthenium complexes were prepared as detailed in Chapter 1, Section 1:3:0.

Measurement of Lifetime Data

Lifetime data were determined on a Fluorescence Microscope Modular Bench (Fig. 2-22).

Fig. 2-22 Diagram Showing Fluorescence Microscope Modular Bench



Lifetimes were measured utilising acetonitrile (HPLC grade, stored over activated 3A molecular sieve under a nitrogen atmosphere) as the solvent.

A Carl Zeiss fluorescence microscope (LAB16), equipped with a 4.0/0.75 Neofuar objective was used in the measurement of lifetime data. Sample excitation was achieved via a helium cadmium laser : model 4240 NB (Liconix, Sunnyvale, USA), wavelength 442nm, output power 50mW; together with a selective mirror FT510, and an emission long pass filter LP520 (Carl Zeiss). Gating of the $4\mu\text{m}$ (diameter) continuous wave beam was produced by an acousto-optical shutter (rise time 50ns (A. A. France)) controlled by a micro-computer C64 (Commodore, Braunschweig, FRG). The photomultiplier tube R446 (Hamamatsu, Japan) was powered by a regulated H-V supply (the Isotope Developments EHT unit, type 532/A). Output from the PMT following the excitation pulse was monitored on an oscilloscope-transient waveform recorder. Digitisation of data points was via a Tektronix digitiser TD20T (Beaverton, USA). A micro-computer (Atari 1040ST) was utilised to apply curvilinear regression routines to analyse the spontaneous decay data (base line reference:- same trigger, no light) in terms of a quadratic expression over defined regions.

At this point, we would like to acknowledge the expertise of Dr. Martin Hilchenbach and thank him for his time spent in the calculation of these results.

Measurement of Quantum Yields

Reagents: All ruthenium complexes were prepared as detailed in Chapter 1, Section 1:3:0.

Solutions of complexes in acetonitrile (HPLC grade, stored over activated 3A molecular sieve under a nitrogen atmosphere) were made up to an optical density of 0.1 at 450nm.

The solutions were degassed utilising 3 freeze thaw cycles under vacuum, and the emission spectra were measured.

Emission spectra were measured with a Perkin Elmer MPF-4 fluorescence spectrophotometer under the following conditions:-

Emission spectral limits	550-750nm
Slits	6/6
Excitation wavelength	450nm
Sensitivity	30 x 10
Chart speed	60mm/min
Scan speed	30nm/min

The area beneath the emission spectrum within the limits 550-750nm was then cut out and weighed.

Using Ru(bipy)₃Cl₂.6H₂O(CH₃CN) as a standard, the quantum yields were calculated from the following equation:-

$$\frac{\Phi_{\text{unknown}}}{\Phi_{\text{standard}}} = \frac{\text{Wt. of unknown}}{\text{Wt. of standard}}$$

$$\Phi_{\text{Of Ru(bipy)}_3\text{Cl}_2\cdot 6\text{H}_2\text{O}(\text{CH}_3\text{CN})} = 0.035$$

Quantum yield of Ru(bipy)₃Cl₂.6H₂O in acetonitrile was calculated using Ru(bipy)₃Cl₂ in water as the standard, utilising the literature quantum yield 0.042 [42], as follows:-

$$\frac{\Phi_{\text{Ru(bipy)}_3\text{Cl}_2(\text{CH}_3\text{CN})}}{\Phi_{\text{Ru(bipy)}_3\text{Cl}_2(\text{H}_2\text{O})}} = \frac{\text{Wt. of Ru(bipy)}_3\text{Cl}_2(\text{CH}_3\text{CN})}{\text{Wt. of Ru(bipy)}_3\text{Cl}_2(\text{H}_2\text{O})}$$

ROOM TEMPERATURE LUMINESCENCE EXPERIMENTAL

Life-time Measurement of the RTL Effect

A rectangular piece of Whatman No.1 filter paper (1.5 x 0.5cm) was dipped into a concentrated solution of Ru(bipy)₃Cl₂.6H₂O in methanol until it was thoroughly soaked, then dried with a hot air blower for approximately 5 minutes. A lifetime measurement was then taken of the dried sample.

Effect of Solid Phase on RTL Signal

Rectangular pieces, (1.5 x 0.5cm) of the following solid phases:-

Whatman No. 1 filter paper
GNT paper (supplied by Wiggins Teape)
100% polyacrylamide 10% PVA binder
100% PVA
100% polyacrylamide
100% 1.8 μ glass fibres
100% polyester fibres
5 μ glass fibres SAN binder
5 μ glass fibres 10% PVA binder + polyacrylonitrile
5 μ glass fibres

were dipped into a concentrated solution of Ru(bipy)₃Cl₂.6H₂O in methanol until thoroughly soaked, then dried for 5 minutes with a hot air blower. All samples of solid phases were prepared in triplicate.

All emission spectra were measured utilising a Perkin-Elmer MPF-4 fluorescence spectrophotometer under the following conditions:-

Spectral limits	500-700nm
Slits	4/4
Excitation wavelength	450nm
Sensitivity	30 x 5
Chart speed	60mm/min
Scan speed	30nm/min

RTL signals were calculated as being the area under the emission curve between the spectral limits 500-700nm.

Blank of the papers between these spectral limits was also measured and subtracted from the RTL signal.

As different sensitivities were used for GNT paper and 100% polyacrylamide 10% PVA binder (sensitivity 30) and 100% PVA (sensitivity 30 x 8), comparison of the results was obtained by the calculation of the ratio of the sample signal on different papers against the RTL signal detected on Whatman No. 1 filter paper. The sample for measurement of the RTL signal from Whatman No. 1 filter paper was prepared by the same method as the above solid phases. The resultant emission spectrum was measured at the same sensitivity at which each individual solid phase was measured; thus resulting in a standard for comparison of results.

MEASUREMENT OF THE LIMIT OF DETECTION OF RTL

The following concentrations of Ru(bipy)₃Cl₂.6H₂O in methanol were prepared:-

0.1M
0.01M
 1×10^{-3} M
 1×10^{-4} M
 1×10^{-5} M

20 μ l aliquots of these solutions were then spotted by capillary action on to Whatman No. 1 filter paper measuring 1.5 x 0.5cm. The samples were then dried using a hot air blower. Each sample at a particular concentration was repeated 5 times.

All emission spectra were measured with a Perkin-Elmer MPF-4 fluorescence spectrophotometer under the following conditions:-

Spectral limits	510-730nm
Slits	4/4
Excitation wavelength	450nm
Sensitivity	30
Chart speed	60mm/min
Scan speed	30nm/min

RTL signals were again calculated as the area under the emission curve between the spectral limits, and a blank of Whatman No. 1 filter paper between the spectral limits was also measured and subtracted from the RTL signal.

IMPROVEMENT OF THE RTL TECHNIQUE

5 μ l of a 0.1M methanol solution of Ru(bipy)₃Cl₂.6H₂O was spotted by capillary action onto Whatman No. 1 paper discs, which had been stored overnight at 80°C. The discs once spotted with analyte were dried at 80°C for 40 minutes.

Emission spectra were then measured with a Perkin-Elmer MPF-4 fluorescence spectrophotometer under the following conditions:-

Spectral limits	500-700nm
Slits	4/4
Excitation wavelength	468nm
Sensitivity	30
Chart speed	60mm/min
Scan speed	30nm/min

All measurements were carried out in triplicate.

The experiment was repeated using a 0.01M solution of ruthenium tris bipyridine in methanol under a new sensitivity reading of 10 x 5.

The whole procedure was repeated substituting Whatman Antibiotic Assay discs (13mm diameter) as the solid phase; spectral conditions were altered as follows:-

0.1M	Sensitivity	10
0.01M	Sensitivity	3 x 5

The RTL signal was measured by photocopying the emission spectrum 3 times, weighing the cut-out area under the curve between the spectral limits, and then averaging the weights, thus producing a one reading result.

VARIATION OF RTL SIGNAL WITH THE SOLID PHASE

Circular discs of 12mm diameter were cut, consisting of the following solid phases:-

Whatman No. 1 filter paper
Whatman No. 42 filter paper
Hardened Whatman No. 50 filter paper
Glass fibre filter paper
Whatman Antibiotic Assay Discs
(supplied as circles 13mm in diameter)

The discs were then stored at 80°C overnight. 5 μ l of a 0.01M solution of Ru(bipy)₃Cl₂.6H₂O in methanol was spotted by capillary action onto the dried solid phase. The samples were dried at 80°C for a further 20 minutes, and an emission spectrum was then measured with a Perkin-Elmer MPF-4 fluorescence spectrophotometer under the following conditions:-

Spectral limits	500-750nm
Slits	4/4
Excitation wavelength	468nm
Sensitivity	3 x 5
Chart speed	60 mm/min
Scan speed	30nm/min

Blanks were run under the same spectral conditions for all the solid phases and subtracted from the relative analyte measurements. RTL readings were taken as the weight of the paper between the spectral limits.

LIMIT OF DETECTION OF THE RTL SIGNAL

The following concentrations of Ru(bipy)₃Cl₂.6H₂O in methanol were prepared:-

0.1M
0.01M
 1×10^{-3} M
 1×10^{-4} M
 1×10^{-5} M

5μl of these solutions were then allowed to drain by capillary action onto a Whatman No. 1 filter paper disc (12mm diameter), previously stored at 80°C overnight. Once the discs had been spotted with analyte, they were returned to 80°C for a further 20 minutes, after which an emission spectrum was measured under the following conditions with a Perkin-Elmer MPF-4 fluorescence spectrophotometer:-

Spectral limits	500-700nm
Slits	4/4
Excitation wavelength	468nm
Sensitivity	10 x 4
Chart speed	60mm/min
Scan speed	30nm/min

A blank reading for the filter paper was measured and subtracted from all the analyte readings. The RTL signal was again calculated as the weight of paper between the spectral limits.

The above experiment was repeated using Whatman antibiotic assay discs (13mm diameter), under the same conditions, but altering the spectral sensitivity to 3 x 5.

VARIATION OF SAMPLING PROCEDURE

5 μ l of a methanol solution of 0.01M Ru(bipy)₃Cl₂.6H₂O was applied to pre-dried Whatman antibiotic assay discs, (dried overnight at 80°C) as follows:-

- i) Allowed to drain onto disc by capillary action.
- ii) Spotted into a medium-size concentrated area on the disc.
- iii) Spotted into a small-size concentrated area on the disc.

The samples thus prepared were then dried for 40 minutes at 80°C and the emission spectra measured using a Perkin-Elmer MPF-4 fluorescence spectrophotometer under the following conditions:-

Spectral limits	500-780nm
Slits	4/4
Excitation wavelength	469nm
Sensitivity	10 x 2
Chart speed	60mm/min
Scan speed	30nm/min

A blank was run of the assay disc alone under the spectral conditions, and this was subtracted from the RTL signals of the analytes, which were calculated as the weight of paper between the spectral limits.

GENERAL TEXTS

- a. PARKER, C.A., Photoluminescence of Solutions, (1968), Pub. Elsevier, Switzerland.
- b. GEOFFROY, G.L. and WRIGHTON, M.S., Organometallic Photochemistry, (1979), Pub. Academic Press Inc., New York.
- c. NICHOLLS, D., Complexes and First-Row Transition Elements, (1974), Pub. The Macmillan Press Ltd., London.

- 1. PARIS, J.P. and BRANDT, W.W., (1959), J. Am. Chem. Soc., 81, 5001.
- 2. PORTER, G.B. and SCHLAFER, H.L., (1964), Ber. Bunsenges Phys. Chem., 68, 316.
- 3. CROSBY, G.A., PERKINS, W.G. and KLASSEN, D.M., (1965), J. Chem. Phys., 43, 1498.
- 4. KLASSEN, D.M. and CROSBY, G.A., (1966), J. Chem. Phys., 48, 1853.
- 5. WATTS, R.J., (1983), J. Chem. Ed., 60, 834.
- 6. ELFRING, W.H. and CROSBY, G.A., (1981), J. Am. Chem. Soc., 103, 2683.
- 7. FELIX, F., FERGUSON, J., GUDEL, H.U. and LUDI, A., (1980), J. Am. Chem. Soc., 102, 4096.
- 8. HIPPS, K.W. and CROSBY, G.A., (1975), J. Am. Chem. Soc., 97, 7042.
- 9. CROSBY, G.A., HIPPS, K.W. and ELFRING, W.H., (1974), J. Am. Chem. Soc., 96, 629.
- 10. HARRIGAN, R.W. and CROSBY, G.A., (1973), J. Chem. Phys., 59, 3468.
- 11. HAGER, G.D. and CROSBY, G.A., (1975), J. Am. Chem. Soc., 97, 7031.
- 12. HAGER, G.D., WATTS, R.J. and CROSBY, G.A., (1975), J. Am. Chem. Soc., 97, 7037.
- 13. DALLINGER, R.F. and WOODRUFF, W.H., (1979), J. Am. Chem. Soc., 101, 4391.
- 14. BELSER, P., DAUL, C. and Von ZELEWSKY, A., (1981), Chem. Phys. Lett., 79, 596.
- 15. HEATH, G.A. and YELLOWLEES, L.J., (1981), J. Chem. Soc. Chem. Comm., 287.

16. CROSBY, G.A. and ELFING, W.,(1976), J. Phys. Chem., 80, 2206.
17. BRADLEY, P.G., KRESS, N., HORNBERGER, B.A., DALLINGER, R.F. and WOODRUFF, W.H.,(1981), J. Am. Chem. Soc.,103, 7441.
18. KOBER, E.M. and MEYER, T.J.,(1984), Inorg. Chem.,23, 3877.
19. Van HOUTEN, J. and WATTS, R.J.,(1976), J. Am. Chem. Soc., 98, 4853.
20. Van HOUTEN, J. and WATTS, R.J.,(1975), J. Am. Chem. Soc., 97, 3843.
21. CHERRY, W.R. and HENDERSON, L.J.,(1984), Inorg. Chem.,23, 983.
22. DURHAM, B., CASPAR, J.V., NAGLE, J.K. and MEYER, T.J., (1982), J. Am. Chem. Soc.,104, 4803.
23. CASPAR, J.V. and MEYER, T.J.,(1983), J. Am. Chem. Soc.,105, 5583.
24. COOK, M.J., LEWIS, A.P., MC AULIFFE, G.S.G., SKARDA, V., THOMSON, A.J., GLASPER, J.L., AND ROBBINS, D.J., (1984), J.Chem.Soc. Parkin Trans. II, 1293.
25. WATTS, R.J. and CROSBY, G.A.,(1972), J. Am. Chem. Soc., 94, 2606.
26. SCHULMAN, E.M. and WALLING, C.,(1972), Science, 178, 53.
27. SCHULMAN, E.M. and WALLING, C.,(1973), J. Phys. Chem., 77, 902.
28. SCHULMAN, E.M. and PARKER, R.T.,(1977), J. Phys. Chem., 81, 1932.
29. SUTER, G.W., KALLIR, A.J., WILD, U.P. and VO-DINH, T., (1986). J. Phys. Chem., 90, 4941.
30. WELLONS, S.L., PAYNTER, R.A. and WINEFORDNER, J.D., (1974), Spectrochim. Acta, 30A, 2133.
31. NIDAY, G.J. and SEYBOLD, P.G.,(1978), Anal. Chem., 50, 1577.
32. McALEESE, D.L., FREEDLANDER, R.S. and DUNLAP, R.B., (1980), Anal. Chem., 52, 2443.
33. Von WANDRUSZKA, R.M.A. and HURTUBISE, R.J., (1977), Anal. Chem., 49, 2164.
34. SEYBOLD, P.G. and WHITE, W., (1975), Anal. Chem., 47, 1199.
35. VO-DINH, T., LUE YEN, E., and WINEFORDNER, J.D., (1976), Anal. Chem., 48, 1186.

36. VO-DINH, T., LUE YEN, E., and WINEFORDNER, J.D., (1977), Talanta, 24, 146.
37. JAKOVIJEVIC, I.M., (1977), Anal. Chem., 49, 2048.
38. Von WANDRUSZKA, R.M.A. and HURTUBISE, R.J., (1976), Anal. Chem., 48, 1784.
39. VO-DINH, T. Room Temperature Phosphorimetry for Chemical Analysis, Chapter 5. (1984). Pub. J.Wiley and Sons Inc., New York.
40. SCHARF, G., SMITH, B.W. and WINEFORDNER, J.D., (1985). Anal. Chem., 57, 1230.
41. VO-DINH, T., WALDEN, G.L., and WINEFORDNER, J.D., (1977), Anal. Chem., 49, 1126.
42. NAKAMARU, K., (1982), Bull. Chem. Soc. Jpn., 55, 2697.

CHAPTER 3

IMMUNOASSAYS AND THE APPLICATION OF RUTHENIUM TRIS BIPYRIDINE
COMPLEXES AS LUMINESCENT LABELS IN IMMUNOASSAY

3:0:0 INTRODUCTION

In the following chapter, we will discuss the use of ruthenium tris-bipyridine complexes as labels in time-resolved luminescent immunoassay. Immunoassay is a technique first reported by **Yalow** and **Berson** [1] for the determination of the level of insulin in the blood. This technique has since expanded rapidly to cover, not only the detection of hormones, but also bacteria, viruses and drug metabolites [2,3,4].

Although there are many different types of assay protocol, all rely on the use of antibodies, as it is the specific nature of these proteins, that is the fundamental basis of the assay detection system. In the following, a brief description will be given of the structure and function of antibodies, as it is important to have an understanding of the basis of antibody function to fully appreciate their use in immunoassay. This will be followed by a discussion of the available assay systems and finally the utilisation of ruthenium complexes in immunoassay.

3:0:1 THE IMMUNE RESPONSE

It is the essential function of the immune system to defend the host against infection. The "non-specific" immune mechanisms (e.g. phagocytosis) of lower animal forms are enhanced in higher animals by the development of an adaptive immunity, which provides a flexible, specific and more effective reaction to different infections.

At the heart of the adaptive immune response, lie three important features; memory, specificity, and the recognition of "non-self".

The first contact with an infectious organism imprints some information, i.e. imparts some memory, so that the host is effectively prepared to repel any later invasion by the organism. This protection is provided by the adaptive immune response, evoked as a reaction to the infectious agent behaving

as an antigen. An antigen (or immunogen) is, therefore, a foreign macromolecule, capable of eliciting antibody function. Proteins, polysaccharides and nucleic acids are usually effective antigens. The antibody (or immunoglobulin) is a protein synthesized by the host's white cells in response to the presence of a foreign substance (antigen).

The antibody has a specific affinity to the foreign material (antigen), that elicited its synthesis. This gives the specificity, mentioned earlier, as a fundamental feature of the adaptive immunological response. The specificity of an antibody is directed against a particular site on an antigen, called the antigenic determinant. The binding between the antigen and antibody is reversible by non-covalent molecular interactions. These include electrostatic, hydrogen-bonding, and Van der Waals forces, which become significant, when the complementarity of shape between antigen and antibody allows them to approach each other closely ("lock and key" fit like enzyme and substrate).

Small foreign molecules do not stimulate antibody formation. However, they can elicit the formation of specific antibody, if they are attached to macromolecules. The macromolecule is then the carrier of the attached chemical group, which is called a haptenic determinant. The small foreign molecule by itself is called a hapten.

As antibodies have more than one available antigen binding site, they are potentially multivalent in their reaction with antigens. Similarly, the antigen can be monovalent or multivalent. If the antigen possesses one antigenic determinant, it can only react with one antigen combining site on the antibody and is, therefore, monovalent. However, many molecules have more than one antigenic determinant, e.g. microorganisms have a large number of antigenic determinants exposed on their surface and hence, are multivalent. When a multivalent antigen combines with more than one of the antibody's binding sites, the binding energy between the two is greater than the sum of the binding energies of the individual sites involved,

since all the antigen-antibody bonds must be broken simultaneously before the antigen and antibody will dissociate.

The strength with which a multivalent antibody binds a multivalent antigen is termed avidity, to differentiate it from the affinity of the bond between a single antigenic determinant and an individual combining site. Therefore, the avidity of an antibody for an antigen is dependent on the affinities of the individual combining sites for the determinants on the antigen, but it is greater than the sum of these affinities if both the antigen and antibody are multivalent. It is because antibodies can discriminate between two antigens, i.e. show specificity by their greater avidity for one rather than the other, that the body can differentiate specifically between two organisms.

The individual must also recognise what is foreign, i.e. is "non-self". The failure to discriminate between "self" and "non-self", could lead to the synthesis of antibodies directed against components of the subject's own body (auto-antibodies). The body must, therefore, develop some mechanism whereby "self" and "non-self" could be distinguished. It has been postulated that those circulating body components, which are able to reach the developing lymphoid system in the perinatal period, could in some way be "learnt" as "self". A permanent unresponsiveness or tolerance would then be created, so that, as immunological maturity was reached, there would normally be an inability to respond to "self" components.

3:1:1 IMMUNOGLOBULINS

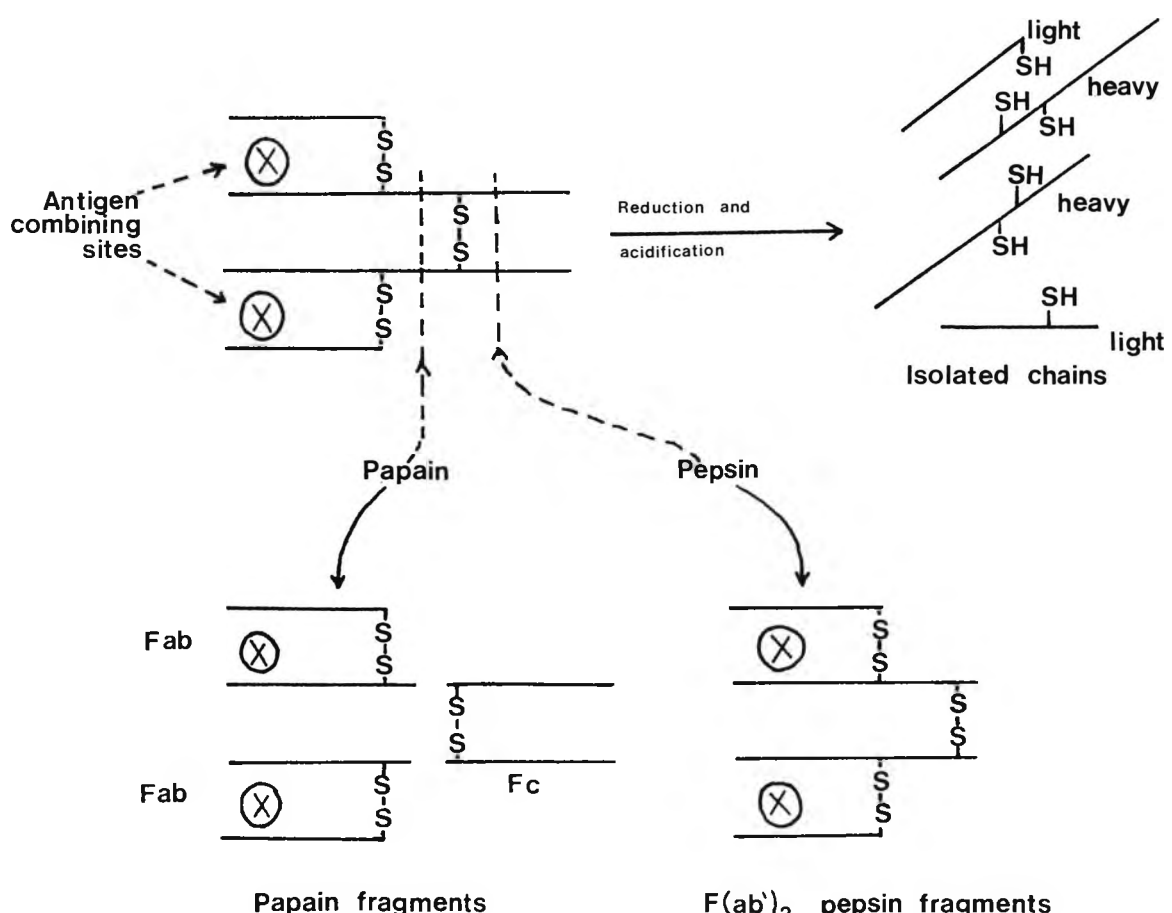
Antibody molecules are secreted by plasma cells, which are derived from B lymphocytes. The other class of lymphocytes, T lymphocytes, mediate the cellular immune response, which complements the humoral response carried out by soluble antibody molecules.

3:1:2 THE BASIC STRUCTURE OF THE IMMUNOGLOBULINS

The antibody fraction of serum is found to consist predominantly of one group of proteins, of molecular weight 150,000 (sedimentation coefficient 7S), whose major component is immunoglobulin G (IgG).

The action of enzymes, such as papain and pepsin on IgG, has led to postulates as to the structure of this group of proteins. IgG is split by papain into three fragments, two of which are identical. These identical fragments combine with antigen to form a soluble complex, which will not precipitate. These fragments are, therefore, univalent antibody fragments and are given the nomenclature Fab ("fragment antibody binding"). The third fragment which cannot combine with antigen is termed Fc ("fragment crystallizable", i.e. obtainable in crystalline form).

Fig. 3-1 Experiments Conducted to Establish Immunoglobulin Structure



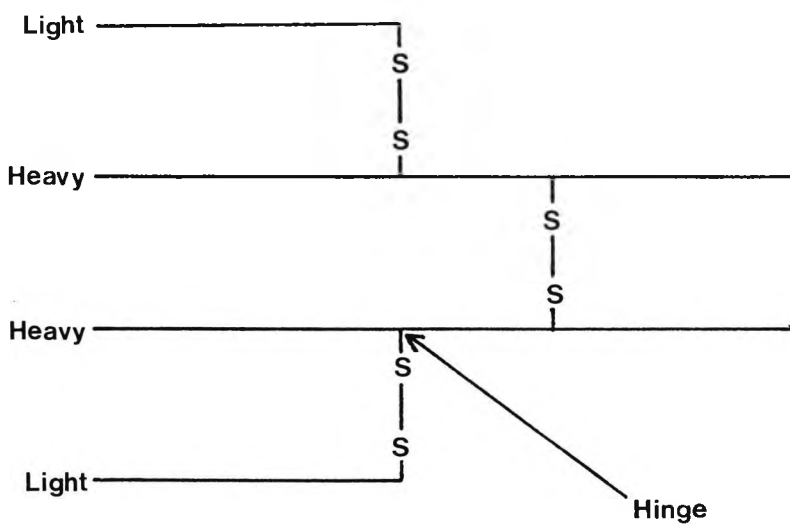
With pepsin, the IgG breaks into two fragments, one again being the Fc fragment. The other fragment can still precipitate in antigen, and is formulated as $F(ab')_2$, since it is clearly still divalent.

The antibodies can also be broken into constituent peptide chains. First the disulphide bridges are broken by reduction, using an excess of a sulphydryl reagent. However, the chains are still held together by non-covalent forces, which are broken by lowering the pH. This, then, results in two sizes of peptide chain, termed heavy and light chains, which can be separated.

These results prompted a model for the structure of immunoglobulins to be put forward by R.R. Porter, see Fig. 3-2 [a]

This model has been confirmed by electron microscope studies showing a Y-shaped structure, whose arms can swing out to an angle of 180° .

Fig. 3-2 Model for the Structure of Immunoglobulins



3:1:3

VARIATIONS IN STRUCTURE OF THE IMMUNOGLOBULINS

From electrophoresis of immunoglobulins, it can be seen, that they occur in different structural classes, and also that they have a wide range of electrophoretic mobilities within each class. These different mobilities are due to variation in the amino acid structure. It is, therefore, almost impossible to analyse the structure of immunoglobulins from normal serum.

One solution to this problem is to study myeloma proteins. There is a human disease called Multiple Myeloma, in which one cell making one particular immunoglobulin divides continuously, like a cancer cell, without regard to the overall requirements of the host. The patient, therefore, has a large number of identical cells derived as a clone from the original cell, all synthesizing the same immunoglobulin.

Purification of the myeloma or M-protein will, therefore, give a preparation of an immunoglobulin, with a unique structure.

3:1:4

STRUCTURAL VARIATION IN RELATION TO ANTIBODY SPECIFICITY

It has been found, that within a major immunoglobulin class, the N-terminal portions of both the heavy and light chains show variations. Other parts of the chains are relatively constant.

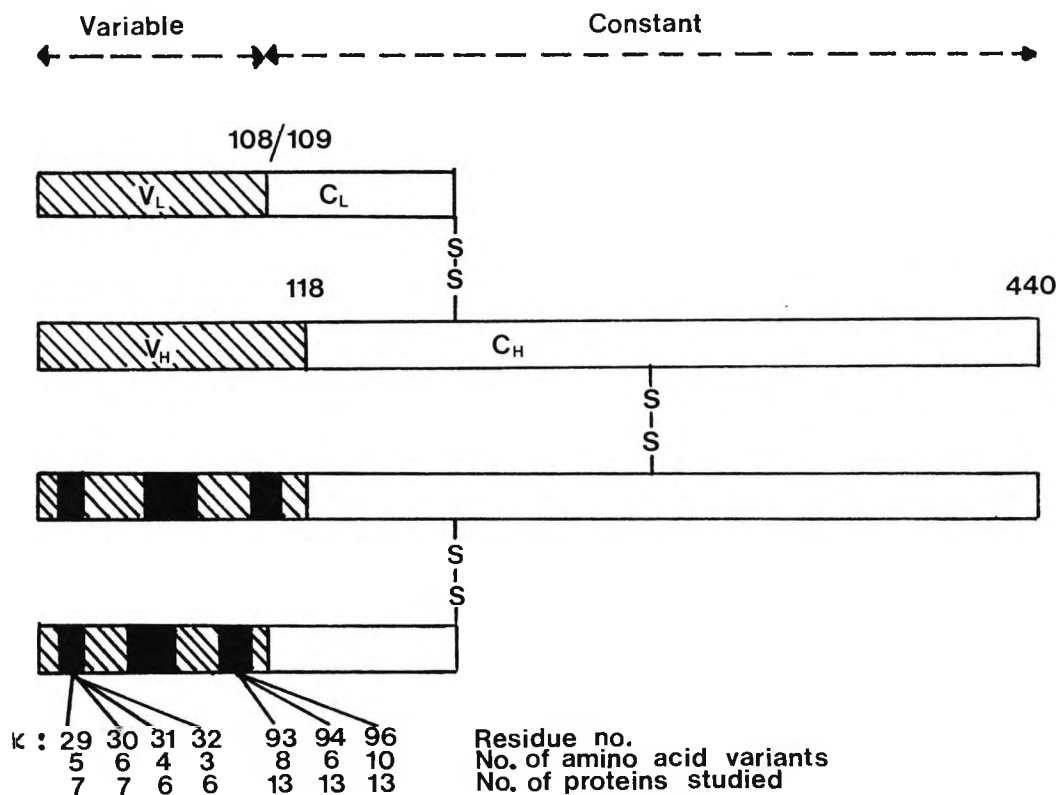
Each variable region has a basic overall amino acid structure, which is common to a number of immunoglobulins with differing specificities. These immunoglobulins are said to be in the same subgroup.

However, this subgroup "framework" structure cannot be related to antibody specificity, as so many different immunoglobulins are in the same subgroup.

Examination of the primary amino acid structure of light and heavy polypeptide chains shows that the variability between the variable regions is not evenly distributed throughout the

length of the region. Some short polypeptide segments show exceptional variability and are termed hypervariable regions. In light chains these hypervariable regions are located near positions 30, 50 and 95. It is generally accepted that the hypervariable regions are directly involved in the formation of the antigen binding site.

Fig. 3-3 Diagram showing the Hypervariability in the Immunoglobulin Structure



Hypervariable regions are sometimes termed complementarity determining regions (CDR) and the intervening peptide segments as framework regions (FR). In both heavy and light chain variable regions, there are three CDRs (CDR1-CDR3) and four FRs (FR1-FR4).

3:1:5 VARIATIONS IN STRUCTURE NOT RELATED TO ANTIBODY SPECIFICITY

Even the "constant" portions of the immunoglobulin peptide chains not directly concerned with antigen binding show heterogeneity.

i) Light Chains

A source of light chains in humans is the urinary Bence-Jones protein, which is found in a proportion of myeloma patients. It is a dimer of light chains, derived from the pool used in the synthesis of myeloma proteins. A study of these light chains show, that there are two distinct groups, Kappa (K) and Lambda (λ); testing with antisera will determine to which group the light chain belongs. The K-group gives precipitation reactions with anti-K sera, but no reaction with anti- λ sera. These chain groups occur on different molecules, i.e. there is no naturally occurring immunoglobulin which has mixed K and λ chains. Approximately 65% of immunoglobulins in normal serum are of K-type; the remainder are of λ -type.

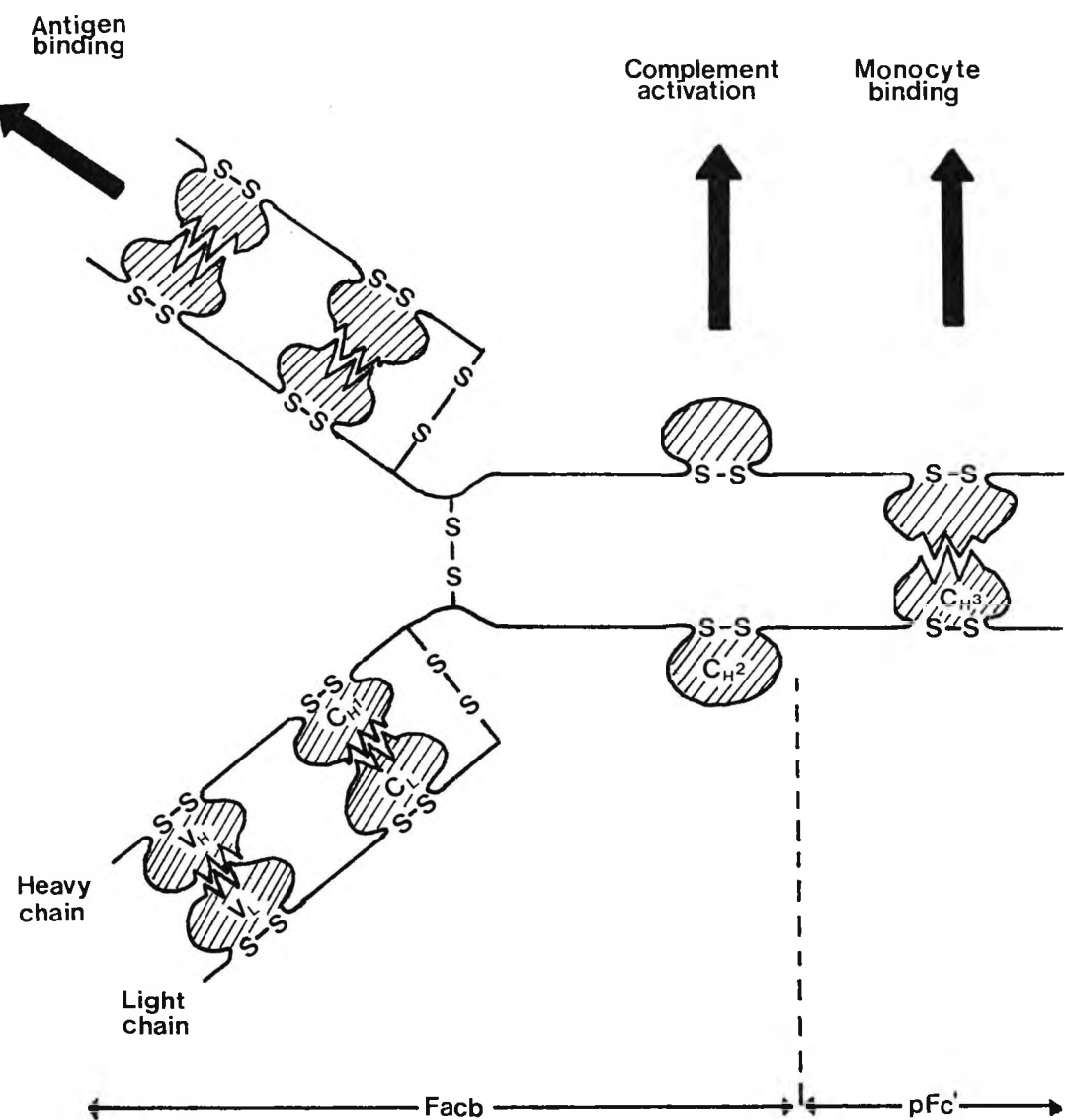
ii) Heavy Chains

Studies using antisera prepared against normal and myeloma proteins, show that there are 5 major types of heavy chain in humans, each of which gives rise to a distinct immunoglobulin class; IgG, IgA, IgM, IgD, and IgE. Though each immunoglobulin class is associated with a particular heavy chain, they all have K- and λ - light chains. It has been found, that the Fc structure directs biological activity, in that it determines the extent of distribution of immunoglobulin through the body. The constant part of the immunoglobulin is, therefore, associated with the different biological properties which vary from one immunoglobulin class to another, depending upon the primary structure, and which may require combination with antigen for their activation.

iii) Immunoglobulin Domains

In addition to interchain disulphide bonds, which bridge the heavy and light chains, there are also internal intrachain disulphide links, which form loops in the peptide chain.

Fig. 3-4 Diagram showing Immunoglobulin Domains



It was predicted, that these loops would be compactly folded to give globular domains, which would interact laterally through their hydrophobic regions, forming V_H/V_L , C_{H1}/C_{L1} , and C_{H2}/C_{H3} diads, the C_{H2} domains remaining separate (Fig. 3-4). Different domains have different functions. The variable region domains (V_L and V_H) are responsible for the formation of a specific antigen-binding site. The C_{H1} region of IgG binds to the fourth component of the complement system (C_{4b}) while the C_{H2} structure can attach C_{1q} , to initiate the classical complement sequence. Since the isolated C_{H2} domain has

the same half-life as the parent IgG molecule, this region must be dominant in controlling the rate of metabolic degradation in vivo. Adherence to the monocyte surface is mediated largely through the terminal C_{H3} domain, but synergism between C_{H2} and C_{H3} appears to be required for optimal binding to Fc receptors on placental syncytiotrophoblast , polymorphonuclear leucocytes and K cells.

TABLE 3-1 PHYSICAL PROPERTIES OF MAJOR HUMAN IMMUNOGLOBULIN CLASSES

WHO Designation	IgG	IgA	IgM	IgD	IgE
Sedimentation Coefficient	,S	,S , ₉ S , ₁₁ S*	₁₉ S	,S	₈ S
Molecular weight	150,000	160,000 and dimer	900,000	185,000	200,000
No. of basic four peptide units	1	1,2*	5	1	1
Heavy chains	γ	α	μ	δ	ε
Light chains κ + λ	κ + λ	κ + λ	κ + λ	κ + λ	κ + λ
Molecular formula	γ ₂ γ ₃ κ ₂ , γ ₂ λ ₂	(α ₂ κ ₂) ₁₋₂ (α ₂ λ ₂) ₁₋₂ (α ₂ κ ₂) ₂ S* (α ₂ λ ₂) ₂ S*	(μ ₂ κ ₂) ₅ (μ ₂ λ ₂) ₅	δ ₂ κ ₂ (δ ₂ λ ₂ ?)	ε ₂ κ ₂ , ε ₂ λ ₂
Valency for antigen binding	2	2,4	5(10)	2	2
Concentration range in normal serum	8-16mg/ml	1.4-4mg/ml	0.5-2mg/ml	0-0.4mg/ml	17-450ng/ml
% Total Immunoglobulin	80	13	6	0-1	0.002
% Carbohydrate content	3	8	12	13	12

* Dimer in external secretions carries secretory component - S

TABLE 3-2

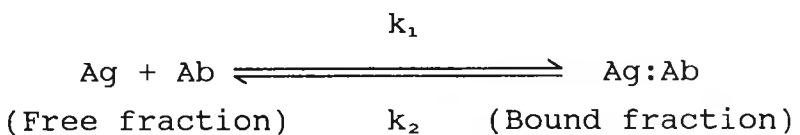
BIOLOGICAL PROPERTIES OF MAJOR IMMUNOGLOBULIN CLASSES IN THE HUMAN

	IgG	IgA	IgM	IgD	IgE
Major characteristics	Most, abundant Ig of internal body fluids particularly extravascular where it combats organisms and their toxins	Major Ig in sero-mucous secretions where it defends external body surfaces	Very effective agglutinator produced early in immune response effective first line defence vs bacteraemia	Most, if not all, present on lymphocyte surface	Protection of external body surfaces. Recruits antimicrobial agents raised in parasitic infections. Responsible for symptoms of atopic allergy
Complement Fixation					
Classical	++	-	+++	-	
Alternative	-	±	-	-	
Cross Placenta	+	-	-	-	-
Fix to homologous mast cells and basophils	-	-	-	-	+
Binding to macrophages and polymorphs	+	+	-	-	-

3:2:1 IMMUNOASSAYS IN GENERAL

Immunoassay is a technique that utilises antibodies as a selective chemical reagent for antigen or hapten analyte determination. It is the very selectivity and specificity of the antibody that has led to its use particularly for the clinical investigation of compounds that are in very low concentrations, and for whose determination chemical methods are not sufficiently specific. Included in these compounds are various proteins (e.g. antibodies and enzymes) [5], hormones (e.g. thyroxine, steroids, and peptide hormones) [6,7,8], and drugs (e.g. digoxin and pentobarbital) [9,10].

As the name implies immunoassay is an analytical procedure based on the reaction between an antigen and a specific antibody, which obeys the Law of Mass Action:



Where Ag represents the antigen, Ab the antibody, and Ag:Ab the bound complex. At equilibrium some of the free reactants will be combining at a rate constant k_1 to form more of the complex while some of the complex will be dissociating at a rate constant k_2 to give free antigen and antibody.

Over the years since Yalow and Berson [1] first reported their immunoassay system in 1960 many different protocols for immunoassay techniques have been reported. However, they are all a variation of two basic procedures which are based on the use of the antibody, (the specific reagent), either as a limited concentration or in excess. The assay in which limited reagent is used is termed immunoassay, while that in which the antibody is in excess is referred to as an immunometric assay. There does exist a third type of assay design which allows the combination of approximately equal proportions of antigen and antibody, e.g. Precipitin test, where the antibody is neither

limited nor in excess. The term immunoassay is, however, generally used in a generic sense to mean assays of all types.

3:2:2 IMMUNOASSAY

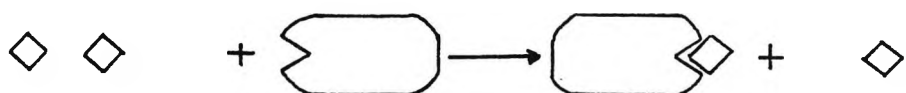
The following is a brief description of the protocol applied in an assay involving a limited amount of reagent.

Varying concentrations of antigen are allowed to react with a constant and limited amount of antibody; limited implies that the molar concentration of antibody is much lower than the molar concentration of the antigen to be assayed, therefore the critical reagent is present in excess.

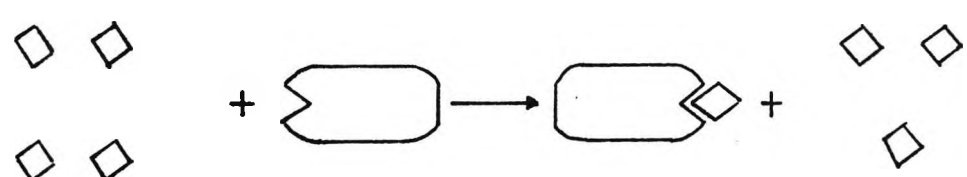
Fig. 3-5 Diagram Representing the Principle of Immunoassay

ANALYTE (Antigen)	REAGENT (Antibody)	BOUNDED ANTIGEN	FREE ANTIGEN
----------------------	-----------------------	--------------------	-----------------

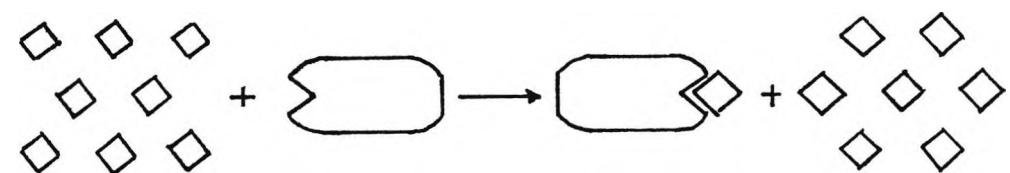
i)



ii)

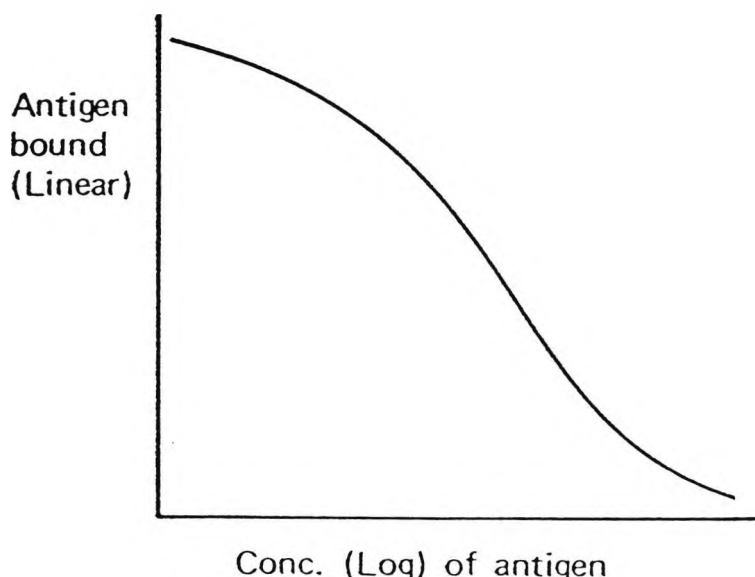
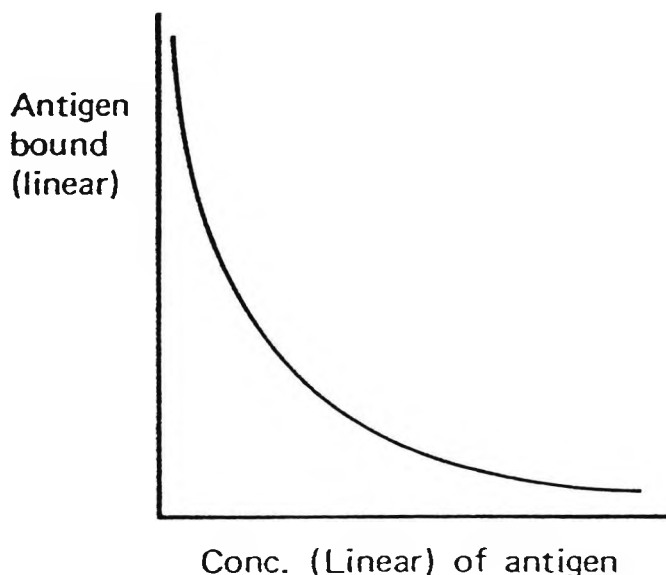


iii)



At equilibrium the situation on the right-hand side of Fig. 3-5 is reached. All of the antibody binding sites are occupied by antigen, with an increasing concentration of antigen not complexed to the antibody. If the amount of free and bound antigen is measured using labelled antigen, it is found that the amount bound, expressed as a percentage, varies inversely to the total concentration of antigen present (Fig. 3-6).

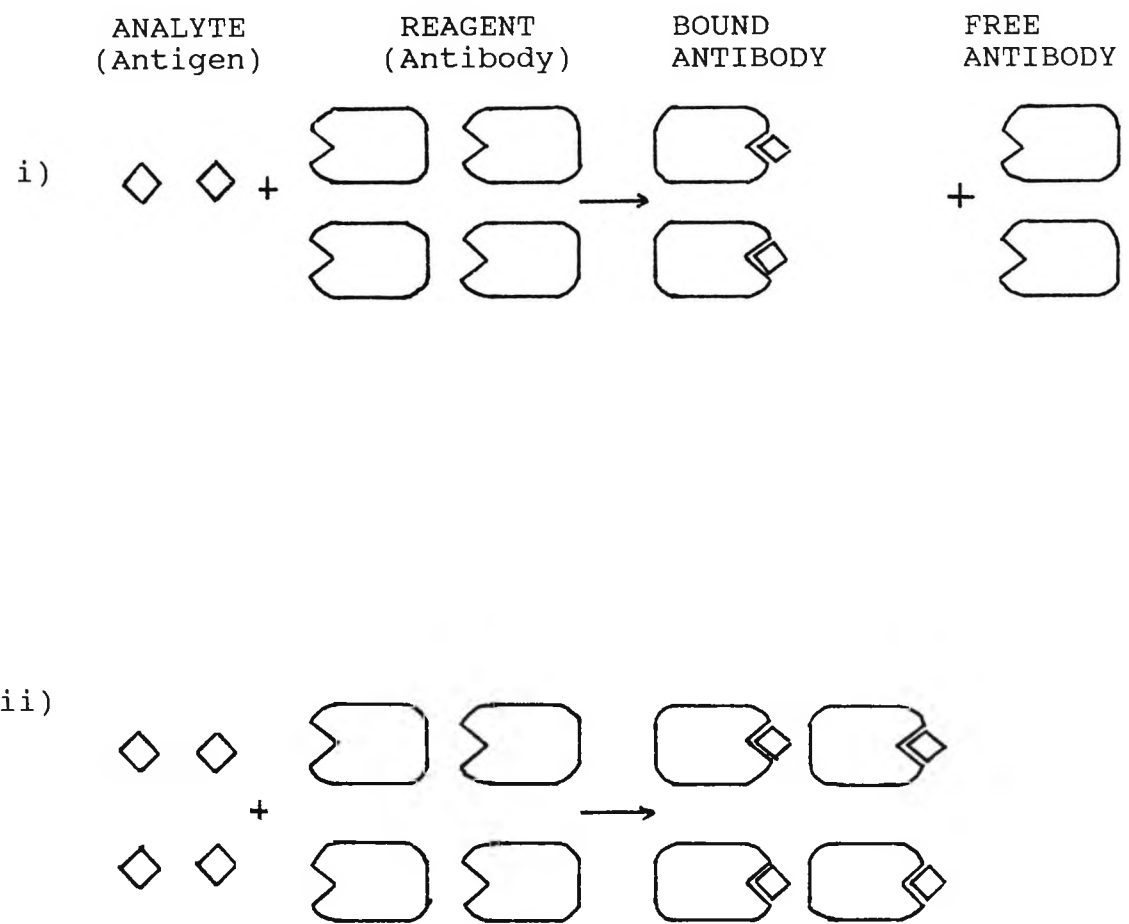
Fig. 3-6 Diagram showing the Relationship of Bound Antigen to Antigen Concentration in Immunoassay



IMMUNOMETRIC ASSAY

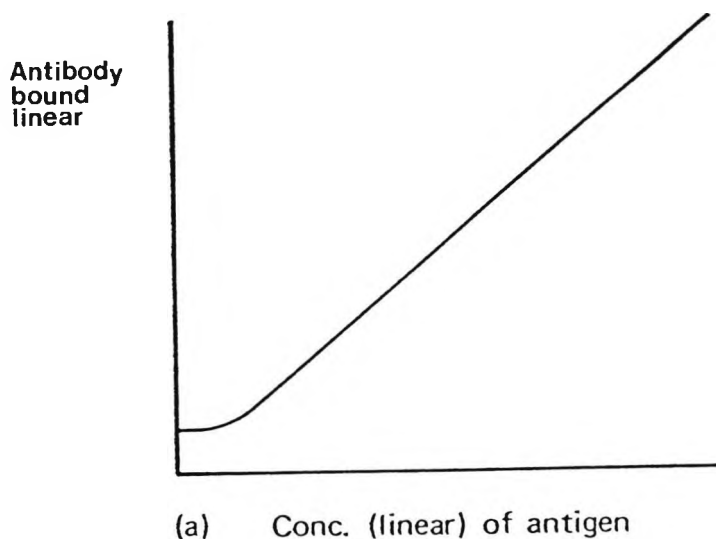
In this type of assay varying concentrations of antigen are allowed to react with a constant, but excess amount of antibody. Excess means a much higher molar concentration of antibody to that of antigen.

Fig. 3-7 Diagram Demonstrating the Principle of Immunometric Assay

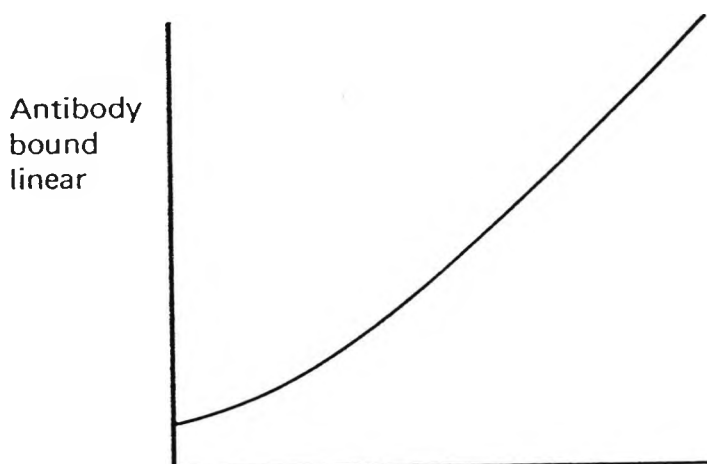


In this type of assay, the distribution of antibody between the bound and the free fractions is measured. When the amount of bound antibody is measured in relation to the concentration of antigen, the graphs (see below) are plotted (Fig. 3-8).

Fig. 3-8 Diagram showing the Relationship of Bound Antibody to Antigen Concentration in Immunometric Assay



(a) Conc. (linear) of antigen



(b) Conc. (log) of antigen

In order to use the immunoassay and immunometric protocols as analytical techniques, the free and bound fractions of the assay must be discriminated between, and quantified in some manner. In earlier techniques, precipitation of the antigen-antibody complex was often used, e.g. immunodiffusion or immunoelectrophoresis assay. Today, it is much more common to attach to the antibody or antigen a cell or particle, which can then be detected, e.g. radioisotope, fluorescent molecule, or enzyme. Such methods, using a label, have led to a considerable improvement in the sensitivity of immunoassay methods.

As the type of label used is often the most distinguishing aspect of the assay, it is, therefore, used as the basis of system classification.

TABLE 3-3 TABLE SHOWING THE APPLICATION OF DETECTION METHODS TO IMMUNOASSAY SYSTEMS

DETECTION METHOD	LIMITED REAGENT	EQUIVALENCE	EXCESS REAGENT
Nitrogen in precipitate		Precipitation test	
Precipitation line (visual)		Immunodiffusion	
Agglutination		Immunoelectrophoresis	
			Haemagglutination
			Latex agglutination
			Nephelometric
Light scattering			Turbidimetric
Radioisotope	Radioimmunoassay		Immunoradiometric
Enzyme	Enzymeimmunoassay		Enzyme-labelled
			Immunosorbent
Fluorescence	Fluoroimmunoassay		Immunofluorometric
Luminescence	Luminoimmunoassay		Immunoluminometric

The most common way of quantifying immunoreaction has been by the use of radioisotopes as labels, which has proved to be an extremely sensitive process. However, there are certain drawbacks associated with the use of radioisotopes:-

- i) the use of radioisotopes requires a special permit and a specially fitted laboratory.
- ii) radiation released during the use of these labels may cause a risk to the health of the user.
- iii) the useful lifetime of an assay kit is limited by the half-life of the radioactive isotopes.
- iv) this method of assay requires relatively expensive instrumentation and reagents.
- v) the counting of a series of samples is generally time-consuming, though it is normally automated.

For these reasons, an alternative to radiolabelling has been sought and consequently alternatives, e.g. enzymatic methods (ELISA, enzyme immunoassay), are already commercially available.

One alternative method available is based on the labelling of samples with fluorescent compounds. The use of this type of label is of advantage over radio labelling in that:-

- i) fluorometric labelling is relatively inexpensive and not a risk to health.
- ii) the useful lifetime of the assay kit is independent of the disintegration of the labelling compound.
- iii) fluorescence can be measured quickly and simply with small, simple and relatively inexpensive instrumentation.

Fluorescent methods are at present widely used in immunohistology [11, 12], in which the sample under examination is either directly or indirectly stained with an antibody labelled with a fluorescent probe. So far, most analytical applications of fluorescence in immunoassays have been limited to their use in fluorescent polarisation assays [13, 14], which deal mainly with therapeutic drug monitoring [15, 16].

The development of a fluorescent assay system as a viable alternative to radioactive assays has, however, been hindered by the relative lack of sensitivity of fluorescent labels. The main reason for the limited sensitivity of fluorescent labels lies in the high background fluorescence, associated with the presence of such materials as plastic and glass in the instrument as well as proteins in the sample. One way to overcome the limitation set by the background, is by using time-resolved fluorescence [17]. This works on the principle, that, if the measurement of the fluorescent signal commences at a time after the background fluorescence has decayed, this background signal would be effectively removed and the net result would be an increase in sensitivity (Fig. 3-9).

The use of time-resolved fluorescence puts considerable constraints on the type of label that can be used. The label's fluorescent life-time must be considerably longer than that of the components giving rise to the background signal. As commonly used fluorescent labels, e.g. dansyl chloride, FITC, have decay times in the same order of magnitude as proteins, the time-resolved technique does not bring an improvement, when these labels are used. It is also of importance for the label for time-resolved assay to possess a high quantum yield of fluorescence, and a wavelength of emission far removed from that of the background emitters.

Fig. 3-9 Principle of Time Delayed Measurement of Fluorescence. [17]

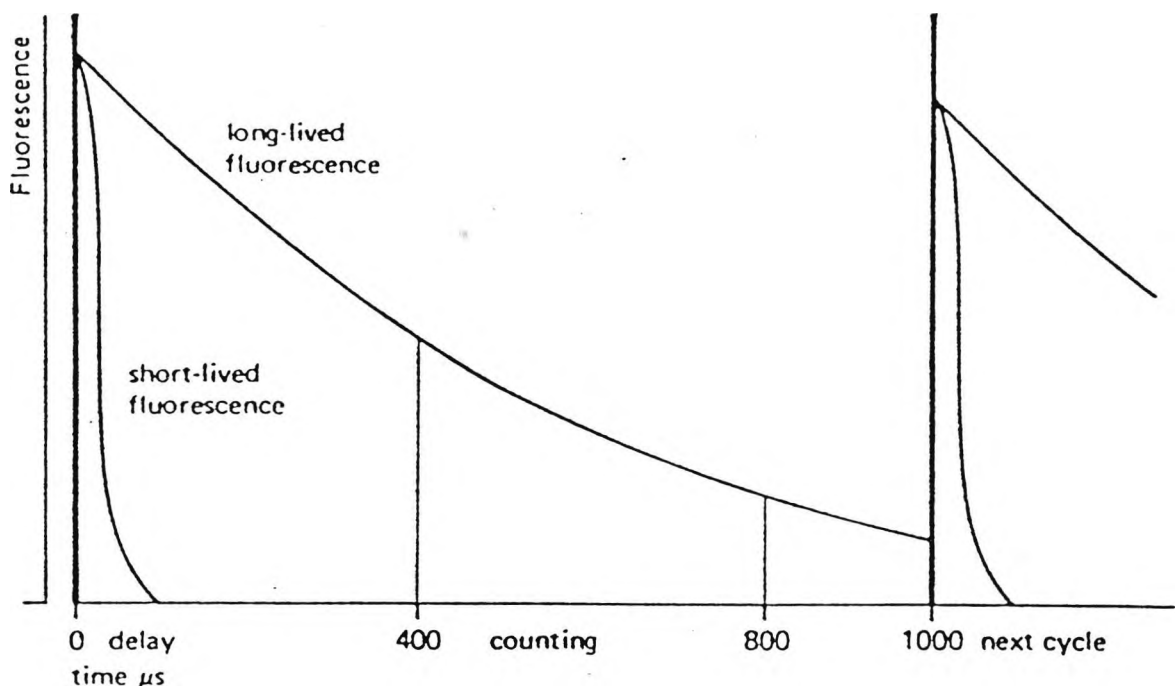


TABLE 3-4 FLUORESCENCE DECAY TIME OF SOME FLUOROPHORES AND PROTEINS

SUBSTANCE	DECAY TIME (ns)
Human Serum Albumin	4.1
Cytochrome C	3.5
Globin (haemoglobin)	3.0
Fluorescein Isothiocyanate	4.5
Dansyl Chloride	14.0
Europium Chelates	$10^3\text{--}10^6$

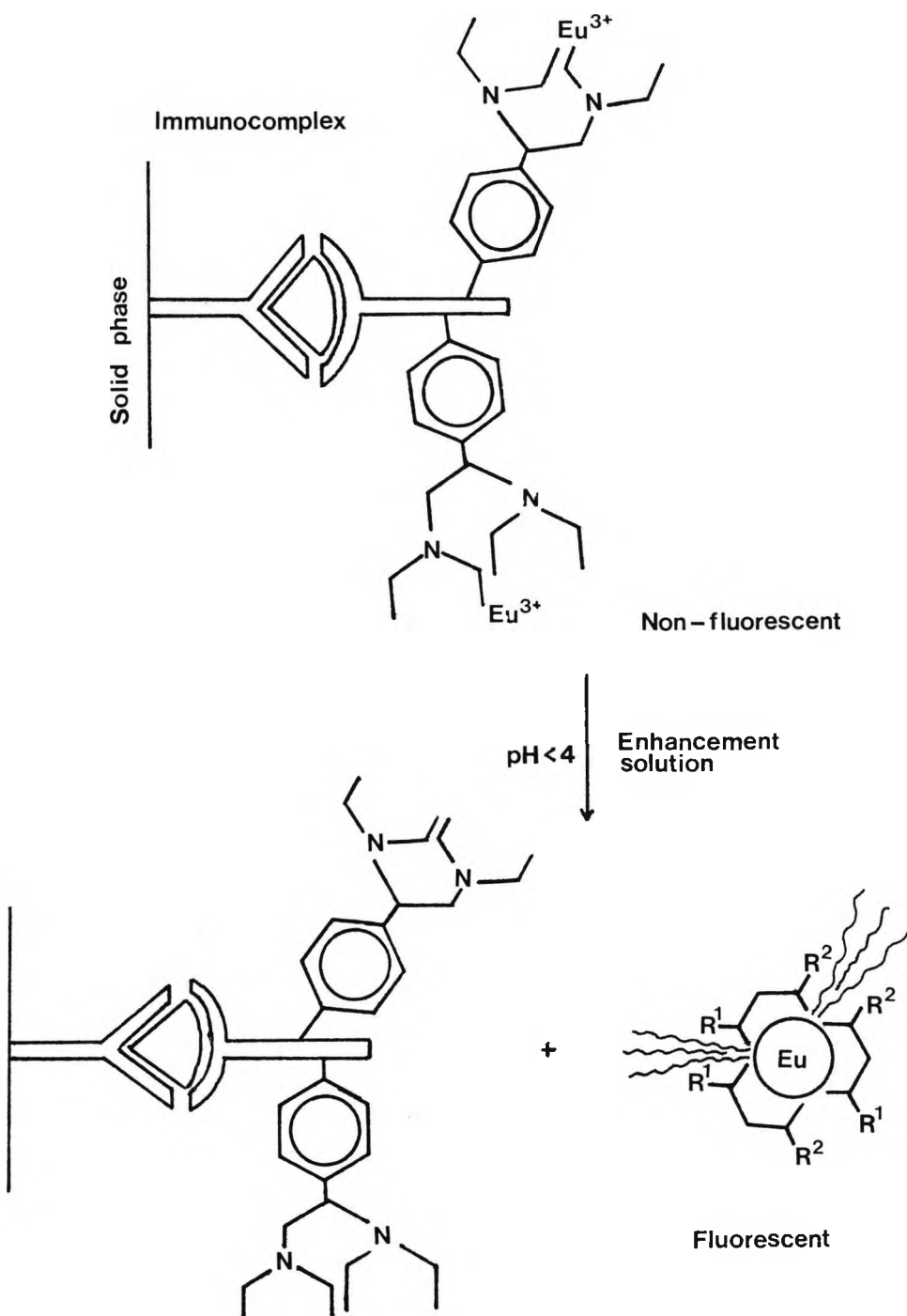
Dissociation-enhanced lanthanide fluoroimmunoassay (DELFIA) is a commercially available assay system which utilises europium complexes as fluorescent labels in a time-resolved immunoassay [18, 19].

A standard DELFIA assay system involves a basic solid phase two-site fluoroimmunoassay, based on the direct sandwich technique, in which two monoclonal antibodies are directed against two separate antigenic determinants of the analyte. Patient, standard, or control samples containing the analyte are reacted with immobilised monoclonal antibodies, which are directed against a specific antigenic site on the analyte. At the same time europium-labelled monoclonal antibodies are incubated with the analyte. As the europium-labelled antibodies are directed against a different specific antigenic site of the analyte than the immobilised antibodies, the result is the formation of a sandwich with the analyte in the middle (Fig. 3-10).

Since the antibody-antigen europium complex thus formed is, however, non-fluorescent, it has to be dissociated and recomplexed into a fluorescent form. The recomplexing of the europium is achieved in the enhancement solution at pH 3.2, in which the europium is complexed to a diketone 2-naphthoyl trifluoroacetone (Fig. 3-10).

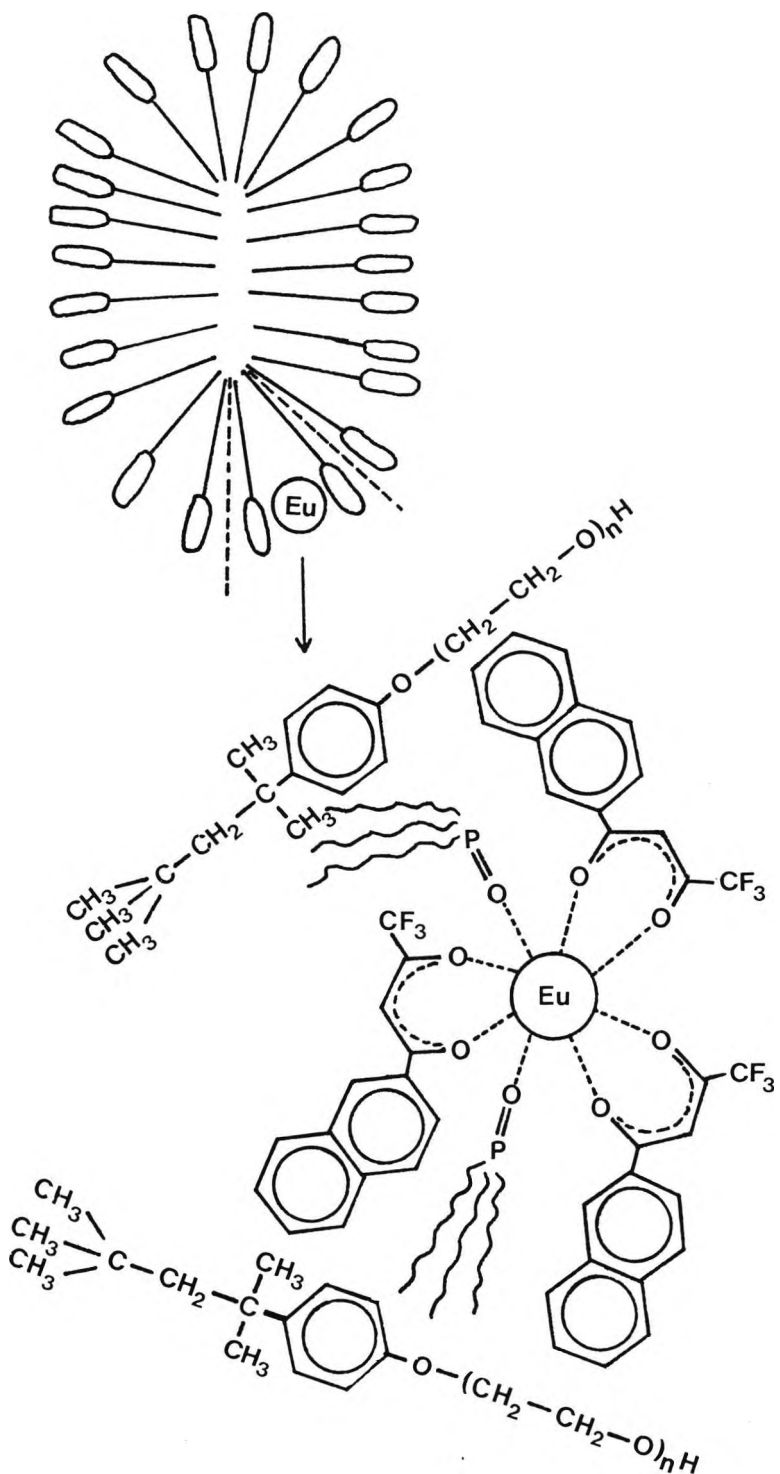
The solution also contains a synergistic agent trioctylphosphine oxide and Triton X-100, which are present to help solubilise the complex and to stop its precipitation (Fig. 3-11). The fluorescent product thus formed is then measured. It is claimed that a system of this type has a detection limit of 10^{-13} mol/L Eu³⁺ [20].

Fig. 3-10 Diagram Illustrating the DELFIA System [18]



Although this assay procedure is highly sensitive it has some limitations, which appear to have been restrictive to its development. First, the dissociation of the europium and its subsequent recomplexation adds an extra step to the assay protocol.

Fig. 3-11 Diagram showing the Form of the Stabilised Fluorescent Europium Chelate [18]



Second, the enhancement solution containing the europium chelates is vulnerable to europium contamination from the environment. Finally, its background fluorescence increases with time even with careful handling.

3:3:0 RUTHENIUM COMPLEXES IN TIME-RESOLVED IMMUNOASSAY

Although the DELFIA assay system outlined above, does increase the limit of detection of fluorescent immunoassays to that area, where it competes directly with radioimmunoassay, its drawbacks have limited its competitiveness. If we were to take a ruthenium tris bipyridine complex and assess its potential performance against the europium chelates in a time resolved fluorescence immunoassay, it would perform well, as it is already luminescent and can also be derivatised with suitable functionalities, e.g. amino groups, for attachment to antibodies, while still maintaining its luminescent properties. Such a complex can, therefore, be measured *in situ* without being recomplexed, which is a major criticism of the DELFIA system. As can be seen in Chapter 2, the ruthenium complexes have a reasonable Stokes shift and quantum yield; they are, therefore, suitable for use in time resolved immunoassay.

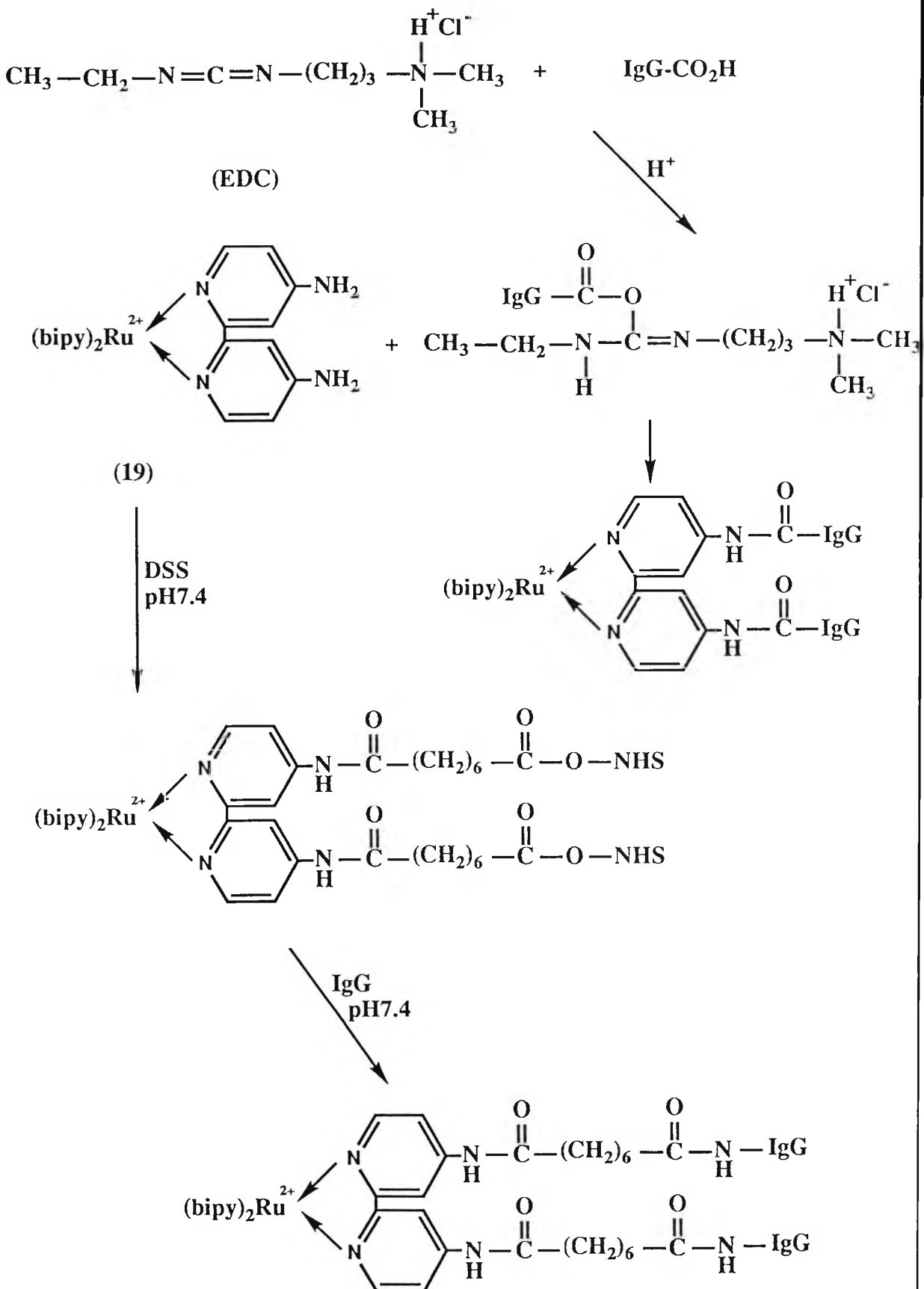
3:3:1 ASSESSMENT OF RUTHENIUM TRIS BIPYRIDINE COMPLEXES AS ANTIBODY LABELS

The first stage in the assessment of the ruthenium complexes as potential antibody labels is to ensure that they do not non-covalently associate with human IgG. This was established using bis(2,2'-bipyridine)(4,4'-dichloro-2,2'-bipyridine) ruthenium (II) hexafluorophosphate (26) which on incubation with human IgG overnight at 2–4°C showed after subsequent separation of the protein fraction by gel filtration chromatography no association with the antibody when examined by fluorescence spectroscopy.

Several ruthenium complexes have been synthesised, (ref. Chapter 1), which bear functionalities on one of their bipyridine ligands that can be activated towards covalent attachment to antibodies. One such functionality is the amino group of bis(2,2'-bipyridine)(4,4'-diamino-2,2'-bipyridine) ruthenium (II) hexafluorophosphate (19), which can be functionalised in numerous ways; two of the most common utilise dicarbodiimide, and N-hydroxy succinimide esters (Scheme 3-1).

SCHEME 3-1

SCHEME SHOWING THE CONJUGATION OF IgG TO BIS(2,2'-BIPYRIDINE)-(4,4'-DIAMINO-2,2'-BIPYRIDINE) RUTHENIUM (II) HEXAFLUOROPHOSPHATE (19)

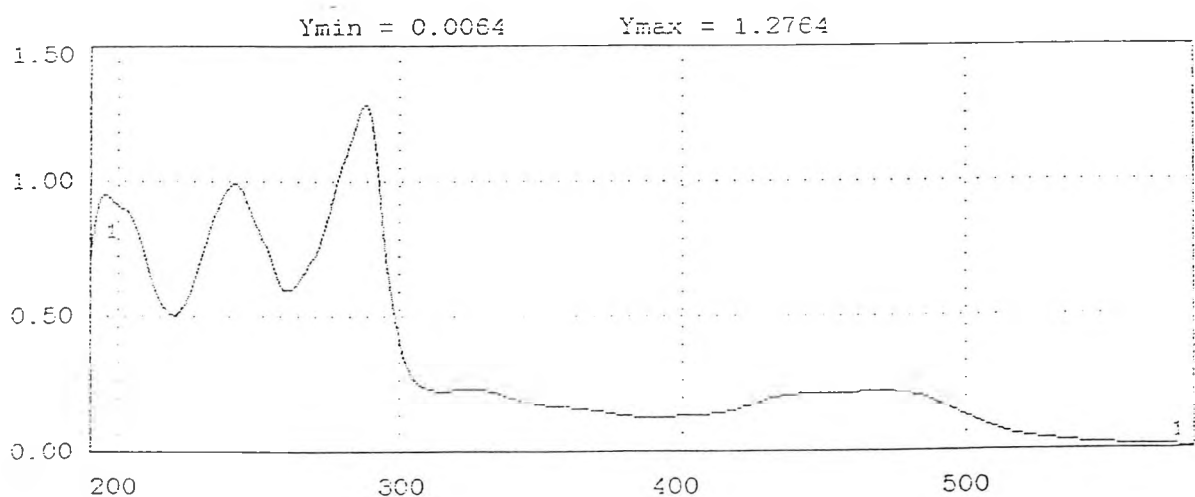


There are many types of commercially available N-hydroxy succinimide esters, which can be used for functionalising antibodies. Disuccinimidyl suberate, DSS, a homobifunctional cross-linking reagent that has NHS-esters at either end of an alkyl chain, was selected for the experiment. The NHS-ester reacts with the amino groups on the ruthenium complex and also the free amino groups on the antibody at pH greater than 7.4. DSS is frequently chosen as a cross-linker, because the alkyl chain between the two NHS-esters serves to separate the label from the antibody, in such a way that the label does not get absorbed into the antibody structure and thus affect the antigenic behaviour of the immunoglobulin.

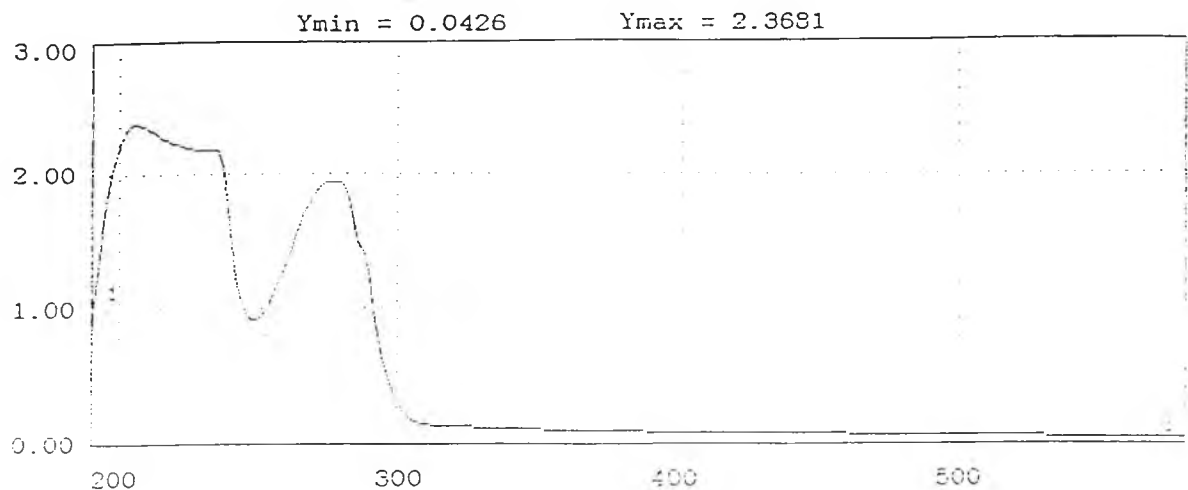
DSS labelled (19) was, therefore, incubated with human IgG for 2 hours at room temperature, after which the reaction mixture was separated by gel filtration chromatography. The protein fraction thus isolated was examined by UV spectroscopy. Examination of the UV spectrum of the isolated protein fraction (Fig. 3-12), did, in fact show incorporation of the ruthenium label into the antibody.

Fig. 3-12 UV Spectra showing Incorporation of Ruthenium Complex (19) into IgG

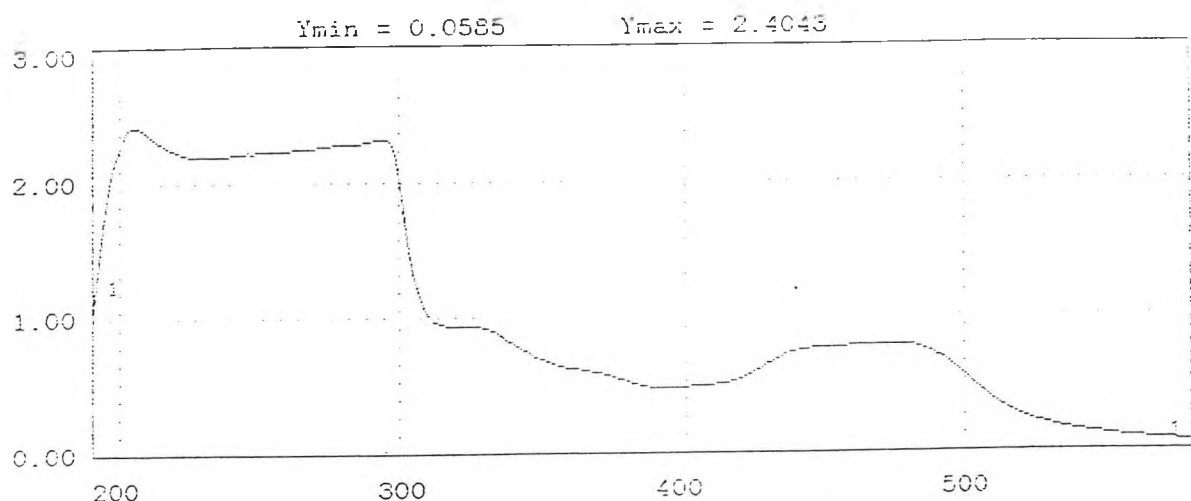
a) $[\text{Ru}(\text{bipy})_2(\text{bipy}\{\text{NH}_2\}_2)]^{2+}$ in 10mM phosphate buffer pH 7.4



b) IgG in 10mM phosphate buffer pH7.4



c) Conjugate in 10mM phosphate buffer pH7.4

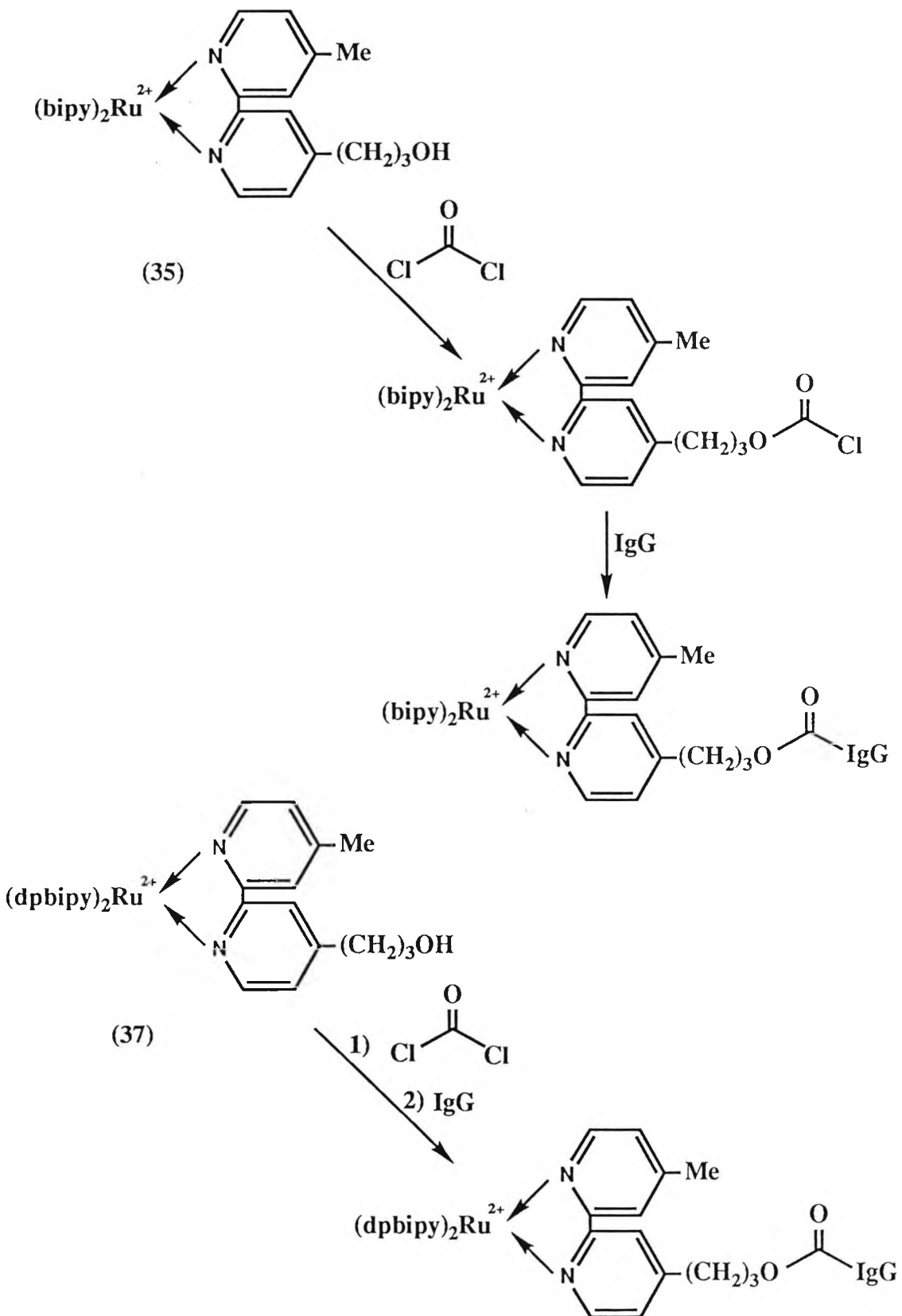


3:3:2

EXAMINATION OF THE LUMINESCENT PROPERTIES OF RUTHENIUM TRIS BIPYRIDINE COMPLEXES LABELLED TO HUMAN IgG

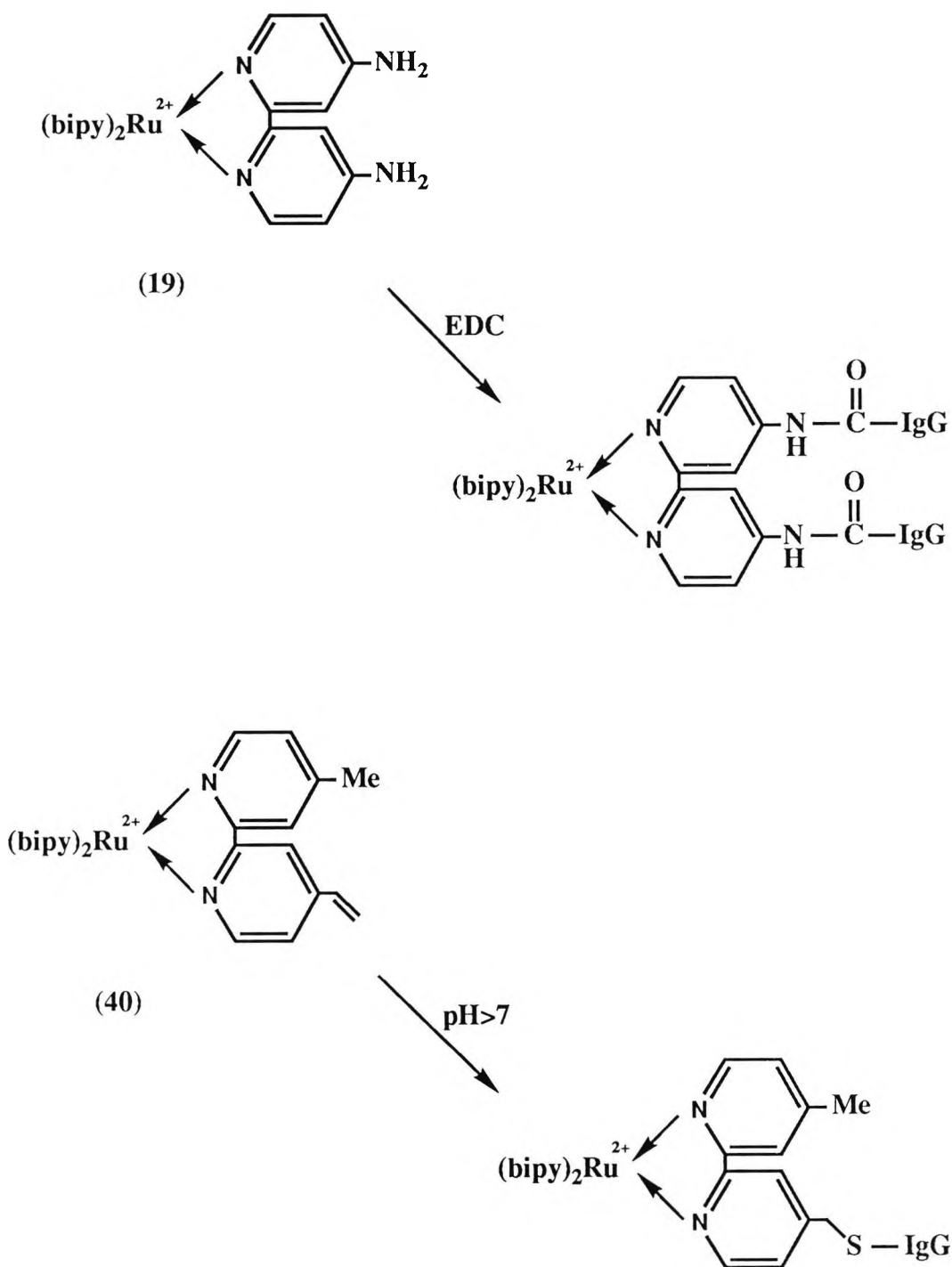
As it had been established that ruthenium complexes bearing suitable functionalities could be conjugated to antibodies, those complexes, that contained suitable groups, were covalently linked to human IgG (Schemes 3-2, 3-3).

SCHEME 3-2
SCHEME SHOWING THE CONJUGATION OF RUTHENIUM COMPLEXES TO IgG
UTILISING PHOSGENE



SCHEME 3-3

SCHEME SHOWING THE CONJUGATION OF IgG TO RUTHENIUM COMPLEXES UTILISING EDC AND VINYL DERIVATIVES



After the reaction mixtures were separated by gel filtration chromatography, the luminescent lifetimes of the resulting IgG fractions were measured, using a fluorescence microscope modular work bench (Ref. Chapter 2). All results are summarised in Table 3-5.

TABLE 3-5 LUMINESCENT LIFETIMES OF RUTHENIUM TRIS BIPYRIDINE ANTIBODY PROBES

	Free Probe	Conjugated Probe (hIgG)
Ru(bipy) ₂ (bipy[NH ₂] ₂) ²⁺ (19)	80 ns *	700 ns
Ru(bipy) ₂ (bipyMe(CH ₂) ₃ OH) ²⁺ (35)	320 ns	2.53μs
Ru(dp bipy) ₂ (bipyMe(CH ₂) ₃ OH) ²⁺ (37)	370 ns	3.00μs
Ru(bipy) ₂ (bipyMe vinyl) ²⁺ (40)	400 ns	3.28μs

* 50ns shutter time

As can be seen from these results, the ruthenium complexes show a luminescent emission, when conjugated to antibody. The results also show an increase in the luminescent lifetime of the ruthenium complexes on conjugation, due possibly to the complexes being held within the matrix of the antibody, thus rendering them less susceptible to other factors, which influence the rate of decay of the excited state, e.g. collisional deactivation, than they would be in a free solution.

3:3:3 EXAMINATION OF CONJUGATED RUTHENIUM PROBES BY RTL

As the feasibility of using RTL as a technique for the detection of ruthenium complexes in solid phase was being investigated, (ref. Chapter 2), it was decided to investigate, whether adsorption of a ruthenium conjugate onto Whatman No. 1 filter paper, would result in the enhancement of the luminescent signal

of the conjugate. Lifetimes were measured using a fluorescence microscope modular work bench (Ref. Chapter 2), the results of which are shown in Table 3-6.

TABLE 3-6 EVALUATION OF THE RTL BEHAVIOUR OF A RUTHENIUM COMPLEX HUMAN IgG CONJUGATE

PROBE	LIFETIME
Ru(bipy) ₂ (bipyMe(CH ₂) ₃ OOC-IgG)* in PBS	467 ns
Ru(bipy) ₂ (bipyMe(CH ₂) ₃ OOC-IgG) on Whatman No. 1 Filter Paper	780 ns
IgG on Whatman No. 1 Filter Paper	269 ns

* Chloroformate activated conjugate of IgG with complex (35).

As can be seen in Table 3-6, adsorption of the conjugate onto Whatman No. 1 filter paper, does result in an increase in the luminescent lifetime; the reasons are explained more fully in Chapter 2. However, adsorption of the conjugate onto the paper would probably result in the conjugate being rigidly held within the paper matrix, so lessening the chances of decay of the ruthenium complex excited state by non-radiative processes, e.g. collisional deactivation.

3:3:4 EVALUATION OF RUTHENIUM TRIS BIPYRIDINE COMPLEXES AS ANTIBODY PROBES IN IMMUNOASSAY

In the above results, it can be seen that, the ruthenium complexes do maintain their luminescent behaviour on conjugation to antibodies, and, as such, they seem to indicate, that they

could be placed in a time-resolved immunoassay system. In such a system, they would appear to have an advantage over the europium chelates in the DELFIA system, because rechelation before fluorescence measurement would not be required. This would remove the use of a wash step, as well as the use of an easily contaminated enhancement solution.

There is, however, more experimentation necessary before the ruthenium conjugates could be used in an immunoassay system. It is important, that the conjugate must be evaluated by electrophoresis, to ensure that the incorporation of the ruthenium complex into the antibody is by covalent attachment. Once this is established, the conjugate must be optimised; a process, which involves the generation of a conjugate, having the correct incorporation ratio of probe to IgG. The resulting conjugate, gives the maximum luminescent signal, without loss of the antigenic affinity of the antibody.

The ability of the ruthenium conjugate to give an enhanced luminescent signal in the solid phase, is also a good indication of the versatility of the ruthenium complexes in immunoassay. It is, therefore, possible that these ruthenium bipyridine complexes may have uses in solid phase and electrochemiluminescent immunoassay, as well as in time-resolved fluorescent immunoassay.

3:4:0 EXPERIMENTAL

Conjugation of bis(2,2'-bipyridine) (4,4'-dichloro-2,2'-bipyridine) ruthenium (II) hexafluorophosphate (26) to human IgG

Human IgG (3mg, 2×10^{-8} moles) was dissolved in phosphate buffer pH 9.4 (1 cm³), to which was added bis(2,2'-bipyridine) (4,4'-dichloro-2,2'-bipyridine) ruthenium (II) hexafluorophosphate (2 mg, 2×10^{-6} moles), to give a 100 molar excess of ruthenium complex to IgG, in DMF (100 µl). The resulting solution was then left at 2-4°C overnight.

After running a column (Sephadex G25) of the above labelling solution and eluting with PBS pH 7.4, the protein containing fractions were pooled. A fluorescence spectrum was run of the isolated protein fraction using the Perkin-Elmer MPF-4 fluorospectrometer, exciting at 470nm and scanning between 580nm and 650nm; no emission was observed.

Conjugation of human IgG to bis(2,2'-bipyridine) (4,4'-diamino-2,2'-bipyridine) ruthenium (II) hexafluorophosphate (19) via DSS

To bis(2,2'-bipyridine) (4,4'-diamino-2,2'-bipyridine) ruthenium (II) hexafluorophosphate (308µl of a 5 mg/ml DMF solution, 3.08 mg, 3.33×10^{-6} moles) was added DSS (123µl of a 5 mg/ml DMF solution, 1.23 mg, 3.33×10^{-6} moles), and the whole left at room temperature for 60 minutes.

After human IgG (10 mg, 6.67×10^{-8} moles) was dissolved in 10 mM phosphate buffer pH 7.4 (2 cm³), it was added to the above incubated mixture, thus giving a 50 times molar excess of ruthenium complex to IgG. The reaction mixture was then left to incubate at room temperature for a further 2 hours. After this incubation period, the mixture was passed down a PD-10 column, eluted with 10 mM phosphate buffer pH 7.4, and the protein fraction collected. A UV spectrum was run of the collected protein fraction on a Kontron UVKON 930 spectrophotometer. The UV spectrum obtained was then compared with that of pure IgG and the ruthenium complex (19), (ref. Section 3:3:1, Fig. 3-12); this spectrum clearly indicated the presence of the ruthenium complex in the protein fraction.

Conjugation of ruthenium complexes to human IgG and measurement of luminescent lifetimes

Ruthenium complexes conjugated to human IgG:-

- i) bis(2,2'-bipyridine) (4,4'-diamino-2,2'-bipyridine) ruthenium (II) hexafluorophosphate (19). Conjugated to human IgG via EDC.
- ii) bis(2,2'-bipyridine) (4-[3-hydroxypropyl]-4'-methyl-2,2'-bipyridine) ruthenium (II) hexafluorophosphate (35). Conjugated to human IgG via the chloroformate derivative of (35) as follows:-

(35) (115.1 mg, 11.15×10^{-4} moles) was dissolved in the smallest possible volume of dry THF. This solution was then added dropwise to 12.5% (w/w) phosgene in toluene (5 cm³). After addition the solution was stirred for a further 30 minutes at room temperature and the excess phosgene removed under reduced pressure. The reaction mixture was then evaporated to dryness to leave an orange coloured solid (the chloroformate derivative of (35)).

To human IgG (2.82 mg, 1.88×10^{-8} moles) in phosphate buffer pH 9.4 (1 cm³) was added the chloroformate derivative of (35) (2.0 mg, 1.88×10^{-6} moles) in DMF (100 μl), and the whole left overnight at 2-4°C.

A column (Sephadex G25) was run of the above solution eluting with PBS buffer pH 7.4, and the fraction containing the protein was collected.

- iii) Bis(4,4'-diphenyl-2,2'-bipyridine) (4-[3-hydroxy-propyl]-4'-methyl-2,2'-bipyridine) ruthenium (II) hexafluorophosphate (37). Conjugated to human IgG via the chloroformate derivative as for (35).

iv) bis(2,2'-bipyridine) (4-vinyl-4'-methyl-2,2'-bipyridine) ruthenium (II) hexafluorophosphate (40). Conjugated to human IgG by elevation of the pH above 8.

At this time, I would like to acknowledge the help of D. Chappell in the preparation of some of the conjugates.

All lifetimes were measured using a fluorescence microscope modular work bench (Ref. Chapter 2).

Lifetime measurement of the RTL effect on the ruthenium conjugate

A rectangular piece of Whatman No. 1 filter paper (1.5cm x 0.5cm) was dipped into a solution of the conjugate of human IgG with ruthenium complex (35) until it was thoroughly soaked. The sample was then left to dry prior to measuring the lifetime.

The lifetime was measured using a fluorescence microscope modular work bench (Ref. Chapter 2). Blanks were also run of IgG adsorbed on to Whatman No. 1 filter paper, and the conjugate in solution in PBS buffer pH 7.4.

3:5:0 REFERENCES

GENERAL TEXTS

- a. ROITT, I.M., Essential Immunology, 5th Edition, (1984), Pub. Blackwell Scientific Publications, Oxford.
 - b. STRYER, L., Biochemistry, 2nd Edition, (1981), Pub. W.H. Freeman and Company, San Francisco.
 - c. EDWARDS, R., Immunoassay An Introduction, (1985), Pub. William Heinemann Medical Books, London.
 - d. ROITT, I.M., BROSTOFF, J. and MALE, D.K., Immunology, (1985), Pub. Gower Medical Publishing Ltd., London.
-
- 1. YALOW, R.S. and BERSON, S.A., (1960), J. Clin. Invest., 39, 1157.
 - 2. COUDRON, P.E., FEDORKO, D.P., DAWSON, M.S., KAPLOWITZ, L.G., BROOKMAN, R.R., DALTON, H.P. and DAVIS, B.A., (1986), Am. J. Clin. Pathol., 85, 89.
 - 3. ALLAIN, J-P., LAURIAN, Y., PAUL, D.A. and SENN, D., (1986), Lancet, 1233.
 - 4. BRASHEAR, J., ZEITVOGEL, C., JACKSON, J., FLEUTGE, C., JANULIS, L., CANTRELL, L., SCHMIDT, B., ADAMCZJK, M., BETEBENNER, D. and VAUGHAN, K., (1989), Clin. Chem., 35, 355.
 - 5. MINORS, S., HORTON, J.K., WEEKS, I., DAVIS, M. and COLES, G.A., (1988), J. Immunological Meth., 115, 119.
 - 6. HEMMILÄ, I., MALMINEN, O., MIKOLA, H. and LÖVGREN, T., (1988), Clin. Chem., 34, 2320.
 - 7. EL-GAMAL, B.A., EREMIN, S.A., SMITH, D.S. and LANDON, J., (1988), Ann. Clin. Biochem., 25, 35.
 - 8. ESKOLA, J.U., NÄNTÖ, V., MEURLING, L. and LÖVGREN, T.N-E., (1985), Clin. Chem., 31, 1731.
 - 9. AL-HAKIEM, M.H.H., NARGESSSI, R.D., POURFARZANEH, M., WHITE, G.W., SMITH, D.S. and HODGKINSON, A.J., (1982), J. Clin. Chem. Clin. Biochem., 20, 151.
 - 10. LI, P.K., LEE, J.T. and SCHREIBER, R.M., (1984), Clin. Chem., 30, 307.
 - 11. HANSEN, W., VRAY, B., MILLER, K., CROKAERT, F. and YOURAS-SOWSKY, E., (1987), J. Clin. Microbiology, 25, 1934.
 - 12. GRASSNER, D., (1986), Eur. J. Cell Biol., 40, 176.
 - 13. HAVER, V.M., AUDINO, N., BURRIS, S. and NELSON, M., (1989), Clin. Chem., 35, 138.

14. JOLLEY, M.E., (1981), J. Anal. Toxicol., 5, 236.
15. COXON, R.E., HODGKINSON, A.J., SIDKI, A.M., LANDON, J. and GALLACHER, G., (1987), Therapeutic Drug Monitoring, 9, 478.
16. KINTZ, P., TRACQUI, A., MANGIN, P., LUGNIER, A. and CHAUMONT, A., (1988), Clin. Chem., 34, 2374.
17. SAVASER, A.N., HOSTEN, N., SCHULZ, E., JORNO, L. and FELIX, R., (1987), Eur. J. Nucl. Med., 13, 397.
18. DIAMANDIS, E.P., (1988), Clin. Biochem., 21, 139.
19. HELSINGIUS, P., HEMMILA, I. and LÖVGREN, T., (1986), Clin. Biochem., 32, 1767.
20. DIAMANDIS, E.P., (1990), Clin. Biochem., 23, 437.